JMT
Journal of Musculoskeletal Trauma
Vol. 39, No. 2, April 2026

JMT Journal of Musculoskeletal Trauma

Vol. 39, No. 2, April 2026
Pages 73-183
The Korean Orthopaedic Trauma Association

pISSN 3058-6267
eISSN 3058-6275

JMT
Journal of Musculoskeletal Trauma | e-jmt.org
Vol. 39, No. 2, April 2026

The Korean Orthopaedic Trauma Association

JMT Journal of Musculoskeletal Trauma

e-jmt.org

pISSN 3058-6267
eISSN 3058-6275

Vol. 39, No. 2, April 2026

Aims and Scope

The Journal of Musculoskeletal Trauma is the official publication of the Korean Orthopaedic Trauma Association. It is an international, peer-reviewed, open access journal dedicated to advancing the science, education, and clinical care of musculoskeletal trauma. The journal provides a platform for the dissemination of high-quality research, innovative techniques, and multidisciplinary approaches that improve patient outcomes in the field of orthopedic trauma and related disciplines.

As an open access journal, all articles are freely available to readers worldwide, ensuring the widest possible dissemination of knowledge and promoting collaboration among researchers, clinicians, and educators.

The scope of the journal encompasses the prevention, diagnosis, treatment, and rehabilitation of musculoskeletal injuries, including but not limited to:

- Fractures, dislocations, and soft tissue injuries of the extremities and axial skeleton
- Advances in surgical techniques, implants, and prosthetic devices
- Biomechanical and biological research related to trauma and tissue healing
- Rehabilitation strategies and innovations for functional recovery
- Clinical and translational research bridging basic science and clinical practice

The journal invites submissions of original research articles, systematic reviews, meta-analyses, technical notes, and correspondence that contribute to the advancement of musculoskeletal trauma care. Submissions are welcomed from all regions of the world, promoting a diverse and inclusive exchange of knowledge and perspectives.

The *Journal of Musculoskeletal Trauma* serves as a resource for orthopedic surgeons, trauma specialists, researchers, rehabilitation professionals, and all healthcare providers involved in the care of musculoskeletal injuries. By fostering collaboration and disseminating cutting-edge findings, the journal aims to elevate the standards of trauma care globally.

Open Access

Publisher: The Korean Orthopaedic Trauma Association
Editor-in-Chief: Jae Ang Sim

Publishing/Editorial Office
The Korean Orthopaedic Trauma Association
2F, 202-a5, 12-16, Dasanjungang-ro 146 beon-gil, Namyangju 12285, Korea
Tel: +82-31-560-2187, Email: office@e-jmt.org

Printed by M2PI
#805, 26 Sangwon 1-gil, Seongdong-gu, Seoul 04779, Korea
Tel: +82-2-6966-4930, Fax: +82-2-6966-4945, Email: support@m2-pi.com

This work is supported by the 'Lottery Fund' of the 'Ministry of Strategy and Finance' and the 'Science and Technology Promotion Fund' of the 'Ministry of Science and ICT,' contributing to the realization of social value and the development of national science and technology.

Published on April 25, 2026

JMT Journal of Musculoskeletal Trauma

e-jmt.org

pISSN 3058-6267
eISSN 3058-6275

Editorial Board

JMT Journal of Musculoskeletal Trauma

e-jmt.org

pISSN 3058-6267
eISSN 3058-6275

Contents

Vol. 39, No. 2, April 2026

Review Articles

Original Articles

Case Report

Letter to the Editor

JMT Journal of Musculoskeletal Trauma

pISSN 3058-6267 · eISSN 3058-6275
J Musculoskelet Trauma 2026;39(2):73-82
https://doi.org/10.12671/jmt.2026.00045

Definitive fixation for traumatic pelvic ring injuries: a dynamically informed, posterior-referenced framework

Jeong-Hyun Koh, Seungyeob Sakong

Department of Orthopedic Surgery, Ajou University School of Medicine, Suwon, Korea

Optimal definitive fixation for traumatic pelvic ring injuries remains challenging because static radiographs and computed tomography, although essential for defining morphology, do not consistently predict load-dependent behavior during early mobilization. This uncertainty contributes to substantial practice variation and continued reliance on simplified displacement thresholds, such as the 2.5 cm rule. Such rules can misclassify instability by underrepresenting posterior competence and by privileging static measurements over functional behavior. In this narrative review, we propose a dynamically informed, posterior-referenced framework composed of three linked elements: (1) decision-linked terminology that explicitly distinguishes dynamic instability, radiographic change, and clinical failure; (2) selective stress-based assessment when uncertainty is likely to alter management; and (3) escalation along a fixation continuum that weighs incremental stability against operative burden. When static imaging cannot establish posterior competence with confidence, we outline selective stress-based approaches to assess pelvic ring behavior and to translate demonstrated instability into fixation selection along a defined continuum. Across all steps, the framework emphasizes minimum necessary fixation and explicitly incorporates the cost of selection as a primary decision variable. The operative question, therefore, shifts from gap width alone to clinically relevant motion and preservation of posterior competence. In doing so, this approach aims to reduce both undertreatment and overtreatment and to improve the consistency and defensibility of definitive fixation strategies across diverse practice environments.

Keywords: Pelvis; Bone fractures; Sacroiliac joint; Fracture fixation, internal

Introduction

Determining the optimal management of traumatic pelvic ring injuries remains clinically challenging. Static radiographs and computed tomography (CT) are essential for defining morphology and planning fixation, yet they do not consistently predict how an injury will behave during early mobilization. As a result, meaningful variation persists in how similar patterns are treated across surgeons and institutions, in part because complex three-dimensional mechanics must be inferred from two-dimensional static images [1-3].

The clinical consequences of this mismatch are substantial. Underestimation of instability can lead to loss of reduction, malunion, persistent pain, and impaired function. In selected cases, it may require revision surgery with considerable morbidity. Overestimation of instability exposes patients to unnecessary operative invasiveness,

Review Article

Received: January 13, 2026
Revised: January 24, 2026
Accepted: January 28, 2026

Correspondence to:
Seungyeob Sakong
Department of Orthopedic Surgery, Ajou University School of Medicine, 164 Worldcup-ro, Yeongtong-gu, Suwon 16499, Korea
Tel: +82-31-219-5220
Email: sgsy4040@gmail.com

greater soft-tissue burden, and implant-related complications. The central problem is therefore not simply whether to operate, but how to select fixation that controls clinically relevant instability while limiting avoidable harm from overtreatment [1,3].

Historically, the field has relied on simplified numeric thresholds because they are teachable and reproducible. Thresholds based on symphyseal diastasis or sacroiliac (SI) widening can assist early stratification, but they do not reliably capture posterior competence, ligament integrity, or load-dependent behavior. In borderline cases, a single static measurement can describe what is seen without forecasting what will occur once the ring is challenged during rehabilitation [1,2].

This review presents a dynamically informed strategy centered on two clinical priorities: posterior competence and the cost of selection. Rigid displacement thresholds—most notably the long-standing "2.5 cm rule"—can misclassify instability. We outline when uncertainty warrants stress-based assessment of behavior and how those findings translate into fixation selection along a construct continuum. The objective is not to promote a single maneuver or construct, but to provide a practical framework that remains applicable across diverse clinical environments [1,4,5].

Shared language: terms that map to decisions

To prevent inconsistent terminology from driving inconsistent surgery, instability and failure should be defined in terms that map directly to decisions. In this review, dynamic instability (Table 1) [1-3,6-11] refers to clinically relevant motion under stress or physiologic loading, regardless of the initial static appearance. This definition shifts emphasis from what an injury looks like to how the pelvic ring behaves when challenged [1,2].

A second distinction is between radiographic change and clinical failure. Radiographic change includes interval widening, minor alignment shifts, and implant loosening on follow-up imaging. These findings—particularly in the anterior ring—may occur without meaningful symptoms or functional compromise. Clinical failure refers to patient-centered deterioration—progressive loss of alignment that compromises the pelvic reference frame, persistent pain or functional limitation that delays rehabilitation, or unplanned revision. Postoperative radiographic changes after anterior fixation do not consistently correlate with poor function or revision, underscoring the risk of escalation driven by imaging alone [6,7].

The gray-zone describes cases in which static imaging does not allow confident classification as stable versus unstable and where management could reasonably differ. Gray-zone injuries are where both undertreatment and overtreatment risks are highest, and interpretation benefits from a consistent reference. In gray-zone injuries, posterior alignment and posterior competence serve as the reference frame for global stability, helping distinguish clinically meaningful anterior instability from expected postoperative variation [2,9].

This logic underpins the review. Static imaging defines morphology and informs planning; however, when uncertainty could change management, controlled stress testing becomes the relevant question. Fixation is then selected by balancing stability benefit against the incremental burden introduced by escalation [1,2]. In this framework, clinically relevant motion refers to reproducible stress- or load-dependent ring motion that plausibly threatens the maintenance of the posterior ring reference frame and/or delays mobilization and rehabilitation. Key working definitions and decision-linked terminology used throughout this review are summarized in Table 1 [1-3,6-11].

Static imaging: necessary but not sufficient

Static imaging remains central to triage and preoperative planning. Radiographs provide an initial characterization of displacement patterns, injury vectors, and associated lesions. CT with multiplanar reconstructions refines assessment of sacral fracture morphology, comminution, and pelvic anatomy relevant to safe fixation corridors. Together, these details guide construct feasibility, technical approach, and operative planning [1,2,12].

A persistent limitation is that morphology and static displacement do not consistently predict functional behavior under physiologic loading. Borderline injuries expose the gap between measured diastasis and clinically meaningful mobility. Two patients with similar symphyseal widening can represent different mechanical states depending on

https://doi.org/10.12671/jmt.2026.00045

Table 1. Working definitions and decision-linked terminology used in the current review

Term	Working definition (current review)	Clinical/surgical implications	Key references
Dynamic instability	Clinically meaningful, demonstrable motion/displacement under stress or early physiologic loading, regardless of initial static alignment.	Shifts decision-making from static diastasis to load-dependent behavior in borderline patterns.	[1,2]
Radiographic change	Interval widening or minor alignment change after treatment without parallel symptom or functional deterioration.	Discourages reactive escalation driven by imaging alone, particularly for anterior constructs.	[6,7]
Clinical failure	Patient-centered deterioration with progressive malalignment that compromises the posterior ring reference frame, persistent disabling symptoms, and/or unplanned revision.	Defines reoperation thresholds by mechanical/functional deterioration rather than radiographic change alone.	[6-8]
Gray-zone injury	Presentations in which static imaging is insufficient to classify stability with confidence and management could reasonably differ.	Identifies cases where selective dynamic assessment or structured surveillance is most defensible.	[2,9]
Posterior competence	Functional integrity of the posterior ring (posterior sacroiliac complex/ligamentous integrity) as the primary determinant of global load transfer.	Supports posterior stabilization when posterior competence is compromised or cannot be established confidently.	[1,2]
Posterior ring reference frame	Interpreting anterior findings and postoperative change through the context of posterior alignment and stability.	Avoids overbuilding the anterior ring to compensate for posterior deficits and reduces radiograph-driven overreaction.	[1,2]
Cost of selection	Incremental burden of escalation (operative time, invasiveness, soft-tissue risk, complications, morbidity).	Requires explicit mechanical justification for construct expansion and reinforces "minimum necessary fixation."	[3,10,11]
Minimum necessary fixation	The least extensive construct that reliably controls demonstrated instability and supports safe mobilization.	Anchors escalation: stabilize what is unstable; escalate only when standard constructs are unlikely to suffice.	[1,3]

Terms are defined to link language to management decisions. Dynamic instability and postoperative anterior findings are interpreted within the posterior ring reference frame, with radiographic change distinguished from clinical failure to avoid imaging-driven escalation. Posterior competence denotes functional integrity of the posterior sacroiliac complex; cost of selection supports the minimum necessary fixation.
CT, computed tomography.

posterior ligament competence, comminution pattern, and mechanical coupling across the ring. Static imaging can be deceptively reassuring: some injuries displace with mobilization, whereas others heal uneventfully without fixation [2,9].

When morphology clearly indicates instability and operative stabilization is indicated, static imaging is typically sufficient for planning. When findings fall in a gray-zone and management could change, displacement thresholds should be treated as risk markers rather than decision rules. The key questions are whether posterior competence is preserved and whether reproducible, clinically relevant motion is demonstrated under stress (Fig. 1) [1,2]. This tension is most visible when practice is organized around numeric cutoffs rather than mechanical behavior. The enduring "2.5 cm rule" is the clearest example of how a single static threshold can oversimplify global pelvic stability [4,13].

Deconstructing the "2.5 cm myth"

The 2.5 cm rule persists because it is simple and historically embedded in pelvic trauma teaching. As a screening heuristic, a numeric cutoff can be useful. However, it should be interpreted as a risk marker—not a decision rule—within the posterior reference-frame logic. The problem arises when it is treated as a definitive boundary for stability across heterogeneous injury patterns and patient contexts [4,13].

A single threshold does not incorporate posterior competence or load-dependent behavior and can therefore misclassify instability. Modest static diastasis may coexist with substantial motion under stress when posterior structures are compromised, whereas larger diastasis may behave relatively stably when posterior competence is preserved. Reducing a three-dimensional mechanical problem to a single static measurement obscures the true determinant of global stability [2,4].

For the practicing surgeon, a more useful question is

whether the pelvic ring shows clinically relevant motion under stress, interpreted within a posterior ring reference frame (Fig. 1). Many borderline cases are better framed as uncertainty about posterior competence rather than a measurement problem. Decision-making should therefore prioritize whether mobility is likely to jeopardize early mobilization or maintenance of reduction [1,2].

Minor postoperative changes in the anterior ring do not automatically represent clinical failure. Small interval widening or implant loosening can occur even when posterior alignment is maintained and functional recovery progresses. Revision and escalation are more appropriate when there is loss of global alignment, persistent instability, or meaningful clinical deterioration rather than isolated radiographic findings [6-8].

Accordingly, the practical question returns to behavior: whether clinically relevant motion is present and whether posterior competence is preserved [2,4].

Dynamic instability assessment: resolving decision-changing uncertainty

Dynamic assessment is a clinical principle rather than a routine test (Fig. 1). Its purpose is to reduce decision-changing uncertainty by clarifying pelvic ring behavior under controlled stress, particularly when static imaging defines morphology but cannot confidently establish posterior competence or global stability. The limitations of rigid cutoffs, exemplified by the 2.5 cm rule, help explain why behavior-based assessment becomes relevant when management hinges on borderline findings [1,2,4].

At the bedside, initial assessment and early reassessment can triage presentations that remain consistent with stability. Focused examination, symptom response during early

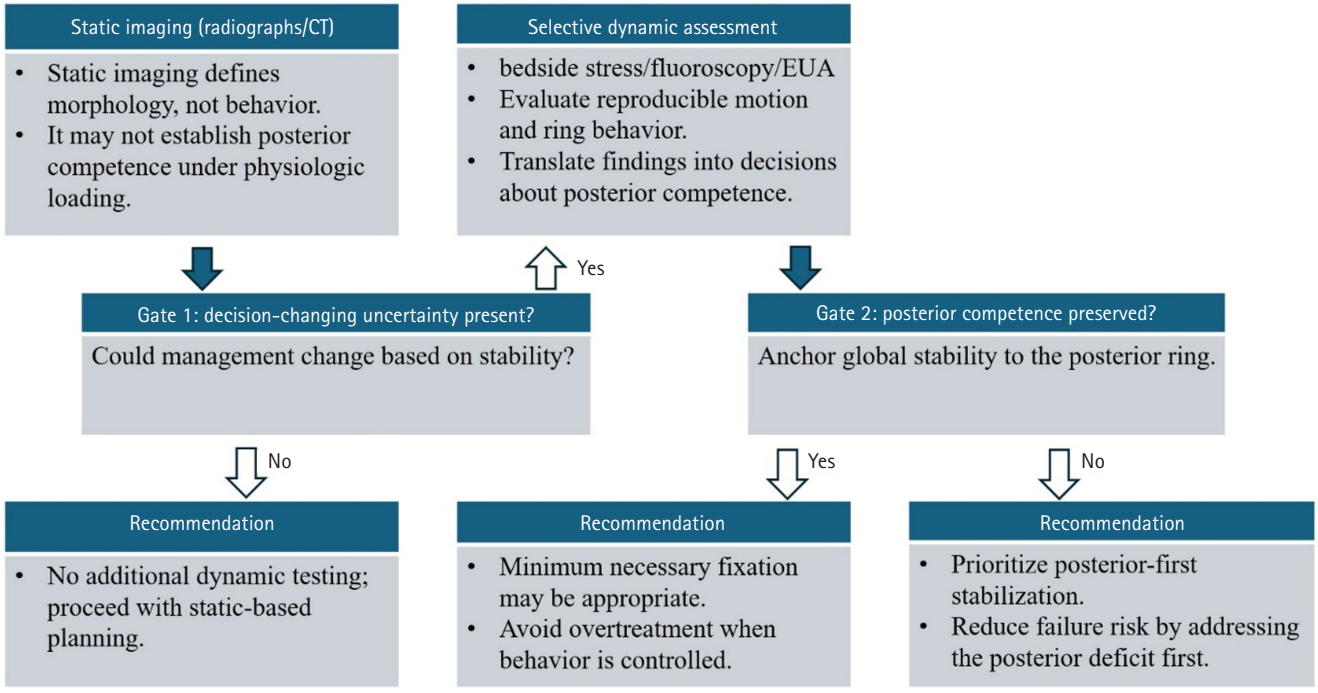

Fig. 1. Gate-based decision framework linking static morphology to selective dynamic assessment. Static imaging using radiographs and computed tomography (CT) defines morphology and informs feasibility and operative planning, but may not reliably establish load-dependent behavior or posterior competence in borderline pelvic ring injuries. In this framework, Gates represent decision checkpoints that determine whether dynamic assessment is required and whether posterior competence should anchor management. When decision-changing uncertainty is present (Gate 1), selective dynamic assessment, such as bedside stress examination, fluoroscopy, or examination under anesthesia, documents reproducible motion and ring behavior. Posterior competence is treated as the primary anchor of global pelvic stability (Gate 2), guiding recommendations that range from static-based planning to minimum necessary fixation or posterior-first stabilization. Construct selection along the fixation continuum is summarized in Fig. 2. EUA, examination under anesthesia.

https://doi.org/10.12671/jmt.2026.00045

mobilization, and serial imaging in standardized views can clarify whether alignment is maintained over time. The objective is not to "prove stability" with a single maneuver, but to determine whether uncertainty meaningfully persists after reasonable observation [2,9].

When uncertainty persists and operative planning is being considered, intraoperative fluoroscopy can provide adjunct information. Controlled stress under fluoroscopy can assess reduction behavior across standard views (anteroposterior [AP], inlet, and outlet). Because applied force and technique vary across operators, these observations are most informative when documented with method details—patient position, direction of stress, and motion pattern—rather than reduced to isolated cutoffs [2,9].

To maximize reproducibility without implying numeric thresholds, minimum documentation should specify:

- Patient position and support (e.g., supine/prone)
- Fluoroscopic views obtained (AP, inlet, and outlet)
- Stress maneuver (direction and method of force application)
- Reproducibility (consistency across repeat maneuvers)
- Qualitative motion pattern (rotational, vertical, or translational)
- Interpretation relative to posterior competence

Examination under anesthesia can serve as a confirmatory option when higher-fidelity information is expected to change management. Full muscle relaxation can improve consistency of stress application, particularly when posterior competence is uncertain and the fixation plan is near a meaningful escalation boundary. It is best used selectively for decision-changing questions rather than as a routine prerequisite [1,14].

The output of dynamic assessment should translate into mechanical decisions: whether posterior competence is preserved and whether observed motion is sufficient to threaten mobilization or reduction maintenance. Interpretation should prioritize posterior competence and reproducible ring behavior under stress rather than absolute millimeter closure. Demonstrated stable behavior may support nonoperative care or limited fixation, whereas persistent motion strengthens the rationale for prioritizing posterior stabilization within the posterior ring reference frame [1,2].

Practical limitations are clinically important. Dynamic testing lacks universal standardization, anesthesia and operating-room constraints vary, and manipulation carries risk. Evidence is heterogeneous, and thresholds for clinically meaningful motion are not consistent across studies or injury patterns. Dynamic assessment is therefore most appropriate when applied to management-relevant questions and reported transparently in context [1,14].

Translating instability into fixation: escalation along a continuum

Fixation selection is best viewed as a continuum in which stability gains must be weighed against the costs of escalation (Fig. 2). Table 2 summarizes representative constructs, decision triggers, and the primary cost of selection across this continuum [1,2,6-12,15-18]. This framework supports minimum necessary fixation: stabilizing what is demonstrably unstable while avoiding construct expansion when it is unlikely to improve patient-centered outcomes. In polytrauma and medically complex patients, added operative time, blood loss, and physiologic stress may themselves be clinically consequential; escalation should therefore be justified by a clear mechanical need [1,3]. A practical translation begins with behavior. When the ring behaves stably under the available assessment method and the clinical course remains concordant, nonoperative management or limited fixation may be reasonable, depending on morphology and patient factors. When behavior is borderline, standard constructs may be appropriate to protect alignment and facilitate mobilization. When clear mobility is demonstrated or posterior competence is compromised, escalation becomes justified. Throughout, decisions are best interpreted within a posterior ring reference frame [1,2].

Posterior stabilization should guide the primary strategy when posterior competence is compromised or strongly suspected. Posterior competence governs global load transfer and strongly influences whether anterior fixation will remain durable. In unstable patterns, posterior stabilization has been associated with fewer anterior construct failures. These observations suggest that loss of posterior competence drives anterior overload more often than isolated anterior implant insufficiency [19].

Anterior fixation is best framed as an adjunct once poste-

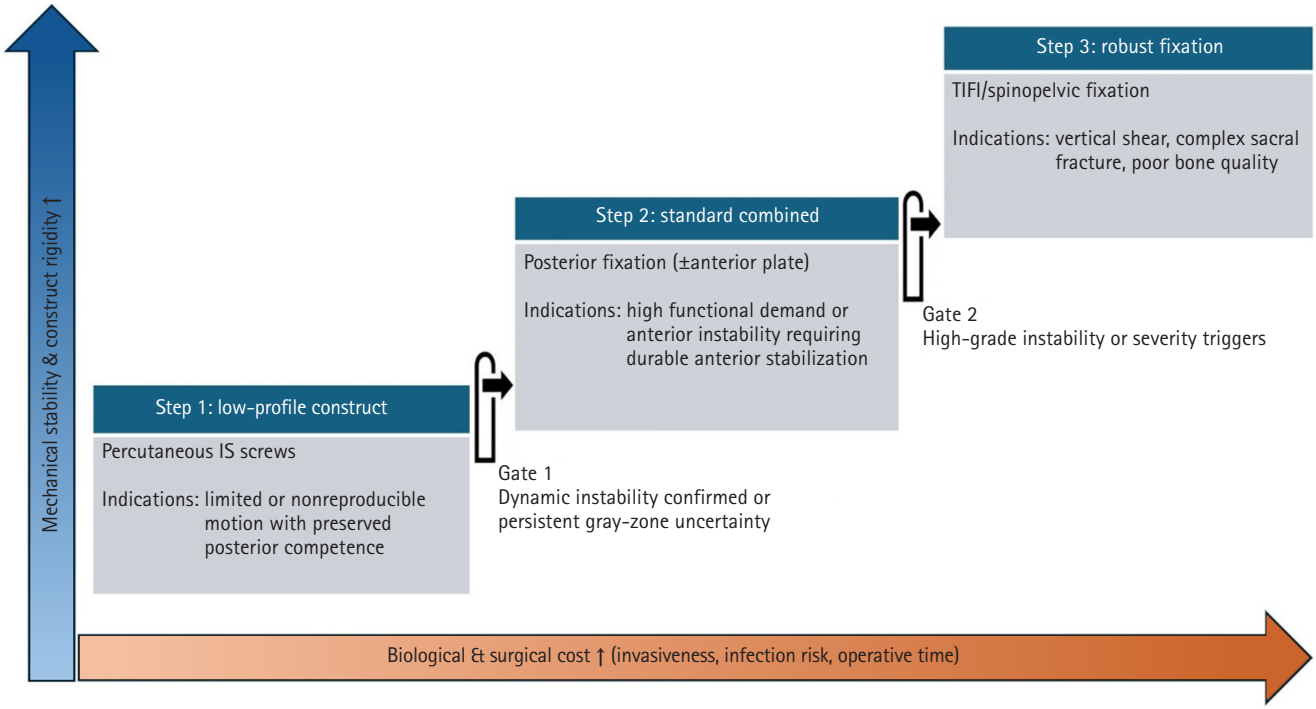

Fig. 2. Fixation escalation along a construct continuum balancing mechanical stability and surgical cost. Fixation constructs are organized from low-profile to more robust strategies, balancing increasing mechanical stability and rigidity against escalating biological and surgical cost, including invasiveness, infection risk, and operative time. Steps represent levels of construct escalation along the fixation continuum. Step 1 reflects low-profile posterior fixation for limited or nonreproducible motion with preserved posterior competence. Step 2 represents standard combined fixation, consisting of posterior fixation with or without an anterior plate, when dynamic instability is confirmed or when persistent gray-zone uncertainty and clinical context favor added stability. Step 3 depicts escalation to robust constructs, such as transiliac internal fixation (TIFI) or spinopelvic fixation, for high-grade instability or severity triggers including vertical shear, complex sacral fracture, or severe osteoporosis. IS, iliosacral.

rior competence is addressed. Its role is to restore anterior alignment, reduce rotational tendency, and protect posterior stabilization in patterns where anterior disruption contributes to symptoms and instability. In this context, minor radiographic changes—such as small interval widening or implant loosening—do not necessarily indicate clinical failure if posterior alignment is preserved and functional recovery is favorable. This distinction reduces escalation driven by radiographic anxiety rather than mechanical necessity [6-8].

The durability of low-profile posterior constructs, including iliosacral screw fixation, depends on patient and technical factors that should be treated as explicit decision variables. Bone quality, reduction accuracy, screw trajectory and length, corridor anatomy, and sacral comminution all influence mechanical performance. Syntheses of the literature associate loosening and failure with these factors, supporting the use of a structured risk checklist during planning rather than defaulting to low-profile constructs in mechanically unfavorable settings [15,16,20].

Escalation to more robust constructs is appropriate when standard posterior fixation is unlikely to control the injury pattern or maintain reduction. Practical triggers include a marked vertical tendency, substantial sacral comminution or compromised corridors, and inability to achieve or maintain acceptable alignment with screws alone. Options such as transiliac internal fixation (TIFI) or spinopelvic constructs can provide stronger control, but indications should remain explicit and mechanically justified [10,12,17]. Percutaneous advances, including TIFI, expand posterior options but require precise corridors [21].

The cost of selection should be incorporated as a primary decision factor. More extensive fixation increases operative complexity and soft-tissue burden compared with low-profile constructs. In selected series and pooled analyses, complex posterior constructs have been associ-

https://doi.org/10.12671/jmt.2026.00045

Table 2. Fixation levels along a continuum: representative constructs, decision triggers, and the primary "cost of selection"

Fixation level (continuum)	Typical construct examples	Decision triggers (indications)	Primary "cost of selection"	Key references
Structured surveillance	Standardized serial radiographs (AP/inlet/outlet) during early mobilization.	When gray-zone presentations show a stable early course, no evidence of clinically relevant motion, and no progressive malalignment.	Risk of delayed displacement; requires disciplined follow-up and a predefined conversion threshold.	[2,9]
Isolated anterior fixation	Symphyseal plating; anterior ramus screw fixation.	When posterior competence is confidently preserved and the anterior injury is the primary driver of symptoms or mobilization limits.	Risk of undertreating occult loss of posterior competence; anterior radiographic change may be overinterpreted as clinical failure.	[1,6,7]
Standard posterior fixation	1–2 Iliosacral screws.	When loss of posterior competence is demonstrated or strongly suspected and is expected to compromise reduction maintenance or safe mobilization.	Technical demand and neurovascular risk; loosening risk in poor bone quality or suboptimal reduction.	[15,16,18]
Augmented posterior fixation	Additional SI screws and/or transiliac–transsacral screw options.	When posterior control is borderline and added stability is required to prevent recurrent motion and anterior construct overload.	Increased radiation and operative time; diminishing mechanical returns in high-grade vertical patterns.	[12,15,17]
Robust posterior fixation	Transiliac internal fixation.	When there is marked vertical tendency, substantial sacral comminution, compromised corridors, or inability to maintain alignment with screws alone.	Greater soft-tissue burden and implant prominence–related symptoms; higher likelihood of implant-related discomfort.	[10,12]
Highest-stability constructs	Lumbopelvic/spinopelvic stabilization.	When spinopelvic dissociation or high-grade vertical shear is present and length and shear control are paramount.	Highest morbidity profile; significant wound complication/infection risk; requires explicit mechanical justification.	[10,11]
Anterior adjunct (cross-cutting add-on)	Symphyseal plating; ramus screws (added after posterior stabilization).	When a posterior ring reference frame is secured, add selectively if residual anterior instability limits ring closure or mobilization.	Overreaction to expected anterior radiographic change can drive unnecessary revision; interpret anterior changes within the posterior ring reference frame and reserve revision for clinical failure.	[6-8]

Indications are expressed as decision triggers rather than static cutoffs and should be interpreted within the posterior ring reference frame. "Isolated anterior fixation" presumes posterior competence; "anterior adjunct" is added selectively after posterior stabilization when residual anterior instability is clinically relevant.
AP, anteroposterior; SI, sacroiliac.

ated with higher complication rates, including infection and wound problems. These risks must be weighed against the consequences of inadequate stabilization, including loss of reduction and revision surgery. In practice, the aim remains minimum necessary fixation: secure posterior mechanics when indicated, add anterior fixation when it meaningfully supports global stability, and escalate only when standard constructs are unlikely to control demonstrated instability [3,10,11].

Definitive fixation strategy and sequencing

With fixation viewed as a continuum (Fig. 2), operative sequencing becomes a practical exercise in establishing a durable posterior ring reference frame (Fig. 1) and adding anterior stabilization only when it contributes meaningful mechanical value. Definitive fixation is most effective when planned around a clear objective: restoring and maintaining global pelvic stability while limiting unnecessary surgical burden. Posterior competence and alignment often define the reference frame that determines whether subsequent steps—particularly anterior reduction—will be meaningful and durable [1,12].

When posterior competence is compromised or uncertain, a posterior-first sequence is typically the most appropriate strategy. Conversely, an anterior-first or ante-

rior-only approach may be reasonable only when posterior competence is clearly preserved, and the decision should still be justified within the posterior ring reference frame. Recent reviews confirm that reduction evolution favors posterior-first sequencing in unstable patterns [22]. Securing posterior alignment establishes the reference on which anterior reduction can be judged and maintained. In this setting, posterior-first fixation is not merely a preference; it is often mechanically necessary for durable anterior stabilization. Anterior constructs cannot reliably compensate for an unaddressed posterior deficit. Attempting to optimize anterior alignment in the presence of unresolved posterior instability can increase surgical burden without reliably improving global stability [12,19,23].

After posterior stabilization, reassessment under fluoroscopy can clarify whether residual anterior instability is mechanically relevant and whether an anterior adjunct is needed to maintain ring closure during mobilization. This step can also help avoid unnecessary anterior escalation when posterior mechanics are adequately controlled and anterior motion is limited [1,2].

Sequencing should also account for physiologic readiness and competing priorities in polytrauma. In patients who have undergone hemorrhage control and temporary stabilization, definitive fixation is best performed when physiology and soft-tissue conditions allow safe surgery, rather than on a rigid timeline. The choice between earlier versus delayed definitive fixation can be individualized based on hemodynamic stability, associated injuries, anticipated invasiveness, and the incremental risk introduced by escalation [3,5].

Technical feasibility is part of the strategy. Posterior fixation options vary in their demands on corridor anatomy, reduction accuracy, and intraoperative imaging. Preoperative CT planning and attention to dysmorphism are essential. Careful fluoroscopic technique reduces malposition risk and increases the likelihood that the selected construct delivers the intended stability [1,15,18].

Special scenarios and failure prevention

Gray-zone injuries managed nonoperatively require an explicit surveillance plan that reflects the same decision logic used for fixation. Early clinical reassessment and standardized serial imaging can identify cases in which alignment is not maintained during mobilization, and recent work highlights how occult instability can declare itself during follow-up despite borderline initial imaging. Conversion to surgery is most appropriate when driven by patient-centered failure, demonstrable progression that threatens global stability, or persistent mechanical symptoms that align with instability, rather than by minor radiographic change alone [2,9].

Certain patient and injury factors increase the likelihood that low-profile constructs will underperform. Poor bone quality, extensive comminution, compromised screw corridors, and malreduction can undermine posterior fixation durability and should influence the decision to augment or escalate. In these scenarios, the goal is not simply to increase fixation, but to select a construct with a realistic likelihood of controlling the observed instability, with a clear mechanical rationale for any escalation [12,15,16].

Open injuries, severe soft-tissue compromise, and contaminated fields require additional caution because the biological cost of fixation rises. When infection risk is high, construct selection should emphasize achieving essential stability with the least additional soft-tissue insult, and definitive internal fixation may need to be staged or modified based on wound management priorities. In such settings, the cost of selection is not an abstract concept but a constraint that should be stated explicitly in the decision rationale [1,3].

Failure prevention also depends on avoiding iatrogenic harm and defining failure appropriately. Malpositioned implants—particularly in the posterior ring—can produce catastrophic neurovascular complications and can convert a borderline mechanical problem into a major clinical failure. Conversely, automatic revision for isolated radiographic findings can drive unnecessary morbidity when the posterior ring reference frame is preserved and functional recovery is favorable. Revision and escalation are most appropriate when there is loss of global alignment, persistent instability, or meaningful clinical deterioration consistent with true failure [6,7,18,20].

Conclusions

Static imaging remains essential for defining morphology and planning treatment, but it does not consistently predict functional instability in borderline pelvic ring injuries.

https://doi.org/10.12671/jmt.2026.00045

The central challenge is to identify clinically meaningful instability and to match fixation to the mechanical problem without defaulting to rigid thresholds or automatic escalation [1,2,4].

A dynamically informed strategy addresses this challenge by anchoring interpretation to posterior competence and using behavior-based assessment selectively when uncertainty is likely to change management. A posterior-referenced strategy supports minimum necessary fixation. It targets demonstrable instability, prioritizes posterior mechanics when indicated, and uses anterior fixation selectively when it adds durable mechanical benefit. This perspective is particularly relevant in polytrauma, where operative burden, timing constraints, and competing priorities are not secondary considerations but part of the outcome [1,3,5].

The practical aim is a decision framework that remains usable across diverse environments. It defines stability in behavioral terms and interprets postoperative changes within a posterior ring reference frame. Escalation is reserved for cases in which standard constructs are unlikely to control demonstrated instability. This helps avoid both undertreatment and unnecessary surgical burden and makes decision-making more consistent [1,2].

Article Information

Author contributions

Conceptualization: JHK; SS. Methodology: JHK; SS. Investigation: JHK. Resources: JHK. Data curation: JHK. Supervision: SS. Project administration: SS. Visualization: JHK. Writing–original draft: JHK. Writing–review & editing: JHK, SS. All authors read and approved the final manuscript.

Conflicts of interest

No potential conflict of interest relevant to this article was reported.

Funding

None.

Data availability

Not applicable.

Acknowledgments

None.

Supplementary materials

None.

References

1. de Ridder VA, Whiting PS, Balogh ZJ, Mir HR, Schultz BJ. Pelvic ring injuries: recent advances in diagnosis and treatment. OTA Int 2023;6(3 Suppl):e261.
2. Elsissy JG, Ruckle DE, LeBrun C, Johnson JP. Pelvic ring injuries: stable or not? J Am Acad Orthop Surg 2024;32:99-107.
3. Halawi MJ. Pelvic ring injuries: surgical management and long-term outcomes. J Clin Orthop Trauma 2016;7:1-6.
4. Gansslen A, Lindahl J, Krappinger D, Lindtner RA, Staresinic M. The myth of 2.5 cm symphyseal diastasis. Arch Orthop Trauma Surg 2025;145:306.
5. Sawauchi K, Esposito L, Kalbas Y, et al. Evolution of management strategies for unstable pelvic ring injuries over the past 40 years: a systematic review. Patient Saf Surg 2024;18:38.
6. Collinge C, Archdeacon MT, Dulaney-Cripe E, Moed BR. Radiographic changes of implant failure after plating for pubic symphysis diastasis: an underappreciated reality? Clin Orthop Relat Res 2012;470:2148-53.
7. Eastman JG, Krieg JC, Routt ML Jr. Early failure of symphysis pubis plating. Injury 2016;47:1707-12.
8. Wheatley BM, Schorr R, Fuhrman H, et al. Can preoperative radiographs predict hardware complication or fracture displacement after operative treatment of pelvic ring injuries? Injury 2021;52:1788-92.
9. Keltz E, Keren Y, Jain A, et al. Surgical stabilisation in equivocal pelvic ring injuries: into the grey zone. Injury 2023;54:110887.
10. Patel S, Ghosh A, Jindal K, Kumar V, Aggarwal S, Kumar P. Spinopelvic fixation for vertically unstable AO type C pelvic fractures and sacral fractures with spinopelvic dissociation: a systematic review and pooled analysis involving 479 patients. J Orthop 2022;29:75-85.
11. Godolias P, Plumer J, Cibura C, Dudda M, Schildhauer TA, Chapman JR. Posterior pelvic ring injuries, lumbosacral junction instabilities and stabilization techniques for spinopelvic dissociation: a narrative review. Arch Orthop Trauma Surg 2024;144:1627-35.
12. Verbeek DO, Routt ML Jr. High-energy pelvic ring disrup-

tions with complete posterior instability: contemporary reduction and fixation strategies. J Bone Joint Surg Am 2018;100:1704-12.
13. Wright RD Jr. Indications for open reduction internal fixation of anterior pelvic ring disruptions. J Orthop Trauma 2018;32 Suppl 6:S18-23.
14. Avilucea FR, Archdeacon MT, Collinge CA, Sciadini M, Sagi HC, Mir HR. Fixation strategy using sequential intraoperative examination under anesthesia for unstable lateral compression pelvic ring injuries reliably predicts union with minimal displacement. J Bone Joint Surg Am 2018;100:1503-8.
15. Hofmann A, Wagner D, Rommens PM. Iliosacral screw osteosynthesis: state of the art. Arch Orthop Trauma Surg 2025; 145:122.
16. Zhou W, Chen J, Pei X, et al. Incidence of and risk factors for screw loosening after iliosacral screw fixation for posterior pelvic ring injury. Orthop Surg 2023;15:1814-22.
17. Muller F, Fuchtmeier B. A systematic review of the transiliac internal fixator (TIFI) for posterior pelvic injuries. SICOT J 2021;7:40.
18. Pishnamaz M, Dienstknecht T, Hoppe B, et al. Assessment of pelvic injuries treated with ilio-sacral screws: injury severity and accuracy of screw positioning. Int Orthop 2016;40:1495-501.
19. Avilucea FR, Whiting PS, Mir H. Posterior fixation of APC-2 pelvic ring injuries decreases rates of anterior plate failure and malunion. J Bone Joint Surg Am 2016;98:944-51.
20. Alzobi OZ, Alborno Y, Toubasi A, et al. Complications of conventional percutaneous sacroiliac screw fixation of traumatic pelvic ring injuries: a systematic review and meta-analysis. Eur J Orthop Surg Traumatol 2023;33:3107-17.
21. Grewal IS, Starr AJ. What's new in percutaneous pelvis fracture surgery. Orthop Clin North Am 2020;51:317-24.
22. Shen L, Xue X, Ping Y, et al. Evolution of the reduction technique for unstable pelvic ring fractures: a narrative review. Eur J Med Res 2025;30:335.
23. Jordan MC, Fuchs KF, Herath SC, Windolf J, Meffert RH, Neubert A. Do we need another screw? Sacroiliac screw fixation in open-book pelvic ring injuries (APC type II). EFORT Open Rev 2024;9:827-36.

https://doi.org/10.12671/jmt.2026.00045

JMT Journal of Musculoskeletal Trauma

pISSN 3058-6267 · eISSN 3058-6275
J Musculoskelet Trauma 2026;39(2):83-92
https://doi.org/10.12671/jmt.2026.00031

Combined acetabular and pelvic ring injuries: a reference-frame algorithm for definitive fixation sequencing

Jeong-Hyun Koh, Seungyeob Sakong

Department of Orthopedic Surgery, Ajou University School of Medicine, Suwon, Korea

Combined acetabular and pelvic ring injuries are not simply "two fractures in one patient." Reduction and fixation of one component can alter the alignment and reducibility of the other, rendering operative sequencing a primary decision variable rather than a secondary consideration. These injuries typically result from high-energy trauma, frequently occur in patients with polytrauma, and are further influenced by physiological tolerance and the feasibility of available operative corridors. The existing evidence base remains constrained by retrospective study designs, inconsistent definitions, variable classification systems, and heterogeneous outcome reporting, all of which limit the strength of comparative recommendations. This state-of-the-art review presents a surgeon-facing, algorithmic approach grounded in a reference-frame mindset. We emphasize computed tomography (CT)-based mapping and the use of consistent terminology to characterize acetabular morphology, pelvic ring instability, deformity vectors, suspicion of mechanical coupling, and feasible operative corridors. Mechanically connected acetabular and pelvic ring injuries (MCAPI) are introduced as a working framework for identifying patterns in which reduction or fixation of one injury predictably influences the other. In cases of suspected MCAPI, a posterior ring-based sequence is generally preferred, typically consisting of posterior ring reduction and fixation, definitive acetabular reconstruction, and subsequent anterior ring fixation. We propose an explicit intraoperative "GO/NO-GO" checkpoint (reference acceptable, stable, corridors feasible) to prevent acetabular reconstruction on a moving target. Acetabulum-first strategies may be appropriate only in selected anteroposterior compression-type configurations in which acetabular fixation plausibly restores sacroiliac congruency and posterior stabilization remains technically feasible. We summarize key outcome domains and complication patterns, highlighting hip dislocation as an important risk factor associated with both neurologic deficits and overall complications. Standardized CT-based definitions and outcome instruments, together with multicenter cohorts employing predefined decision pathways, are required to test sequencing strategies and to determine whether improved radiographic reduction translates into durable functional benefit.

Keywords: Acetabulum; Pelvic bones; Bone fractures; Internal fracture fixation; Multiple trauma

Introduction

Combined acetabular and pelvic ring injuries represent a distinct and challenging subset of pelvic trauma. Unlike isolated acetabular or pelvic ring fractures, these combined patterns often occur after high-energy mechanisms and are frequently

Review Article

Received: January 8, 2026
Revised: January 18, 2026
Accepted: January 25, 2026

Correspondence to:
Seungyeob Sakong
Department of Orthopedic Surgery, Ajou University School of Medicine, 164 Worldcup-ro, Yeongtong-gu, Suwon 16499, Korea
Tel: +82-31-219-5220
Email: sgsy4040@gmail.com

accompanied by substantial associated injuries, creating a narrow therapeutic window in which surgeons must balance physiological priorities with the technical demands of achieving stable pelvic alignment and accurate articular reconstruction [1,2]. Early reports and subsequent series have consistently emphasized that these injuries behave differently from "two independent fractures," because the reduction and fixation of one component may influence the alignment and reducibility of the other [3,4].

Despite their clinical importance, the evidence remains fragmented. Definitions of what constitutes a "true" combined injury vary across studies, classification usage is inconsistent, and outcome reporting is heterogeneous—factors repeatedly highlighted in systematic reviews [5,6]. In addition, the spectrum of pelvic ring instability and acetabular fracture morphology is broad, and shared terminology is essential for translating published experiences into reproducible surgical decision-making [7-9]. Consequently, surgical strategies, particularly the optimal sequence of fixation and approach planning, continue to show substantial variations across centers [10,11].

To address this gap, we adopted the concept of mechanically connected acetabular and pelvic ring injuries (MCAPI) as a practical working framework rather than a rigid taxonomy. MCAPI highlights combined patterns in which the acetabulum and pelvic ring function as a mechanically coupled system, such that the fixation order and reduction strategy are decisive for achieving a stable reference frame and a congruent hip joint [2,12]. Building on contemporary state-of-the-art perspectives and representative clinical series, we synthesized the decision points most relevant to pelvic and acetabular surgeons, including pattern recognition, fixation sequencing, approach and positioning considerations, and staging and timing modifiers, and translated them into an actionable algorithm (Fig. 1) [13-15]. The key studies underpinning this framework are summarized in Table 1 [1,2,4-6,10,12,13,16,17].

To populate Table 1, we used a pragmatic evidence-selection approach aligned with the goals of a surgeon-facing narrative review. We identified relevant publications through targeted database searching and reference-list screening of major reviews and clinical series, then prioritized studies that (1) explicitly addressed combined acetabular-pelvic ring injuries, (2) provided decision-relevant information on sequencing, reference-frame stability, or corridor feasibility, and (3) reported reproducible clinical or radiographic outcomes and complication signals. The final set of 'key studies' was selected by author consensus to represent the spectrum of definitions and sequencing strategies and to foreground decision-relevant signals, rather than to provide an exhaustive systematic synthesis.

This surgeon-facing narrative review aimed to provide a standardized decision-making framework to address the current ambiguity surrounding surgical sequencing. To achieve this, our objective was threefold: (1) to standardize key terminology and classification language for combined injuries, (2) to provide a practical MCAPI-based approach to operative sequencing with clearly stated "generally favored" principles and selected exceptions, and (3) to summarize outcome expectations and complication risk signals that can inform preoperative counseling and intraoperative strategy [16,17].

Scope, terminology, and classification

Combined acetabular and pelvic ring injuries involve multiple threats, including high injury severity, frequently associated visceral and vascular injuries, and competing priorities between restoring pelvic stability and articular congruity [1,4]. Definitive management is often a sequential problem, in which the order of reduction and fixation determines whether the acetabulum is reconstructed on a stable reference frame [12]. Definitions vary because fracture lines near the pubic root and anterior column can be interpreted differently across centers. High pubic root or ramus injuries may be mislabeled as low anterior column fractures, whereas some acetabular fractures extend toward the sacroiliac (SI) region without meaningfully destabilizing the ring [5]. In this review, we included injuries with a true acetabular articular component and pelvic ring disruption, where at least one component was potentially operative, and the interaction could influence the reduction strategy or fixation sequence.

Computed tomography (CT)-based mapping is essential, and a practical "common language" is to describe acetabular morphology using Judet-Letournel patterns and pelvic ring instability using AO/OTA (Arbeitsgemeinschaft für Osteosynthesefragen/Orthopedic Trauma Association) descriptors, with Young-Burgess anteroposterior compression (APC) and lateral compression (LC) concepts as

https://doi.org/10.12671/jmt.2026.00031

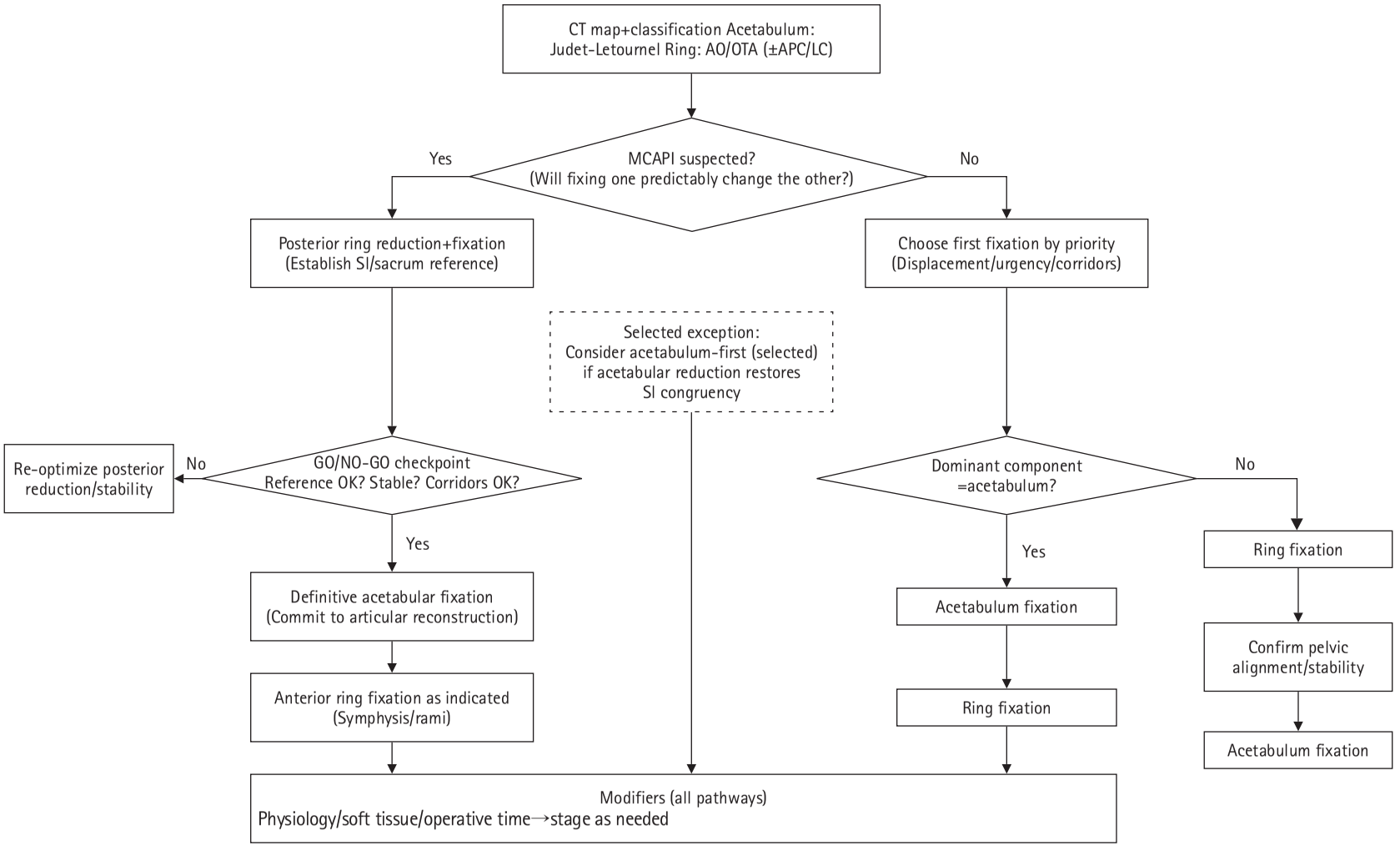

Fig. 1. Reference-frame algorithm for definitive fixation sequencing in combined pelvic ring and acetabular injuries. Following computed tomography (CT)-based morphological mapping (Judet-Letournel for the acetabulum; AO/OTA ± APC/LC for the pelvic ring), the surgical sequence is guided by the presence or absence of mechanical coupling (MCAPI). In suspected MCAPI patterns, posterior ring stabilization is performed to establish a stable sacroiliac and sacral reference, after which a critical GO/NO-GO checkpoint is applied to confirm reference stability and operative corridor feasibility before proceeding with definitive articular reconstruction. In non-MCAPI patterns, the initial fixation target is selected based on the degree of displacement, clinical urgency, and corridor feasibility. Regardless of the chosen sequence, pelvic alignment and overall stability must be reconfirmed before committing to final joint surface reconstruction. Staged surgery may be required in some cases because of physiological status or soft-tissue considerations. CT, computed tomography; AO/OTA, Arbeitsgemeinschaft für Osteosynthesefragen/Orthopedic Trauma Association; APC/LC, anteroposterior compression/lateral compression; MCAPI, mechanically connected acetabular and pelvic ring injuries; SI, sacroiliac.

https://doi.org/10.12671/jmt.2026.00031

Table 1. Core evidence matrix for combined acetabular-pelvic ring injuries (10 key studies)

Study (yr)	Design	No./scope	Definition/inclusion (as used)	Classification	Sequencing/strategy (key message)	Outcome highlights	Complications/ risk signals
Halvorson et al. 2014 [4]	Narrative review	Evidence synthesis	Combined acetabular fracture with pelvic ring injury; definitions vary across series	Judet-Letournel ring described with OTA/Young-Burgess concepts	Integrated planning based on mechanical interaction identifies scenarios where acetabular fixation facilitates SI joint reduction	Higher injury burden (ISS) and morbidity than isolated fracture patterns	Emphasizes multidisciplinary care and physiological optimization to manage systemic morbidity
Veerappa et al. 2020 [6]	Systematic review (PRISMA)	8 Retrospective series (≥20 cases)	Combined pelvic and acetabular injuries (heterogeneous definitions)	Lack of standardized terminology	Consensus-based sequencing: reinforces "ring first" standard (posterior → acetabulum → anterior) based on pooled series	Reported incidence: 5%–16% of pelvic/acetabular injuries; transverse and both-column patterns are most frequent	Confirms that heterogeneous definitions and a lack of standardized terminology limit strong comparative conclusions
Ross et al. 2023 [5]	Systematic review (PRISMA)	11 Series (985 patients)	Combined pelvic ring + acetabular fractures (ipsilateral/contralateral included)	Lack of standardized terminology	Sequencing remains debated; unstable rings are often managed with ring first logic; acetabular reduction quality is emphasized	Across studies: mean ISS ~23; pooled mortality ~8%; functional metrics inconsistently reported	Calls for standardized definitions, radiographic metrics, and PROMs
Puchwein et al. 2024 [2]	State-of-the-art review	Algorithmic framework	Emphasizes mechanically connected patterns (MCAPI) vs. less connected combinations	Judet-Letournel (acetabulum) + AO/OTA (ring); APC/LC as adjunct	For MCAPI: pelvic ring first (sacrum/SI joint) is generally favored; acetabulum-first is reserved for selected cases with stable posterior rings	Definitive fixation within an early window (~3 to 7 days) is ideal, subject to physiologic and soft-tissue status	Temporary stabilization pitfalls: inadequate initial stability can compromise definitive reduction; emphasize planning for complex coupling
Suzuki et al. 2010 [12]	Retrospective cohort (Level I)	82 Combined (68 operative)	Unstable pelvic injury plus displaced acetabular fracture treated at a Level I center	OTA/Young-Burgess (ring); OTA acetabulum descriptors	Reference-frame principle: prioritizes posterior ring reduction to establish a stable foundation before articular fixation	Mean time to surgery: 5.7 days; Mean postoperative acetabular displacement: 2.2 mm	Residual posterior pelvic displacement is a significant predictor of poor acetabular reduction quality
Osgood et al. 2013 [1]	Retrospective pattern study	40 Combined (institutional database)	Combined pelvic ring disruption + acetabular fracture identified from institutional registry	Young-Burgess (ring); Letournel (acetabulum)	Morphological mapping: defines common injury combinations, providing a basis for initial planning and corridor assessment	Distribution: APC (53%), LC (45%), VS (3%); Posterior wall fractures are significantly less common (~5%) than in isolated cohorts	High systemic injury burden: mortality rate of ~13%, characterized by high ISS and frequent associated injuries
Cai et al. 2017 [10]	Retrospective case series	21 Operative	Unstable pelvic fractures with concomitant acetabular fractures are managed operatively	Tile (pelvis) & Letournel (acetabulum) approach- and fixation-based reporting; Matta and functional scores used	Individualized planning: focuses on patient-specific surgical approach and corridor selection when a standardized sequence is not applicable	Functional success: Majeed excellent/good in 85.7% (18/21) at final follow-up	Reports specific complications, including heterotopic ossification, femoral head necrosis, and iatrogenic neurovascular injury
Li et al. 2023 [17]	Retrospective case series	24 Tile B/C	Unstable pelvic fractures combined with acetabular fractures (single center)	Tile (ring); Judet-Letournel (acetabulum)	Posterior-first preference: emphasizes stabilizing posterior ring alignment to provide a reliable template for complex acetabular reconstruction	High functional success: Majeed excellent/good (87.5%) and Merle d'Aubigne excellent/good (83.3%) at final follow-up	Reinforces that anatomic restoration through morphology-based sequencing yields favorable long-term functional results

(Continued on the next page)

https://doi.org/10.12671/jmt.2026.00031

Table 1. Continued

Study (yr)	Design	No./scope	Definition/inclusion (as used)	Classification	Sequencing/strategy (key message)	Outcome highlights	Complications/ risk signals
Cunningham et al. 2023 [16]	Retrospective risk-factor study	70 (≥1-yr follow-up)	Operatively treated combined ring + acetabulum injuries (single Level I center)	Not classification-driven; focuses on predictors of complications	Percutaneous acetabular methods are associated with fewer complications than open approaches	Overall complication rate: 44%; Hip dislocation incidence: 40%	Hip dislocation is a major predictor of all-cause complications and residual neurologic deficits; angio/embolization is not linked to deep infection
Fratus et al. 2025 [13]	Retrospective comparative cohort	45 (posterior-first vs. others)	Adults requiring operative management; excluded are stable ring/nonoperative acetabulum/nondisplaced percutaneous acetabulum	Postoperative CT step-off and gapping endpoints	Posterior-first preference: validates that addressing the posterior ring first leads to superior anatomic reduction of the acetabulum on CT	CT-based endpoints: anatomic step-off (68.2% vs. 30.4%) and gapping (27.3% vs. 4.4%) significantly favor the posterior-first approach	Reinforces reduction quality but notes that correlation with long-term PROMs remains uncertain

Definitions and outcomes vary across studies; this table summarizes dominant decision points and sequencing signals rather than prescribing a single universal protocol.

OTA, Orthopedic Trauma Association; ISS, injury severity score; PRISMA, Preferred Reporting Items for Systematic Reviews and Meta-analyses; PROM, patient-reported outcome measure; MCAPI, mechanically connected acetabular and pelvic ring injuries (working framework); AO/OTA, Arbeitsgemeinschaft für Osteosynthesefragen/Orthopedic Trauma Association; APC/LC/VS, anteroposterior compression/lateral compression/vertical shear (Young-Burgess); SI joint, sacroiliac joint; CT, computed tomography;

deformity-oriented adjuncts when needed [7-9]. Imaging deliverables should address three operative questions: mechanical linkage (suspected MCAPI), dominant deformity and reduction targets, and corridor feasibility in the context of soft tissues and physiology [2]. Although combined patterns represent a small proportion of acetabular and pelvic ring fractures, they carry disproportionate resource utilization and complication risks; the mechanisms are typically high-energy, and polytrauma physiology frequently necessitates staged definitive fixation [1,2,5,18].

Most evidence consists of retrospective series with heterogeneous inclusion criteria and variable outcome instruments, and systematic reviews have concluded that these limitations preclude strong comparative recommendations on timing, sequencing, or surgical approach [5,6,19]. Nevertheless, an algorithmic approach can add value by standardizing key decision points (mechanical linkage, reference frame selection, and sequence checkpoints) and aligning terminology across studies (Table 1) [2,11].

Working framework: MCAPI vs. non-MCAPI

MCAPI refers to combined injuries in which the reduction or fixation of one component predictably affects the other, whereas non-MCAPI refers to injuries that behave more independently [2]. This distinction is important because it promotes a reference-frame mindset: the first fixation step should be selected to make subsequent acetabular reduction reliable and reproducible [4,12].

For practical application, MCAPI can be suspected using a concise checklist: (1) an ipsilateral unstable pelvic ring likely requiring fixation (commonly AO/OTA B2–B3 or C-type), (2) acetabular morphology with a transverse or anterior-column–linked component (including T-type or both-column variants), (3) CT features suggesting coupled displacement such that hemipelvic reduction is expected to change acetabular alignment, and (4) anticipated interdependence in corridor feasibility or positioning where the first fixation step predictably alters reducibility or deliverability of the other component. As a high-risk coupling signal, hip dislocation or central instability—particularly with transverse-oriented morphology—should heighten suspicion and may justify earlier stability decisions to protect neurologic risk and optimize final congruity [2,12,16]. In contrast, non-MCAPI is more likely when the acetabular injury involves an isolated wall or column pattern, or when the injuries are contralateral without a plausible mechanical linkage [2,11]. In these settings, the fixation sequence is determined by displacement, urgency, and corridor feasi-

bility; regardless of the order, pelvic stability should be reverified before committing to final articular reconstruction.

Clinically, combined-injury cohorts often show higher injury severity, more frequent associated injuries, and more frequent staging than isolated injuries [1,17]. In particular, hip dislocation has been associated with residual neurologic deficits and overall complications and should be treated as a key risk signal during counseling and operative planning [16]. Finally, MCAPI is most useful because it clarifies which structure must be reduced and stabilized first to establish a reliable reference for acetabular reconstruction; when coupling is likely, posterior ring reduction and stabilization commonly precede definitive acetabular fixation, with explicit checkpoints before articular reconstruction (Fig. 1) [2,3,12].

Epidemiology, injury patterns, and assessment pearls for definitive planning

Combined cohorts tend to present with greater injury severity, multisystem trauma, and a higher likelihood of staged definitive fixation than isolated injuries [1,17]. These contextual factors often drive timing, positioning tolerance, and corridor selection as much as fracture morphology itself [18].

A mechanism-informed language is useful because it predicts deformity vectors. APC patterns suggest external rotation and anterior instability that can alter acetabular relationships, whereas LC patterns suggest internal rotation and impaction tendencies that may influence reduction strategy and corridor selection [4,7]. In practice, several "red flags" commonly modify definitive strategy, including hip dislocation, major posterior ring displacement, and soft-tissue or visceral constraints that limit early corridors; early identification of these factors helps anticipate sequence, staging, and operative time requirements [1,10,12].

CT should provide a reproducible and shared map for the team, including ring deformity and instability, acetabular articular displacement, evidence of coupling, and feasible corridors in the context of soft-tissue and physiology [2,4]. Two practical pearls repeatedly influence definitive planning. First, definitive acetabular fixation should be avoided until the pelvic reference frame is acceptable and stable; otherwise, the acetabulum is reconstructed on a moving target [3,12]. Second, deciding early whether a case is likely to represent MCAPI helps avoid unplanned repositioning and prolonged operative time [2].

Decision points and operative planning

The primary goal in combined acetabular and pelvic ring injuries is to create a reliable hemipelvic reference frame for acetabular reduction by addressing instability that can shift acetabular alignment. Therefore, the fixation sequence is often more important than approach selection, particularly when the two injuries interact mechanically [2,4]. Before committing to definitive acetabular fixation, preoperative planning should explicitly state what provides the reference frame and what constitutes an acceptable checkpoint for proceeding with definitive acetabular reconstruction [12].

MCAPI triage can be performed preoperatively using CT and pattern recognition. An ipsilateral unstable ring combined with transverse- or anterior-column-linked acetabular morphology, along with CT features suggesting coupled displacement, increases the likelihood that reduction or fixation of one component will predictably affect the other [2,17]. The goal is not to force cases into a rigid category, but to use coupling suspicion as a trigger to plan an explicit reference-frame sequence and to anticipate situations in which indirect reduction may fail.

A simple intraoperative checkpoint can improve reproducibility and help avoid reconstruction of the acetabulum on a "moving target." In practice, definitive acetabular fixation should proceed only if the GO/NO-GO checkpoint is met: (1) reference acceptable (posterior ring reduction acceptable), (2) reference stable (temporary or definitive fixation has converted the hemipelvis into a reliable platform), and (3) corridors feasible (positioning/approach constraints reconciled without compromising reduction priorities) [2,3,12,14].

Staging is common and should be planned deliberately, driven by physiology, soft tissues, and operative time rather than treated as an afterthought [4,18]. Early coordination between pelvic and acetabular teams helps preserve the intended sequence when physiological constraints require staged corridors [2,10]. Approach and positioning should follow the planned sequence: when MCAPI is likely, posterior ring reduction and stabilization often precede acetab-

https://doi.org/10.12671/jmt.2026.00031

ular reconstruction, and corridor choice should minimize repositioning without compromising establishment of the reference frame first [2,3]. Finally, fixation philosophy (percutaneous vs. open) should be framed as a constraint-driven decision point. Percutaneous strategies may reduce soft-tissue insult and operative time in polytrauma but require a stable reference frame, accurate imaging, and clear reduction targets, whereas an open strategy may be necessary to achieve accurate articular reduction in complex coupled patterns [2,10,15,17].

Definitive fixation strategy and sequence

Combined acetabular and pelvic ring injuries are not simply "two fractures in one patient." Operative planning must integrate approach, positioning, and fixation order, because reduction of one component can influence the reduction (or reducibility) of the other. Fig. 1 provides an algorithmic overview of the key decision points and generally favors specific sequencing strategies in this setting [2,4,5].

The term MCAPI has been proposed to distinguish patterns in which reduction or fixation of one injury is expected to affect the other from "coexisting but noninteracting" combinations (non-MCAPI) [2]. CT-based characterization is typically required to define fracture morphology and associated injuries, and the use of a unified classification language (such as Judet-Letournel for the acetabulum and AO/OTA for the pelvic ring) supports consistent decision-making across patterns [5,8,9].

From a practical standpoint, MCAPI should be suspected in ipsilateral acetabular patterns with an anterior column or transverse component (including T-type and both-column variants) combined with an unstable pelvic ring injury (commonly AO/OTA B2–B3 or C patterns), in which indirect posterior reduction through anterior-only maneuvers may be unreliable because of an "interrupting fracture" [2,12]. In these mechanically coupled patterns, definitive treatment is best framed as a reference frame problem, and the fixation sequence should be chosen to establish a stable hemipelvic platform before committing to definitive acetabular reconstruction.

For definitive treatment of MCAPI, a posterior ring-based sequence is generally favored in contemporary series and strategy articles [2,12]. The rationale is that incomplete posterior ring reduction may compromise acetabular reduction, particularly in transverse-oriented acetabular patterns [4,12].

Accordingly, a commonly adopted sequence is (1) reduction and fixation of the displaced posterior ring, (2) definitive acetabular fixation, and (3) fixation of the anterior ring (such as symphysis or rami), as indicated [2,4]. Clinical observations support this linkage, which reports of worse acetabular reduction quality in the presence of residual posterior displacement or SI separation [12,17]. Therefore, an intraoperative checkpoint is reasonable: if meaningful residual posterior malreduction persists (especially in transverse-oriented acetabular fractures), re-optimization of the posterior reduction should precede definitive acetabular fixation [2,12].

An MCAPI-centered approach should also acknowledge pattern-driven exceptions. An acetabulum-first sequence may be considered in selected configurations, most notably transverse acetabular fractures combined with an AO/OTA B2.3 (APC2) pelvic ring injury, in which acetabular fixation may nearly restore SI congruency and allow percutaneous fixation or case-dependent nonoperative management of the posterior ring [2]. An acetabulum-first strategy may also be discussed when percutaneous acetabular fixation is appropriate and can be performed efficiently before pelvic ring fixation; however, these scenarios should be regarded as selected exceptions rather than routine alternatives [2,5,6].

Sequence decisions are inseparable from approach, positioning, and staging. Planning should minimize unnecessary repositioning while accepting staged corridors when required by fracture morphology and patient physiology [2,10]. When posterior acetabular components, such as a posterior wall fracture, are present, posterior approaches (such as Kocher-Langenbeck) are commonly required for reliable fixation [8,9]. Given that pelvic ring disruptions may be immediately life-threatening and physiological tolerance can limit operative duration, staged fixation is frequently necessary. Stabilizing the pelvic ring first and staging acetabular reconstruction is reasonable when blood loss, operative time, or cardiopulmonary status preclude a single-stage procedure [5,12]. Definitive fixation should proceed once physiological optimization is achieved and soft-tissue conditions permit. In published series, surgery commonly occurs within an early window (approximately

3–7 days), although substantial variation exists, and timing should be individualized based on concomitant injuries, competing priorities, and operative logistics [2,5].

Outcomes, complications, and postoperative considerations

Outcomes of combined acetabular and pelvic ring injuries are best interpreted across three domains: acetabular articular congruity, pelvic alignment and stability, and patient-centered function. However, heterogeneous definitions and outcome instruments continue to limit cross-study comparisons and preclude firm conclusions regarding an optimal strategy [5,6,19].

Complication burdens are substantial across reported series, although exact rates vary with inclusion criteria and injury severity. Hip dislocation is a particularly important risk factor associated with residual neurologic deficits and overall complications, and should be highlighted during preoperative counseling and planning [16]. Recent studies further examine predictors of complications and support practical risk stratification, physiological staging, and sequence discipline rather than maximal reconstruction in a single setting when physiological tolerance is limited [13].

Postoperative care should remain principle-based and focus on protection of the reconstruction until pelvic stability and hip congruity are secure; surveillance for thromboembolism, infection, and heterotopic ossification according to institutional protocols; and tailoring weight-bearing progression to construct stability, fixation quality, and associated injuries [2,4]. Follow-up imaging should be consistent, with a low threshold for CT when symptoms or radiographs suggest loss of reduction or when articular congruity is uncertain.

Discussion: pitfalls, controversies, and future directions

Although combined acetabular and pelvic ring injuries are increasingly recognized as a meaningful subset of pelvic trauma, the evidence base remains constrained by retrospective study designs, inconsistent definitions, variable classifications, and heterogeneous outcome reporting. Systematic reviews consistently highlight these limitations and caution against overgeneralizing "best" strategies from small case series [5,6,19]. Accordingly, the most defensible contribution of a modern review is not to prescribe a single universal protocol, but to clarify decision points and identify principles that are repeatedly supported across contemporary experiences [2,4].

The MCAPI concept is attractive because it translates a complex fracture spectrum into a clinically actionable question: are the acetabulum and pelvic ring mechanically coupled such that reduction of one will change the other? As a working framework, MCAPI helps surgeons prioritize reference frames and sequencing decisions, particularly in transverse-oriented acetabular patterns with unstable posterior ring injury [2,12,15]. However, MCAPI should not be treated as a definitive classification system. Its boundaries are still evolving, and real-world cases exist along a continuum from "more connected" versus "less connected," with patient physiology and corridor feasibility frequently overriding purely morphologic considerations [13,14].

The most debated practical question is fixation order. Earlier experience and mechanistic reasoning support a posterior ring-based sequence in mechanically connected patterns, emphasizing that residual posterior malreduction can compromise acetabular reduction quality [2,4,12,13]. More recent cohort studies continue to evaluate whether posterior-first sequencing improves postoperative acetabular reduction metrics and whether such improvements translate into meaningful functional benefits [13]. The selected exceptions remain clinically plausible. In specific configurations, classically described for transverse acetabular fractures with an APC-type ring pattern, acetabular fixation may nearly restore SI congruency, and an acetabulum-first pathway may be reasonable if a stable reference can be reliably achieved and posterior fixation can be performed percutaneously or in a staged fashion [2,6]. A defensible stance is therefore to frame posterior-first sequencing as "generally favored" in MCAPI, while explicitly acknowledging exceptions and emphasizing intraoperative checkpoints rather than rigid rules.

A second practical controversy concerns whether definitive reconstruction should be completed in a single setting or intentionally staged. Combined injuries frequently occur in physiologically stressed patients with multisystem trauma, and unplanned prolonged surgery can amplify risk, even when the technical plan is sound [4,18]. Staging should not be seen as a failure of planning, but rather as

https://doi.org/10.12671/jmt.2026.00031

a deliberate strategy to secure the reduction reference, limit operative burden, and return for definitive articular reconstruction when conditions permit [2,6]. Similarly, the choice between open and percutaneous strategies is rarely a matter of pure technical preference, as it is often dictated by displacement, comminution, and the need for direct articular reduction. Reported complication burdens reinforce the importance of minimizing soft-tissue morbidity when percutaneous methods can achieve stable alignment without sacrificing articular goals, while recognizing that selection bias remains unavoidable in retrospective evidence [5,15,16].

Progress in this field depends on three practical steps. First, a consistent CT-based definition of "combined injury," distinguishing true articular acetabular involvement from high pubic root variants, would reduce heterogeneity across reports [2,5]. Second, standardized outcome reporting should include articular metrics (step-off and gapping), pelvic alignment, and patient-reported outcomes with minimum follow-up thresholds to enable meaningful comparison of sequencing and staging strategies [13,19]. Third, multicenter registries or prospective cohorts with predefined decision pathways could clarify whether posterior-first sequencing confers functional advantages beyond improved radiographic reduction in selected MCAPI patterns [14,15].

Summary and key messages

Combined acetabular and pelvic ring injuries represent a distinct subset of pelvic trauma in which reduction or fixation of one component may influence the other, making operative sequencing a primary decision variable rather than an afterthought [2,4]. The MCAPI concept is useful as a working framework to identify mechanically coupled patterns and guide reduction priorities and sequencing; however, it should be applied with "generally favored" principles with explicit exceptions rather than rigid rules [2,15]. Future studies should focus on correlating these sequencing algorithms with long-term patient-reported outcome measures through prospective multicenter registries.

Key messages

- Use CT-based mapping and consistent classification languages for both injuries [2,8,9].
- Suspect MCAPI when an ipsilateral unstable pelvic ring coexists with transverse- or anterior-column-linked acetabular morphology and coupled displacement features; in these cases, establish an acceptable and stable posterior ring reference before definitive acetabular fixation [2,3,12].
- Use a simple intraoperative GO/NO-GO checkpoint (reference acceptable, stable, corridors feasible) to avoid reconstructing the acetabulum on a moving target [2,14].
- Consider an acetabulum-first strategy only in selected APC-type configurations in which acetabular fixation plausibly restores SI congruency and posterior stabilization remains feasible [2].
- Counsel patients regarding substantial complication risks; hip dislocation is a key risk signal and may indicate a higher risk of neurologic deficits and overall complications [13,16].
- The evidence base remains heterogeneous; standardized definitions and outcome measures are required to test sequencing strategies in comparable cohorts [5,6].

Article Information

Author contributions

Conceptualization: JHK, SS. Methodology: JHK, SS. Investigation: JHK. Resources: JHK. Data curation: JHK. Supervision: SS. Project administration: SS. Visualization: JHK. Writing–original draft: JHK. Writing–review & editing: JHK. SS. All authors read and approved the final manuscript.

Conflicts of interest

No potential conflict of interest relevant to this article was reported.

Funding

None.

Data availability

Not applicable.

Acknowledgments

None.

Supplementary materials

None.

References

1. Osgood GM, Manson TT, O'Toole RV, Turen CH. Combined pelvic ring disruption and acetabular fracture: associated injury patterns in 40 patients. J Orthop Trauma 2013;27:243-7.
2. Puchwein P, Sandersjoo G, Lindahl J, Eibinger N. Combined pelvic ring and acetabular fractures: strategies and sequence of surgery. State of the art. Arch Orthop Trauma Surg 2024;144:4577-86.
3. Gänsslen A, Pohlemann T, Paul C, Lobenhoffer P, Tscherne H. Epidemiology of pelvic ring injuries. Injury 1996;27 Suppl 1:S-A13-20.
4. Halvorson JJ, Lamothe J, Martin CR, et al. Combined acetabulum and pelvic ring injuries. J Am Acad Orthop Surg 2014;22:304-14.
5. Ross H, Stine S, Blue K, Wolterink TD, Vaidya R. Systematic review of combined pelvic ring and acetabular injuries: what do we know from the literature? Cureus 2023;15:e41843.
6. Veerappa LA, Tippannavar A, Goyal T, Purudappa PP. A systematic review of combined pelvic and acetabular injuries. J Clin Orthop Trauma 2020;11:983-8.
7. Burgess AR, Eastridge BJ, Young JW, et al. Pelvic ring disruptions: effective classification system and treatment protocols. J Trauma 1990;30:848-56.
8. Judet R, Judet J, Letournel E. Fractures of the acetabulum: classification and surgical approaches for open reduction. Preliminary report. J Bone Joint Surg Am 1964;46:1615-46.
9. Letournel E. Acetabulum fractures: classification and management. Clin Orthop Relat Res 1980;81-106.
10. Cai L, Lou Y, Guo X, Wang J. Surgical treatment of unstable pelvic fractures with concomitant acetabular fractures. Int Orthop 2017;41:1803-11.
11. Porter SE, Schroeder AC, Dzugan SS, Graves ML, Zhang L, Russell GV. Acetabular fracture patterns and their associated injuries. J Orthop Trauma 2008;22:165-70.
12. Suzuki T, Smith WR, Hak DJ, et al. Combined injuries of the pelvis and acetabulum: nature of a devastating dyad. J Orthop Trauma 2010;24:303-8.
13. Fratus A, Nirunsuk P, Tucker NJ, Parry JA, Mauffrey C. Combined pelvic and acetabular injuries: Decision making and clinical results. Injury 2025;56:112364.
14. Gansslen A, Lindahl J, Krappinger D, Lindtner RA, Staresinic M. Outcome of pelvic ring injuries. Arch Orthop Trauma Surg 2024;145:47.
15. Mauffrey C, Bellas N, David G, Le Baron M. Understanding acetabular fractures: a comprehensive review. J Am Acad Orthop Surg 2025 Dec 22 [Epub]. https://doi.org/10.5435/JAAOS-D-25-00741.
16. Cunningham B, Pearson J, McGwin G, et al. What are the risk factors for complications after combined injury of the pelvic ring and acetabulum? Eur J Orthop Surg Traumatol 2023;33:341-6.
17. Li R, Zhao P, Guan J, Wang X, Liu L, Wu M. Combined pelvic, acetabular injuries: clinical features and treatment strategies of a unique injury pattern. J Orthop Surg Res 2023;18:415.
18. Marchand LS, Sepehri A, Hannan ZD, et al. Pelvic ring injury mortality: are we getting better? J Orthop Trauma 2022;36:81-6.
19. Cuthbert R, Walters S, Ferguson D, et al. Epidemiology of pelvic and acetabular fractures across 12-mo at a level-1 trauma centre. World J Orthop 2022;13:744-52.

https://doi.org/10.12671/jmt.2026.00031

JMT Journal of Musculoskeletal Trauma

pISSN 3058-6267 · eISSN 3058-6275
J Musculoskelet Trauma 2026;39(2):93-102
https://doi.org/10.12671/jmt.2026.00024

Nonoperative management of distal radius fractures: when and how?

Shin Woo Choi[1], Jae Kwang Kim[2]

[1]Department of Orthopedic Surgery, Gangneung Asan Hospital, University of Ulsan College of Medicine, Gangneung, Korea
[2]Department of Orthopedic Surgery, Asan Medical Center, University of Ulsan College of Medicine, Seoul, Korea

Distal radius fractures are among the most common injuries of the upper extremity, particularly in the elderly population. Although the use of volar locking plate fixation has increased in recent years, evidence from randomized and prospective studies demonstrates that, while operative treatment may achieve superior radiographic alignment and enable more rapid early recovery, these advantages tend to diminish over time and do not result in superior long-term patient-reported functional outcomes in elderly patients. In addition, radiographic parameters show only a limited correlation with functional recovery. Consequently, nonoperative treatment remains a valid and important treatment option for distal radius fractures. The decision to pursue nonoperative management should be based on a comprehensive assessment of radiographic parameters—including dorsal tilt, radial shortening, and intraarticular displacement—together with patient-specific factors such as age, activity level, comorbidities, and functional expectations. For stable or minimally displaced fractures, an immobilization period of 3–4 weeks is generally recommended, whereas displaced fractures typically require immobilization for 5–6 weeks. In cases requiring manual reduction, traditional treatment protocols recommend weekly radiographic follow-up during the first 2–3 weeks to monitor for secondary displacement. Successful nonoperative management should also emphasize effective swelling control through limb elevation, as well as the initiation of early finger exercises to prevent hand stiffness. After removal of the cast or splint, active wrist mobilization is essential for restoring optimal range of motion and achieving functional recovery.

Keywords: Wrist fractures; Conservative treatment; Surgical cast; Recovery of function; Treatment outcome

Review Article

Received: January 6, 2026
Revised: January 28, 2026
Accepted: January 29, 2026

Correspondence to:
Jae Kwang Kim
Department of Orthopedic Surgery, Asan Medical Center, University of Ulsan College of Medicine, 88 Olympic-ro 43-gil, Songpa-gu, Seoul 05505, Korea
Tel: +82-2-3010-3523
Email: orth4535@gmail.com

Introduction

Distal radius fractures are the most common fractures occurring in the elderly and are known to account for approximately 18% of all fractures in patients over 65 years of age [1]. As an initial treatment strategy, stable and nondisplaced fractures are immobilized immediately with a splint without attempting reduction, whereas in fractures with marked displacement—such as pronounced angular deformity or radial shortening—manual reduction is performed to decrease swelling and pain prior to splint application. Subsequently, decisions regarding operative versus nonoperative management are made by considering radiographic stability and morphology of the fracture, the patient's age, activity level, underlying comorbidities, and the functional

level the patient desires to achieve after recovery. This decision-making process is often challenging.

Operative treatments for distal radius fractures have included closed reduction and percutaneous pinning or external fixation. Over the past several decades, with the development and advancement of locking plates, the frequency of open reduction and internal fixation has increased. In particular, the introduction of anatomically contoured volar locking plates has made it easier to improve and maintain anatomical alignment without displacement even in distal radius fractures where metaphyseal bone quality is poor [2]. However, percutaneous pinning and external fixation have been associated with weak fixation strength, difficulty in obtaining and maintaining articular reduction, and the risk of joint or fracture-site infection due to externally exposed hardware. Volar locking plate fixation also carries a significant complication profile, ranging from mild issues such as flexor tendon irritation and median nerve symptoms to serious complications such as surgical site infection, flexor tendon rupture, and carpal tunnel syndrome; complication rates as high as 16.5% have been reported [3].

Given that such complications remain a concern, that a considerable proportion of distal radius fractures are stable, and that in elderly patients even unstable fractures do not always show a direct correlation between the accuracy of anatomic reduction and functional outcome [4], nonoperative treatment continues to represent an important treatment principle. Accordingly, the authors review established knowledge and current perspectives regarding the nonoperative management of distal radius fractures.

Aims and scope

The aim of this narrative review is to synthesize contemporary evidence on the nonoperative management of distal radius fractures and to provide practical, stepwise guidance for fracture reduction, immobilization, follow-up imaging, and rehabilitation. Rather than advocating uniform radiographic thresholds across all patients, we present an evidence-informed decision-making framework stratified by patient age, comorbidity burden, and functional demand. Particular emphasis is placed on older, lower-demand patients, in whom long-term patient-reported outcomes after operative and nonoperative treatment may converge despite differences in radiographic alignment.

Ethics statement

Written informed consent was obtained from the patients for publication of their images in this review.

Literature search strategy

This narrative review was informed by a targeted search of PubMed/Medline from inception through December 2025 (last searched December 2025). Search terms were combined using Boolean operators and truncation and included distal radius fracture, nonoperative treatment, casting, splinting, immobilization, and volar locking plate. An example query was ("distal radius fracture" OR "wrist fracture") AND (cast OR splint OR immobilization) AND (nonoperative OR conservative). We prioritized randomized clinical trials, systematic reviews and meta-analyses, and clinical practice guidelines; reference lists of key articles were also screened. We focused on adults with displaced or potentially unstable distal radius fractures. Because this is a narrative review, study selection was pragmatic rather than exhaustive, and recommendations were anchored to higher-level evidence when available.

Clinical considerations in nonoperative treatment

Indications for nonoperative treatment

The general goal of fracture treatment is to achieve bony union in the original anatomical position or in a position close to it, thereby preventing sequelae associated with the fracture. Distal radius fractures mainly involve the metaphyseal region, where abundant soft tissue and vascular supply allow relatively reliable bone healing compared with other anatomical areas. Thus, the role of nonoperative treatment is to maintain the anatomical or near-anatomical alignment during the healing process to prevent long-term complications. Common sequelae associated with distal radius fractures include posttraumatic arthritis, decreased wrist range of motion, ulnar-sided wrist pain, and decreased grip strength. Therefore, clinicians must evaluate the condition of the distal radius fracture at the time of injury to determine whether nonoperative treatment is appropriate, identify radiographic parameters or criteria associated with the development of sequelae, and determine whether nonoperative treatment can be continued

https://doi.org/10.12671/jmt.2026.00024

if displacement occurs during the course of conservative management.

Radiographic parameters for assessing anatomical displacement

Radial shortening and positive ulnar variance caused by metaphyseal impaction of the distal radius increase tension on the triangular fibrocartilage complex and load on the distal radioulnar joint (DRUJ), potentially leading to articular surface damage, pain, and restricted forearm rotation. Specifically, compared with normal anatomy, a radial shortening of 2.5 mm increases the load on the distal ulna by approximately 18%–42% [5], and a shortening of 10 mm may result in a loss of 47% of pronation and 29% of supination [6].

Improper reduction of intraarticular fractures is a representative cause of posttraumatic arthritis and subsequent limitation of joint motion and pain. Even 1–2 mm of intraarticular incongruity is known to induce arthritis and lead to poor outcomes. Knirk and Jupiter [7] reported that >1 mm of intraarticular incongruity resulted in radiographic arthritis in 91% of cases, and that all patients with ≥2 mm of incongruity developed radiographic arthritis.

Abnormal volar or dorsal tilt of the distal radius in the sagittal plane is associated with wrist range of motion, particularly flexion and extension. As dorsal tilt increases, the load-bearing area shifts from the volar-radial side to the dorsal-ulnar side, leading to compensatory flexion at the midcarpal joint. This can result in painful synovitis and a form of dorsal intercalated segment instability [8,9]. Conversely, excessive volar tilt reduces wrist extension and may cause dorsal subluxation of the ulnar head and restricted supination [10].

Changes in radial inclination affect grip strength, radial and ulnar deviation, and load distribution across the wrist. It has been reported that patients with radial inclination less than 5° experience poor outcomes in 100% of cases [11].

Radiographic and clinical indications

To consider nonoperative treatment immediately after injury, criteria that predict the likelihood of subsequent displacement are necessary, and numerous studies have been conducted on this topic. Weber [12] defined unstable fractures as those in which dorsal cortical comminution exceeds 50% of the anteroposterior diameter of the fracture site on the sagittal view. Cooney [13] classified fractures as unstable if initial radiographs demonstrated >25° of dorsal tilt, >10 mm of radial shortening, or bilateral radius fractures. Lafontaine et al. [14] proposed more specific criteria, widely used for assessing instability, including: >20° dorsal tilt, >5 mm radial shortening, >50% dorsal comminution, intraarticular displacement, associated ulnar metaphyseal fracture, shear fracture of the distal radius, DRUJ fracture-dislocation, and early loss of reduction after initial reduction—meeting three or more of these conditions suggests an unstable fracture.

Radiographic criteria for determining whether to proceed with operative treatment after successful reduction have also been extensively studied. With advances in surgical techniques and implants, operative treatment has shown improved outcomes, narrowing the indications for conservative management, especially in younger patients with high functional demands. Radial shortening of >2 mm, DRUJ subluxation, and significant anteroposterior translation of the distal ulna are generally considered unsuitable for conservative treatment. However, acceptable thresholds for intraarticular incongruity (<1 mm vs. <2 mm) and dorsal tilt (allowing up to 10° vs. allowing only neutral alignment) remain controversial (Fig. 1) [15-19]. Randomized controlled trials comparing conservative and operative treatment for displaced distal radius fractures have consistently demonstrated superior radiographic alignment following surgical fixation, particularly with respect to volar tilt and radial inclination at final follow-up [20]. Several studies have also reported modest advantages in early functional recovery and grip strength in surgically treated patients during the initial postoperative period [21,22]. However, long-term follow-up data in elderly populations indicate that these early advantages do not persist over time. Large prospective studies have shown that although volar locking plate fixation may facilitate faster early recovery, it does not confer superior patient-reported outcomes at 12 months when compared with cast immobilization [23,24]. In line with these findings, a comprehensive systematic review and meta-analysis by Gutierrez-Espinoza et al. [25] concluded that while statistically significant differences in radiologic and functional outcomes favor volar plate fixation, these differences do not exceed minimal clinically important difference thresholds. Furthermore, ulnar variance did not differ significantly between treatment groups, and radiographic parameters showed

Fig. 1. Successful conservative treatment of a displaced distal radius fracture in a 20-year-old female patient. (A) Immediate posttrauma wrist anteroposterior and lateral radiographs demonstrating a dorsally displaced intraarticular distal radius fracture of the right wrist. (B) Wrist radiographs obtained after manual reduction, showing restoration of volar tilt and radial length. (C) Wrist radiographs at 3 months posttrauma, demonstrating maintenance of fracture alignment and satisfactory fracture union.

limited correlation with long-term clinical outcomes (Table 1) [20,22,24,26-28]. Collectively, these data suggest that despite the potential for radiographic malunion in conservatively managed cases, long-term functional recovery is not inferior to surgical intervention, supporting nonoperative management as a viable primary treatment option.

Rather than applying strict radiographic criteria uniformly across all patients, more stringent criteria may be appropriate for younger, active individuals, while more flexible thresholds may be suitable for elderly patients with comorbidities or low functional demands. In particular, several studies have reported that unsatisfactory radiographic results do not always correlate with unsatisfactory functional outcomes in elderly patients [29,30]. Kyung et al. [31] reported that dorsal metaphyseal comminution did not significantly affect radiographic or functional outcomes in patients treated nonoperatively. Kim et al. [32] compared elderly patients (≥65 years) treated nonoperatively versus operatively for unstable distal radius fractures and found that although radial shortening was more pronounced in the nonoperative group, functional evaluation and wrist range of motion did not differ significantly between groups. A recent randomized trial of intraarticular fractures found that intraarticular incongruity did not significantly affect functional outcomes, even though radiographic differences were present (Fig. 2) [16]. These findings support the premise that in elderly patients with lower functional demands, nonoperative treatment can achieve satisfactory outcomes even when anatomical restoration is not perfect.

In addition to radiographic findings, clinical features such as concomitant fractures in the ipsilateral upper extremity, carpal fractures or dislocations, severe soft-tissue damage, or associated neurovascular injury warrant consideration of operative treatment as a priority [15].

Methods of nonoperative treatment

Reduction of the fracture and postinjury management

When dorsal metaphyseal comminution is mild, radial length is relatively preserved, or angulation/displacement is minimal, additional fracture reduction is not required. In displaced fractures, longitudinal traction is applied along the forearm with adequate pronation of the hand while directing the distal fragment opposite to the direction of displacement in order to achieve reduction. Typically, the wrist is immobilized in approximately 20°–30° of flexion with ulnar deviation. If needed, local injection of lidocaine at the dorsal aspect of the fracture may be used before attempting reduction to provide pain relief and allow effective traction.

Elevation of the hand is essential to prevent swelling after injury. The use of a sling is not recommended because it positions the hand below the level of the heart; instead, the hand should always be kept above the elbow. Continuous finger motion is necessary. Importantly, finger motion must include full metacarpophalangeal (MCP) joint flexion and full interphalangeal (IP) joint extension rather than motion limited to the IP joints alone (Fig. 3). If active exercise alone is insufficient, assisted active exercise using the contralateral hand should be performed so that the patient can fully clench the fist and achieve full finger extension.

https://doi.org/10.12671/jmt.2026.00024

Table 1. Summary of randomized controlled trials comparing nonoperative and operative treatment for distal radius fracture

Study	Included patients	Type of treatment	No.	Age (yr)	Sex (male: female)	Severity of fracture (AO type)	Clinical outcomes at final F/U			Radiologic outcomes								
							Wrist flexion/extension[a]	Grip strength[a]	Patient-reported outcomes	Dorsal angulation (°)[b]			Radial inclination (°)[b]			Ulnar variance (mm)[b]		
										Pre	Post	F/U	Pre	Post	F/U	Pre	Post	F/U
2005, Azzopardi et al. [20]	Unstable, extraarticular fractures	Nonoperative	27	71	2:25	A3	88.5%	72%	SF-36 physical: 38.2	29±16	−5±7	4±8	18±6	21±3	19±6	3±3	0±1	3±2
		Percutaneous pinning	27	72	4:23	A3	90.5%	77%	SF-36 physical: 42.2	35±15	−4±7	−3±10[c]	16±6	22±3	22±5	4±3	0±1	3±2
2010, Wong et al. [28]	Unstable, extraarticular fractures	Nonoperative	30	71	5:25	Frykman classification I:II (18:12)	143°	9.0 kg	Mayo wrist scores: 80.5±7.5	31±6	−7.5±1	3±1	13±3	23±4	16±2	4.3±1.2	0.5±0.2	3.2±1.4
		Percutaneous pinning	30	70	6:24	Frykman classification I:II (17:13)	145°	8.5 kg	Mayo wrist scores: 82.2±6.2	33±6	−8±1	−4±1[c]	13±4	23±2	20±2[c]	5.2±1.8	0.3±0.1	2.1±1.1
2011, Arora et al. [26]	Displaced, unstable fractures	Nonoperative	37	77.4	10:27	A2-3, A3-9, C1-11, C2-8, C3-6	103.7%[c]	92.6%	DASH scores: 8.0±9.3		3.6±11.2	10.4±19.1		20.3±3.3	15.9±9.0		0.8±1.7	3.2±2.9
		ORIF with volar locking plate	36	75.9	8:28	A2-3, A3-7, C1-4, C2-12, C3-10	92.8%	102.4%[c]	DASH scores: 5.7±11.1		−3.6±6.9[c]	−0.5±4.7[c]		21.8±2.7[c]	21.2±2.6[c]		0.6±1.6	0.7±1.8[c]
2014, Sharma et al. [27]	AO type B and C fractures	Nonoperative	32	48.1	10:22	B-13, C-19	135.0°	72.2%	DASH scores: 14.0±10.2		−8.4±0.4	−5.2±0.5		18.1±0.9	15.2±0.8		0.2±0.1	0.3±0.1
		ORIF with volar locking plate	32	52.4	9:23	B-19, C-17	168.2°[c]	89.1%[c]	DASH scores: 5.0±9.4[c]		−10.1±1.5[c]	−8.4±1.0[c]		20.5±1.3[c]	17.9±0.8[c]		−0.3±0.3	−0.3±0.2
2019, Saving et al. [22]	Dorsally displaced fractures (≥20° dorsal tilt)	Nonoperative	64	78	8:56	A2-10,A3-28, C1-20, C2-6, C3-0	107°	80.9%	PRWE scores: 22.4±21.4 DASH scores: 23.1±19.8	27±8	8±8	14±13	14±8	18±6	14±7	2.3±2.2	0.6±1.6	2.7±2.2
		Volar locking plate	58	80	3:55	A2-6, A3-33, C1-11, C2-7, C3-1	118°	96.0%[c]	PRWE scores: 12.7±15.0 DASH scores: 15.6±17.0[c]	31±10	−1±7[c]	1±9[c]	14±13	18±8	19±8[c]	2.4±2.1	0.0±0.3[c]	0.5±1.3[c]
2021, Hassellund et al. [24]	Displaced, unstable fractures	Nonoperative	50	73.9	8:42	A2-2, A3-12, C1-11, C2-18, C3-7	112°	77%	QuickDASH median: 5 PRWE median: 2	23	13	20	18	19	18	3	5	5
		Volar locking plate	50	73.4	3:47	A2-3, A3-9, C1-13, C2-16, C3-9	119°	88%[c]	QuickDASH median: 0 PRWE median: 0[c]	21	−1[c]	−1[c]	19	24[c]	25[c]	3	2[c]	2[c]

Table 1 summarizes key comparative studies. Differences in fracture classification, definitions of instability, and outcome instruments limit direct comparisons across studies. For patient-reported outcomes, statistical significance should be interpreted alongside clinical relevance (e.g., the minimal clinically important difference, when available). Follow-up intervals vary; early functional differences may not persist at later assessments. All of the continuous values are presented as mean or mean±standard deviation.

DASH, Disabilities of the Arm, Shoulder and Hand; SF-36, Short Form-36 Health Survey; QuickDASH, Quick Disabilities of the Arm, Shoulder and Hand; PRWE, Patient-Rated Wrist Evaluation.

[a]Wrist flexion/extension arc and grip strength of the involved hand are presented as raw data or ratios compared with the contralateral side. [b]Pre denotes the values before the reduction or operation. Post means the values after the reduction or operation. F/U refers to values that were measured at the final follow-up period. [c]The value of this group is statistically significantly better than that of the comparison group.

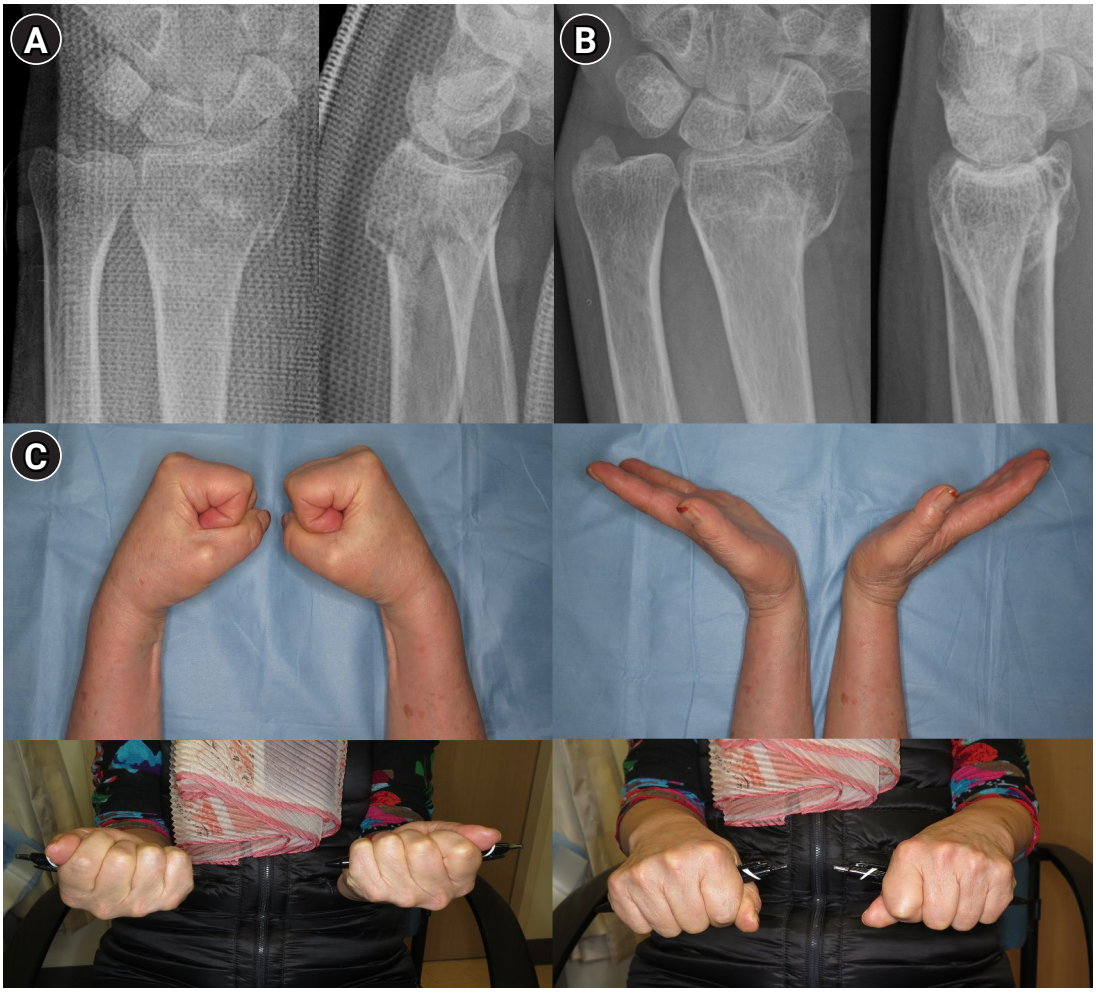

Fig. 2. Outcome of conservative treatment in an older patient with a displaced distal radius fracture. Radiographs of a 71-year-old female patient. (A) Wrist anteroposterior and lateral radiographs obtained after initial reduction, demonstrating distal radius and ulnar styloid fractures with intraarticular comminution of the left wrist. Volar tilt and radial length were well restored after reduction. (B) Wrist radiograph obtained 1 year after trauma, showing radial shortening and dorsal tilt of the distal radius. (C) Range of motion of the left wrist was slightly decreased compared with the right side; however, the patient was able to perform daily activities without pain at one year after trauma.

Assisted exercises should apply sustained, gentle pressure rather than abrupt force to the joints. Additionally, during prolonged immobilization, contractures may develop in nonimmobilized joints such as the shoulder or elbow; therefore, these joints should be moved regularly from the time of injury [33].

Type and duration of splint or cast immobilization

Because considerable swelling is present immediately after injury, excessive compression during initial bandage or plaster application should be avoided. Joints not requiring immobilization—such as the shoulder and the MCP joints—should remain as mobile as possible. In particular, excessive pressure during plaster wrapping can lead to circulatory compromise, and improper molding before the plaster sets may result in pressure over bony prominences (e.g., radial or ulnar styloid, posterior ulna), causing skin necrosis, nerve palsy, or vascular insufficiency [33].

Various immobilization techniques for conservative treatment of distal radius fractures include sugar-tong splints, long-arm splints or casts, short-arm double splints, short-arm splints or casts, and radial gutter short-arm splints. Among these, sugar-tong splint is most commonly used immediately after injury. It partially restricts elbow motion while preventing forearm rotation in an effort to

https://doi.org/10.12671/jmt.2026.00024

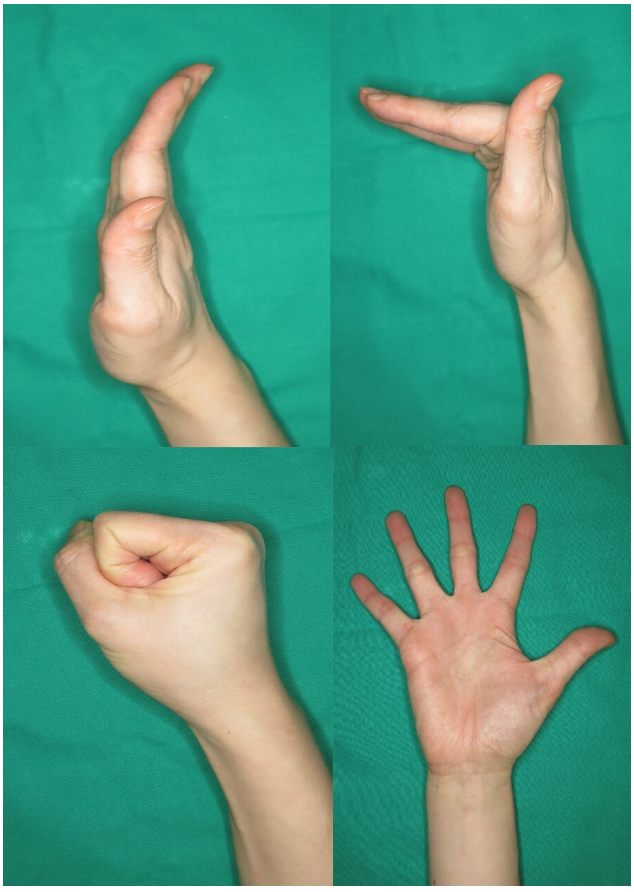

Fig. 3. Active finger range of motion exercise to prevent finger stiffness.

reduce loss of reduction [34]. However, sugar-tong splints may be uncomfortable during elevation due to their weight, and restriction of elbow motion can lead to elbow stiffness [35,36].

Randomized controlled trials have demonstrated that immobilization methods not involving the elbow provide stability comparable to elbow-including methods, with fewer immobilization-related complications [17,37]. Therefore, the necessity of elbow immobilization in conservative management of distal radius fractures remains controversial. Grafstein et al. [38] also reported no significant differences in redisplacement rates or functional recovery among sugar-tong splints, short-arm double splints, and short-arm casts in displaced distal radius fractures, recommending that physicians use the method they are most familiar with. The American Academy of Orthopaedic Surgeons (AAOS) clinical practice guideline similarly states that there is insufficient evidence to determine the superiority or necessity of elbow immobilization in conservative treatment of distal radius fractures [39].

Emerging technologies such as 3D-printed custom splints have been introduced as alternatives to conventional immobilization. These patient-specific devices, designed based on forearm surface scanning and fabricated using additive manufacturing, offer potential advantages including reduced weight, improved ventilation, and water resistance. A recent randomized controlled trial comparing 3D-printed splints to fiberglass casts in minimally displaced distal radius fractures demonstrated equivalent patient satisfaction and clinical effectiveness, although minor complications such as pressure points and splint breakage occurred more frequently in the 3D-printed group and required design modifications [40].

Regardless of the immobilization technique, it is essential to avoid crossing the metacarpal heads with the distal end of the splint or cast to permit MCP flexion to 90° and to prevent finger stiffness. After splint or cast application, the patient should be instructed to move the MCP joints to confirm absence of discomfort.

The recommended duration of immobilization is generally 3–4 weeks for impacted or minimally displaced fractures and 5–6 weeks for displaced fractures [33,35,41]. Recent evidence suggests that shorter immobilization periods may be appropriate for stable fractures. Multiple studies have demonstrated that 1 week of cast immobilization is safe and feasible for nondisplaced or minimally displaced distal radius fractures, potentially resulting in better functional outcomes and faster return to activities [42]. In displaced fractures, long-arm immobilization using a sugar-tong splint or long-arm cast is applied for the first 2–3 weeks, followed by a short-arm cast for an additional 3–4 weeks; however, actual duration may vary depending on fracture characteristics, patient status, and progression of bone healing [19,43,44]. In cases requiring reduction, weekly radiographs for the first 2–3 weeks are necessary to detect redisplacement or deformity, and if present, treatment should be converted to operative management [33].

Rehabilitation after immobilization

After planned immobilization is completed, active mobilization is required to restore wrist range of motion. With the elbow flexed and the upper arm supported on the table, the patient performs wrist flexion, extension, pronation, and supination through active and assisted active exercises

[33]. Pain during early rehabilitation is common after prolonged immobilization; nonsteroidal anti-inflammatory drugs and heat therapy may help alleviate symptoms [33].

Evidence integration

Across randomized and prospective comparative studies summarized in Table 1, operative fixation more consistently improves radiographic alignment at final follow-up than function. Functional benefits are less consistent and often time dependent. Interpretation is limited by heterogeneity in fracture patterns (extraarticular vs. intraarticular), definitions of instability and acceptable alignment, baseline functional demand, outcome measures (e.g., the Disabilities of the Arm, Shoulder and Hand [DASH/QuickDASH], the Patient-Rated Wrist Evaluation [PRWE], range of motion, grip strength), and follow-up duration (commonly 12 months). Early between-group differences in motion, strength, or patient-reported outcomes may diminish over time, and statistically significant effects may not meet thresholds for patient-important change (e.g., minimal clinically important difference). Overall, treatment goals should be individualized: radiographic restoration may be more consequential for younger, high-demand patients, whereas many older, lower-demand patients can achieve acceptable long-term function with nonoperative care when early stability is maintained through structured radiographic surveillance and rehabilitation.

Limitations of the evidence and this review

The existing evidence base is heterogeneous with respect to fracture patterns, definitions of instability and acceptable alignment, treatment and rehabilitation protocols, outcome measures, and duration of follow-up, which limits direct cross-study comparison and consistent interpretation of effect sizes. Many trials are underpowered to detect uncommon but clinically important complications, and follow-up is frequently limited to approximately one year, potentially underestimating late sequelae in younger or higher-demand patients. As a narrative review, this synthesis does not include a formal risk-of-bias assessment or structured evidence grading, and the literature search was not intended to be exhaustive. Accordingly, the conclusions presented should be interpreted as evidence-informed guidance to support individualized clinical decision-making rather than as pooled comparative estimates of treatment efficacy.

Conclusions

Nonoperative treatment remains a fundamental option for distal radius fractures, particularly in elderly patients. Treatment selection should integrate radiographic parameters with patient-specific factors including age, activity level, comorbidities, and functional expectations. During nonoperative management, attention must extend beyond fracture reduction and union to include swelling control and prevention of hand stiffness through finger exercises. Following immobilization, active wrist motion should be encouraged to restore range of motion.

Article Information

Author contributions

Conceptualization: SWC, JKK. Supervision: JKK. Writing-original draft: SWC. Writing-review & editing: SWC, JKK. All authors have read and approved the final version of the manuscript.

Conflicts of interest

No potential conflict of interest relevant to this article was reported.

Funding

None.

Data availability

Not applicable.

Acknowledgments

None.

Supplementary materials

None.

References

1. Baron JA, Karagas M, Barrett J, et al. Basic epidemiology of fractures of the upper and lower limb among Americans

 https://doi.org/10.12671/jmt.2026.00024

over 65 years of age. Epidemiology 1996;7:612-8.
2. Orbay JL, Fernandez DL. Volar fixation for dorsally displaced fractures of the distal radius: a preliminary report. J Hand Surg Am 2002;27:205-15.
3. Bentohami A, de Burlet K, de Korte N, et al. Complications following volar locking plate fixation for distal radial fractures: a systematic review. J Hand Surg Eur Vol 2014;39:745-54.
4. Kodama N, Takemura Y, Ueba H, Imai S, Matsusue Y. Acceptable parameters for alignment of distal radius fracture with conservative treatment in elderly patients. J Orthop Sci 2014;19:292-7.
5. Palmer AK, Werner FW. Biomechanics of the distal radioulnar joint. Clin Orthop Relat Res 1984;187:26-35.
6. Bronstein AJ, Trumble TE, Tencer AF. The effects of distal radius fracture malalignment on forearm rotation: A cadaveric study. J Hand Surg Am 1997;22:258-62.
7. Knirk JL, Jupiter JB. Intra-articular fractures of the distal end of the radius in young adults. J Bone Joint Surg Am 1986;68:647-59.
8. Kazuki K, Kusunoki M, Yamada J, Yasuda M, Shimazu A. Cineradiographic study of wrist motion after fracture of the distal radius. J Hand Surg Am 1993;18:41-6.
9. Miyake T, Hashizume H, Inoue H, Shi Q, Nagayama N. Malunited Colles' fracture: analysis of stress distribution. J Hand Surg Br 1994;19:737-42.
10. Fernandez DL. Malunion of the distal radius: current approach to management. Instr Course Lect 1993;42:99-113.
11. Altissimi M, Antenucci R, Fiacca C, Mancini GB. Long-term results of conservative treatment of fractures of the distal radius. Clin Orthop Relat Res 1986;206:202-10.
12. Weber ER. A rational approach for the recognition and treatment of Colles' fracture. Hand Clin 1987;3:13-21.
13. Cooney WP. Fractures of the distal radius: a modern treatment-based classification. Orthop Clin North Am 1993;24:211-6.
14. Lafontaine M, Hardy D, Delince P. Stability assessment of distal radius fractures. Injury 1989;20:208-10.
15. Lee JH. Surgical indications for distal radius fractures. J Korean Soc Surg Hand 2015;20:72-6.
16. Martinez-Mendez D, Lizaur-Utrilla A, de-Juan-Herrero J. Intra-articular distal radius fractures in elderly patients: a randomized prospective study of casting versus volar plating. J Hand Surg Eur Vol 2018;43:142-7.
17. Park MJ, Kim JP, Lee HI, et al. Is a short arm cast appropriate for stable distal radius fractures in patients older than 55 years? A randomized prospective multicentre study. J Hand Surg Eur Vol 2017;42:487-92.
18. Simic PM, Weiland AJ. Fractures of the distal aspect of the radius: changes in treatment over the past two decades. Instr Course Lect 2003;52:185-95.
19. Song SW. Osteoporotic distal radius fracture-conservative treatment. J Korean Fract Soc 2008;21:81-6.
20. Azzopardi T, Ehrendorfer S, Coulton T, Abela M. Unstable extra-articular fractures of the distal radius: a prospective, randomised study of immobilisation in a cast versus supplementary percutaneous pinning. J Bone Joint Surg Br 2005;87:837-40.
21. Haslhofer DJ, Froschauer SM, Gotterbarm T, Schmidt M, Kwasny O, Holzbauer M. Comparison of surgical and conservative therapy in older patients with distal radius fracture: a prospective randomized clinical trial. J Orthop Traumatol 2024;25:46.
22. Saving J, Wahlgren SS, Olsson K, et al. Nonoperative treatment compared with volar locking plate fixation for dorsally displaced distal radial fractures in the elderly: a randomized controlled trial. J Bone Joint Surg Am 2019;101:961-9.
23. Chung KC, Kim HM, Malay S, et al. The wrist and radius injury surgical trial: 12-month outcomes from a multicenter international randomized clinical trial. Plast Reconstr Surg 2020;145:1054e-1066e.
24. Hassellund SS, Williksen JH, Laane MM, et al. Cast immobilization is non-inferior to volar locking plates in relation to QuickDASH after one year in patients aged 65 years and older: a randomized controlled trial of displaced distal radius fractures. Bone Joint J 2021;103-B:247-55.
25. Gutierrez-Espinoza H, Araya-Quintanilla F, Olguin-Huerta C, et al. Effectiveness of surgical versus conservative treatment of distal radius fractures in elderly patients: a systematic review and meta-analysis. Orthop Traumatol Surg Res 2022;108:103323.
26. Arora R, Lutz M, Deml C, Krappinger D, Haug L, Gabl M. A prospective randomized trial comparing nonoperative treatment with volar locking plate fixation for displaced and unstable distal radial fractures in patients sixty-five years of age and older. J Bone Joint Surg Am 2011;93:2146-53.
27. Sharma H, Khare GN, Singh S, Ramaswamy AG, Kumaraswamy V, Singh AK. Outcomes and complications of fractures of distal radius (AO type B and C): volar plating versus nonoperative treatment. J Orthop Sci 2014;19:537-44.

28. Wong TC, Chiu Y, Tsang WL, Leung WY, Yam SK, Yeung SH. Casting versus percutaneous pinning for extra-articular fractures of the distal radius in an elderly Chinese population: a prospective randomised controlled trial. J Hand Surg Eur Vol 2010;35:202-8.
29. Jaremko JL, Lambert RG, Rowe BH, Johnson JA, Majumdar SR. Do radiographic indices of distal radius fracture reduction predict outcomes in older adults receiving conservative treatment? Clin Radiol 2007;62:65-72.
30. Young BT, Rayan GM. Outcome following nonoperative treatment of displaced distal radius fractures in low-demand patients older than 60 years. J Hand Surg Am 2000;25:19-28.
31. Kyung MG, Chung HW, Kim JS, et al. Closed reduction and cast immobilization for the treatment of distal radius fracture: does dorsal metaphyseal comminution predict radiographic and functional outcomes? J Korean Soc Surg Hand 2013;18:29-36.
32. Kim JM, Seo HJ, Jeon YD, Lee HM, Son JH. Comparative study of outcomes between operative and non-operative treatment of unstable distal radius fracture in the elderly patients. J Korean Soc Surg Hand 2015;20:43-50.
33. The Korean Society for Surgery of the Hand. Surgery of the hand. Panmuneducation; 2014.
34. Lee JH, Hong SH, Kim YJ, Back JH, Lee JS. Effect of different splints on displacement after closed reduction of the distal radius fractures: a comparison of short arm double splint and sugar-tong splint. J Korean Soc Surg Hand 2015;20:104-9.
35. Cho JH, Park DY, Kim JY, Han KJ. A comparison of sugar tong splint and radial gutter short arm splint after closed reduction of distal radius fracture. Arch Hand Microsurg 2009;14:194-8.
36. Frykman G. Fracture of the distal radius including sequelae–shoulder-hand-finger syndrome, disturbance in the distal radio-ulnar joint and impairment of nerve function: a clinical and experimental study. Acta Orthop Scand 1967; Suppl 108:3.
37. Bong MR, Egol KA, Leibman M, Koval KJ. A comparison of immediate postreduction splinting constructs for controlling initial displacement of fractures of the distal radius: a prospective randomized study of long-arm versus short-arm splinting. J Hand Surg Am 2006;31:766-70.
38. Grafstein E, Stenstrom R, Christenson J, et al. A prospective randomized controlled trial comparing circumferential casting and splinting in displaced Colles fractures. CJEM 2010;12:192-200.
39. Lichtman DM, Bindra RR, Boyer MI, et al. American Academy of Orthopaedic Surgeons clinical practice guideline on: The treatment of distal radius fractures. J Bone Joint Surg Am 2011;93:775-8.
40. Guebeli A, Thieringer F, Honigmann P, Keller M. In-house 3D-printed custom splints for non-operative treatment of distal radial fractures: a randomized controlled trial. J Hand Surg Eur Vol 2024;49:350-8.
41. McAuliffe TB, Hilliar KM, Coates CJ, Grange WJ. Early mobilisation of Colles' fractures. A prospective trial. J Bone Joint Surg Br 1987;69:727-9.
42. de Bruijn MA, van Ginkel LA, Boersma EZ, et al. The past, present and future of the conservative treatment of distal radius fractures. Injury 2023;54 Suppl 5:110930.
43. Bucholz R, Rockwood C, Green D. Rockwood and Green's fractures in adults. 7th ed. Philadelphia, PA: Wolters Kluwer Health/Lippincott Williams & Wilkins; 2010.
44. Jung M, Sung S, Choi I. Textbook of fractures. 3rd ed. Gunja; 2008.

https://doi.org/10.12671/jmt.2026.00024

JMT Journal of Musculoskeletal Trauma

pISSN 3058-6267 · eISSN 3058-6275
J Musculoskelet Trauma 2026;39(2):103-116
https://doi.org/10.12671/jmt.2026.00066

Sex-specific bottlenecks and risk zones in the retrograde superior pubic ramus screw corridor: a 3D CT-based morphometric cadaver study

Ji Won Jeong[1], Jung Tae Ahn[1], Gu Hee Jung[2,3], Kun Tae Kim[1,4]

[1]Department of Orthopedic Surgery, Gyeongsang National University Hospital, Gyeongsang National University College of Medicine, Jinju, Korea
[2]Department of Orthopedic Surgery, GIJANG Hospital, Busan, Korea
[3]Planner.surgery Co., Busan, Korea
[4]Department of Orthopedic Surgery, Gyeongnam Regional Trauma Center, Jinju, Korea

Background: Superior ramus screw fixation is commonly used to stabilize anterior pelvic ring injuries but is constrained by a narrow, irregular, and curved intraosseous corridor. Trajectory-based morphometric analysis may assist in screw diameter selection and enable identification of reproducible anatomic constriction zones.

Methods: We conducted a cross-sectional computed tomography (CT)-based morphometric study of 82 cadaveric pelvises (42 males, 40 females). Bottleneck diameter was defined as the diameter of the largest fully contained virtual cylinder along the planned trajectory, and cylinder length was recorded. Orthogonal cross-sections at 9.5-mm intervals (up to 12 segments) were generated to measure segment-wise effective diameter (defined as twice the minimum centerline-to-cortex distance) and cortical clearance, which was used as a diameter-based safety margin. Segments were realigned to the acetabular start segment to define relative segment positions (Δ seg). Feasibility was assessed for prespecified screw diameters ranging from 3.5 to 7.3 mm.

Results: Mean bottleneck diameter was larger in males than in females (7.34±1.10 vs. 5.93±0.98 mm), whereas trajectory length was similar between sexes (127.85±8.54 vs. 128.85±8.20 mm). Δ seg realignment localized corridor constriction to two discrete zones: a preacetabular zone (Δ seg −6 to −4) and a periacetabular zone (Δ seg 1 to 2), where effective diameter and cortical clearance were most limited. Feasibility rates were 100% at 3.5–4.5 mm, 95.2% vs. 82.5% at 5.0 mm, 81.0% vs. 27.5% at 6.5 mm, and 59.5% vs. 10.0% at 7.3 mm in males and females, respectively.

Conclusions: Female models demonstrated smaller trajectory-wide bottleneck diameters and segment-wise effective diameters than male models. Acetabular-referenced Δ seg realignment identified two reproducible anatomic risk zones: a preacetabular zone adjacent to the obturator neurovascular bundle and a periacetabular zone near the external iliac vessels. At diameters ≥6.5 mm, cortical proximity increased more prominently in females than in males.

Level of evidence: III.

Keywords: Bone screws; Internal fracture fixation; Pubic bone; X-ray computed tomography; Sex factors

Original Article

Received: January 22, 2026
Revised: February 1, 2026
Accepted: February 7, 2026

Correspondence to:
Kun Tae Kim
Department of Orthopedic Surgery, Gyeongsang National University Hospital, Gyeongsang National University College of Medicine, 79 Gangnam-ro, Jinju 52727, Korea
Tel: +82-55-750-9509
Email: os.tkra@gmail.com

Introduction

Background

Retrograde superior ramus screw fixation is widely used to stabilize the anterior pelvic ring in superior ramus fractures [1,2]. Compared with open approaches, this technique can be performed through small incisions with limited soft-tissue dissection, which can reduce blood loss and surgical morbidity. It is also increasingly applied to fragility fractures in older patients [2]. However, safe screw placement is constrained by the narrow, irregular, and variably curved intraosseous corridor of the superior ramus [3,4]. Corridor geometry differs by sex and pelvic morphotype, with parameters including the limiting diameter and the available intraosseous trajectory length. These anatomic differences may increase the risk of cortical breach and injury to the acetabular articular cartilage or intrapelvic neurovascular structures [3,4]. The superior ramus screw corridor originates just inferior to the pubic tubercle adjacent to the pubic symphysis and courses through the superior ramus toward the superior acetabular area [5]. In 1995, Routt et al. [6] described retrograde intramedullary fixation for anterior pelvic ring injuries, establishing the corridor as the anatomic basis for percutaneous superior ramus screw techniques.

Anatomic studies describe a double-curved configuration with midcourse angulation, suggesting that both the limiting cross-section and local curvature change along the path [7]. The trajectory follows the superior ramus margin, passes through the anterior acetabular column, and continues toward the sacroiliac tubercle region near the sacroiliac joint [5]. The most constricted region was reported between the iliopsoas gutter and the obturator neurovascular canal [8,9]. The superior isthmus was defined as the distance between the acetabular joint surface and the superior boundary of the corridor [8,9]. The reported measurements differ by the anatomic level at which they are obtained [7,10-12]. These features suggest that screw feasibility is determined primarily by localized constrictions and morphologic variability. Detailed morphometric characterization is needed to guide selection of screw diameter and length to support preoperative planning.

When planning retrograde superior ramus screw insertion, safe accommodation of a screw matched to corridor size requires estimating the minimum intraosseous diameter and the intraosseous trajectory length. Preoperative planning should also localize the segment containing the minimum diameter along the intended trajectory and characterize how the intraosseous diameter changes along the path [7,13-15].

Objectives

Accordingly, in this cross-sectional, computed tomography (CT)-based morphometric study, we quantified anatomic constraints of the retrograde superior ramus screw corridor along a predefined trajectory using three-dimensional reconstructions. Specifically, we aimed to (1) measure the trajectory-wide minimum intraosseous diameter ($D_{bottleneck}$) and intraosseous trajectory length, (2) compare these morphometric parameters between male and female pelvic models, and (3) identify the bottleneck segment and characterize the pattern of diameter variation along the trajectory. We hypothesized that the trajectory-wide minimum diameter would be smaller in female models than in male models, whereas intraosseous trajectory length would be similar between sexes.

Methods

Ethics statement

This study used anonymized cadaveric pelvic CT datasets provided by the Korea Institute of Science and Technology Information (KISTI). The research involved secondary analysis of deidentified imaging data and did not involve living human participants or identifiable private information. Therefore, Institutional Review Board approval and informed consent were not applicable.

Study design

We performed a cross-sectional, CT-based morphometric study of the superior ramus osseous corridor using anonymized cadaveric pelvic CT datasets provided by the KISTI.

Setting

This morphometric analysis was conducted from November 2025 to January 2026. The cadaveric pelvic CT datasets were obtained as deidentified secondary data from the Korea Institute of Science and Technology Information (KISTI), and the original CT acquisition/collection dates were not available in the provided dataset.

https://doi.org/10.12671/jmt.2026.00066

Variables

Exposures included sex, injury side (left or right hemipelvis), and pelvic morphology (shape and structure of the pelvis). Primary outcome measures were the minimum bottleneck diameter (narrowest screw pathway) and screwable length (maximum length in bone for a screw) of the retrograde superior pubic ramus screw corridor. Secondary safety outcomes were segment-wise cortical clearance in the preacetabular (Δ seg –6 to –4, in front of the hip socket) and periacetabular (Δ seg 1–2, near the hip socket) zones. This was defined as the minimum perpendicular distance from the virtual screw surface to the cortical boundary (outer bone edge) at each cross-sectional plane.

Subjects/data sources

We screened pelvic CT scans from 105 adult cadavers and excluded those with pelvic pathology based on medical record review or imaging, such as retained hardware, deformity from a prior fracture, or suspected osseous tumor, as well as scans with image quality insufficient for reliable three-dimensional reconstruction and measurement. Twenty-three cadavers met these exclusion criteria, leaving 82 cadavers (42 males and 40 females) for analysis. The mean age was 52.1 years (standard deviation [SD], 9.2; range, 21–60 years) and the mean height was 161.3 cm (SD, 7.1; range, 146–176 cm).

Measurement

All cadavers underwent supine CT scanning with a 1.0-mm section thickness (Pronto [Hitachi, Tokyo, Japan]). CT data in Digital Imaging and Communications in Medicine (DICOM) format were imported into Mimics (Materialise, Leuven, Belgium) to reconstruct three-dimensional pelvic models including the sacrum and both iliac bones. Using Mimics, we simulated pelvic radiographic projections, including pelvic anteroposterior (AP), inlet, outlet, and obturator oblique outlet views, to center the virtual cylinder within the intraosseous corridor while avoiding cortical violation and virtually placed a retrograde superior ramus screw trajectory (Fig. 1).

After initial virtual cylinder placement, an experienced pelvic trauma surgeon (KTK) adjusted and verified the entry point and trajectory using standardized multiplanar reconstructions and fluoroscopic-equivalent views. The trajectory originated at an osseous entry point inferior to the pubic tubercle and lateral to the symphyseal meniscus and was directed toward the lateral iliac cortex above the acetabulum to represent the intended superior ramus

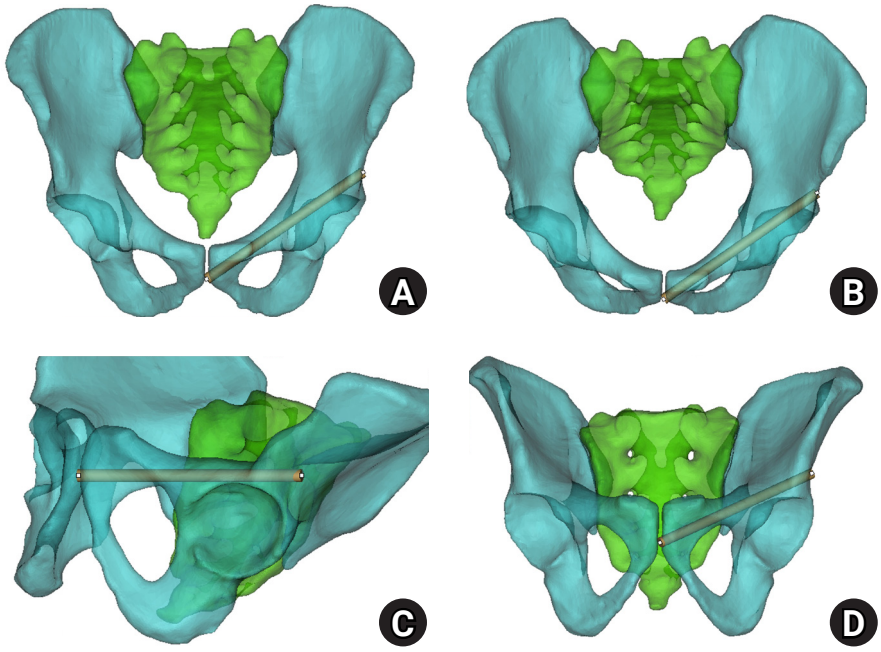

Fig. 1. Virtual cylinder positioning and biomechanical orientation. (A) Pelvis anteroposterior view. (B) Pelvis inlet view. (C) Obturator oblique outlet view. (D) Outlet view.

corridor [6]. Corridor boundaries were defined by the surrounding cortices of the superior ramus (medial [inner], lateral [outer], superior, and inferior). In the periacetabular region, boundaries were defined by the supracetabular cortex superiorly, the quadrilateral plate cortex medially, the acetabular surface inferiorly, and the anterior wall of acetabulum laterally (Fig. 2).

To quantify the intraosseous diameter of the retrograde ramus screw corridor, we defined two morphometric outcomes, including the trajectory-wide bottleneck diameter and the corresponding corridor cylinder length. A virtual cylinder representing the screw was aligned with the predefined trajectory to avoid cortical violation and evaluated uniformly across all models.

The cylinder diameter was incrementally increased until the cylinder first contacted the cortical boundary at any point along the trajectory. For each pelvis, the largest cylinder diameter that remained fully contained within the corridor along the entire path was recorded as the bottleneck, representing the trajectory-wide maximum allowable diameter. The corresponding cylinder length was defined as the intraosseous distance along the trajectory from the

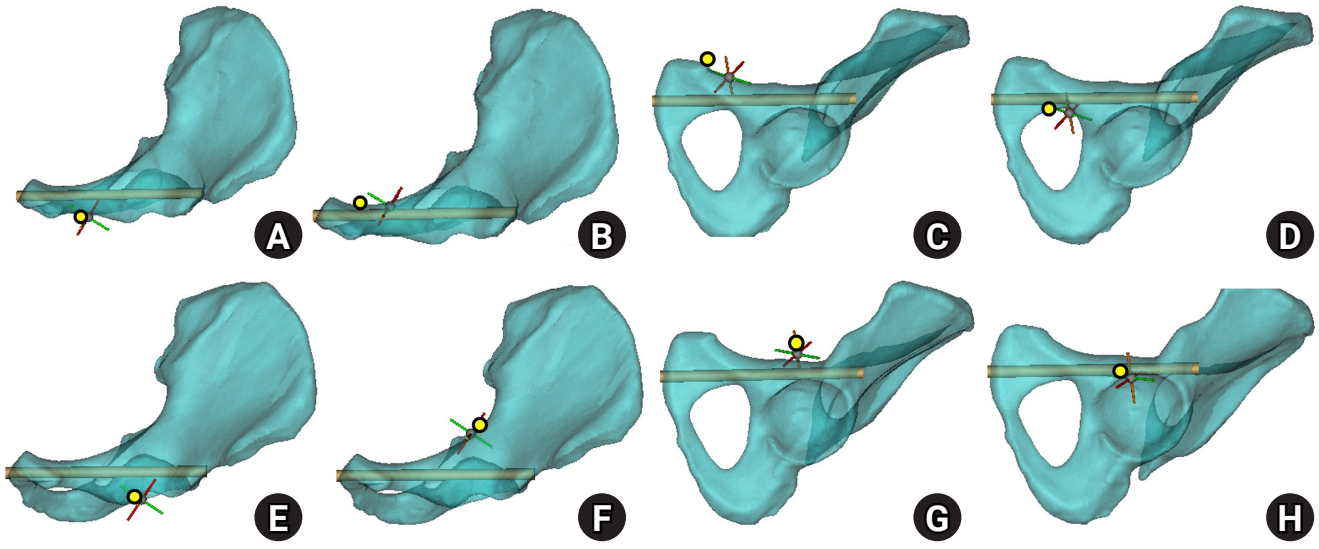

Fig. 2. Corridor boundaries in the preacetabular and periacetabular regions. In the three-dimensional hemipelvis model, yellow dots delineate the boundaries of the preacetabular zone: the lateral (A) and medial (B) margins on the inlet view, the superior margin on the obturator oblique outlet (OOO) view (C), and the inferior margin (D). Corresponding boundaries of the periacetabular zone include the lateral (E) and medial (F) margins on the inlet view, the superior margin on the OOO view (G), and the inferior margin (H).

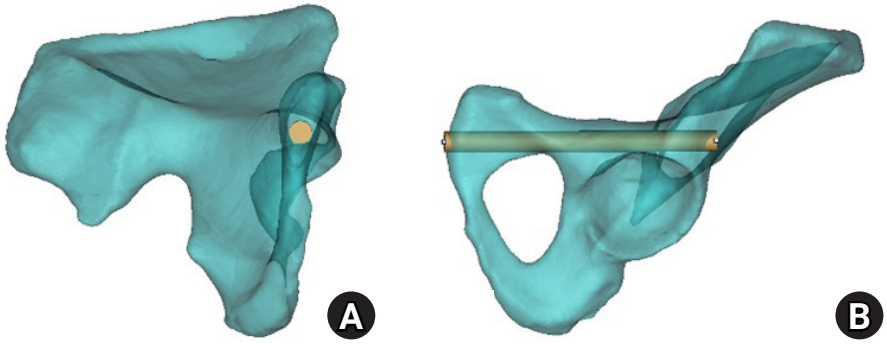

Fig. 3. Axial cylinder and obturator oblique outlet views for measurement of bottleneck diameter and intraosseous corridor length. (A) On the axial cylinder view, the superior ramus screw corridor was assessed, and the bottleneck diameter was measured as the largest cylinder diameter that could be accommodated without cortical violation. (B) On the obturator oblique outlet view, the total cylinder length was measured to define the intraosseous corridor length.

https://doi.org/10.12671/jmt.2026.00066

proximal entry point to the distal endpoint (Fig. 3).

To characterize local corridor geometry along the trajectory, we resliced each pelvic model into orthogonal cross-sections at 9.5-mm intervals along the cylinder axis, generating sequential segments from the entry region to the distal endpoint at the lateral iliac cortex (maximum of 12 segments per model). This spacing was selected a priori as a pragmatic compromise between spatial resolution and measurement reproducibility and burden across models, providing approximately 1-cm sampling and a manageable number of cross-sections over the typical corridor length (approximately 120–130 mm). This sampling density is sufficient to capture clinically interpretable regional trends while limiting excessive multiplicity from very fine reslicing by reducing the number of segment-level comparisons. (Fig. 4).

At each segment, the perpendicular distances from the cylinder centerline to the surrounding cortical boundaries were measured in four directions (medial, lateral, superior, and inferior). The segment-wise limiting radius ($r_{\text{min, seg}}$) was defined as the minimum of the four perpendicular distance: $r_{\text{min, seg}}=\min(d_{\text{medial}}, d_{\text{lateral}}, d_{\text{superior}}, d_{\text{inferior}})$. The effective corridor diameter at each segment was defined as $D_{\text{eff, seg}}=2r_{\text{min, seg}}$, representing the maximum cylinder diameter accommodated at that segment without cortical violation assuming a fixed trajectory axis. For the segment-wise anal-

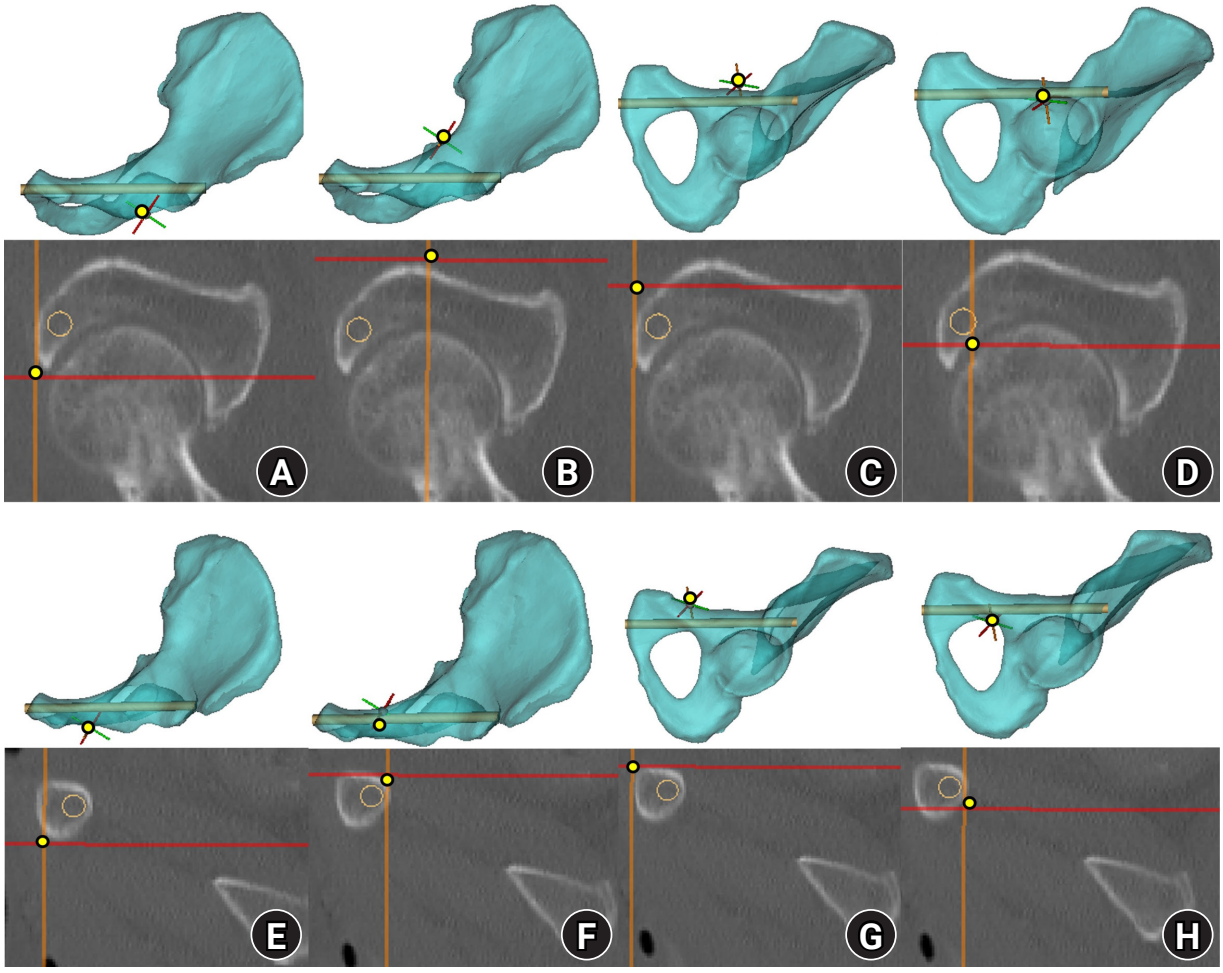

Fig. 4. Corridor boundaries in the preacetabular and periacetabular zones on resliced computed tomography (CT) images. The three-dimensional hemipelvis model and corresponding resliced CT images illustrate the spatial correspondence of each corridor boundary. (A–D) CT images demonstrate the medial, lateral, superior, and inferior margins of the preacetabular zone. (E–H) CT images demonstrate the medial, lateral, superior, and inferior margins of the periacetabular zone. Yellow dots indicate corridor boundaries, and orange circles indicate the virtual cylinder.

ysis, segments were numbered 1-12 in a sequential order along the trajectory, from entry-side to the distal endpoint. To quantify the segment-specific diameter margin relative to the bottleneck diameter, we defined segment-wise cortical clearance ($Clearance_{seg}$) as a diameter-based difference between the segment-wise effective corridor diameter ($D_{eff, seg}$) and the trajectory-wide bottleneck diameter ($D_{bottleneck}$): $Clearance_{seg}=D_{eff, seg}-D_{bottleneck}$. $Clearance_{seg}=0$ at the bottleneck segment. Values greater than 0 indicate segments in which $D_{eff, seg}$ exceeds $D_{bottleneck}$. We defined the acetabular start segment (ASS) as the segment immediately preceding the acetabular dome along the trajectory and used it to divide the corridor into the preacetabular and periacetabular regions. All measurements followed a prespecified protocol with fixed intersegment interval and standardized cortical boundary definitions. The corresponding author independently reviewed trajectory placement to ensure consistent application of the protocol.

To standardize comparisons across models by aligning segment numbers to a consistent anatomic landmark, we referenced segment position to the ASS using a segment-offset variable (Δ seg), calculated by subtracting the acetabular segment number from the segment. For each model, we defined the ASS as the first segment in which the acetabular articular surface formed the inferior corridor boundary. Δ Seg was defined as 0 at ASS. Negative values indicate preacetabular (proximal) segments toward the entry point, whereas positive values indicate periacetabular (distal) segments along the trajectory toward the lateral ilium, where acetabular involvement contributes to the inferior corridor boundary (Fig. 5).

Interobserver reliability was assessed in a representative subset of 20 models that were independently processed by two observers using the same prespecified protocol for trajectory planning, ASS identification, and morphometric derivation. Reliability was quantified using the intraclass correlation coefficient (ICC), specifically a two-way random-effects model with absolute agreement for single measurements (ICC [2,1]) and was reported with 95% confidence intervals (CIs).

Feasibility was assessed for five prespecified cylinder diameters (3.5, 4.5, 5.0, 6.5, and 7.3 mm) to reflect commonly used implant sizes. For each diameter, models were classified as feasible if the model-level bottleneck diameter was greater than or equal to the threshold diameter.

All measurements were performed using a prespecified protocol with fixed segment spacing and standardized cortical boundary definitions. Trajectory placement was independently reviewed by the corresponding author to ensure measurement consistency.

Bias

We applied several steps to mitigate potential bias. Trajectory definition, intersegment interval, and boundary measurements followed a prespecified protocol applied uniformly to all models (Fig. 6). When minor trajectory adjustments were required, such adjustments were restricted to refinements within the same anatomic entry region and were verified by the corresponding author. During measurement, sex information was concealed to minimize sex-related observer bias.

Study size

Sample size was determined by the number of eligible cadaveric pelvic CT datasets available during the study period. No a priori sample size calculation was performed for the present morphometric analysis.

Statistical methods

Continuous variables ($D_{bottleneck}$, cylinder length, $D_{eff, seg}$, and $Clearance_{seg}$; all in millimeters) were presented as mean±SD, and categorical outcomes were presented as counts and percentages. Sex was the primary grouping

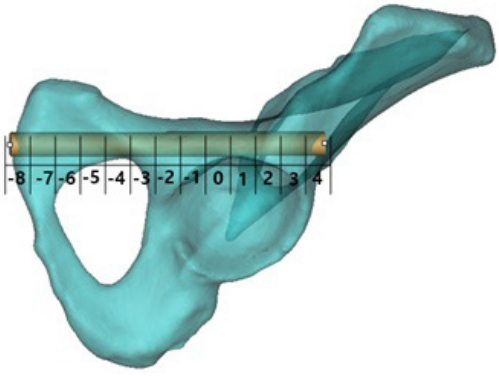

Fig. 5. Acetabular-referenced Δ seg analysis. Using acetabulum-referenced alignment, effective corridor diameter ($D_{eff, seg}$) and cortical clearance (clearance seg) were calculated at each Δ seg position using all available measurements. Bottleneck frequency was defined as the number and percentage of pelvises in which the bottleneck occurred at each Δ seg position.

https://doi.org/10.12671/jmt.2026.00066

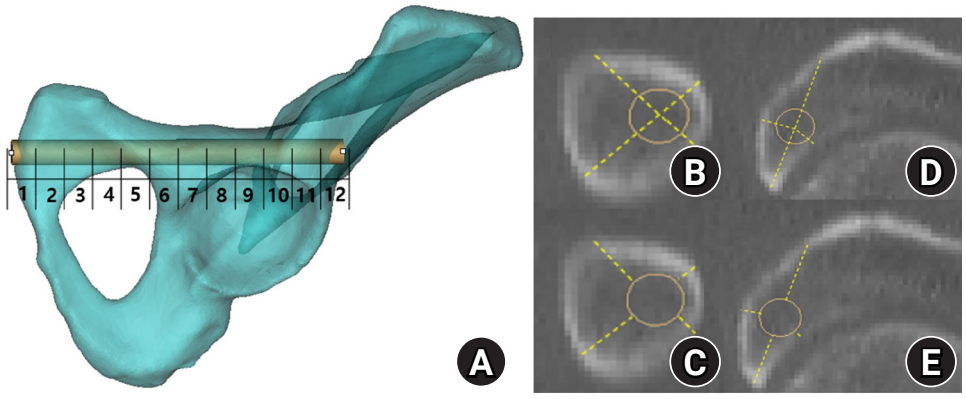

Fig. 6. Segment numbering and distance measurements for segment-wise corridor assessment. (A) In the three-dimensional hemipelvis model, the obturator oblique outlet view illustrates division of the corridor into up to 12 segments from the entry point to the distal lateral iliac cortex, with segments numbered sequentially; segment 8 was designated as the acetabular start segment. In the preacetabular region (proximal to the acetabular start segment), (B) effective distance was defined as the minimum perpendicular distance from the cylinder centerline to each cortical boundary, and (C) cortical clearance was defined as the minimum perpendicular distance from the cylinder surface to each cortical boundary. In the periacetabular region (distal to the acetabular start segment), (D) effective distance and (E) cortical clearance were defined analogously. All segment definitions and boundary measurements were performed according to a prespecified protocol uniformly applied across models.

variable. Global outcomes ($D_{\text{bottleneck}}$ and cylinder length) were compared between males and females using 2-sample t-tests; the Welch t-test was used when the equal-variance assumption was not met. Effect sizes were reported as mean differences with 95% CIs. Sex differences in segment-wise outcomes ($D_{\text{eff, seg}}$, and $Clearance_{\text{seg}}$) were evaluated using independent 2-sample t-tests at each segment and at each Δ seg position relative to acetabular start, with multiplicity control across segment-wise comparisons using the Benjamini-Hochberg false discovery rate (FDR) procedure. Segment-wise and Δ seg measurements are repeated observations within each pelvis; therefore, adjacent segments are anatomically correlated and not statistically independent. Accordingly, these analyses are intended to describe spatial patterns along the corridor rather than to support segment-specific causal inference, and P-values should be interpreted cautiously. Sex differences in feasibility were evaluated using the Fisher exact test; effect sizes are reported as risk ratios with 95% CIs. To account for multiple comparisons across the prespecified cylinder diameters (3.5, 4.5, 5.0, 6.5, and 7.3 mm), feasibility analyses used Benjamini-Hochberg FDR-adjusted P-values. Distributional assumptions were evaluated visually using the line plots used for data visualization. Statistical analyses and development of graphs were performed using R ver. 4.4.3 (R Foundation for Statistical Computing).

Results

Interobserver reliability

Interobserver reliability was high in the subset of 20 models. ASS identification showed complete agreement (ICC, 1.00; weighted κ, 1.00). Continuous measures were highly reproducible, with ICC values of 0.980 (95% CI, 0.952–0.992) for cylinder length and 0.962 (95% CI, 0.907–0.985) for bottleneck diameter (Supplementary Table 1).

Study sample and model-level corridor metrics

In this study, 82 pelvic models were analyzed, including 42 male and 40 female models. The mean model-level bottleneck diameter was larger in males than in females, with mean values of 7.34±1.10 mm in males and 5.93±0.98 mm in females, for a mean difference of 1.41 mm. Mean cylinder length was similar between sexes, averaging 127.85±8.54 mm in males and 128.85±8.20 mm in females, for a mean difference of –1.00 mm (Supplementary Table 2). All included models yielded complete measurements, and no imputation was performed. Sensitivity analyses were consistent with the primary results (Supplementary Table 3).

Segment-wise effective corridor diameter

Segment-wise effective corridor diameters were compared between sexes across 12 predefined segments. Effective diameters were larger in males than in females in segments 2 through 11. This pattern suggested sex differences across most of the trajectory. The largest sex difference was observed at segment 11. In males, the mean segment-wise effective diameter ranged from 8.14±1.45 mm at segment 4 to 17.34±5.21 mm at segment 12. The diameter decreased to the minimum at segment 4. This was followed by an increase to approximately 11 mm at segments 6 and 7. The diameter subsequently decreased again to approximately 9 mm across segment 8 through 10. The diameter increased at segment 11 and peaked at segment 12. In females, the mean effective diameter ranged from 6.77±1.35 mm at segment 10 to 13.59±2.57 mm at segment 12. The diameter decreased through segment 4. This was followed by a gradual increase across segment 5 through 7 with a local maximum at segment 7. The diameter then decreased to the minimum at segment 10. The largest increase occurred between segments 11 and 12. The diameter reached the maximum at segment 12 (Fig. 7, Supplementary Table 4).

Segment-wise cortical clearance

Segment-wise cortical clearance used as a safety margin was compared between sexes across 12 segments. Sex differences were identified in 5 of 12 segments. These were segments 1, 6, 7, 8, and 11. At segment 1, females had greater cortical clearance than males. Mean clearance was 2.55±2.11 mm in females and 1.51±1.35 mm in males. In contrast, males had greater clearance at segment 6, 7, 8 and 11. No sex differences were detected in segment 2 through 5, 9, 10 or 12. In males, cortical clearance ranged from 0.80±0.99 mm at segment 4 to 9.67±4.81 mm at segment 12. The pattern decreased to a minimum at segment 4. This was followed by a mid-trajectory increase with mean clearance of approximately 3 to 4 mm across segments 6 through 8. Clearance then declined across segments 9 and 10 to approximately 1 to 2 mm. A distal increase followed that began at segment 11 and peaked at segment 12. In females, cortical clearance ranged from 0.86±1.14 mm at segment 10 to 7.59±2.54 mm at segment 12. The trajectory decreased through segment 4. This was followed by a mid-trajectory increase with a local peak near segment 7 with mean clearance of approximately 2 to 3 mm. Clearance then declined to minimum at segment 10. The largest increase occurred between segments 11 and 12. Clearance peaked at segment 12 (Fig. 8, Supplementary Table 5).

Acetabular-referenced effective diameter

After realignment to the acetabular transition segment Δ seg 0, effective corridor diameters were presented by sex

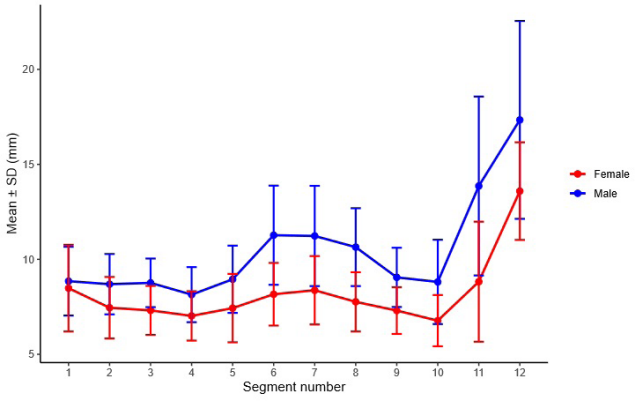

Fig. 7. Segment-wise effective diameter by sex across 12 segments. Between-sex comparisons were performed using independent-samples t-tests, and P-values were adjusted using the Benjamini-Hochberg false discovery rate for 12 segment-wise comparisons. Sex differences were significant for segments 2–11 (all P_FDR<0.001) but not for segments 1 or 12 (P_FDR=0.423 and 0.123, respectively). SD, standard deviation.

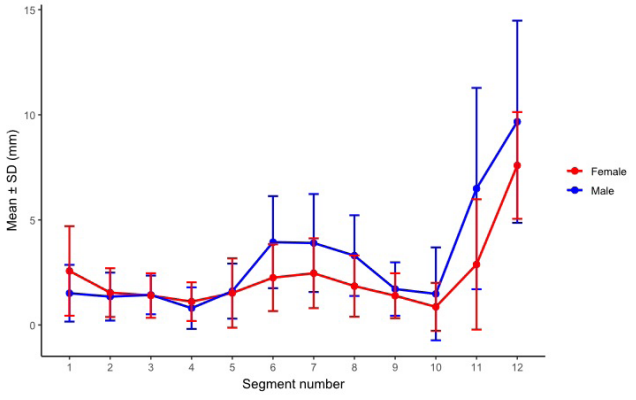

Fig. 8. Segment-wise cortical clearance (safety margin) by sex across 12 absolute segments. Sex-based differences were significant in segments 1, 6, 7, 8, and 11 (P_FDR=0.0249, 0.00095, 0.00458, 0.00095, and 0.00133, respectively) and were not significant in the remaining segments (all P_FDR ≥0.203). SD, standard deviation; FDR, false discovery rate.

https://doi.org/10.12671/jmt.2026.00066

at each relative segment using all available measurements. Statistical comparisons were performed only at Δ seg positions with adequate sex-specific sample sizes. Positions with insufficient data in either sex were presented descriptively. No sex difference was observed at Δ seg –7. From Δ seg –6 through Δ seg 3, males had larger effective diameters than females. In both sexes, effective diameter was larger in the preacetabular segments and decreased toward and immediately after acetabular start. The narrowest region occurred around Δ seg 1 to 2. Distally, the corridor increased again at Δ seg 3. The increase was more pronounced in males. When segment position was referenced to acetabular start (Δ seg), males showed a gradual preacetabular narrowing toward Δ seg –4. This was followed by a marked periacetabular expansion from Δ seg –2 through Δ seg 0. The profile then narrowed in the periacetabular region from Δ seg 1 through Δ seg 2 and expanded distally at Δ seg ≥3. In females, the profile showed a gradual preacetabular narrowing toward Δ seg –4. A slight expansion was observed from Δ seg –2 through Δ seg –1. The trajectory then narrowed from Δ seg 0 through Δ seg 2. The minimum occurred at Δ seg 2. The trajectory increased again at Δ seg 3 (Fig. 9, Supplementary Table 6).

Acetabular-referenced cortical clearance

After realignment to Δ seg 0, cortical clearance as a safety margin was reported by sex at each relative segment using all available measurements. Males had significantly greater cortical clearance than females at Δ seg –2, Δ seg –1, Δ seg 0, and Δ seg 1. No significant differences were detected from Δ seg –7 through Δ seg –3 or from Δ seg 2 through Δ seg 3. When segment position was referenced to acetabular start (Δ seg), males showed an initial decrease in cortical clearance toward a local minimum at Δ seg –4. This was followed by a marked periacetabular increase from Δ seg –2 through Δ seg 0. Clearance then decreased in the periacetabular region from Δ seg 1 through Δ seg 2. A second low point occurred at Δ seg 2. Clearance increased distally at Δ seg ≥3 and reached the largest values at Δ seg 4. In females, clearance decreased gradually from Δ seg –8 toward Δ seg –4. A slight periacetabular increase occurred from Δ seg –2 through Δ seg –1. Clearance then decreased from Δ seg 0 through Δ seg 2 and reached the minimum at Δ seg 2. Clearance increased distally at Δ seg 3 (Fig. 10, Supplementary Table 7).

Bottleneck location distribution and diameter

Bottleneck locations at more proximal positions (Δ seg –7 to –5) and at Δ seg 0 or 3 were uncommon. At shared Δ seg positions, mean bottleneck diameters were generally larger in males than in females. At the most common bottleneck location (Δ seg 2), the mean bottleneck diameter was 7.54±0.96 mm in males (n=16) and 6.27±1.08 mm in females (n=12). Several Δ seg positions had small sample

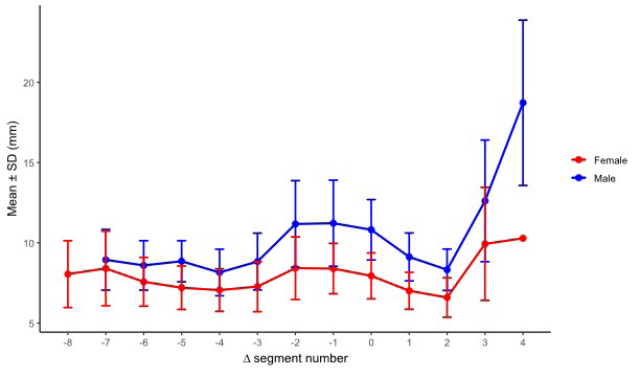

Fig. 9. Segment-wise effective diameter by sex after realignment to the acetabular start segment (Δ seg). No sex-based difference was detected at Δ seg –7 (P_FDR=0.282), whereas males exhibited larger effective diameters than females from Δ seg –6 through Δ seg 3 (all P_FDR≤0.00369). SD, standard deviation; FDR, false discovery rate.

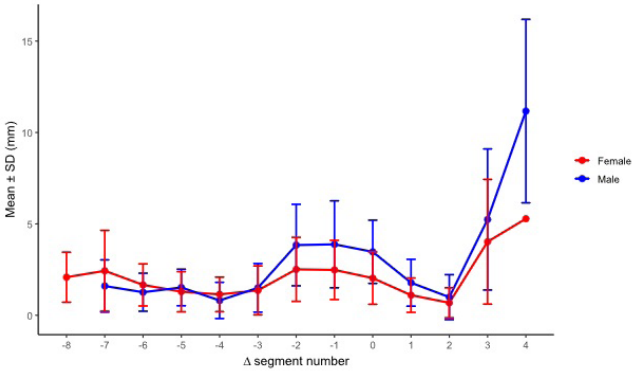

Fig. 10. Segment-wise cortical clearance (safety margin) by sex after realignment to the acetabular start segment (Δ seg). Males demonstrated greater cortical clearance at Δ seg –2, –1, 0, and 1 (P_FDR=0.0107, 0.0107, 0.000664, and 0.0131, respectively), whereas no significant sex-based differences were observed at other Δ seg levels with adequate sample size. SD, standard deviation; FDR, false discovery rate.

sizes, including cells with n=1 in one sex. Bottleneck location occurred most frequently at specific Δ seg positions in both sexes. In males (n=42), the bottleneck most frequently occurred at Δ seg 2 (16/42, 38.1%), followed by Δ seg −4 (7/42, 16.7%) and Δ seg 1 (4/42, 9.5%). In females (n=40), the bottleneck most frequently occurred at Δ seg 2 (12/40, 30.0%), followed by Δ seg −3 (7/40, 17.5%) and Δ seg 1 (6/40, 15.0%) (Fig. 11, Supplementary Table 8).

Diameter-dependent feasibility for virtual cylinders

Feasibility for accommodating a virtual cylinder was evaluated at five diameters of 3.5 mm, 4.5 mm, 5.0 mm, 6.5 mm, and 7.3 mm. All models were feasible for a 3.5 mm and 4.5 mm, including 42 of 42 male models and 40 of 40 female models. At 5.0 mm, feasibility remained 95.2% in males, with 40 of 42 models feasible, and decreased to 82.5% in females, with 33 of 40 models feasible. At larger diameters, feasibility declined and differed by sex. At 6.5 mm, feasibility was 81.0% in males, with 34 of 42 models feasible, and 27.5% in females, with 11 of 40 models feasible (P<0.001). At 7.3 mm, feasibility was 59.5% in males, with 25 of 42 models feasible, and 10.0% in females, with 4 of 40 models feasible (P<0.001) (Fig. 12, Supplementary Table 9).

Cortical breach localization among infeasible models

Among models classified as infeasible at a given diameter, the primary cortical breach occurred at the bottleneck segment. When breach locations were grouped into clinically defined Δ seg regions, females most frequently breached in the periacetabular zone (Δ seg 1 to 2) at both 6.5 mm (13/29, 44.8%) and 7.3 mm (16/36, 44.4%). In contrast, males showed a higher proportion of preacetabular breaches at 7.3 mm (9/17, 52.9%). Regarding the breached cortical boundary, superior-boundary breaches predominated in females at 6.5 mm (14/29, 48.3%) and 7.3 mm (17/36, 47.2%) In males, boundary involvement was vari-

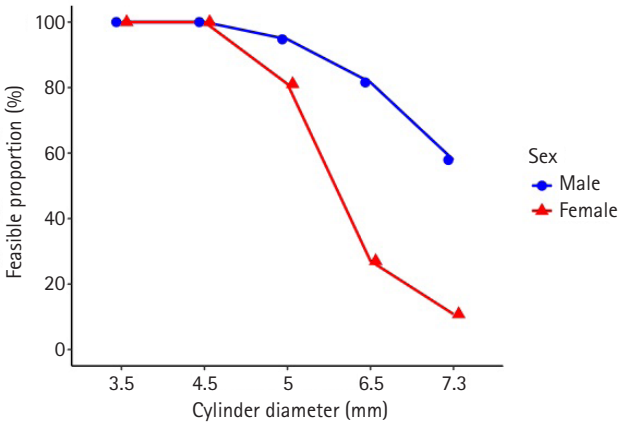

Fig. 12. Diameter-dependent feasibility by sex. Proportion of pelvis models accommodating the cylinder diameter along the retrograde superior pubic ramus trajectory. Feasibility was 100% at 3.5–4.5 mm in both sexes, declined at 5.0 mm (male 95.2% vs. female 82.5%; P_FDR=0.084), and showed significant sex differences at 6.5 mm (81.0% vs. 27.5%) and 7.3 mm (59.5% vs. 10.0%). FDR, false discovery rate.

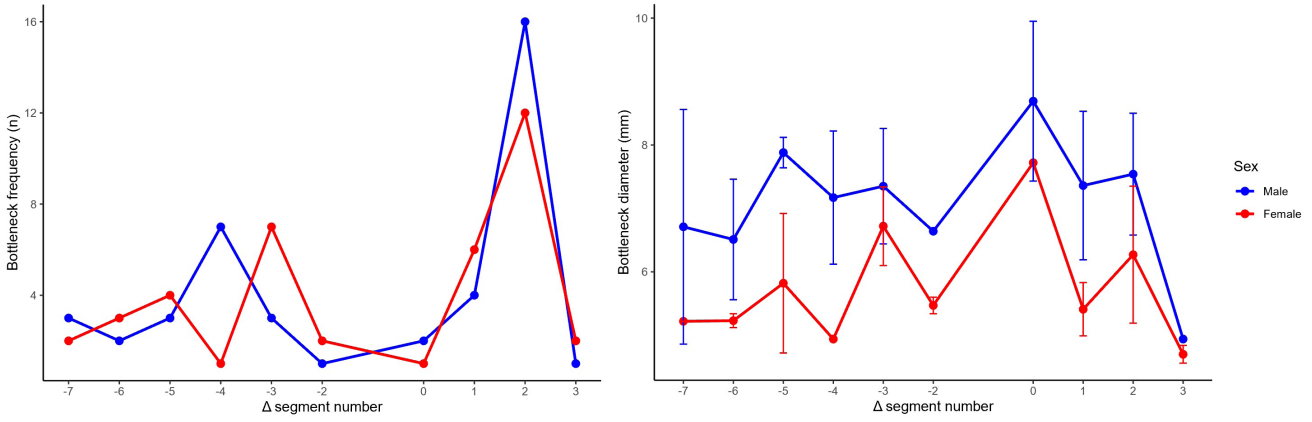

Fig. 11. Bottleneck location frequency and diameter by sex after realignment to the acetabular start segment (Δ seg). The distribution of bottleneck locations across relative segments (Δ seg −7 to 3) did not differ by sex (Fisher exact test with Monte Carlo simulation, P=0.461). Within Δ seg positions, the most pronounced sex-based difference in bottleneck diameter was observed at Δ seg 2 (Welch t-test P=0.0038; Benjamini-Hochberg FDR-adjusted P=0.023), whereas nominal differences at Δ seg −5 and 1 did not remain significant after FDR correction. SD, standard deviation; FDR, false discovery rate.

https://doi.org/10.12671/jmt.2026.00066

able at 6.5 mm, whereas at 7.3 mm the inner boundary was most frequently breached (6/17, 35.3%). Small sample size counts limited inference at 5.0 mm, particularly in males (n=2), in whom breaches were evenly split between preacetabular and distal periacetabular locations and between superior and outer boundaries (each 50%). The distribution of breached cortical boundaries and location did not differ significantly by sex within each diameter (Supplementary Table 10).

The full numeric values, sex-specific sample sizes, and corresponding test statistics for all segment-wise and Δ seg analyses are provided in Supplementary materials.

Discussion

Key results

In this cross-sectional CT morphometric study, we identified clinically meaningful sex differences in the retrograde superior ramus screw corridor. Female models had smaller corridor diameter along the trajectory than male models, with smaller segment-wise effective diameters and a smaller model-level bottleneck diameter. These morphometric differences had clinically relevant implications for diameter-dependent feasibility. Feasibility was universal at 3.5 mm and 4.5 mm diameters in both sexes but decreased markedly at 6.5 mm and 7.3 mm, with a greater relative decline in females.

Interpretation/comparison with previous studies

Our findings are consistent with prior CT-based morphometric studies showing that narrowest canal diameter is larger in males than in females [5,7,12,14]. Similarly, the marked decline in female feasibility at screw diameters ≥6.5 mm aligns with a large CT morphometric study (n=231) reporting that 6.5 mm and 7.3 mm screws may not be safely accommodated in a substantial proportion of female patients [15]. Taken together, these findings provide practical guidance for screw diameter selection along the trajectory.

A key strength of our approach is that it localizes constrictions along the entire trajectory rather than at a single anatomic cross-section. We resliced a series of orthogonal cross-sections at 9.5 mm intervals along the selected cylinder centerline and calculated the segment-wise effective diameter as twice the minimum distance from the centerline to any cortical boundaries. The minimum effective diameter across the trajectory defined the model-level bottleneck. We also quantified segment-wise cortical clearance as the minimum residual distance between the cylinder surface and the nearest cortical boundaries. This clearance served as the safety margin. This combined description of corridor diameter and safety margin is clinically useful. A segment may accommodate a given screw diameter but provide minimal safety margin to the cortex, increasing the risk of cortical violation if intraoperative trajectory adjustments are required. Therefore, our analysis provides both the spatial variation in corridor diameter along the superior ramus trajectory and, for each segment, the cortical boundary most susceptible to violation.

Our feasibility thresholds were derived from intact cadaveric pelves along a prespecified, idealized trajectory and therefore represent an idealized anatomic corridor. In clinical superior ramus fractures, displacement, residual malreduction, and limitations of intraoperative fluoroscopy may alter corridor geometry, narrowing the usable diameter and shifting the location of the limiting segment. Therefore, the reported thresholds should be interpreted as an anatomic reference rather than fixed intraoperative cutoffs for displaced fractures.

The segment numbers (Seg 1–12) may not correspond to anatomically comparable locations across individuals because the acetabular articular surface begins at variable positions. Accordingly, we realigned segment position to the ASS (Seg $_{ASS}$) using a relative coordinate (Δ seg=Seg–Seg $_{ASS}$). Using segment numbering, both effective diameter and cortical clearance (safety margin) showed a nonmonotonic profile with two constriction zones. The first zone was a proximal constriction (Seg 2–4), and the second zone was a periacetabular constriction (Seg 9–10). After realignment to acetabular start, these zones were standardized as a preacetabular zone (Δ seg –6 to –4; Seg 2–4) and a periacetabular zone (Δ seg 1 to 2; Seg 9–10). These findings suggest that anchoring segment position to the ASS improves consistency in identifying anatomically corresponding bottleneck sites along the corridor.

Sex-specific patterns were observed within these acetabular-referenced intervals. In the preacetabular segments (Δ seg –6 to –4), the greatest male constriction was at Δ seg –4, followed by Δ seg –6. Females also showed narrowing at Δ seg –4 and Δ seg –5. In the periacetabular zone (Δ seg

1 to 2), both sexes exhibited concurrent decreases in diameter and safety margin, but the decreases were greater in females. These findings identify the segment immediately distal to the acetabular start as a clinically important risk zone, particularly in females, where both corridor diameter and safety margin decrease most markedly.

Diameter-specific feasibility represented the clinical impact of these morphometric differences. Feasibility was universal at 3.5 mm and 4.5 mm in both sexes but decreased markedly at larger diameters, especially in females. Males were approximately three times more likely to accommodate a 6.5-mm cylinder than females, and nearly six times more likely to accommodate a 7.3-mm cylinder. These results suggest that the safety margin may be limited when selecting screws ≥6.5 mm in females and support patient-specific, corridor-based preoperative planning for screw diameter selection.

Failure patterns differed by sex and diameter in both Δ seg location and the dominant limiting cortical boundary. At 6.5 mm, most failures occurred in females (29/37). In females, failures clustered immediately after acetabular start (Δ seg 1 to 2) and were most often limited by the superior cortex, accounting for approximately half of infeasible cases at 6.5 mm and 7.3 mm. A second female cluster was observed in the entry-side preacetabular range (Δ seg –6 to –5). These models had smaller bottleneck diameters and showed a shift in dominant limiting boundary from the superior cortex to the medial-lateral cortices (inner/outer). Male failures at 6.5 mm were irregular and were distributed across Δ seg without a single dominant boundary phenotype. At 7.3 mm, failures remained largely female, with persistent clustering at Δ seg 2 and predominantly superior-boundary limitation. In contrast, males demonstrated an additional cluster centered around Δ seg –4 that was characterized by medial-boundary limitation. Overall, these patterns suggest sex-specific failure patterns, with periacetabular superior-boundary limitation more prominent in females and proximal medial-boundary limitation more evident in males.

The retrograde superior ramus screw corridor lies close to major neurovascular structures, including the obturator neurovascular bundle and the external iliac vessels [14]. In this CT-based morphometric study, we modeled the osseous corridor only along a standardized trajectory; therefore, our findings do not quantify clinical neurovascular risk, which is additionally influenced by soft-tissue anatomy, fracture displacement and reduction, and intraoperative conditions. However, cortical contact with, or breach of, specific corridor boundaries may be anatomically relevant when interpreting where a larger-diameter screw is most constrained. For screws ≥6.5 mm, infeasible male models more frequently demonstrated medial-boundary limitation in the preacetabular region, whereas infeasible female models more frequently demonstrated superior-boundary limitation in the periacetabular region. These boundary-specific patterns are consistent with prior anatomic descriptions placing the obturator neurovascular bundle approximately 36–44 mm lateral to the pubic symphysis and 2–4 mm posterior to the superior ramus, and the external iliac vessels approximately 63–73 mm lateral and 3–8 mm posterior [16]. These landmark ranges broadly correspond to our preacetabular (Δ seg –6 to –4) and periacetabular (Δ seg 1 to 2) intervals. Accordingly, our results should be viewed as hypothesis-generating anatomic context that may help prioritize direction-specific corridor assessment in these Δ seg zones during preoperative planning, rather than as evidence of segment-level or sex-specific neurovascular injury risk.

Minor intraoperative deviations in the entry point or trajectory may materially influence both bottleneck location and safety margins because the corridor is narrow, irregular, and curved. Even small angular changes can disproportionately affect the periacetabular portion of the trajectory, where cortical boundaries are closely apposed. These deviations may shift the limiting segment and reduce cortical clearance, even when the idealized intact-model corridor appears adequate. Therefore, our segment-wise bottleneck mapping should be viewed as trajectory dependent and is most applicable when the planned trajectory closely matches the prespecified trajectory.

Limitations

Our study has several limitations. First, the effective diameter and cortical clearance reported in this study were trajectory dependent and were determined along a single prespecified path. Therefore, our diameter thresholds should not be used as fixed intraoperative cutoffs. Instead, they should be interpreted as morphology-based reference values and confirmed on a patient-specific basis when substantial trajectory modification is required. Second, as a

https://doi.org/10.12671/jmt.2026.00066

morphometric analysis, our study did not account for fracture displacement, reduction, or intraoperative imaging constraints. Accordingly, feasibility estimates for specific screw diameters in displaced superior ramus fractures may differ and should be interpreted as morphology-based, exploratory reference values rather than definitive clinical thresholds. Third, our cadaveric cohort had a relatively young mean age, 52.1 years (SD, 9.2; range, 21–60 years), compared with the typical fragility-fracture population in whom minimally invasive anterior ring fixation, including retrograde superior ramus screws, is commonly considered. Age-related changes may influence absolute corridor dimensions and, importantly, bone quality in ways not captured by morphology alone; therefore, the feasibility proportions and suggested diameter thresholds reported here may not directly translate to older, osteoporotic patients. Nonetheless, we expect the observed sex-related patterning of constriction zones to remain directionally informative for anatomic risk mapping. Future validation in geriatric cohorts with osteoporosis, ideally incorporating bone quality metrics, is warranted before clinical generalization. Fourth, our segment-wise and acetabular-referenced (Δ seg) analyses are based on repeated measurements obtained within the same pelvis; therefore, values from contiguous segments are anatomically correlated and not statistically independent. Although we controlled multiplicity across segment-level comparisons using the Benjamini-Hochberg FDR procedure, this adjustment does not address within-pelvis correlation. Accordingly, segment-level P-values should be interpreted cautiously, and these analyses should be viewed primarily as descriptive topographic mapping of spatial patterns (narrowing and cortical clearance) along the corridor rather than as evidence supporting segment-specific causal inference. Future studies may incorporate correlation-aware approaches, such as mixed-effects or marginal models, to strengthen segment-level inference while preserving spatial resolution. Fifth, segment-wise effective diameter was computed from four orthogonal centerline-to-cortex distances on each cross-section. Because the true minimum distance may occur along an oblique direction in nonelliptical or irregular corridor shapes, our approach may not capture the strict minimum in every segment and could modestly overestimate $D_{\text{eff, seg}}$ and the corresponding clearance in some locations.

Conclusions

In this cross-sectional CT-based morphometric study, we identified clinically meaningful sex-specific differences in the retrograde superior ramus screw corridor. Female models had a smaller trajectory-wide bottleneck diameter and smaller segment-wise effective diameters than male models, whereas intraosseous trajectory length was comparable between sexes. After acetabular-referenced realignment (Δ seg), we identified two constriction zones, including a preacetabular narrowing (Δ seg –6 to –4) and a periacetabular risk zone (Δ seg 1 to 2). In these zones, corridor capacity and cortical clearance, a segment-level safety margin, were lowest, most prominently in females. These constraints translated into diameter-dependent feasibility. Cylinders of 3.5 mm and 4.5 mm were feasible in most models in both sexes, whereas feasibility decreased substantially at 6.5 mm and 7.3 mm, with a greater decline in females. Because these estimates are trajectory dependent and derived from intact pelvic models rather than clinical outcome data, and because pelvic morphology varies across populations, the results should be generalized cautiously.

Article Information

Author contributions

Conceptualization: JWJ, JTA, GHJ, KTK. Data curation: JTA. Formal analysis: JWJ, JTA. Investigation: GHJ. Resources: GHJ. Visualization: JWJ, GHJ, KTK. Writing–original draft: JWJ. Writing–review & editing: JWJ, JTA, GHJ, KTK. All authors read and approved the final manuscript.

Conflicts of interest

No potential conflict of interest relevant to this article was reported.

Funding

None.

Data availability

Restrictions apply to the availability of these data. The human body digital datasets were obtained from the Korea Institute of Science and Technology Information and are available upon reasonable request with the permission of Korea Institute of Science and Technology Information.

Acknowledgments
None.

Supplementary materials
Supplementary materials related to this article can be found online at https://doi.org/10.12671/jmt.2026.00066.

Supplementary Table 1. Interobserver reliability for acetabular start segment identification and key morphometric measures

Supplementary Table 2. Bottleneck diameter and planned cylinder length by sex

Supplementary Table 3. Sensitivity analyses of sex differences in global corridor outcomes

Supplementary Table 4. Segment-wise effective diameter by sex across 12 segments

Supplementary Table 5. Segment-wise cortical clearance (safety margin) by sex across 12 absolute segments

Supplementary Table 6. Segment-wise effective diameter by sex after realignment to acetabular start (Δ seg)

Supplementary Table 7. Segment-wise cortical clearance (safety margin) sex after realignment to acetabular start (Δ seg)

Supplementary Table 8. Bottleneck diameter by acetabular start segment (Δ seg)

Supplementary Table 9. Infeasibility rates by cylinder diameter and relative risk of infeasibility (male vs. female)

Supplementary Table 10. Dominant failure pattern in infeasible models (by diameter and sex)

References

1. Heiman E, Gencarelli P Jr, Tang A, Yingling JM, Liporace FA, Yoon RS. Fragility fractures of the pelvis and sacrum: current trends in literature. Hip Pelvis 2022;34:69-78.
2. Wilson DG, Kelly J, Rickman M. Operative management of fragility fractures of the pelvis: a systematic review. BMC Musculoskelet Disord 2021;22:717.
3. Arand C, Wagner D, Richards RG, et al. Anatomical evaluation of the transpubic screw corridor based on a 3D statistical model of the pelvic ring. Sci Rep 2021;11:16677.
4. Rommens PM, Graafen M, Arand C, Mehling I, Hofmann A, Wagner D. Minimal-invasive stabilization of anterior pelvic ring fractures with retrograde transpubic screws. Injury 2020;51:340-6.
5. De Bondt S, Carette Y, van Lenthe GH, Herteleer M. Evaluation of the superior pubic ramus and supra acetabular corridors using statistical shape modelling. Surg Radiol Anat 2024;46:1189-97.
6. Routt ML Jr, Simonian PT, Grujic L. The retrograde medullary superior pubic ramus screw for the treatment of anterior pelvic ring disruptions: a new technique. J Orthop Trauma 1995;9:35-44.
7. Chen KN, Wang G, Cao LG, Zhang MC. Differences of percutaneous retrograde screw fixation of anterior column acetabular fractures between male and female: a study of 164 virtual three-dimensional models. Injury 2009;40:1067-72.
8. Attias N, Lindsey RW, Starr AJ, Borer D, Bridges K, Hipp JA. The use of a virtual three-dimensional model to evaluate the intraosseous space available for percutaneous screw fixation of acetabular fractures. J Bone Joint Surg Br 2005;87:1520-3.
9. Shahulhameed A, Roberts CS, Pomeroy CL, Acland RD, Giannoudis PV. Mapping the columns of the acetabulum: implications for percutaneous fixation. Injury 2010;41:339-42.
10. Bi C, Ji X, Wang F, Wang D, Wang Q. Digital anatomical measurements and crucial bending areas of the fixation route along the inferior border of the arcuate line for pelvic and acetabular fractures. BMC Musculoskelet Disord 2016;17:125.
11. Puchwein P, Enninghorst N, Sisak K, et al. Percutaneous fixation of acetabular fractures: computer-assisted determination of safe zones, angles and lengths for screw insertion. Arch Orthop Trauma Surg 2012;132:805-11.
12. Suzuki T, Soma K, Shindo M, Minehara H, Itoman M. Anatomic study for pubic medullary screw insertion. J Orthop Surg (Hong Kong) 2008;16:321-5.
13. Altınayak H, Balta O. Is percutaneous fixation of the superior pubic ramus possible in all types of pelvis. Ulus Travma Acil Cerrahi Derg 2023;29:419-29.
14. Fernandes ML, Dos Santos DG, Costa-Santos C, Pereira PA, Pinho AR, Leite MJ. Iliopubic rami morphology and its vascular relationships in percutaneous retrograde fixation. Surg Radiol Anat 2025;47:200.
15. Jarragh A, Lari A, Shaikh M. A computed tomography (CT) based morphometric study of superior pubic ramus anatomy among Arabs to determine safe intramedullary pubic rami screw insertion. Surg Radiol Anat 2023;45:603-9.
16. Hammond E, Nassereddin A, Costanza M. Anatomy, abdomen and pelvis: external iliac arteries [Internet]. StatPearls Publishing; 2025 [cited 2026 Jan 10]. Available from: https://www.ncbi.nlm.nih.gov/books/NBK519552/.

JMT Journal of Musculoskeletal Trauma

pISSN 3058-6267 · eISSN 3058-6275
J Musculoskelet Trauma 2026;39(2):117-129
https://doi.org/10.12671/jmt.2025.00311

Percutaneous anterior leverage technique for anteromedial cortical support in intertrochanteric femur fractures: a computed tomography–based validation study

Whee Sung Son*, Bum Jin Shim*, Oog-jin Shon

Department of Orthopedic Surgery, Yeungnam University Medical Center, Yeungnam University College of Medicine, Daegu, Korea

Background: Anteromedial cortical support (AMCS) enhances stability in intertrochanteric femur fractures. However, reproducible, validated methods of achieving AMCS have not previously been reported. This study introduces a percutaneous anterior leverage technique and validates its AMCS effects using computed tomography (CT).

Methods: We retrospectively reviewed patients treated by a single surgeon between March 2022 and December 2024. The inclusion criteria were an AO/OTA classification of A1–A3, application of the percutaneous anterior leverage technique, available pre- and postoperative CT, and ≥6 months follow-up. Outcomes included CT-based AMCS (anterior on axial and medial on coronal images, classified as positive, neutral, or negative), time to union, union rate, changes in neck-shaft angle, and treatment failure (varus collapse, blade cut-through, or nonunion without the former two). The risk factors for failure were analyzed.

Results: Of 273 patients reviewed, 53 met the inclusion criteria. Follow-up was at least 6 months in all cases. Positive anterior support was achieved in 37 patients (69.8%) and positive medial support in 42 (79.25%). No patient demonstrated negative anterior support; one (1.9%) had negative medial support. Cortical support improved significantly after surgery. CT images demonstrated significant postoperative improvements (anterior P=0.026; medial P<0.001). Bone union was achieved in 50 patients (94.34%) at a mean of 3.93±1.48 months. The mean change in the neck-shaft angle at last follow-up was 1.75°±2.34° varus. Three patients (5.66%) experienced treatment failure. Anteromedial cortical breakage during follow-up differed between failure and nonfailure groups (P=0.002), but regression identified no independent predictors. No technique-related complications were observed.

Conclusions: Our percutaneous anterior leverage technique produced favorable CT-confirmed AMCS and high union with low failure, supporting its safety and effectiveness in intertrochanteric femur fractures.

Level of evidence: IV.

Keywords: Hip fractures; X-ray computed tomography; Internal fracture fixation; Aged

Original Article

Received: September 24, 2025
Revised: December 9, 2025
Accepted: December 10, 2025

Correspondence to:
Whee Sung Son
Department of Orthopedic Surgery, Yeungnam University Medical Center, Yeungnam University College of Medicine, 170 Hyonchung-ro, Nam-gu, Daegu 42415, Korea
Tel: +82-53-620-3640
Email: oswsson@gmail.com

Co-Correspondence to:
Oog-jin Shon
Department of Orthopedic Surgery, Yeungnam University Medical Center, Yeungnam University College of Medicine, 170 Hyonchung-ro, Nam-gu, Daegu 42415, Korea
Tel: +82-53-620-3640
Email: ossoj@ynu.ac.kr

*These authors contributed equally to this work as first authors.

Introduction

Background

Femoral intertrochanteric fractures are among the most common types in the geriatric population, and they are considered a life-threatening injury [1]. Potentially fatal complications related to immobilization are frequent, so early rehabilitation is essential [2]. However, early rehabilitation is often difficult to achieve in such patients owing to the high risk of reduction loss, making femoral intertrochanteric fractures particularly challenging to treat.

Anteromedial cortical support (AMCS) is a well-recognized means of addressing these challenges and achieving stable fixation in femoral intertrochanteric fractures [3]. Several studies have reported favorable outcomes, with AMCS providing support between the anteromedial cortex of the head-neck segment and the distal segment. This achieves secondary stability and promotes fracture healing [4-6].

However, surgical methods for achieving AMCS have not been described in detail in the existing literature, and there has been no validation of such techniques. Kim et al. [7] have described eight cases in which a bone hook leverage technique was used. This is performed through the entry incision for intramedullary nailing. Kozono et al. [8] have reported direct reduction using a small elevator in six cases. They note that closed reduction of the anterior cortex is challenging due to the strong attachment of the iliofemoral ligament to the anterior intertrochanteric crest. However, both of these studies were limited by a small number of cases and lacked validation. Furthermore, other studies addressing AMCS did not provide detailed descriptions of surgical methods. Consequently, no study has validated a single technique in an adequately-sized sample.

Objectives

Therefore, the authors of the present study considered it necessary to establish and validate a surgical technique that allows surgeons to obtain AMCS in a reproducible manner. This study introduces the percutaneous anterior leverage technique, providing a detailed description of the method. It also aims to validate its effectiveness. As computed tomography (CT) provides a more accurate assessment than plain radiography, validation was based on CT evaluation.

Methods

Ethics statement

The study adhered to the principles of the 1964 Declaration of Helsinki and its subsequent revisions, and was approved by the Institutional Review Board (IRB) of Yeungnam University Medical Center (IRB No. YUMC 2025-09-019). In accordance with institutional and ethical guidelines, informed consent was obtained from all participants.

Study design

This study was a single-center retrospective case series of patients treated for femoral intertrochanteric fractures.

Setting

This study was conducted at Yeungnam University Medical Center, Daegu, Korea, between March 2022 and December 2024. The surgical indication criteria for applying the technique were as follows: if preoperative CT in either the axial or coronal plane demonstrated loss of AMCS, a closed reduction maneuver was performed before draping. When fluoroscopic evaluation in both the anteroposterior (AP) and lateral views failed to restore positive AMCS, the percutaneous anterior leverage technique was subsequently applied to achieve adequate AMCS (Fig. 1). The procedure was performed by a single orthopedic trauma surgeon (WSS) between March 2022 and December 2024.

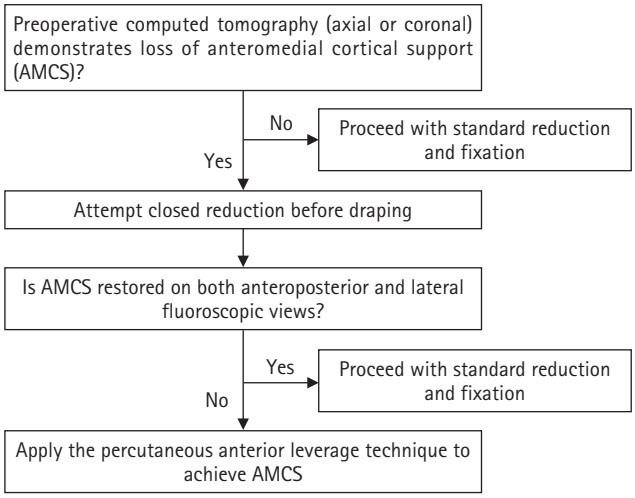

Fig. 1. Clinical decision-making algorithm for applying the percutaneous anterior leverage technique.

https://doi.org/10.12671/jmt.2025.00311

Surgical technique

Each patient was positioned on a fracture table, and their overall limb length and approximate neck-shaft angle were restored using the fracture table prior to draping. A 2 cm incision was made along the Smith-Petersen interval (Fig. 2A). Blunt dissection was then performed using blunt Kelley hemostatic forceps to reach the anterior cortex of the femur. Under a fluoroscopic AP view, the position was adjusted to ensure that the forceps were located at the anteromedial cortex of the fracture site, taking care not to extend medially toward the femoral artery (Fig. 2B, 2C). The forceps were then exchanged for a freer retractor, which was safely advanced and positioned at the anteromedial cortex of the fracture site. Subsequently, fluoroscopy was switched to the lateral view. This enabled confirmation of the correct advancement of the freer retractor into the fracture site (Fig. 2D, 2E). The anteromedial cortex of the proximal segment is usually displaced into the intramedullary space of the distal segment. Therefore, the retractor is advanced obliquely, from cephalad to caudal and from medial to lateral, to gain access. Once fluoroscopic confirmation was obtained, the intramedullary-displaced proximal anteromedial cortex was levered into an extramedullary reduced state with the freer retractor. This achieved a positive AMCS state (Fig. 2F, 2G). A 3.2 mm Steinmann pin was then introduced from the anterolateral cortex of the distal segment and advanced toward the proximal segment through an anterior trajectory for temporary fixation. This avoids the passage of the intramedullary nail (Fig. 2F) [9]. During the procedure, the lateral fluoroscopic view was used to verify positive anterior cortical support, and the AP view was used to verify positive medial cortical support. Following these steps, conventional intramedullary nailing was performed using the TFN-ADVANCED Proximal Femoral Nailing System (TFNA; DePuy Synthes). The anteriorly placed freer retractor did not interfere with nail insertion and maintained AMCS of the proximal segment (Fig. 2H, 2I). After blade insertion, compression was applied through the blade as the retractor was gradually withdrawn. This ensured final compression in a complete positive AMCS state (Fig. 2J). Finally, distal interlocking screws were placed, completing the procedure (Figs. 2K, 3). Throughout the procedure, the lateral fluoroscopic view was obtained not as an axial projection aligning the femoral head-neck with the femoral shaft, but rather, as a 30° oblique tangential projection. This allowed optimal visualization of the anteromedial cortical state [10].

Postoperative management

Postoperatively, weight bearing was initiated as soon as the patient's pain became tolerable, and walker-assisted ambulation was achieved within 2 weeks. The patient was

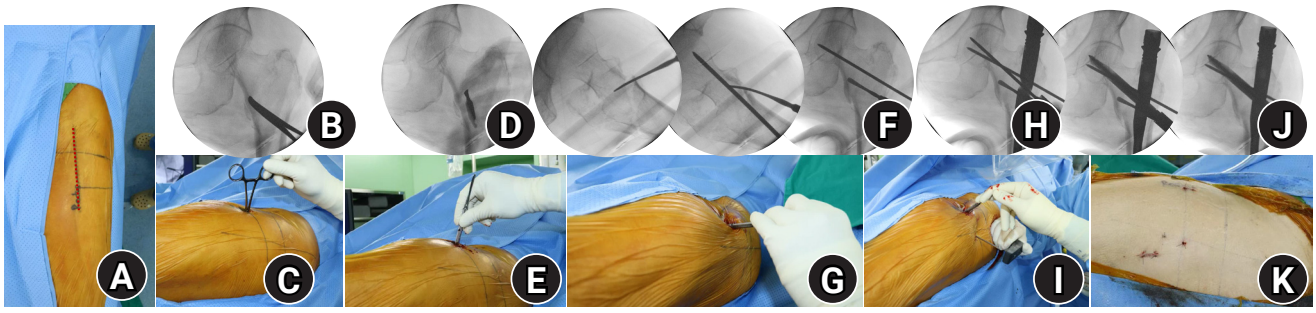

Fig. 2. Intraoperative photographs and fluoroscopic images illustrating the percutaneous anterior leverage technique for achieving anteromedial cortical support (AMCS) in intertrochanteric femur fractures. (A) The red dotted line represents the lateral margin of the rectus femoris, corresponding to the Smith-Petersen interval used for the procedure; (B, C) A small incision is made along the Smith-Petersen interval, followed by blunt dissection with Kelley hemostatic forceps to reach the anteromedial cortex of the femur; (D, E) The forceps are replaced with a freer retractor, which is advanced to the fracture site at the anteromedial cortex; (F, G) The leverage maneuver, in which the freer retractor is used to elevate the intramedullary-displaced proximal anteromedial cortex into an extramedullary reduced position to achieve positive AMCS. This is followed by temporary fixation with a 3.2 mm Steinmann pin; (H, I) The freer retractor remains in place during intramedullary nailing without interfering with the procedure; (J) After blade insertion, compression is applied through the blade while the freer retractor is gradually withdrawn, ensuring final compression with complete positive AMCS; (K) Photograph showing the minimally invasive nature of this approach.

Fig. 3. Radiographic, fluoroscopic, and computed tomography (CT) images from an 83-year-old female patient with a left femoral intertrochanteric fracture (AO/OTA classification A3). (A) Preoperative plain radiographs and CT showing a negative anteromedial cortical support (AMCS) state; (B) Intraoperative fluoroscopic images illustrating the percutaneous anterior leverage technique; (C) Comparative postoperative images from plain radiographs and CT showing that lateral plain radiographs alone do not clearly reveal the AMCS state. This CT shows positive AMCS in both the coronal and axial views; (D) Plain radiographs obtained 3 months postoperatively, showing bone union without complications.

then transferred to a rehabilitation hospital. Follow-up evaluations to monitor rehabilitation progress and assess for any complications were conducted at 1, 2, 3, 5, 7, 10, and 13 months postoperatively.

Participants

The inclusion criteria were (1) femoral intertrochanteric fractures classified as AO/OTA types A1, A2, and A3; (2) use of the percutaneous anterior leverage technique; (3) availability of preoperative and postoperative CT scans; (4) a minimum postoperative follow-up period of 6 months; and (5) availability of complete medical records and radiographic data for review.

Variables

The index exposure (intervention) was the application of the percutaneous anterior leverage technique. The primary outcome was CT-based postoperative AMCS, assessed as anterior cortical support on axial CT, and medial cortical support on coronal CT, each classified as positive, neutral, or negative. Secondary outcomes included bone union (yes/no) and time to union (months), change in neck-shaft angle, treatment failure, and technique-related complications.

Data sources/measurement

Data were collected from institutional medical records on patient demographics, operative times, AO/OTA fracture classifications, and Dorr types. Tip to apex distance (TAD), blade position, the difference between the postoperative and contralateral neck-shaft angles (representing varus or valgus alignment relative to the contralateral hip), and the occurrence of anteromedial cortical breakage during follow-up were assessed using plain radiographs and CT images. These variables were included in an analysis of risk factors for treatment failure. Anteromedial cortical breakage during follow-up was included in the failure analysis because it was anticipated that, even if AMCS was initially achieved, subsequent cortical breakage could nullify this support.

Outcomes were assessed using plain radiographs and CT images. Plain radiographic evaluations assessed time to union, achievement of bone union (defined as bridging callus formation across at least three cortices with no signs of implant failure or further displacement), and the difference in neck-shaft angle between the postoperative period and the final follow-up. This latter measure reflects the degree of varus displacement during the follow-up period. Varus collapse (defined as a decrease in the neck-shaft angle of >10° compared with the postoperative measurement) [11], blade cut-through, and nonunion in the absence of varus collapse or blade cut-through were also evaluated. The presence of any of these three was defined as treatment failure.

https://doi.org/10.12671/jmt.2025.00311

Axial CT images were used to evaluate anterior cortical support, which was classified as positive, neutral, or negative. When the anteromedial cortex of the proximal segment was located anterior to that of the distal segment, anterior cortical support was classified as positive. When both cortices were aligned, it was classified as neutral. When the proximal cortex was located posterior to the distal cortex, it was classified as negative. Coronal CT images were used to assess medial cortical support. This was also classified as positive, neutral, or negative. When the anteromedial cortex of the proximal segment was located medial to that of the distal segment, medial cortical support was classified as positive. When both cortices were aligned, it was classified as neutral. When the proximal cortex was located lateral to the distal cortex, it was classified as negative (Fig. 4). These assessments were performed on both preoperative and postoperative CT scans. Postoperative AMCS status was evaluated as an outcome of the percutaneous anterior leverage technique and was included in the treatment failure risk factor analysis. It was also compared with the preoperative status in each patient to assess the changes resulting from the use of the technique. In addition, we performed subgroup analyses based on patient demographics and fracture characteristics (AO/OTA classification and Dorr type), reporting the postoperative AMCS within each subgroup. Complications such as femoral artery injury associated with the percutaneous anterior leverage technique were also assessed.

Bias

To mitigate bias in this retrospective, single-center study, we employed prespecified eligibility criteria and an indication pathway, including only patients with paired pre- and postoperative CTs, complete records, and a minimum of 6 months of follow-up. CT-based grading of anterior and medial cortical support reduced misclassification compared to plain radiographs. Outcomes—such as union, neck-shaft angle change, and failure components—were defined as a priori using objective radiographic criteria. A single surgeon performed all procedures to minimize variability, while potential confounders, including age, fracture type, position, and TAD, were examined using univariate and multivariable analyses.

Study size

Because this was a single-center retrospective review, no a priori sample-size calculation was performed; instead, the study size was determined by the number of patients who met all eligibility criteria during the study period.

Statistical methods

We used IBM SPSS ver. 27.0 (IBM Corp.) for all analyses. Continuous data were tested for normality of distribution. Accordingly, the Student t-test or the Mann-Whitney U test was used to compare two groups. Categorical data were evaluated using Pearson chi-square test or Fisher exact test. Variables associated with treatment failure were assessed

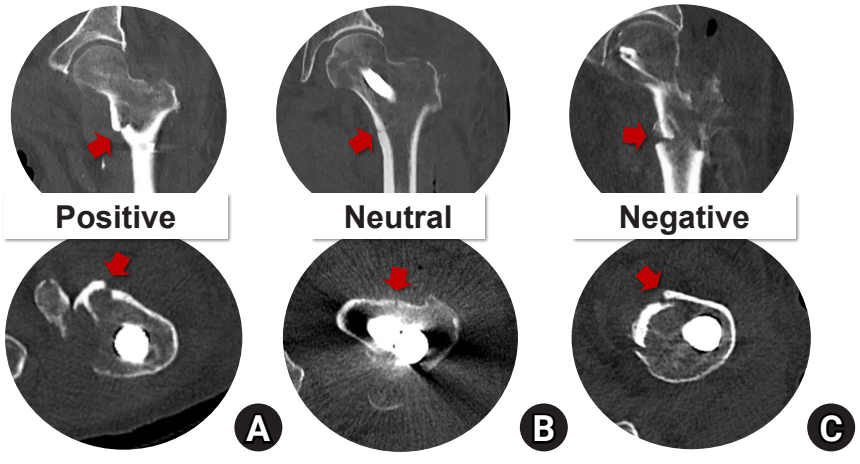

Fig. 4. Computed tomography (CT) images of the anteromedial cortical support states in intertrochanteric femur fractures. The upper row shows coronal CT images illustrating medial cortical support, and the lower row shows axial CT images illustrating anterior cortical support. (A) Positive cortical support; (B) neutral cortical support; (C) negative cortical support. The red arrow indicates the anteromedial cortical state.

using univariate analysis. A multivariate logistic regression model was intended to further analyze the variables found to be statistically significant in the univariate analysis. P-values <0.05 were deemed statistically significant.

Results

Participants

Among 273 patients reviewed, 53 patients met the inclusion criteria and were enrolled in the study (Fig. 5). The mean age of the enrolled patients was 81.36±8.43 years, and the sample comprised 22 males and 31 females. The AO/OTA classification was type A1 in 24 cases (45.28%), type A2 in 21 cases (39.62%), and type A3 in eight cases (15.09%). The Dorr classification was type A in 16 patients (30.19%), type B in 24 patients (45.28%), and type C in 13 patients (24.53%).

On preoperative axial CT scans, anterior cortical support was positive in three patients (5.66%), neutral in four patients (7.55%), and negative in 46 patients (86.79%). In the coronal view, medial cortical support was positive in five patients (9.43%), neutral in nine patients (16.98%), and negative in 39 patients (73.58%). Thus, most patients demonstrated negative AMCS in both the axial and coronal views.

The mean TAD was 10.75±3.77 mm, and no patient had a TAD greater than 25 mm. Blade position was center-center in 12 patients (22.64%), inferior-center in 38 patients (71.70%), and inferior-posterior in three patients (5.66%). The mean difference between the postoperative and contralateral neck-shaft angles was 3.09°±4.16° in valgus. This indicated that the postoperative neck-shaft angle was slightly more valgus than the contralateral side. The mean operative time was 34.15±10.21 minutes. During the follow-up period, there were two cases (3.77%) of anteromedial cortical breakage (Table 1).

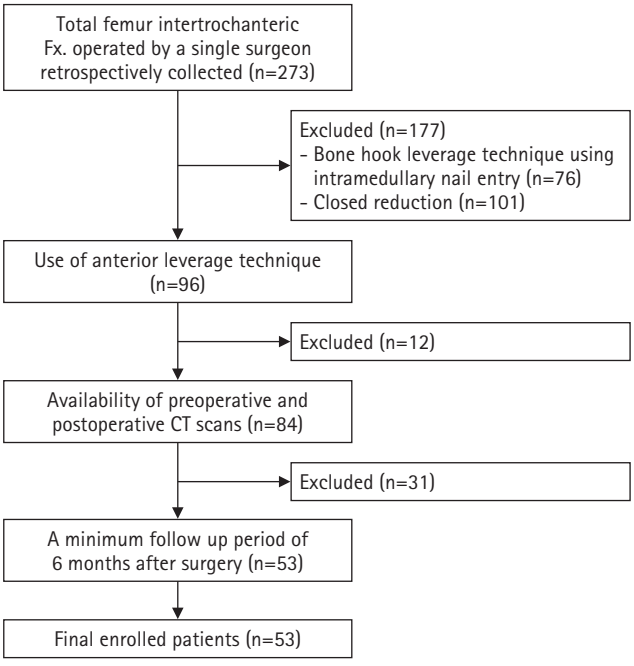

Fig. 5. Flowchart illustrating the patient selection process. Fx, fracture; CT, computed tomography.

Main results

The postoperative axial CT scans revealed that 37 patients (69.81%) had positive anterior cortical support, 16 patients (30.19%) had neutral support, and none had negative support. In the coronal CT scans, 42 patients (79.25%)

Table 1. Demographic and fracture characteristics of patients (n=53)

Characteristic	Value
Age (yr)	81.36±8.43
Sex (male:female)	22:31
AO/OTA classification	
A1	24 (45.28)
A2	21 (39.62)
A3	8 (15.09)
Dorr type	
A	16 (30.19)
B	24 (45.28)
C	13 (24.53)
Preoperative anterior cortical support	
Positive	3 (5.66)
Neutral	4 (7.55)
Negative	46 (86.79)
Preoperative medial cortical support	
Positive	5 (9.43)
Neutral	9 (16.98)
Negative	39 (73.58)
Tip to apex distance (mm)	10.75±3.77
Blade position	
Center (anteroposterior)–center (lateral)	12 (22.64)
Inferior (anteroposterior)–center (lateral)	38 (71.70)
Inferior (anteroposterior)–posterior (lateral)	3 (5.66)
Neck-shaft valgus angle difference (postoperative–contralateral) (°)	3.09±4.16
Operative time (min)	34.15±10.21
Follow-up (mo)	8.79±4.35

Values are presented as mean±standard deviation or number (%).

https://doi.org/10.12671/jmt.2025.00311

demonstrated positive medial cortical support, 10 patients (18.87%) neutral support, and one patient (1.89%) negative support. There was a significant preoperative to postoperative improvement in anterior cortical support on the axial CT views (P=0.026), as well as in medial cortical support on the coronal views (P<0.001) (Table 2).

Bone union was achieved in 50 patients (94.34%), with a mean time to union of 3.93±1.48 months. The mean change in the neck-shaft angle between the postoperative period and the final follow-up was 1.75°±2.34° in varus. Nonunion in the absence of varus collapse or blade cut-through occurred in one patient (1.89%), and blade cut-through in one patient (1.89%). Varus collapse was seen in one patient (1.89%), despite the achievement of bone union during long-term follow-up. This case was classified as a treatment failure. Thus, three cases (5.66%) in total were categorized as treatment failures (Table 3). Interestingly, all instances of anteromedial cortical breakage during follow-up were in patients who experienced treatment failure (Fig. 6). Specifically, it occurred in the patients with blade cut-through and varus collapse. It was not seen in the patient with nonunion in the absence of varus collapse or blade cut-through, in whom reduction was maintained, but bone union was not achieved. This patient had multiple comorbidities—including bladder cancer, chronic kidney disease, cerebral infarction, alcoholic liver cirrhosis, diabetes, and hypertension—and it is presumed that these host factors contributed to the development of nonunion.

In subgroup analyses evaluating postoperative AMCS across demographic and fracture-related subgroups, age and Dorr type showed significant differences in postop-

Table 2. Preoperative and postoperative anterior and medial cortical support in patients with intertrochanteric femur fractures treated with the percutaneous anterior leverage technique

Cortical support	Preoperative	Postoperative	P-value
Anterior cortical support			0.026*
Positive	3 (5.66)	37 (69.81)	
Neutral	4 (7.55)	16 (30.19)	
Negative	46 (86.79)	0 (0.00)	
Medial cortical support			<0.001*
Positive	5 (9.43)	42 (79.25)	
Neutral	9 (16.98)	10 (18.87)	
Negative	39 (73.58)	1 (1.89)	

Values are presented as number (%).
*P<0.05

Table 3. Clinical and radiographic characteristics of treatment failure patients

Case	Age (yr)	Sex	AO/OTA classification	Dorr type	Preoperative anterior cortical support	Preoperative medial cortical support	Tip to apex distance (mm)	Blade position	Neck-shaft valgus angle (°) difference (postoperative–contralateral)	Operative time (min)	Postoperative anterior cortical support	Postoperative medial cortical support	Anteromedial cortical breakage during follow-up
8. Nonunion in the absence of varus collapse or blade cut-through	81	Male	A2	B	Negative	Neutral	9.2	Inferior (AP)–center (lateral)	4[a]	33	Positive	Positive	None
20. Varus collapse	88	Female	A2	B	Negative	Negative	15.2	Center (AP)–center (lateral)	0	50	Neutral	Neutral	Occurred
51. Blade cut-through	80	Female	A3	C	Negative	Negative	7.7	Inferior (AP)–center (lateral)	7[a]	48	Neutral	Positive	Occurred

AP, anteroposterior.
[a]Positive values indicate valgus alignment compared with the contralateral hip, and negative values indicate varus alignment.

erative anterior cortical support. Patients with postoperative positive anterior cortical support had a mean age of 83.0±6.6 years, whereas those with neutral cortical support had a mean age of 77.6±11.0 years (P=0.030). Regarding Dorr classification, type C showed 11 postoperative anterior cortical positive (84.62%) and two neutral (15.38%); type B showed 19 positive (79.17%) and five neutral (20.83%); and type A showed seven positive (43.75%) and nine neutral (56.25%; P=0.037). No significant differences were observed in the other subgroup categories with respect to postoperative AMCS (Table 4).

In a comparison of the treatment failure and success groups for risk factor analysis, we found no significant differences in the demographic or fracture variables. Only anteromedial cortical breakage during follow-up differed significantly between the two groups (P=0.002) (Table 5). As univariate logistic regression analysis did not identify any significant factors, multivariate logistic regression analysis was not performed (Table 6). No complications associated with the percutaneous anterior leverage technique occurred.

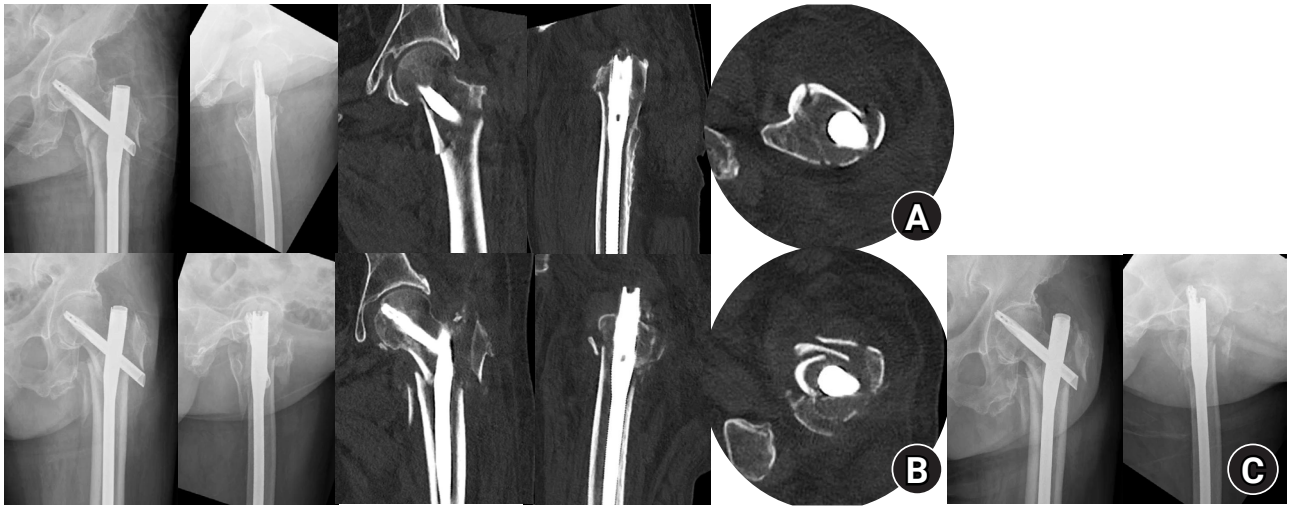

Fig. 6. Radiographic images of an 82-year-old female patient with an AO/OTA A3 intertrochanteric femur fracture treated with the percutaneous anterior leverage technique. (A) Postoperative radiographs showing positive medial cortical support and neutral anterior cortical support. (B) Radiographs obtained 3 weeks postoperatively at the first outpatient visit, showing progression to negative anteromedial cortical support with cortical breakage. (C) Radiographs obtained 7 weeks postoperatively, demonstrating blade cut-through.

Table 4. Subgroup analyses of postoperative anteromedial cortical support according to patient demographics and fracture characteristics

Variable	Anterior cortical support				Medial cortical support			
	Positive (n=37)	Neutral (n=16)	Negative (n=0)	P-value	Positive (n=42)	Neutral (n=10)	Negative (n =1)	P-value
Age (yr)	83.0±6.6	77.6±11.0		0.030*	81.2±9.1	81.8±5.9	83±0	0.847
Sex				0.068				0.287
Male (n=22)	12 (54.55)	10 (45.45)	0		16 (72.73)	6 (27.27)	0	
Female (n=31)	25 (80.65)	6 (19.35)	0		26 (83.87)	4 (12.90)	1 (1.89)	
AO/OTA classification				0.778				0.199
A1 (n=24)	18 (75.00)	6 (25.00)	0		21 (87.50)	3 (12.50)	0	
A2 (n=21)	14 (66.67)	7 (33.33)	0		16 (76.19)	5 (23.81)	0	
A3 (n=8)	5 (62.50)	3 (37.50)	0		5 (62.50)	2 (25.00)	1 (12.50)	
Dorr type				0.037*				0.278
A (n=16)	7 (43.75)	9 (56.25)	0		11 (68.75)	5 (31.25)	0	
B (n=24)	19 (79.17)	5 (20.83)	0		21 (87.50)	3 (12.50)	0	
C (n=13)	11 (84.62)	2 (15.38)	0		10 (76.92)	2 (15.38)	1 (7.69)	

Values are presented as mean±standard deviation or number (%).
*P<0.05.

https://doi.org/10.12671/jmt.2025.00311

Table 5. Comparisons between the treatment success and treatment failure groups in intertrochanteric femur fractures managed with the percutaneous anterior leverage technique

Characteristic		Treatment success group (n=50)	Treatment failure group (n=3)	P-value
Age (yr)		81.3±8.4	83.0±4.4	0.732
Sex	Male	21 (42)	1 (33)	>0.999
	Female	29 (58)	2 (67)	
AO/OTA classification	A1	24 (48)	0	0.185
	A2	19 (38)	2 (67)	
	A3	7 (14)	1 (33)	
Dorr type	A	15 (30)	1 (33)	0.787
	B	22 (44)	2 (67)	
	C	13 (26)	0	
Tip to apex distance (mm)		10.7±3.8	10.7±4.0	0.983
Blade position	Center (AP)–center (lateral)	11 (22)	1 (33)	>0.999
	Inferior (AP)–center (lateral)	36 (72)	2 (67)	
	Inferior (AP)–posterior (lateral)	3 (6)	0	
Neck-shaft angle (°) difference (postoperative–contralateral)		3.06±4.23	3.51±2.03	0.809
Anterior cortical support	Positive	36 (72)	1 (33)	0.213
	Neutral	14 (28)	2 (67)	
	Negative	0	0	
Medial cortical support	Positive	40 (80)	1 (33)	0.510
	Neutral	9 (18)	2 (67)	
	Negative	1 (2)	0 (0)	
Anteromedial cortical breakage during follow-up	Occurred	0	2 (67)	0.002*
	None	50 (100)	1 (33)	

Values are presented as mean±standard deviation or number (%).
AP, anteroposterior.
*P<0.05.

Table 6. Univariate logistic regression analysis of factors associated with treatment failure

Characteristic		OR	95% CI	P-value
Age		1.028	0.881–1.200	0.726
Sex	Male	1	-	-
	Female	1.448	0.123–17.041	0.768
AO/OTA classification	A1	1	-	-
	A2	170,049,980.6	0.000–0.000	0.998
	A3	230,782,116.5	0.000–0.000	0.998
Dorr type	A	1	-	-
	B	1.364	0.113–16.423	0.807
	C	0.000	0.000–0.000	0.999
Tip to apex distance		0.997	0.729–1.363	0.983
Blade position	Center (AP)–center (lateral)	1		-
	Inferior (AP)–center (lateral)	0.611	0.050–7.397	0.699
	Inferior (AP)–posterior (lateral)	0.000	0.000–0.000	0.999
Neck-shaft angle difference (postoperative–contralateral)		1.034	0.795–1.345	0.805
Anterior cortical support	Positive	1	-	-
	Neutral	5.143	0.431–61.324	0.195
Medial cortical support	Positive	1	-	-
	Neutral	2.222	0.181–27.262	0.532
	Negative	0.000	0.000–0.000	>0.999
Anteromedial cortical breakage during follow-up	Occurred	1	-	-
	None	80,773,742,143	0.000–0.000	0.999

OR, odds ratio; CI, confidence interval; AP, anteroposterior.
*P<0.05.

Discussion

Key results

This study demonstrates that the percutaneous anterior leverage technique is a reproducible and effective method for achieving AMCS in intertrochanteric femur fractures. Using CT for validation, the technique consistently converted preoperative negative AMCS into positive or neutral states, resulting in a high union rate and low incidence of treatment failure. Importantly, no complications related to the procedure were observed. To our knowledge, this is the first study to provide a detailed description of a surgical method for obtaining AMCS and to validate its clinical effectiveness through CT-based evaluation, thereby addressing a critical unresolved issue in the current literature.

Interpretation/comparison with previous studies

To date, only two studies have provided specific descriptions of direct reduction techniques aimed at achieving AMCS. Kozono et al. [8] reported six cases treated with various direct reduction approaches, in which five cases (83.33%) achieved neutral or positive anterior cortical support, while one case (16.67%) demonstrated negative support. Medial cortical support outcomes were not reported in their study. Kim et al. [7] described the use of bone hook leverage via incision of the intramedullary nail entry in eight cases. Although they assessed reduction quality based on whether displacement of the anterior and medial cortices was <1 cortical thickness, they did not classify outcomes into positive, neutral, or negative categories. Among the eight cases, five cases (62.50%) demonstrated <1 cortical thickness displacement in both the anterior and medial cortices, whereas the remaining three cases (37.50%) had ≥1 cortical thickness displacement in at least one of the two cortices. Because their study did not employ a clear classification system for AMCS, the interpretation of their outcomes is limited with respect to the AMCS concept.

In this study, we observed negative AMCS in only one patient (1.89%), with all other patients achieving at least neutral AMCS. Positive anterior cortical support was achieved in 69.81% and positive medial cortical support in 79.25%. Although AMCS appeared to be restored on intraoperative fluoroscopy, postoperative CT did not demonstrate positive support in all cases. This discrepancy is likely attributable to differences between plain radiographic and CT-based assessments of AMCS, as described in detail later in the Discussion. A direct comparison with other techniques is not feasible because previous studies have not validated a single method for achieving AMCS. Nevertheless, the bone union rate of 94.34% in this older cohort (mean age, 81.36±8.43 years) may be considered favorable. The percutaneous anterior leverage technique for achieving AMCS offers several advantages. First, it utilizes a separate incision and anterior plane, which do not interfere with the intramedullary nailing procedure. Second, maintaining leverage with the freer retractor throughout the nailing process helps to prevent re-displacement during intramedullary nail fixation. Finally, because the procedure is performed percutaneously, it is minimally invasive and does not appear to substantially increase operative time (mean operative time, 34.15±10.21 minutes), although no direct comparison with other methods was possible. However, potential pitfalls of this technique include the risk of injury to the medial femoral circumflex artery and the possibility of lateral femoral cutaneous nerve injury, even though no such events were observed in the present cohort. Therefore, careful attention to these anatomical structures is warranted during the procedure.

Subgroup analyses of postoperative AMCS across demographic and fracture-related categories revealed that older patients were more likely to achieve postoperative positive anterior cortical support than neutral support. Similarly, patients with Dorr type C and type B demonstrated higher rates of postoperative positive anterior cortical support compared with neutral support. Notably, no cases of negative anterior cortical support were observed in this study. These findings suggest that the percutaneous anterior leverage technique may offer particular advantages in patient groups—such as older individuals and those with Dorr type B or C morphology—who are generally considered at higher risk for treatment failure.

Our risk factor analysis for treatment failure found no significant relationships between treatment failure and patient variables, including age, sex, AO/OTA classification, and Dorr type. Notably, eight patients (15.09%) had AO/OTA type A3 fractures, which are generally considered to carry a high risk of fixation failure, yet no significant association was observed. This suggests that favorable outcomes may be achieved even in A3 intertrochanteric fractures when AMCS is obtained using this technique. The mean TAD was 10.75±3.77 mm, and no patient had a TAD greater than 25 mm. Blade position was not unfavorable in any of the patients [12], and the neck-shaft angle compared with the contralateral side was, on average, 3.09°±4.16° in valgus. All of these fracture characteristics are considered acceptable. However, anteromedial cortical breakage during follow-up was significantly correlated with treatment failure (P=0.002 in a comparison between the treatment failure and success groups). However, statistical significance was not confirmed in a regression analysis. Anteromedial cortical breakage was observed in the patient with varus collapse and the patient with blade cut-through. In contrast, reduction was maintained in the patient with nonunion without varus collapse or blade cut-through, and anteromedial cortical breakage did not occur. These findings suggest that, even when AMCS is initially achieved, subse-

https://doi.org/10.12671/jmt.2025.00311

quent anteromedial cortical breakage can result in reduction loss, thereby increasing the risk of treatment failures such as varus collapse or blade cut-through. Thus, careful monitoring for anteromedial cortical breakage during follow-up is warranted. However, further studies with more cases of treatment failure are required to validate this observation. Moreover, because the temporal relationship could not be determined, it remains unclear whether anteromedial cortical breakage was a cause or a consequence of treatment failure, limiting the interpretation of this finding. In addition, although not observed in the cohort of the present study, it is reasonable to assume that preoperative anteromedial cortical comminution would diminish the effectiveness of the percutaneous anterior leverage technique, as the technique relies on an intact cortical buttress to achieve and maintain reduction. In such cases, the method may be insufficient to provide durable stability, and the development of additional strategies or adjunctive techniques to ensure reliable fixation may be required.

Previous studies have raised concerns about neutral cortical support. Li et al. [13] reported that among 46 patients, 16 patients (34.8%) with intraoperative neutral medial cortical support progressed to negative cortical support at 6 months postoperatively. They concluded that neutral cortical support, particularly medial, as assessed by fluoroscopy, is associated with a high rate of fracture reduction loss during follow-up. In the present study, CT imaging found that 16 of the 53 patients (30.19%) had neutral anterior cortical support, and 10 (18.87%) had neutral medial cortical support. However, despite these numbers, only three cases (5.66%) of treatment failure were observed. This may be explained by Mao et al. [4]'s suggestion that previous studies may have misclassified cases of negative cortical support as neutral because evaluations were based on plain radiographs rather than CT. As our study validated cortical support states using CT, the assessments were likely to have been more accurate. Moreover, we did not find neutral cortical support to be a significant risk factor in our treatment failure analysis, suggesting that neutral cortical support may be acceptable. Mao et al. [4] have further posited that poor outcomes following neutral cortical support could result from secondary interfragmentary movement or sliding, which may lead to loss of immediate postoperative neutral reduction. However, in the percutaneous anterior leverage technique, the freer retractor used to maintain AMCS is removed only after compression has been performed through the blade. This ensures that compression is achieved in the AMCS position. This approach may have helped to prevent changes from neutral to negative cortical support [11]. In summary, neutral cortical support, as assessed by CT, combined with intraoperative blade compression to prevent secondary interfragmentary movement, does not appear to be a risk factor for treatment failure and may be considered an acceptable outcome.

Limitations

First, it included only 53 patients, so further studies with larger sample sizes are needed. However, to our knowledge, this is the largest study to date that has focused on a single technique for achieving AMCS. Second, only three patients experienced treatment failure, which limited the validity and reliability of the risk factor analysis. Studies with larger samples are needed to obtain larger numbers of treatment failure cases. Third, bone mineral density (BMD) was not included as a variable in this study. Because incorporating only patients with available BMD measurements would have substantially reduced the sample size, it was excluded; nevertheless, given that bone quality can significantly influence fixation stability and fracture healing, this remains an important limitation. Fourth, comparative studies that include other techniques are needed to fully establish the utility of this method. Finally, all surgeries were performed by a single surgeon. Future multicenter studies with multiple surgeons would strengthen the generalizability of the findings.

Despite these limitations, the findings of this study allow for the proposal of a practical clinical decision pathway for applying the percutaneous anterior leverage technique. In patients with intertrochanteric femur fractures—particularly unstable AO/OTA A2 or A3 patterns—preoperative CT should first be evaluated for loss of AMCS. When the AMCS loss is identified and the anteromedial cortex is intact without comminution, a closed reduction maneuver is recommended before draping. If intraoperative fluoroscopic assessment in both AP and lateral views confirms restoration of AMCS, standard reduction and fixation may proceed. However, if both anterior and medial cortical support cannot be restored, the percutaneous anterior leverage technique should be applied to achieve adequate reduction, followed by fracture site compression to maintain

the achieved AMCS. Postoperative CT should then be used to confirm both anterior and medial cortical support in either a neutral or positive state, as discrepancies between intraoperative fluoroscopy and postoperative CT assessment may occur. When postoperative AMCS is confirmed on CT, immediate weight bearing should be initiated, with continued surveillance for potential anteromedial cortical breakage during the follow-up period (Fig. 7).

Conclusions

The percutaneous anterior leverage technique for AMCS in femoral intertrochanteric fractures resulted in positive anterior cortical support in 69.81% and positive medial cortical support in 79.25% of cases, as evidenced by CT imaging. Only one of the 53 patients showed negative medial cortical support. In addition, 94.34% of patients achieved bone union without technique-related complications. These findings suggest that the percutaneous anterior leverage technique is a safe and effective method with which to achieve AMCS in femoral intertrochanteric fractures.

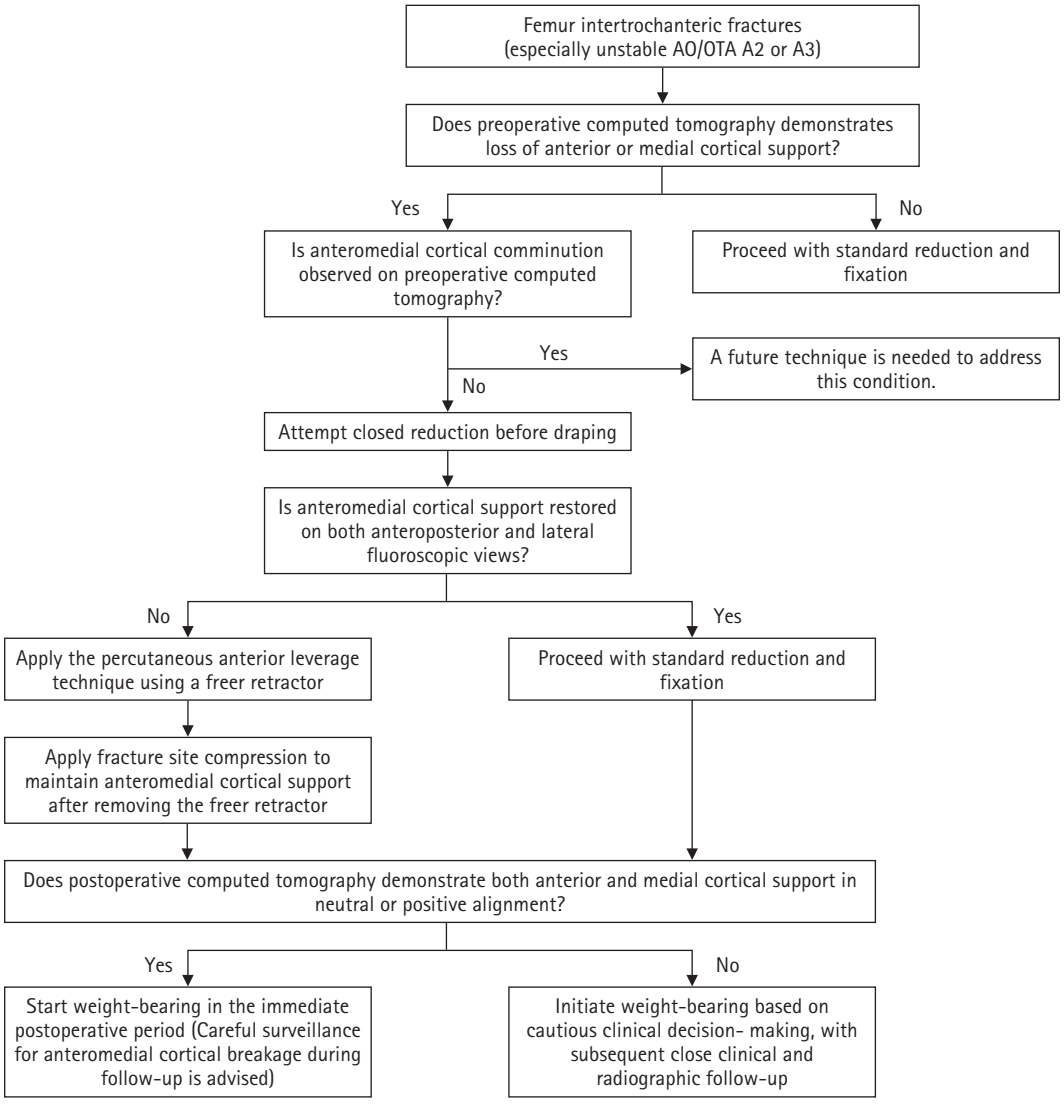

Fig. 7. Clinical algorithm providing practical guidance for application of the percutaneous anterior leverage technique.

https://doi.org/10.12671/jmt.2025.00311

Article Information

Author contributions

Conceptualization: WSS. Data curation: WSS, BJS, OS. Formal analysis: WSS, BJS, OS. Funding acquisition: WSS. Investigation: WSS, BJS, OS. Methodology: WSS. Validation: WSS, BJS, OS. Writing–original draft: WSS, BJS. Writing–review & editing: WSS, BJS, OS. All authors read and approved the final manuscript.

Conflicts of interest

No potential conflict of interest relevant to this article was reported.

Funding

This work was supported by the 2024 Yeungnam University Research Grant (224A580029).

Data availability

Contact the corresponding author for data availability.

Acknowledgments

None.

Supplementary materials

None.

References

1. Kim SH, Jang SY, Cha Y, et al. The impact of hospital volume and region on mortality, medical costs, and length of hospital stay in elderly patients following hip fracture: a nationwide claims database analysis. Clin Orthop Surg 2025;17:80-90.
2. Jang BW, Kim JW, Nho JH, et al. Hip fractures in centenarians: functional outcomes, mortality, and risk factors from a multicenter cohort study. Clin Orthop Surg 2023;15:910-6.
3. Lim EJ, Sakong S, Son WS, Cho JW, Oh JK, Kim CH. Comparison of sliding distance of lag screw and nonunion rate according to anteromedial cortical support in intertrochanteric fracture fixation: a systematic review and meta-analysis. Injury 2021;52:2787-94.
4. Mao W, Liu CD, Chang SM, Yang AL, Hong CC. Anteromedial cortical support in reduction of trochanteric hip fractures: from definition to application. J Bone Joint Surg Am 2024;106:1008-18.
5. Chang SM, Zhang YQ, Ma Z, Li Q, Dargel J, Eysel P. Fracture reduction with positive medial cortical support: a key element in stability reconstruction for the unstable pertrochanteric hip fractures. Arch Orthop Trauma Surg 2015;135:811-8.
6. Xie W, Shi L, Zhang C, et al. Anteromedial cortical support reduction of intertrochanteric fractures-A review. Injury 2024;55:111926.
7. Kim Y, Dheep K, Lee J, et al. Hook leverage technique for reduction of intertrochanteric fracture. Injury 2014;45:1006-10.
8. Kozono N, Ikemura S, Yamashita A, Harada T, Watanabe T, Shirasawa K. Direct reduction may need to be considered to avoid postoperative subtype P in patients with an unstable trochanteric fracture: a retrospective study using a multivariate analysis. Arch Orthop Trauma Surg 2014;134:1649-54.
9. Cho WT, Cho JW, Yoon YC, Kim Y, Oh CW, Oh JK. Provisional pin fixation: an efficient alternative to manual maintenance of reduction in nailing of intertrochanteric fractures. Arch Orthop Trauma Surg 2016;136:55-63.
10. Chen SY, Chang SM, Tuladhar R, et al. A new fluoroscopic view for evaluation of anteromedial cortex reduction quality during cephalomedullary nailing for intertrochanteric femur fractures: the 30° oblique tangential projection. BMC Musculoskelet Disord 2020;21:719.
11. Song H, Chang SM, Hu SJ, Du SC, Xiong WF. Calcar fracture gapping: a reliable predictor of anteromedial cortical support failure after cephalomedullary nailing for pertrochanteric femur fractures. BMC Musculoskelet Disord 2022;23:175.
12. Lee CH, Su KC, Chen KH, Pan CC, Wu YC. Impact of tip-apex distance and femoral head lag screw position on treatment outcomes of unstable intertrochanteric fractures using cephalomedullary nails. J Int Med Res 2018;46:2128-40.
13. Li SJ, Kristan A, Chang SM. Neutral medial cortical relation predicts a high loss rate of cortex support in pertrochanteric femur fractures treated by cephalomedullary nail. Injury 2021;52:3530-1.

JMT Journal of Musculoskeletal Trauma

pISSN 3058-6267 · eISSN 3058-6275
J Musculoskelet Trauma 2026;39(2):130-139
https://doi.org/10.12671/jmt.2025.00353

Biomechanical comparison of anatomically precontoured patellar plate, anterior tension wiring through cannulated screws, and double-sided plating in patellar fractures using a synthetic bone model

Abdullah M. Aljeaid[1,*], Wonseok Choi[2,*], Jeong-Seok Choi[2], Youngsig Choi[3], Jiyeon Bae[3], Jong-Keon Oh[2], Jae-Woo Cho[2]

[1]Department of Orthopedic Surgery, Prince Sultan Military Medical City, Riyadh, Saudi Arabia
[2]Department of Orthopedic Surgery, Korea University Guro Hospital, Korea University School of Medicine, Seoul, Korea
[3]Jeil Medical Corporation R&D Center, Seoul, Korea

Background: Patellar fractures are common injuries that require stable fixation to achieve optimal healing and restoration of knee function. This study aimed to analyze the mechanical properties of an anatomically precontoured patellar plate and to compare its maximum tensile load-bearing capacity with that of anterior tension wiring through cannulated screws and double-sided plating for the fixation of patellar fractures.

Methods: Artificial Sawbones with a standardized transverse fracture line were used to simulate patellar fractures. Each sawbone was attached to polyester bands, and this fracture model was applied consistently across all test samples. To evaluate mechanical properties of the anatomically precontoured patellar plate (model code 25-ANPA-209) made of ASTM F67 titanium, static tensile strength testing and dynamic tensile strength testing were performed, with seven samples prepared for each test. For comparison of maximum tensile load capacity among the anatomically precontoured patellar plate, anterior tension wiring through cannulated screws, and double-sided plating, five samples were prepared for each fixation group. All specimens were tested using a tension/compression testing machine.

Results: In the static tensile strength test, all seven samples exhibited a maximum tensile load capacity above 844 N without any fractures or failure points. The dynamic tensile strength test showed that all seven samples completed 10,000 cycles without deformation or damage to the anatomically precontoured patellar plate. When comparing maximum tensile load capacity, the anatomically precontoured patellar plate exhibited a significantly higher maximum tensile load-bearing capacity than anterior tension wiring through cannulated screws and double-sided plating.

Conclusions: The anatomically precontoured patellar plate demonstrated satisfactory mechanical performance, successfully meeting the criteria of both static and dynamic tensile strength testing, and showed superior maximum tensile load-bearing capacity compared with the other fixation methods evaluated. These findings suggest that the anatomically precontoured patellar plate may represent a reliable fixation option for the management of patellar fractures.

Level of evidence: V.

Keywords: Patella; Fracture; Bone plates; Plating; Biomechanical phenomena

Original Article

Received: November 14, 2025
Revised: February 6, 2026
Accepted: February 10, 2026

Correspondence to:
Jae-Woo Cho
Department of Orthopedic Surgery, Korea University Guro Hospital, 148 Gurodong-ro, Guro-gu, Seoul 08308, Korea
Tel: +82-2-2626-1869
Email: jaewoocho@korea.ac.kr

*Abdullah M. Aljeaid and Wonseok Choi contributed equally to this study as co-first authors.

Introduction

Background

Patellar fractures are rare, comprising merely 0.5%–1.5% of total bone fractures [1]. The primary objective in managing patellar fractures is to achieve accurate anatomical alignment of the fracture and articular surface while providing stable fixation to enable early knee joint rehabilitation [2]. Several approaches have been used in recent decades to stabilize patellar fractures, with various clinical and biomechanical investigations comparing and evaluating these approaches [3,4]. Traditional tension-band wiring with K-wires has been commonly employed to treat patellar fractures by converting the tensile forces of the quadriceps on the anterior surface of the patella into compressive forces at the articular surface. Modified techniques using cannulated screws with anterior tension wiring have also been developed to provide enhanced stability [5]. Despite their potential to yield favorable clinical outcomes, these methods are associated with several drawbacks, including the possibility of pin migration, which can lead to soft tissue irritation, and low mechanical properties, which are a risk factor for loss of reduction and thus are not suitable for comminuted patellar fractures [6,7].

Nowadays, plates are a promising alternative for the fixation of patellar fractures. These implants are characterized by their relatively smaller size and versatile design, offering distinct advantages over traditional techniques (tension-band wiring with K-wires or cannulated screws). Multiple biomechanical studies have shown superior outcomes of patellar plates compared with traditional fixations. Besides being biomechanically robust, patellar plates offer further advantages. They are favorable for comminuted fractures, reducing complications and minimizing reoperation procedures [8]. The empty holes in the plate can be effectively used for suture fixation of the retinaculum or tendinous tissues (quadriceps and patellar tendons). However, there are concerns associated with their use. For example, low-profile mesh plates require extensive intraoperative contouring to fit the patella's anatomy, whereas locking plates, with their uniplanar anterior surface design, provide inadequate coverage for comminuted inferior pole fractures [9,10]. Similarly, with double-sided plating, collisions of the drill with already inserted screws on the opposite side might occur [11].

Therefore, we designed our plate to address the potential disadvantages of other patellar plates. Specifically, the plate was designed to fit the anterior surface of the patella with a low-profile so that bending of the plate would not be necessary and to cover the inferior pole of patella.

Objectives

We hypothesized that anterior plating using an anatomically precontoured patellar plate would demonstrate comparable or superior maximum load-bearing capacity compared with other fixation methods, including anterior tension wiring using cannulated screws and double-sided plating.

This study aimed to perform a biomechanical analysis of the anatomically precontoured patellar plate and compare its maximum tensile load-bearing capacity to anterior tension wiring through cannulated screws and double-sided plating for patellar fractures.

Methods

Ethics statement

This biomechanical study was conducted at the Jeil Medical Corporation Test Lab in Seoul, Korea. Institutional Review Board approval was not required as this study utilized artificial sawbone models.

Fracture model

Synthetic bone blocks with a density of 30 pound per cubic foot (PCF; Sawbones, model 1522-04, Pacific Research Laboratories) with dimensions of 130 mm×180 mm×40 mm were used for biomechanical testing. Thirty PCF was chosen to replicate the characteristics of the human patella, which has a compressive strength between 3 and 30 MPa, and a tensile strength of 2–20 MPa [12]. We developed an artificial patellar fracture model (width, 44 mm; thickness, 20 mm) composed of cortical and cancellous bone, attached to a polyester band (width, 24 mm; thickness, 12 mm) to simulate the quadriceps and patellar tendons, representing the knee joint's extensor mechanism. We created a transverse fracture line on the middle of the sawbone based on our previous study, which included using a three-dimensional computed tomography scan to analyze the location and frequency of fracture lines in patellar fractures [13]. This transverse fracture model was selected

for several important clinical reasons. First, in comminuted patellar fractures (type C3 according to the AO/OTA classification), the surgical strategy involves converting the complex fracture pattern to a simplified configuration using auxiliary fixation methods such as screws and miniplates before applying the main definitive fixation [2,13]. This approach neutralizes vertical fracture lines, coronal splits, or satellite fragments, effectively reducing a type C3 fracture to a type C1 pattern with a primary horizontal fracture line [13]. Second, the transverse fracture model allows for consistent and reproducible testing across all samples, eliminating variables associated with complex fracture geometries. Most importantly, this model represents the biomechanically critical condition where the main fixation construct must resist tensile forces along the primary horizontal fracture line—the predominant mechanism of clinical fixation failure, nonunion, and delayed union in patellar fractures [14-16].

Biomechanical test environment

The biomechanical tests were conducted using a tension/compression testing machine (Instron) via a custom-made jig designed to control the location and motion of the parts. The jig was fixed to the testing machine using screws. The lower part of the sample, representing the patellar tendon, was connected to the jig with an M-6 stainless steel D-type fixation ring. The upper part of the polyester band, representing the quadriceps tendon, was affixed to the jig using another M-6 stainless steel D-type fixation ring. This fixation ring was linked to a 3.3 mm metal cable, secured to the jig with screws. The polyester band angle connected to the sawbone was set at lower 60°, upper 60°, and final 120°, where maximum tension of the quadriceps muscle occurs (Fig. 1).

Study groups

Our biomechanical test consisted of two parts. The first part analyzed the mechanical properties (static tensile strength test and dynamic tensile strength test) of our designed implant, the anatomically precontoured patellar plate (Jeil Medical Corp.) (Fig. 2). The second part compared the maximum tensile load-bearing capacity between

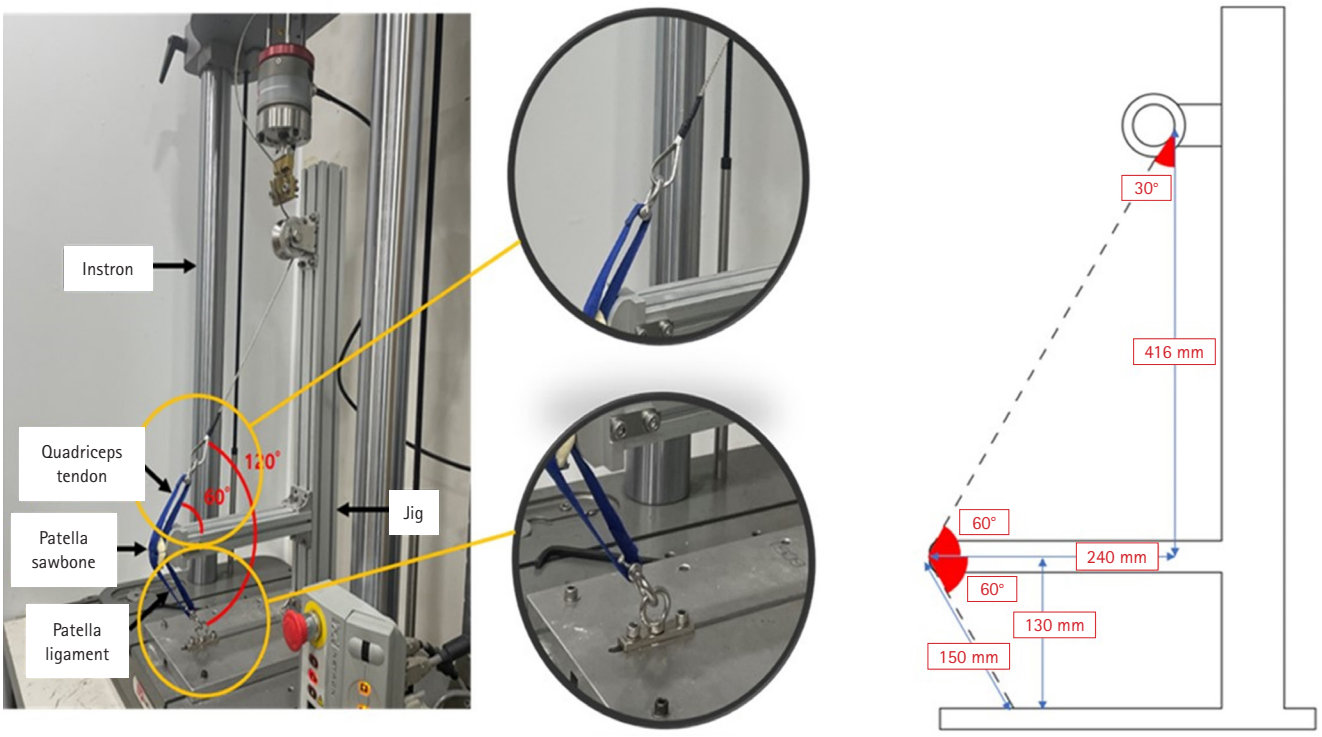

Fig. 1. Biomechanical testing environment illustrating the experimental setup, including the Instron testing machine, simulated quadriceps tendon, patellar sawbone, and patellar ligament, with detailed measurements and joint angles. A knee flexion angle of 120° was maintained consistently throughout testing of all specimens.

https://doi.org/10.12671/jmt.2025.00353

the anatomically precontoured patellar plate, anterior tension wiring through cannulated screws, and double-sided plating.

The anatomically precontoured patellar plate was applied to the anterior surface of the patella, with two cortical screws (diameter, 2.8 mm; length, 46 mm) inserted from the inferior to the superior aspect of the patella, perpendicular to the transverse fracture line. One cortical screw was inserted in the proximal fragment (diameter, 2.5 mm; length, 12 mm) and two cortical screws in the distal fragment (diameter, 2.5 mm; length, 12 mm) to fit the plate against the anterior surface. Three locking screws (diameter, 2.5 mm; length, 12 mm) in the proximal fragment and one locking screw (diameter, 2.5 mm; length, 12 mm) in the distal fragment were added in the locking screw holes of the plate. The tension wiring through cannulated screws was performed with two headless cannulated screws (diameter, 4 mm; length, 36 mm) and a cerclage wire (diameter, 1 mm) used as a tension construct. In double-sided plating, following the technique described by Wild et al. [11,17,18], bilateral fixed-angle plates were applied to the medial and lateral borders of the patella. Specifically, two 2.8-mm small-fragment plates (Jeil Medical Corp.) with six holes were applied on both sides of the patella, which were placed to insert three locking screws perpendicular to the surface of the plate in the proximal and the distal fragment at each side (screw diameter, 2.8 mm; length, 20-40 mm). Plates were placed in different sagittal planes to prevent screw collisions. Screws were inserted perpendicular to the screw holes and longest screws up to 40 mm were inserted. During instrumentation, screw trajectories from the medial and lateral plates occasionally intersected within the limited thickness of the patellar model. When screw collision was anticipated or encountered, screw length was reduced incrementally to avoid interference while maintaining bicortical or near-bicortical purchase when possible. This approach was applied consistently across all specimens to ensure reproducibility of the construct configuration (Fig. 3).

Fig. 2. Anatomically precontoured patellar plate fabricated from ASTM F67 titanium (model code 25-ANPA-209). Two 2.8-mm cortical screws can be inserted from the inferior to the superior fragment. Three 2.5-mm cortical screws and four 2.5-mm locking screws can be inserted from the anterior aspect of the plate.

Static tensile strength test

Seven samples of precontoured plates were tested. After

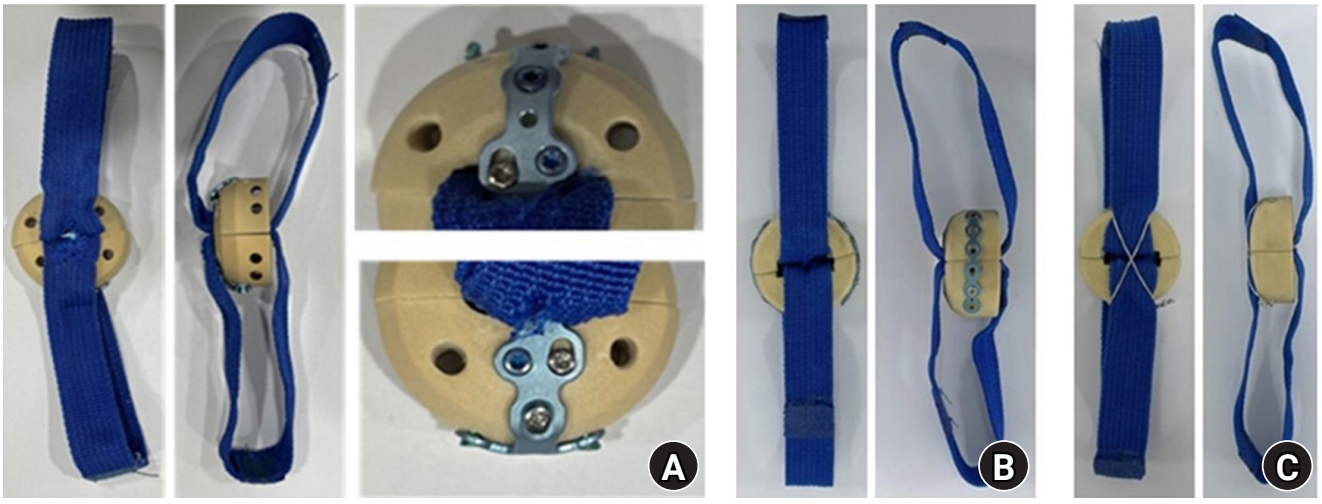

Fig. 3. Frontal and lateral views of each fixation construct: (A) anatomically precontoured patellar plate, (B) double-sided plating, and (C) anterior tension wiring through cannulated screws. All specimens were prepared using synthetic sawbone models with identical transverse fracture patterns and simulated quadriceps and patellar tendon attachments (blue bands) to ensure standardized biomechanical testing conditions.

applying a preload of 100 N, a tensile load was applied at a speed of 5 N/min. Testing protocol focused on construct survival as the endpoint. A threshold of 844 N was established as the minimum acceptable load-bearing capacity, reflecting a safety factor of two times the maximum load value of 422 N that the patellofemoral joint receives during walking [19]. Although the value reported by Matthews et al. represents patellofemoral joint reaction force, this value was used as a reference load because the quadriceps–patellar tendon complex transmits tensile forces across the patella during knee extension, and previous biomechanical studies have used comparable magnitudes to simulate physiologic loading conditions of the extensor mechanism [20,21]. These studies support the use of simplified tensile loading models to represent the forces transmitted through the patella during knee extension. The test was continued with progressively increasing load to evaluate the maximum load-bearing capacity of the construct. Failure was defined as fracture of the plate or sawbone, screw pull-out, or visible structural damage to the fixation construct. The maximum load reached during testing and the mode of failure, if present, were recorded for each specimen.

Dynamic tensile strength test

Seven samples of precontoured plates were tested, each subjected to a preload of 100 N. This preload was applied to remove slack and ensure consistent initial tension in the loop simulating the patellar tendon and quadriceps prior to cyclic loading. Each sample was then subjected to sinusoidal cyclic loading between 100 N and 300 N for 10,000 cycles at a frequency of 1 Hz (R-ratio, 0.33). The cyclic loading range of 100–300 N was selected based on previous biomechanical studies indicating that physiologic tensile loads across the patella during routine activities typically fall within this range [20,22]. After completion of cyclic loading, each patellar plate sample was examined for damage [22]. The testing protocol focused on construct survival as the endpoint. The acceptance criterion was no damage to the plate after 10,000 cycles. Assessment of construct integrity after cyclic loading was performed by visual inspection for plate deformation, screw loosening, or structural damage. Quantitative measurements of interfragmentary displacement or construct stiffness were not performed in this study.

Statistical methods

Five samples were prepared for each fixation construct as follows: the anatomically precontoured patellar plate, anterior tension wiring through cannulated screws, and double-sided plating. The maximum tensile load was applied to each sample, and results were recorded using a tension/compression testing machine. Normality was assessed using the Shapiro-Wilk test (anterior tension wiring: W=0.8506, P=0.1963; anatomical plate: W=0.6983, P=0.0092; double-sided plating: W=0.9517, P=0.7494). Homogeneity of variance was confirmed using Levene's test ($F(2,12)=1.3139$, P=0.3048). Given the robustness of one-way ANOVA to moderate deviations from normality in balanced experimental designs, one-way ANOVA was used to compare the maximum tensile load-bearing capacity among the three fixation methods, followed by Tukey's honestly significant difference (HSD) post-hoc testing.

To ensure the robustness of the statistical inference, a nonparametric sensitivity analysis was additionally performed. The Kruskal-Wallis test demonstrated a significant difference in maximum tensile load among fixation constructs (H=12.50, P=0.0019). Post-hoc pairwise comparisons using Dunn's test with Bonferroni correction confirmed significant differences between all fixation methods (adjusted P=0.0238 for all comparisons). Importantly, the nonparametric analysis demonstrated the same pattern of significant differences among fixation constructs as observed in the parametric one-way ANOVA with Tukey's HSD test, supporting the robustness of the primary findings.

Results

Static tensile strength test

All seven samples passed the static tensile strength test and were capable of bearing a load above 844 N. The maximum tensile load applied was 1,360.2 N, and the minimum was 1,216.2 N, with a standard deviation of 56.51. No construct failure was observed within the loading range achieved during testing, which was a failure criterion for this test. No deformation of the fixation constructs or fracture models was observed in any of the samples.

Dynamic tensile strength test

All seven samples completed 10,000 cycles without defor-

https://doi.org/10.12671/jmt.2025.00353

mation or structural damage. Visual inspection after cyclic loading revealed no evidence of plate deformation, screw loosening, or construct failure. Quantitative measurements of interfragmentary displacement or stiffness were not performed. All plates maintained their original contour without evidence of plastic deformation. The screw-plate interfaces showed no signs of loosening or toggle. No gross displacement or separation was evident at the fracture interface that would indicate construct instability.

Comparison of maximum tensile load-bearing capacity

The individual maximum tensile loads for each sample and the corresponding mean (SD) values for each group are provided in Table 1. One-way analysis of variance results for maximum tensile load among study groups are summarized in Table 2. The results revealed significant differences in the maximum tensile load between the different fixation groups. The anatomically precontoured patellar plate group had the highest mean maximum tensile load at 2,242.93 N (SD, 120.56), followed by the anterior tension wiring through cannulated screws group with a mean of 1,954.43 N (SD, 64.87), and the double-sided plating group with a mean of 1,255.17 N (SD, 231.72).

In the post-hoc tests, all group comparisons were significant at the 0.05 level (Table 3). The anatomically precontoured patellar plate group had a significantly greater tensile load than both the cannulated screw through anterior tension wiring group and the double-sided plating group. Similarly, the anterior tension wiring through cannulated screws group had a significantly greater tensile load than the double-sided plating group.

Table 1. Maximum tensile load applied on each sample

Case	Anterior tension wiring through cannulated screws	Anatomically precontoured patellar plate	Double-sided plating
1	1,983.98	2,211.56	971.95
2	1,845.79	2,166.29	1,258.35
3	1,980.78	2,455.55	1,608.03
4	1,948.64	2,173.29	1,157.97
5	2,012.98	2,207.97	1,279.56
Mean±SD	1,954.43±64.87	2,242.93±120.56	1,255.17±231.72
Median (IQR)	1,980.78 (1,948.64–1,983.98)	2,207.97 (2,173.29–2,211.56)	1,258.35 (1,157.97–1,279.56)

SD, standard deviation; IQR, interquartile range.

Table 2. One-way analysis of variance results for maximum tensile load among study groups

Source	Sum of squares	Degrees of freedom	Mean square	F-value	P-value
Between groups	2,579,780	2	1,289,890	53.42	<0.001**
Within groups (error)	289,745	12	24,145	-	-
Total	2,869,525	14	-	-	-

**P<0.001.

Table 3. Post-hoc pairwise comparisons of maximum tensile load among fixation groups (Tukey HSD test)

Group comparison	Mean difference (N)	SE	95% CI	P-value
Anterior tension wiring through cannulated screws vs. anatomical plate	−288.50	98.28	−519.45 to −57.55	0.031*
Anterior tension wiring through cannulated screws vs. double-sided plating	699.26	98.28	468.31 to 930.21	<0.001**
Anatomical plate vs. double-sided plating	987.76	98.28	756.81 to 1,218.71	<0.001**

Negative values indicate the first group had lower tensile load than the second group.
HSD, honestly significant difference; SE, standard error; CI, confidence interval.
*P<0.05, **P<0.001.

Discussion

Key results

The present study revealed that the anatomically precontoured patellar plate demonstrated adequate mechanical performance under physiologic-range cyclic loading, with no catastrophic failure observed during 10,000 loading cycles. This patellar plate withstood loads ≥844 N without construct failure and remained stable throughout 10,000 cycles of nondestructive dynamic tensile loading (100–300 N). The anatomically precontoured patellar plate was the most capable of bearing a maximum tensile load compared to anterior tension wiring through cannulated screws and double-sided plating. All load-displacement curves showed a consistent pattern with minimal or no deviation in all samples of the anatomically precontoured patellar plate. Although physiologic tensile loads across the patella during routine activities are lower than the ultimate loads measured in this study, greater load-bearing capacity may provide an additional safety margin against unexpected peak loads. Therefore, the higher ultimate load observed in the anatomically precontoured plate construct may indicate a greater mechanical reserve under extreme loading conditions.

Interpretation/comparison with previous studies

Although comminuted patellar fractures are quite common, we applied our biomechanical test to the transverse fracture pattern for two main reasons. First, comminuted type C3 patellar fractures (34C3 according to the current AO/OTA classification) typically feature a primary horizontal fracture line, while additional vertical lines, coronal splits, or satellite fragments can be neutralized to convert the fracture pattern to type C1 [13]. Second, using a simplified transverse pattern allowed us to create identical fractures in all Sawbones samples for consistent testing.

Stoffel et al. [23] conducted a biomechanical investigation of anterior variable-angle locked plating versus tension-band wiring of simple and complex patellar fractures. Their findings showed that anterior locked plating of both simple and complex patellar fractures resulted in less interfragmentary displacement under extended cyclic loading. Similarly, Thelen et al. [22] performed a biomechanical analysis comparing bilateral, polyaxial, fixed-angle plates to modified tension wiring with K-wires and cannulated screws with anterior tension wiring. They found that the plate is significantly stronger, with less fracture gap dehiscence than other osteosynthesis methods. Another study conducted biomechanical cadaveric testing of a fixed-angle plate compared with tension-band wiring and screw fixation in transverse patellar fractures. Both wiring and screw constructs showed significant fracture displacement, whereas the plate showed no significant fracture gap widening [24]. In daily activities, most of the tension around the patella is within 300 N, as recorded in previous biomechanical tests [22,23]. In the present study, our anatomically precontoured patellar plate passed the dynamic tensile load of 300 N.

In general, stable fixation is crucial in patellar fracture fixation, especially in the comminuted pattern. Wagner et al. [3] conducted a biomechanical comparison of a 3.5 mm anterior locking plate to cannulated screws with anterior tension-band wiring in comminuted patellar fractures. The findings revealed that the plate biomechanically provides better primary stability compared to cannulated screws with anterior tension-band wiring. Traditional tension-band wiring with cannulated screws or K-wires, while widely used, has been associated with complications including pin migration, soft tissue irritation, and symptomatic hardware that may require additional surgery for removal [16]. Furthermore, loss of reduction is another complication of these fixation methods [14]. Therefore, stable fixation is necessary, and our anatomically precontoured patellar plate may provide a reliable solution to the potential complications of traditional fixation constructs.

The inclusion of double-sided plating as a comparator in our study warrants clarification, as this technique may not be the most commonly used method for simple transverse fractures. However, bilateral plating using fixed-angle plates applied to the medial and lateral borders of the patella has been established as a viable and effective treatment option for patellar fractures, with several clinical studies demonstrating favorable outcomes [11,17,18]. These studies validate double-sided plating as a clinically relevant comparator. Contrary to previous studies, our study demonstrated that double-sided plating showed inferior mechanical stability compared to anterior tension wiring. This discrepancy may be attributed to differences in plate design and specifications used across studies, as well as variations in screw length and positioning that

https://doi.org/10.12671/jmt.2025.00353

could affect construct rigidity. Furthermore, bilateral plating represents an alternative plating strategy that differs from anterior single-plate fixation, making it an appropriate comparison to evaluate the relative biomechanical advantages of different plate configurations. Our study therefore contributes to the understanding of how different plate positioning strategies—anterior single-plate versus double-sided plates—perform under standardized biomechanical testing conditions.

Limitations

There are some limitations to this study that should be considered when interpreting the findings. First, our biomechanical study is not clinically verified and needs to be followed by a clinical study. While our findings require clinical validation, Moore et al. [25] have reported good to excellent functional outcomes following fixed-angle plate fixation of comminuted patellar fractures in a retrospective series of 20 patients (mean follow-up 154 weeks).

Second, the use of synthetic bone models, while providing consistency and reproducibility, does not fully replicate the biological and biomechanical properties of human bone, including bone quality variations, fracture healing responses, and soft tissue interactions. However, the primary advantage of synthetic bone models lies in their standardized material properties, which eliminate variability inherent in cadaveric specimens and allow for controlled comparative biomechanical testing under identical conditions. To minimize these potential sources of bias, we implemented the following standardization measures: all specimens were prepared and instrumented by a single experienced orthopedic surgeon to ensure consistency in surgical technique; screw insertion was performed using a standardized torque driver set at uniform torque settings across all specimens; and implant positioning was verified by photographic documentation to ensure reproducibility. Despite these precautions, minor variations in bone-implant interface contact and screw purchase within the synthetic bone material may still have occurred, particularly in the double-sided plating group where bilateral symmetric placement is more technically demanding. These factors may have contributed to the observed variability in biomechanical performance and represent an inherent limitation of *ex vivo* biomechanical testing that should be considered when interpreting our results. Third, although our study was limited to the transverse fracture pattern, this model was specifically chosen to represent the biomechanical condition after conversion of complex comminuted fractures to a simplified configuration using auxiliary fixation, as is standard in clinical practice. In comminuted patellar fractures, additional fixation modalities such as screws or mini-plates are employed to neutralize secondary fracture lines and convert the complex pattern into a primary horizontal fracture line, upon which the main definitive fixation is applied [13]. Therefore, our transverse fracture model reflects the clinically relevant scenario where the main fixation construct must effectively resist tensile forces along the primary horizontal fracture line—the predominant mechanism of fixation failure, nonunion, and delayed union in patellar fractures [14,15]. Our uniaxial tensile loading protocol was therefore specifically designed to evaluate this primary failure mechanism under controlled conditions, enabling standardized biomechanical comparison among fixation techniques. Fourth, the small sample size of five specimens per group in the comparative testing represents a limitation that may affect the statistical power of our findings. However, the use of synthetic bone models with consistent material properties reduces inter-specimen variability compared to biological specimens, and the statistically significant differences observed between groups suggest that the sample size was adequate to detect meaningful biomechanical differences. Notably, the double-sided plating group exhibited greater variability in our results, which may be explained by the technical sensitivity of this construct. Double-sided plating requires precise bilateral plate placement and symmetric screw positioning, and minor variations in plate contouring, screw length selection, or screw trajectory between specimens could substantially affect the overall construct stability and load distribution, leading to increased variability in biomechanical performance. Finally, our cyclic testing protocol evaluated construct survival without quantifying interfragmentary displacement at the fracture site. Future studies employing optical tracking systems (e.g., digital image correlation) or extensometers would enable detailed characterization of displacement evolution and stiffness degradation under cyclic loading. Nevertheless, our findings demonstrate that the anatomically precontoured plate can withstand physiologically relevant cyclic loads without catastrophic failure, which is clinically relevant for early postoperative rehabili-

tation protocols.

It should also be noted that the double-sided plating construct used in this study was not identical to the specific implant systems evaluated in previous biomechanical studies. Variations in plate geometry, screw trajectory, and screw length selection may influence construct rigidity in bilateral plating configurations. Therefore, the inferior mechanical performance observed in the present study should be interpreted within the context of the specific implant configuration tested, rather than as a general conclusion regarding all double-sided plating techniques for patellar fractures.

Conclusions

In conclusion, the anatomically precontoured patellar plate offered stable fixation for patellar fracture models. The mechanical analysis of this plate showed that it could withstand maximum static and dynamic tensile loads without any damage or failure and was the most capable of bearing a maximum tensile load. These findings support the potential clinical utility of the anatomically precontoured patellar plate as a main fixation construct for both simple transverse and converted complex patellar fractures, although cadaveric study or clinical validation is needed to confirm these biomechanical advantages.

Article Information

Author contributions

Conceptualization: YC, JB, JWC. Methodology: YC, JB. Data curation: YC, JB, JSC. Formal analysis: AMA, WC. Project administration: JWC. Supervision: JKO, JWC. Writing-original draft: AMA, WC. Writing-review & editing: AMA, WC, YC, JB, JSC, JKO, JWC. All authors read and approved the final manuscript.

Conflicts of interest

No potential conflict of interest relevant to this article was reported.

Funding

This study was partially funded by Seoul R&BD Program (BT230060).

Data availability

Contact the corresponding author for data availability.

Acknowledgments

The authors thank the Jeil Medical Corporation for their support in conducting the biomechanical tests.

Supplementary materials

None.

References

1. Sebastian P, Michael Z, Frederik G, et al. Influence of patella height after patella fracture on clinical outcome: a 13-year period. Arch Orthop Trauma Surg 2022;142:1557-61.
2. Cho JW, Kent WT, Cho WT, et al. Miniplate augmented tension-band wiring for comminuted patella fractures. J Orthop Trauma 2019;33:e143-50.
3. Wagner FC, Neumann MV, Wolf S, et al. Biomechanical comparison of a 3.5 mm anterior locking plate to cannulated screws with anterior tension band wiring in comminuted patellar fractures. Injury 2020;51:1281-7.
4. Lee KH, Lee Y, Lee YH, Cho BW, Kim MB, Baek GH. Biomechanical comparison of three tension band wiring techniques for transverse fracture of patella: Kirschner wires, cannulated screws, and ring pins. J Orthop Surg (Hong Kong) 2019;27:2309499019882140.
5. Hsu KL, Chang WL, Yang CY, Yeh ML, Chang CW. Factors affecting the outcomes of modified tension band wiring techniques in transverse patellar fractures. Injury 2017;48:2800-6.
6. Banks KE, Ambrose CG, Wheeless JS, Tissue CM, Sen M. An alternative patellar fracture fixation: a biomechanical study. J Orthop Trauma 2013;27:345-51.
7. Avery MC, Jo S, Chang A, et al. Cannulated screw prominence in tension band wiring of patella fractures increases fracture gapping: a cadaver study. Clin Orthop Relat Res 2019;477:1249-55.
8. Tsotsolis S, Ha J, Fernandes AR, et al. To plate, or not to plate? A systematic review of functional outcomes and complications of plate fixation in patellar fractures. Eur J Orthop Surg Traumatol 2023;33:3287-97.
9. Verbeek DO, Hickerson LE, Warner SJ, Helfet DL, Lorich DG. Low profile mesh plating for patella fractures: video of a novel surgical technique. J Orthop Trauma 2016;30 Suppl 2:S32-3.

https://doi.org/10.12671/jmt.2025.00353

10. Wurm S, Buhren V, Augat P. Treating patella fractures with a locking patella plate: first clinical results. Injury 2018;49 Suppl 1:S51-5.
11. Wild M, Thelen S, Jungbluth P, et al. Fixed-angle plates in patella fractures: a pilot cadaver study. Eur J Med Res 2011;16:41-6.
12. Wurm S, Augat P, Buhren V. Biomechanical assessment of locked plating for the fixation of patella fractures. J Orthop Trauma 2015;29:e305-8.
13. Cho JW, Yang Z, Lim EJ, et al. Multifragmentary patellar fracture has a distinct fracture pattern which makes coronal split, inferior pole, or satellite fragments. Sci Rep 2021;11:22836.
14. Smith ST, Cramer KE, Karges DE, Watson JT, Moed BR. Early complications in the operative treatment of patella fractures. J Orthop Trauma 1997;11:183-7.
15. Klassen JF, Trousdale RT. Treatment of delayed and nonunion of the patella. J Orthop Trauma 1997;11:188-94.
16. Hoshino CM, Tran W, Tiberi JV, et al. Complications following tension-band fixation of patellar fractures with cannulated screws compared with Kirschner wires. J Bone Joint Surg Am 2013;95:653-9.
17. Wild M, Eichler C, Thelen S, Jungbluth P, Windolf J, Hakimi M. Fixed-angle plate osteosynthesis of the patella: an alternative to tension wiring. Clin Biomech (Bristol) 2010;25:341-7.
18. Wild M, Fischer K, Hilsenbeck F, Hakimi M, Betsch M. Treating patella fractures with a fixed-angle patella plate: a prospective observational study. Injury 2016;47:1737-43.
19. Matthews LS, Sonstegard DA, Henke JA. Load bearing characteristics of the patello-femoral joint. Acta Orthop Scand 1977;48:511-6.
20. Carpenter JE, Kasman RA, Patel N, Lee ML, Goldstein SA. Biomechanical evaluation of current patella fracture fixation techniques. J Orthop Trauma 1997;11:351-6.
21. Scilaris TA, Grantham JL, Prayson MJ, Marshall MP, Hamilton JJ, Williams JL. Biomechanical comparison of fixation methods in transverse patella fractures. J Orthop Trauma 1998;12:356-9.
22. Thelen S, Schneppendahl J, Baumgartner R, et al. Cyclic long-term loading of a bilateral fixed-angle plate in comparison with tension band wiring with K-wires or cannulated screws in transverse patella fractures. Knee Surg Sports Traumatol Arthrosc 2013;21:311-7.
23. Stoffel K, Zderic I, Pastor T, et al. Anterior variable-angle locked plating versus tension band wiring of simple and complex patella fractures - a biomechanical investigation. BMC Musculoskelet Disord 2023;24:279.
24. Thelen S, Schneppendahl J, Jopen E, et al. Biomechanical cadaver testing of a fixed-angle plate in comparison to tension wiring and screw fixation in transverse patella fractures. Injury 2012;43:1290-5.
25. Moore TB, Sampathi BR, Zamorano DP, Tynan MC, Scolaro JA. Fixed angle plate fixation of comminuted patellar fractures. Injury 2018;49:1203-7.

JMT Journal of Musculoskeletal Trauma

pISSN 3058-6267 · eISSN 3058-6275
J Musculoskelet Trauma 2026;39(2):140-146
https://doi.org/10.12671/jmt.2026.00094

Biomechanical analysis of medial distal tibial locking plate fixation for distal-third spiral tibial shaft fractures

Yao-Jen Liu

Department of Orthopedic Surgery, Hsinchu MacKay Memorial Hospital, Hsinchu, Taiwan

Background: Distal spiral fractures of the tibial shaft present fixation challenges, particularly in patients who are not suitable candidates for intramedullary nailing. This study evaluated the biomechanical stability of medial minimally invasive percutaneous plating osteosynthesis (MIPO) under various physiological loading conditions.

Methods: A finite-element model of a distal AO/OTA 42-A1.1c spiral fracture of the tibia was created using computed tomography data. A precontoured titanium medial distal tibia locking compression plate with nine locking screws was simulated. Material properties were assigned to cortical and cancellous bone. The loading conditions included axial compression (750 N), varus/valgus bending (300 N at a 9° offset), and internal/external torsion (7.5 N·m). von Mises stress and fracture displacement were analyzed.

Results: Axial loading produced a peak plate stress of 508.06 MPa and a displacement of 2.17 mm. Valgus and varus loading generated stresses of 490.17 MPa and 324.08 MPa, respectively, with corresponding displacements of 3.86 mm and 2.01 mm. External and internal torsion resulted in stresses of 354.23 MPa and 358.9 MPa, respectively, with corresponding displacements of 2.64 mm and 2.22 mm.

Conclusions: Medial distal tibial plating demonstrated favorable biomechanical performance in this finite-element model; however, clinical extrapolation should be made cautiously.

Level of evidence: V.

Keywords: Finite element analysis; Tibial fractures; Biomechanical phenomena; Mechanical stress

Original Article

Received: February 4, 2026
Revised: February 24, 2026
Accepted: March 9, 2026

Correspondence to:
Yao-Jen Liu
Department of Orthopedic Surgery, Hsinchu MacKay Memorial Hospital, No. 690, Sec. 2, Guangfu Rd., East Dist., Hsinchu City 300, Taiwan
Tel: +886-3-6889595
Email: lyjs93311132@gmail.com

Introduction

Tibial shaft fractures represent the most common long bone fractures. According to the AO/OTA classification system, spiral fractures (AO/OTA 42-A1) represent approximately 34% of tibial shaft fractures, followed by oblique fractures (AO/OTA 42-A2), which account for 17% [1]. Externally rotated spiral fractures are the most frequently observed and are often accompanied by a concurrent fibular fracture. These injuries can occur as a result of high-energy trauma—such as traffic accidents or falls in young males, or due to low-energy mechanisms like ground-level falls in the elderly individuals [1,2].

Especially in geriatric patients, bone quality and overall physical condition are often compromised, making early mobilization and weight bearing essential to prevent complications related to immobilization [3]. Therefore, it is crucial to choose a

fixation technique that provides sufficient stability and can support early weight bearing.

While intramedullary (IM) nailing remains the gold standard treatment for tibial shaft fractures, it may not be suitable in certain patients due to soft tissue conditions, associated injuries, or the aging population with prior total knee arthroplasty or technical limitations [4]. In such cases, techniques such as blocking screws, locking screws, or percutaneous reduction may be unfeasible, and there may also be an increased risk of pulmonary complications [5-7]. Recently, minimally invasive percutaneous plating osteosynthesis (MIPO) has gained traction as a viable alternative, particularly in cases with compromised anterior and medial soft tissue coverage where open reduction and internal fixation may increase the risk of wound complications. In addition, MIPO can also be used in patients with combined multiple injuries in whom IM reaming is contraindicated because of the potential increased risk of pulmonary complications or in cases where blocking screws, locking screws, or percutaneous repositioning techniques are difficult to perform.

Kati et al. [6] have proposed MIPO as an effective method for managing spiral and spiral wedge tibial shaft fractures, hypothesizing that it provides improved alignment and torsional stability. Biomechanical studies further support the use of medial plating, showing superior stiffness in both axial and torsional loading and reduced fracture site displacement and rotation compared to lateral plating [8,9]. However, limited studies have specifically evaluated the biomechanical performance of the medial plates in the treatment of distal tibial spiral fractures. This study aimed to evaluate the biomechanical performance of the medial plate for the stability of distal tibial spiral fracture under different physiological loads.

Methods

Ethics statement

This study is a biomechanical simulation using a finite-element model based on an anonymized dataset from the Visible Human Project [10]. As the study did not involve any live human participants or animal subjects, Institutional Review Board approval and informed consent were not required. All computational procedures were conducted in accordance with the ethical standards of the institutional and/or national research committee.

Tibial model reconstruction and fracture simulation

A three-dimensional (3D) lower-leg finite-element model that included the tibia of a normal adult was developed. The bony structures were generated using a computed tomography data set segmentation from the Visible Human Project [10]. The 3D tibia model was reconstructed via the cortical shell and cancellous core. Cortical and cancellous regions were segmented anatomically during reconstruction, with the cortical shell defined as the outer layer of the tibial shaft and the cancellous bone assigned to the IM core. A simple spiral fracture model (AO/OTA 42-A1.1c) was made at the distal-third of the tibia shaft (Fig. 1A). The distal fracture initiation point was located 50 mm proximally to the distal tibial joint line, with a spiral fracture orientation of 50°. The fracture line extended approximately 40 mm in length from distal to proximal.

Implant specifications and fixation strategy

A common implant, a Zimmer periarticular distal tibial locking plate, was utilized in this simulation. This medial distal tibial plate features an anatomical precontoured titanium plate and is used with 10 holes and is 168 mm in length. The plate was affixed to the tibial shaft with three 3.5 mm locking screws whereas six 3.5 mm locking screws were used for the articular fixation. The plate and screw models were simplified without threads. The placement of the medial tibial plate on the simulated spiral fracture is shown in Fig. 1B.

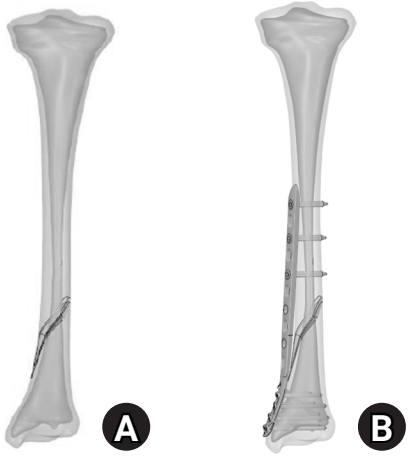

Fig. 1. The reconstructed tibial model with (A) a simulated spiral fracture and (B) an implanted medial distal locking plate.

Computational modeling and material properties

The ANSYS Workbench 19 (ANSYS Inc.) was used for computational analysis. A frictional contact behavior was defined between the fracture fragments with a coefficient of friction of 0.2 for possible contact after loading while a coefficient of friction of 0.42 was used at the interfaces between the bone and the plate [11]. Fully constrained treatments were applied between the screws and the surrounding bone, as well as between the contact surfaces of the plate and the screw head, to simulate the mechanism of tightened locking. Both plate and screws were made of titanium and modeled according to specifications described in previous studies (Young's modulus, 110,000 MPa; Poisson ratio, 0.3), while the cortical bone was modeled with Young's modulus of 17,500 MPa and 0.3 Poisson ratio. Material properties for the cancellous bone were assigned with a Young's modulus of 1,500 MPa and Poisson ratios of 0.12. Bones and implants were modeled as linear elastic, isotropic, and homogeneous materials.

Physiological loading conditions and evaluation metrics

A vertical compressive load of 750 N was applied to simulate physiological weight bearing, corresponding to loading conditions ranging from cane-assisted walking to fast walking [12]. For varus-valgus bending tests, a load of 300 N was applied at the medial side of the distal tibial articular surface in a direction deviated 9° medially from the mechanical axis of the lower limb to simulate varus stress [13]. Conversely, a 300 N load was applied to the lateral side of the distal tibial articular surface at a 9° lateral deviation to simulate valgus stress. For torsional loading, the distal articular surface of the tibia was fixed, and internal and external torques of 7.5 N·m were applied to the proximal articular surface to simulate internal and external rotation forces, respectively [12]. Maximum von Mises stress in the bone plate and the maximum displacement of the fracture surface were calculated for evaluation.

Results

Under vertical loading (Fig. 2), the bone plate exhibited a maximum von Mises stress of 508.06 MPa, with a corresponding fracture site displacement of 2.17 mm. Valgus loading (Fig. 3) resulted in a relatively high von Mises stress of 490.17 MPa among the three loading modes and a displacement of 3.86 mm. In contrast, varus loading (Fig. 4) produced a lower von Mises stress of 324.08 MPa among three loading modes and lower displacement of 2.01 mm. Under external rotational loading (Fig. 5), the maximum stress was 354.23 MPa, with a fracture displacement of 2.64 mm. Internal rotational loading (Fig. 6) resulted in a peak von Mises stress of 358.9 MPa and lower fracture displacement observed than that observed under external rotation, at 2.22 mm.

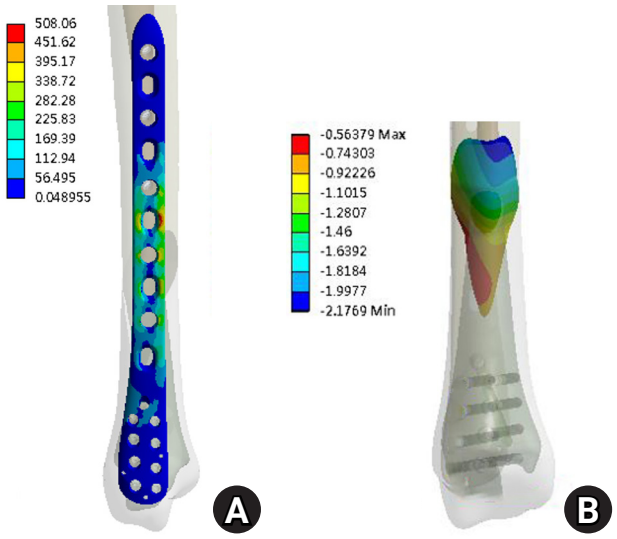

Fig. 2. The results under compression load. (A) von Mises stress distribution on the plate and (B) the displacement on the fracture surface.

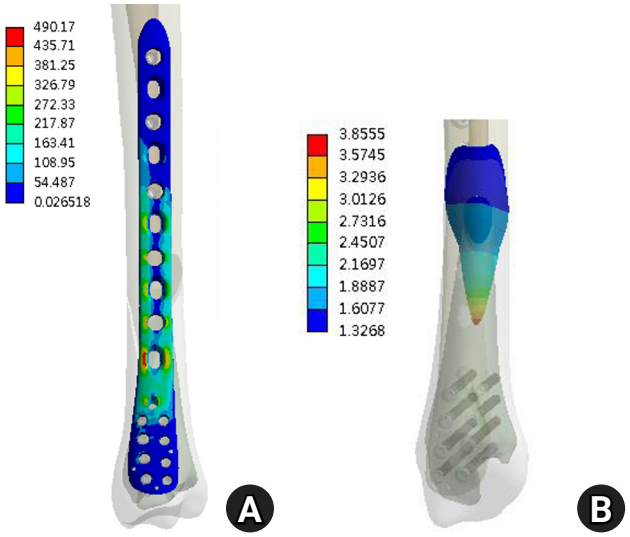

Fig. 3. The results under valgus load. (A) von Mises stress distribution on the plate and (B) the displacement on the fracture surface.

https://doi.org/10.12671/jmt.2026.00094

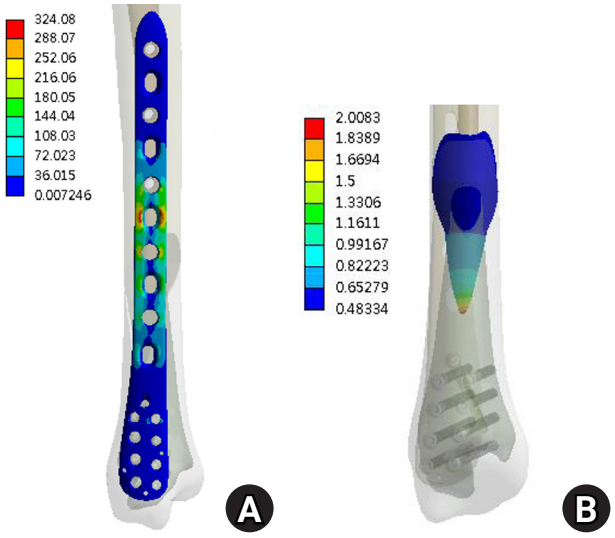

Fig. 4. The results under varus load. (A) von Mises stress distribution on the plate and (B) the displacement on the fracture surface.

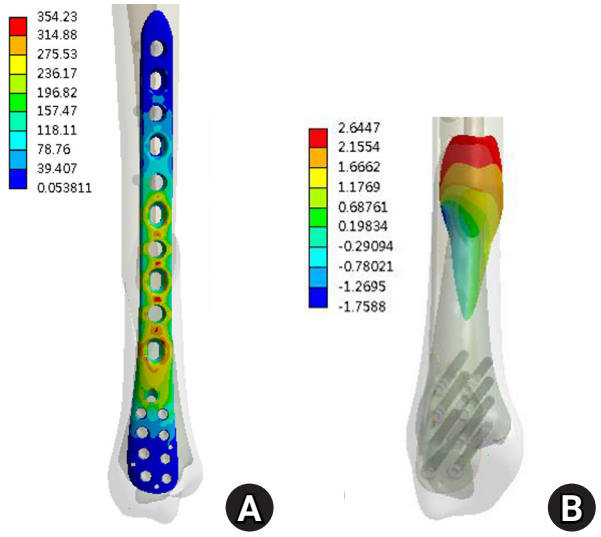

Fig. 5. The results under external torque. (A) von Mises stress distribution on the plate and (B) the displacement on the fracture surface.

Discussion

This study investigated the biomechanical performance of a medial distal tibial plate for the stabilization of distal-third spiral tibial shaft fractures under various physiological loading conditions. Biomechanically, the failure displacement of a fracture fragment is 3 mm [14]. The finite-element analysis (FEA) demonstrated that the medial plate provided sufficient stability under vertical compressive, varus, and internal/external rotation loadings, with relatively low fracture displacement (approximately 2 mm).

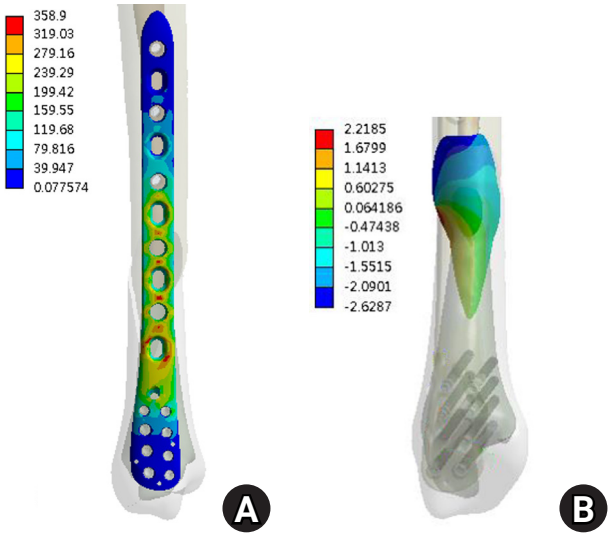

Fig. 6. The results under internal torque. (A) von Mises stress distribution on the plate and (B) the displacement on the fracture surface.

Vertical loading, which simulates normal weight bearing, produced the highest von Mises stress (508.06 MPa) in the plate, yet the corresponding fracture displacement was limited to 2.17 mm, indicating effective load transfer and structural stiffness. In Jia et al. [15]'s study, which used the finite-element method to evaluate a distal transverse fracture type under comparable loading conditions, the lateral plate sustained a peak stress of 738 MPa with 5.74 mm of displacement. These findings suggest the superiority of medial plating in resisting vertical compressive loading. Importantly, while the maximum stress remained below the commonly cited fatigue strength of titanium alloy (approximately 600 MPa), it approached this threshold. This is clinically significant, as repeated loading cycles—especially during activities such as walking or stair climbing—can lead to fatigue failure over time if the stress approaches or exceeds the fatigue endurance limit of the implant material. Therefore, although acute performance under single-cycle loading is acceptable, the proximity to fatigue limits warrants caution in high-demand patients or those with delayed healing (such as elderly patients).

Varus loading resulted in the lowest stress (324.08 MPa) and minimal displacement (2.01 mm), likely because the loading vector aligned with the medial plate's position and

construct geometry. In contrast, valgus loading, which applies a bending moment opposite to the plate's location, produced higher stress (490.17 MPa) and increased displacement (3.86 mm), reflecting the plate's biomechanical disadvantage under medially-directed bending forces. These findings are consistent with prior biomechanical studies showing superior stiffness in axial and varus directions for medial plates, but increased vulnerability under valgus loading [8,9]. The increased stress and displacement observed under valgus loading highlight a potential coronal-plane vulnerability of medial distal tibial plating, as the bending moment acts opposite to the plate location. Clinically, this warrants careful attention to construct optimization and alignment control. The use of a longer plate to increase working length, higher distal screw density, bicortical fixation when feasible, and multiplanar locking screw orientation may enhance resistance to valgus bending. Anatomical reduction in the coronal plane is essential, as residual valgus malalignment may further amplify tensile stress on the medial plate. Additionally, the present model did not include the fibula, which *in vivo* may provide lateral column support and reduce valgus instability; therefore, fibular fixation should be considered in distal-third fractures when coronal stability is a concern.

Under torsional conditions, both internal and external rotational loading resulted in moderate stress (354.23–358.9 MPa), but the highest displacement at the fracture site (2.22–2.64 mm), suggesting limited torsional control. In Jia et al. [15]'s study, lateral plating fixation demonstrated a peak stress of 355.04 MPa with a displacement of 1.39 mm. These findings suggest that medial plating may provide a safer construct than lateral plating under comparable loading conditions. This may be due to the geometric limitations of the plate and screw configuration in resisting rotational moments. While Kati et al. [6] advocated medial MIPO for spiral fractures, citing improved alignment and torsional resistance, our findings suggest that the construct alone may be insufficient to fully counteract torsional instability. In clinical practice, this may necessitate supplemental fixation techniques or altered screw configurations to optimize rotational stability, especially in active patients or complex fracture patterns.

The proximity of observed stress values to the fatigue strength of titanium emphasizes the need for careful patient selection and postoperative load management. Though none of the loading scenarios exceeded the fatigue threshold, repeated high-load activities or delayed union could potentially result in cyclic fatigue and implant failure. Therefore, long-term implant durability should be a consideration, particularly in younger or heavier patients and in those expected to return to high levels of activity.

Several biomechanical studies have evaluated fixation strategies for distal tibial fractures using both finite-element modeling and experimental testing.

Jia et al. [15] performed a finite-element comparison of medial plating, lateral plating, and IM nailing for distal tibial fractures under axial and torsional loading. Their results demonstrated differences in stress distribution and displacement between fixation methods, with medial plating showing favorable axial stiffness but variable torsional performance depending on screw configuration. However, differences in fracture pattern and model assumptions limit direct comparison with the present study.

Cao et al. [16] investigated the biomechanical effects of plate length, fibular integrity, and plate position in tibial shaft fracture models. Their findings emphasized that fibular fixation significantly enhances coronal-plane stability and reduces implant stress in distal fractures. They also reported that longer plates distribute stress more evenly and improve construct durability, underscoring the importance of construct configuration.

Unal et al. [17] performed biomechanical testing and FEA comparing a newly designed tibial IM nail with distal supportive locking versus medial distal tibial plating. Their results demonstrated that under axial loading, the IM nail construct showed greater force resistance, greater stiffness, and lower fracture displacement than the plate group, suggesting superior load transfer and structural stability of nail fixation under axial loads.

Collectively, previous biomechanical studies indicate that fixation performance in distal tibial fractures is strongly influenced by fracture pattern, implant position, plate length, screw configuration, and fibular integrity. The present findings are consistent with prior reports showing that medial plating provides satisfactory axial stability but may demonstrate increased stress under coronal-plane bending, particularly without fibular support. In comparison, IM nailing generally offers superior axial load-sharing and stiffness, whereas plating constructs may allow more precise alignment control in selected fracture configurations.

https://doi.org/10.12671/jmt.2026.00094

Limitations

Several limitations must be acknowledged. The finite-element model utilized homogeneous, isotropic, and linear elastic assumptions for bone and implant materials, which may not fully represent *in vivo* mechanical behavior. Thread features of the screws were not modeled, and biological healing or callus formation over time was not considered. Only single plate length was evaluated, and it was not compared with IM nailing to further prove the ability of enabling early weight bearing. Only simple spiral fracture type was analyzed. The findings primarily apply to simple distal spiral fractures rather than highly comminuted patterns. This study references a titanium fatigue threshold of 600 MPa to explain the safety of medial plating for the fixation of the spiral tibial shaft fracture. However, the actual fatigue performance of a bone plate depends on multiple factors, including alloy type, surface condition, loading cycles, and stress ratios. Additionally, this study is based on FEA, which evaluates construct mechanics under controlled, idealized, and primarily static loading conditions. Although FEA provides valuable insight into stress distribution and interfragmentary motion, it cannot directly predict clinical outcomes such as fracture union, implant failure, complication rates, or patient function. Therefore, the present findings should be interpreted as biomechanical evidence rather than direct clinical recommendations. Furthermore, the loading conditions applied in this model do not fully replicate the complex *in vivo* biomechanical environment of the tibia. In reality, tibial loading is influenced by dynamic muscle forces, joint reactions, and patient-specific gait patterns, with relatively stronger lateral muscular forces that may amplify valgus-directed bending moments. In this context, the increased stress and displacement observed under valgus loading may represent a potential mechanical vulnerability of the medial plating construction, particularly during functional activities such as walking or stair climbing. Accordingly, the clinical implications of these findings should be interpreted with caution, and further *in vivo* or clinical studies are necessary to validate their translational relevance. The cited reference [15] used for comparison did not involve an equivalent fracture type to that investigated in the present study. As no methodologically comparable reference was available, this comparison was intended only to verify that the analyzed results of the current study fell within reasonable ranges. Nonetheless, the controlled and comparative nature of the simulated loading conditions provides valuable insight into the mechanical performance of the medial plating construct.

Conclusions

This finite-element study evaluated the mechanical behavior of a medial distal tibial plate construct in a normal adult tibial model with a distal-third spiral fracture in the absence of the fibula under idealized loading conditions. The results demonstrated that, within the constraints of the model, the medial plating construct maintained fracture displacement within the simulated parameters, and the calculated von Mises stresses remained below the referenced fatigue threshold of titanium alloy. Increased stress and displacement were observed under axial compression and valgus loading, indicating relative mechanical sensitivity to these loading modes. These findings describe only the biomechanical performance of the specific construct configuration analyzed and should not be interpreted as direct clinical recommendations or as evidence of surgical technique superiority.

Article Information

Author contributions

All the work was done by Yao-Jen Liu.

Conflicts of interest

No potential conflict of interest relevant to this article was reported.

Funding

None.

Data availability

Not applicable.

Acknowledgments

None.

Supplementary materials

None.

References

1. Larsen P, Elsoe R, Hansen SH, Graven-Nielsen T, Laessoe U, Rasmussen S. Incidence and epidemiology of tibial shaft fractures. Injury 2015;46:746-50.
2. Laurila J, Huttunen TT, Kannus P, Kaariainen M, Mattila VM. Tibial shaft fractures in Finland between 1997 and 2014. Injury 2019;50:973-7.
3. Kammerlander C, Pfeufer D, Lisitano LA, Mehaffey S, Bocker W, Neuerburg C. Inability of older adult patients with hip fracture to maintain postoperative weight-bearing restrictions. J Bone Joint Surg Am 2018;100:936-41.
4. Tamburini L, Zeng F, Neumann D, et al. A review of tibial shaft fracture fixation methods. Trauma Care 2023;3:202-11.
5. Lai TC, Fleming JJ. Minimally invasive plate osteosynthesis for distal tibia fractures. Clin Podiatr Med Surg 2018;35:223-32.
6. Katı YA, Oken OF, Yıldırım AO, Kose O, Unal M. May minimally invasive plate osteosynthesis be an alternative to intramedullary nailing in selected spiral oblique and spiral wedge tibial shaft fractures. Jt Dis Relat Surg 2020;31:494-501.
7. Xue XH, Yan SG, Cai XZ, Shi MM, Lin T. Intramedullary nailing versus plating for extra-articular distal tibial metaphyseal fracture: a systematic review and meta-analysis. Injury 2014;45:667-76.
8. Aizat RM, Kadir MR, Ab Rahman S, Md Shihabudin TM, Robson N, Kamarul T. Biomechanical comparative analyses between the anterolateral and medial distal tibia locking plates in treating complex distal tibial fracture: a finite element study. J Med Imaging Hlth Inform 2013;3:532-7.
9. Pirolo JM, Behn AW, Abrams GD, Bishop JA. Anterolateral versus medial plating of distal extra-articular tibia fractures: a biomechanical model. Orthopedics 2015;38:e760-5.
10. Oken OF, Yildirim AO, Asilturk M. Finite element analysis of the stability of AO/OTA 43-C1 type distal tibial fractures treated with distal tibia medial anatomic plate versus anterolateral anatomic plate. Acta Orthop Traumatol Turc 2017;51:404-8.
11. Lin K, Tarng Y, Lin K, Wei H. Biomechanical superiority of locking plate designed with cluster of head screws compared to conventional buttress plate for fixation of posteromedial tibial plateau fractures: a computational assessment. J Med Biol Eng 2022;42:189-95.
12. Ebramzadeh E, Knutsen AR, Sangiorgio SN, Brambila M, Harris TG. Biomechanical comparison of syndesmotic injury fixation methods using a cadaveric model. Foot Ankle Int 2013;34:1710-7.
13. Jiang D, Zhan S, Wang Q, Ling M, Hu H, Jia W. Biomechanical comparison of locking plate and cancellous screw techniques in medial malleolar fractures: a finite element analysis. J Foot Ankle Surg 2019;58:1138-44.
14. Ali AM, El-Shafie M, Willett KM. Failure of fixation of tibial plateau fractures. J Orthop Trauma 2002;16:323-9.
15. Jia J, Tang C, Yue J, Li F. Finite element analysis of three different fixation methods for distal tibial fracture. Chin J Tissue Eng Res 2019;23:5188-94.
16. Cao Y, Zhang Y, Huang L, Huang X. The impact of plate length, fibula integrity and plate placement on tibial shaft fixation stability: a finite element study. J Orthop Surg Res 2019;14:52.
17. Unal OK, Dagtas MZ, Najafov T, Demir C, Ugutmen E, Akpinar F. Medial plating versus newly designed intramedullary nail with distal interlocking system for distal tibia fractures: a biomechanical study with finite element analysis. Jt Dis Relat Surg 2025;37:477-88.

https://doi.org/10.12671/jmt.2026.00094

JMT Journal of Musculoskeletal Trauma

pISSN 3058-6267 · eISSN 3058-6275
J Musculoskelet Trauma 2026;39(2):147-155
https://doi.org/10.12671/jmt.2025.00325

Clinical and radiographic outcomes of hemiarthroplasty for proximal humeral fractures in Korea with three or more years of follow-up: a retrospective cohort study

Sang Jin Cheon[1], Kyu-Hak Jung[2], Min Hyeok Choi[3], Suk-Woong Kang[4]

[1]Department of Orthopedic Surgery, Pusan National University Hospital, Pusan National University School of Medicine, Busan, Korea
[2]Department of Orthopedic Surgery, Yeson Hospital, Bucheon, Korea
[3]Department of Preventive and Occupational & Environmental Medicine, Office of Public Healthcare Service, Research Institute for Convergence of Biomedical Science and Technology, Pusan National University Yangsan Hospital, Pusan National University School of Medicine, Yangsan, Korea
[4]Department of Orthopedic Surgery, Research Institute for Convergence of Biomedical Science and Technology, Pusan National University Yangsan Hospital, Pusan National University School of Medicine, Yangsan, Korea

Background: Shoulder hemiarthroplasty (HA) is an established treatment option for complex proximal humeral fractures, particularly in cases involving severe comminution or osteoporotic bone. This study investigated the clinical and radiographic outcomes of HA with a minimum follow-up of 3 years and aimed to identify prognostic factors associated with postoperative function.

Methods: We retrospectively reviewed 44 patients (16 males and 28 females; mean age, 61.2 years; range, 23–83 years) who underwent shoulder HA for complex proximal humeral fractures between 2005 and 2018. The mean follow-up duration was 70.4 months (range, 36–168 months). Clinical evaluations included the Constant score, visual analog scale pain score, patient satisfaction, and range of motion. Radiographic assessments examined tuberosity healing, radiolucent lines, acromiohumeral distance (AHD), and glenoid arthrosis.

Results: At the 3-year follow-up, 64% of patients reported being satisfied or very satisfied. The mean Constant score was 46.6 (range, 13–71), and the age- and sex-adjusted Constant score was 53.5 (range, 19–92). Radiographically, 23% of patients demonstrated radiolucent lines, and 41% showed evidence of glenoid arthrosis. Tuberosity absorption occurred in 39% of patients, with a mean onset of 11.2 months postoperatively, and was significantly associated with lower Constant scores and reduced range of motion. Patients younger than 60 years demonstrated better functional outcomes and lower rates of tuberosity absorption. The mean AHD decreased from 8.4 mm postoperatively to 4.4 mm at the 3-year follow-up (P<0.001).

Conclusions: Shoulder HA for complex proximal humeral fractures yielded satisfactory pain relief and functional outcomes, particularly when tuberosity healing was preserved. However, elderly patients with diminished bone quality were more likely to develop tuberosity absorption and experience poorer functional recovery. Meticulous surgical technique and careful postoperative surveillance remain essential to achieving optimal results.

Level of evidence: III.

Keywords: Hemiarthroplasty; Osteoarthritis; Osteoporosis; Prognosis; Shoulder fractures

Original Article

Received: October 27, 2025
Revised: December 1, 2025
Accepted: December 8, 2025

Correspondence to:
Suk-Woong Kang
Department of Orthopedic Surgery, Pusan National University Yangsan Hospital, 20 Geumo-ro, Mulgeum-eup, Yangsan 50612, Korea
Tel: +82-55-360-2125
Email: redmaniak@naver.com

Introduction

Background

Proximal humeral fractures are among the most common osteoporotic injuries in the elderly, accounting for approximately 5% of all fractures. Anatomical reduction and stable fixation are often difficult, making arthroplasty a reasonable option. Historically, hemiarthroplasty (HA) has been widely used in such cases. Recently, the use of reverse total shoulder arthroplasty (RSA) has increased; however, it is generally limited to carefully selected elderly patients with proximal humeral fractures. Several studies have reported that in this specific subgroup, particularly in those with poor bone quality or rotator cuff insufficiency, RSA may provide better clinical outcomes and lower complication rates than HA [1-3].

Although RSA provides reliable pain relief and restoration of elevation in elderly individuals, complications such as instability, scapular notching, glenoid component loosening, and comparatively lower implant survival rates than hip and knee arthroplasty remain concerns. Therefore, in younger and more active patients, HA is still considered an alternative to preserve the bone stock and restore near-anatomic biomechanics [4]. Nevertheless, the clinical outcomes of HA are often unsatisfactory, and tuberosity healing has been identified as a major prognostic factor for postoperative function [5-7].

Malunion or nonunion of the tuberosities leads to decreased strength, a limited range of motion, and poor patient satisfaction. Boileau et al. [5] reported that resorption or malposition of the tuberosity was the primary cause of poor results after HA, and Kralinger et al. [6] also demonstrated significantly lower Constant scores in the nonunion group than in the healing group.

Another concern following HA is the development of secondary glenoid changes, including erosion or arthrosis, which may deteriorate the long-term outcomes. Zhao et al. [8] observed glenoid erosion in 64.9% of patients at an average follow-up of 14.7 years and reported significantly worse clinical outcomes in this group. Parsons et al. [9] also found progressive glenoid wear and joint-space narrowing in all young active patients after HA, which correlated with reduced function. However, the clinical significance and progression pattern of glenoid arthrosis remain unclear.

Objectives

Therefore, this study aimed to evaluate the clinical and radiographic outcomes of HA performed for proximal humeral fractures with a minimum follow-up of 3 years. This study focused on the influence of tuberosity healing, changes in the acromiohumeral distance (AHD), and the occurrence of glenoid arthrosis to clarify the midterm results and prognostic factors for HA.

Methods

Ethics statement

This study was conducted at Pusan National University Hospital. The study protocol and data use were approved by the Institutional Review Board (IRB) of Gachon University Gil Medical Center, with appropriate data-sharing agreements in place (IRB No. GFIRB 2018-382).

Study design

This was a single-arm retrospective cohort study. It was described according to the STROBE statement available at https://www.strobe-statement.org/.

Setting

This study was conducted in Pusan National University Hospital, Korea. Patients were treated between January 2005 and December 2018 and were followed in an outpatient setting according to a standardized postoperative schedule (1, 3, 6, 9, and 12 months and annually thereafter).

Surgical approach and postoperative care

Before surgery, templating was performed on both shoulder radiographs and both sides were compared. An appropriate insertion length was determined for implant insertion. All patients underwent a 30° beach-chair position under general anesthesia. A deltopectoral approach was used in all the cases. During the operation, a trial stem was inserted and the tension of the biceps tendon and deltoid muscle was adjusted. Traction was applied to confirm proper reduction and humeral head height. Cement was used to fix humeral stems. The tuberosity was fixed with Ethibond No. 5 (Ethicon) and attached to the stem. The cancellous bone was taken from the surrounding humeral head, and the sutures were bundled. To confirm whether the soft tissues, including the tuberosity, were properly

https://doi.org/10.12671/jmt.2025.00325

sutured after surgery, we investigated whether a forward elevation of 140°, internal rotation of 50°–70°, and external rotation of 40° were possible, and whether 10–15 mm posterior subluxation was possible. Postoperatively, a shoulder abduction brace was applied for 6 weeks. Passive pendulum and isometric exercises were performed on the first postoperative day. One week postoperatively, passive shoulder motion began, and the range of motion gradually increased. Active range of motion was measured 6 weeks after surgery, and resistance strengthening exercises were allowed at 12 weeks.

Participants

Eligible participants were patients who underwent primary shoulder HA for proximal humeral fractures during the study period. During this period, HA was selected when fixation was not feasible because of severe comminution or poor bone quality. Patients were included in the final cohort if they had postoperative follow-up for at least 3 years with available clinical outcomes and radiographic evaluation. Patients were excluded if follow-up was shorter than 3 years (including death before minimum follow-up) or if they were lost to follow-up. A total of 47 patients were initially identified. Among them, two patients died and one was lost to follow-up. Consequently, 44 patients (16 males and 28 females) who were followed up for at least three years were included in the study.

Variables

The primary clinical outcome was the Constant score at the 3-year follow-up. Age- and sex-adjusted Constant scores were also evaluated. Secondary clinical outcomes included pain during active motion, measured using a 0–10 visual analog scale; patient satisfaction; and active range of motion. Radiographic outcomes comprised AHD measured on true anteroposterior radiographs; radiolucent lines around the humeral stem at the cement-bone or implant-bone interface; glenoid arthrosis, characterized by joint-space narrowing, subchondral sclerosis or cysts, or osteophyte formation on anteroposterior or axillary views; and tuberosity absorption, defined as nonunion with radiographic absorption or loss of the greater tuberosity.

Data sources/measurement

Demographic and perioperative variables were obtained from electronic medical records and operative reports.

Clinical assessment

All patients were assessed 1 day preoperatively, and postoperative evaluation was regularly performed during outpatient visits (1, 3, 6, 9, and 12 months, and once a year thereafter). The clinical results were defined according to the Constant score and postoperative age- and sex-adjusted Constant scores. Subjective pain during active motion was measured using a visual analog scale (VAS) [10], with 0 indicating no pain and 10 indicating extremely severe pain. The patients' self-assessment scale was measured as very satisfied, satisfied, acceptable, and disappointed. We also assessed the patients' active range of motion in forward elevation, abduction and external rotation (at the side).

Radiographic assessment

True anteroposterior and axillary radiographs were obtained preoperatively, postoperatively, and at regular visits. Radiographic evaluations included the assessment of AHD, radiolucent lines, glenoid arthrosis, and tuberosity absorption. The AHD was measured on true anteroposterior radiographs. Radiolucent lines were assessed at the cement-bone or implant-bone interface around the humeral stem [11]. Glenoid arthrosis was defined radiographically as the presence of joint space narrowing, subchondral sclerosis, subchondral cysts, or osteophyte formation on the true anteroposterior or axillary views [9]. Tuberosity absorption was evaluated and defined as nonunion with radiographic absorption or loss of the greater tuberosity (Figs. 1, 2) [12].

Statistical methods

Paired comparisons of the AHD between immediate postoperative radiographs and radiographs obtained at the 3-year follow-up were performed using the Wilcoxon signed-rank test. The Mann-Whitney U test and Fisher exact test were used for between-group comparisons (tuberosity absorption vs no absorption; ≥60 vs. <60), as appropriate. All statistical analyses were performed using IBM SPSS ver. 20.0 (IBM Corp.). A P-value <0.05 was considered statistically significant.

Fig. 1. Radiography of the right proximal humerus fracture in a 52-year-old female patient. (A) Preoperative anteroposterior radiograph demonstrating a four-part fracture. (B) Immediate postoperative anteroposterior radiograph following hemiarthroplasty. (C) Anteroposterior radiograph at the 3-year follow-up showing decreased acromiohumeral distance and progression of glenoid arthrosis.

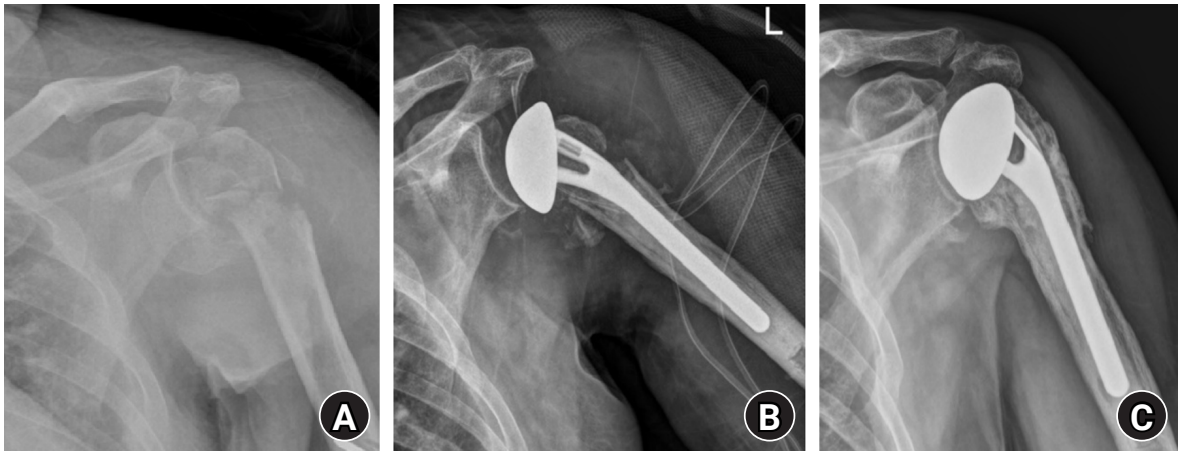

Fig. 2. Radiography of the left proximal humerus fracture and dislocation in a 65-year-old male patient. (A) Preoperative anteroposterior radiograph demonstrating a four-part fracture-dislocation. (B) Immediate postoperative anteroposterior radiograph following hemiarthroplasty. (C) Anteroposterior radiograph at the 3-year follow-up demonstrating tuberosity healing.

Results

The mean age at the time of surgery was 61.2 years (range, 23–83 years), and the mean follow-up duration was 70.4 months (range, 36–168 months) (Table 1). Fractures were categorized according to the Neer classification, which defines displaced proximal humerus fractures by the number of involved parts; based on this system, 16 cases were identified as three-part fractures and 28 as four-part fractures.

The implants used in this study were the Global Shoulder System (DePuy Inc.), Bipolar Shoulder System (Biomet Inc.), and Bigliani/Flatow Shoulder System (Zimmer Inc.).

Table 1. Preoperative demographic data of patients (n=44)

Variable	Value
Patient	44
Age (yr)	61.2±15.7 (23–83)
Male sex	16 (36.4)
Follow-up duration (mo)	70.4±53.1 (36–168)
Fracture type	
3-Part	16 (36.4)
4-Part	28 (63.6)

Values are presented as mean±standard deviation (range) or number (%).

https://doi.org/10.12671/jmt.2025.00325

Overall clinical results

At the 3-year follow-up, the mean VAS score was 2.1 (range, 0–5). Regarding patient satisfaction, 12 patients (27%) reported being very satisfied and 16 patients (36%) were satisfied with the operated shoulder. The mean Constant score was 46.6 (range, 13–71), the age- and sex-adjusted Constant score was 53.5 (range, 19–92). The mean active shoulder range of motion was as follows: forward elevation, 120.6 (range, 20–145); abduction, 114.5 (range, 20–140) and external rotation, 52.4 (range, 10–65) (Table 2).

Radiographic findings

At the 3-year follow-up, all stems were radiographically stable without evidence of loosening; however, radiolucent lines were observed in 10 patients (23%). The radiolucent lines were first detected at a mean of 25.2 months (range, 12–36). Glenoid arthrosis was observed in 18 patients (41%) at a mean of 34.4 months (range, 12–36) after surgery. At the 3-year follow-up, absorption of the tuberosity was observed in 17 cases (39%), with a mean of 11.2 months (range, 6–24) after surgery. The AHD was 8.4 mm immediately after surgery and 4.4 mm at 3-year follow-up (P<0.001) (Table 3).

Comparison of outcomes according to absorption of tuberosity

Among the 44 patients, 17 showed tuberosity absorption and 27 did not. The median age was 72 years (interquartile range [IQR], 65–76 years) in the absorption group and 59 years (IQR, 47–72 years) in the nonabsorption group. At the 3-year follow-up, the median VAS score was 3 (IQR, 1–4) in the absorption group and 2 (IQR, 1–3) in the nonabsorption group. The median Constant score was significantly lower in the absorption group than in the nonabsorption group (35 [IQR, 34–35] vs. 50 [IQR, 49–71]; P=0.004), as was the median age- and sex-adjusted Constant score (40 [IQR, 30–50] vs. 60 [IQR, 44–78]; P=0.002). The median forward elevation, abduction, and external rotation were 80° (IQR, 50°–105°), 95° (IQR, 85°–100°), and 30° (IQR, 30°–35°), respectively, in the absorption group, compared with 145° (IQR, 145°–160°), 130° (IQR, 120°–140°), and 60° (IQR, 55°–70°) in the nonabsorption group. Differences in all range of motion parameters were statistically significant between the two groups (all P<0.001) (Table 4).

Comparison of outcomes between patients aged <60 and ≥60 years

Among the 44 patients, 24 were aged ≥60 years and 20 were aged <60 years. The median age was 73.5 years (IQR, 68.5–78 years) in patients aged ≥60 years and 46.5 years (IQR, 38.5–56.5 years) in those aged <60 years. At the 3-year follow-up, the median VAS score was 2 (IQR, 1–3) in patients aged ≥60 years and 2 (IQR, 0.5–4) in patients aged <60 years. The median Constant score was significantly lower in patients aged ≥60 years than in those aged <60 years (35 [IQR, 34–49.5] vs. 50 [IQR, 50.0–70.5]; P=0.001), as was the

Table 2. Clinical outcomes after hemiarthroplasty at the 3-year follow-up

Variable	Value
Patient	44
Visual analog scale	2.1±1.6 (0–5)
Patient satisfaction score	
Very satisfied	12 (27.3)
Satisfied	16 (36.4)
Acceptable	12 (27.3)
Disappointed	4 (9.1)
Constant score	46.6±16.4 (13–71)
Age- and sex-adjusted Constant	53.5±19.1 (19–92)
Forward elevation (°)	120.6±45.1 (20–145)
Abduction (°)	114.5±24.0 (20–140)
External rotation (°)	52.4±17.7 (10–65)

Values are presented as mean±standard deviation (range) or number (%).

Table 3. Radiographic findings after hemiarthroplasty at the 3-year follow-up

Variable	Value
Patient	44
Radiolucent line	10 (23)
Time until development of radiolucent line (mo)	25.2±7.8 (12–36)
Glenoid arthrosis	18 (41)
Time until development of glenoid arthrosis (mo)	34.4±5.8 (12–36)
Tuberosity absorption	17 (39)
Time until development of tuberosity absorption (mo)	11.2±5.2 (6–24)
Acromiohumeral distance after surgery (mm)	8.4±2.9
Acromiohumeral distance at the 3-year follow-up (mm)	4.4±3.1

Values are presented as number (%) or mean±standard deviation (range).

median age- and sex-adjusted Constant score (46 [IQR, 34.5–58.5] vs. 60 [IQR, 40–80]; P=0.014). Glenoid arthrosis was observed in 10 patients (41.7%) aged ≥60 years and eight patients (40.0%) aged <60 years, with no statistically significant difference between the groups (P=1.0). Tuberosity absorption occurred more frequently in patients aged ≥60 years than in those aged <60 years (13 [54.2%] vs. 4 [20.0%]; P=0.030). Patients aged <60 years demonstrated greater range of motion. The median forward elevation and abduction were significantly higher in patients aged <60 years than in those aged ≥60 years (150° [IQR, 145°–160°] vs. 110° [IQR, 72.5°–145°], P<0.001; and 135° [IQR, 119°–140°] vs. 100° [IQR, 90°–120°], P<0.001, respectively). External rotation was also significantly greater in patients aged <60 years (65° [IQR, 61°–80°] vs. 33° [IQR, 30°–57.5°]; P<0.001) (Table 5).

Complications and reoperations

One patient underwent plate fixation for a periprosthetic fracture. One patient underwent revision surgery because of a postoperative infection. Two patients experienced axillary nerve injury after trauma, and conservative treatment was administered.

Discussion

Key results

This study investigated the midterm clinical and radio-

Table 4. Comparison of outcomes according to the tuberosity absorption at the 3-year follow-up

Variable	Absorption	No absorption	P-value
Patient	17	27	-
Age (yr)	72 (65–76)	59 (47–72)	0.141
Visual analog scale score	3 (1–4)	2 (1–3)	0.457
Constant score	35 (34–35)	50 (49–71)	0.004
Age- and sex-adjusted Constant score	40 (30–50)	60 (44–78)	0.002
Forward elevation (°)	80 (50–105)	145 (145–160)	<0.001
Abduction (°)	95 (85–100)	130 (120–140)	<0.001
External rotation (°)	30 (30–35)	60 (55–70)	<0.001
Radiolucent line	4 (23.5)	6 (22.2)	1
Glenoid arthrosis	12 (70.6)	6 (22.2)	0.004
Difference in acromiohumeral distance (mm)	5.9 (4.1–7.3)	3 (1.5–4.3)	<0.001

Values are presented as median (interquartile range) or number (%). Continuous variables were analyzed using the Mann-Whitney U test, and categorical variables were compared using Fisher exact test.

Table 5. Comparison of outcomes between patients aged ≥60 and those aged <60 years at the 3-year follow-up

Variable	≥60 Years	<60 Years	P-value
Patient	24	20	-
Age (yr)	74 (69–78)	47 (39–57)	<0.001
Visual analog scale score	2 (1–3)	2 (0.5–4)	0.644
Constant score	35 (34–49.5)	50 (50.0–70.5)	0.001
Age- and sex-adjusted Constant score	46 (34.5–58.5)	60 (40.0–80.0)	0.014
Forward elevation (°)	110 (72.5–145)	150 (145–160)	<0.001
Abduction (°)	100 (90–120)	135 (119–140)	<0.001
External rotation (°)	33 (30–57.5)	65 (61–80)	<0.001
Radiolucent line	4 (16.7)	6 (30.0)	0.472
Glenoid arthrosis	10 (41.7)	8 (40.0)	1
Tuberosity absorption	13 (54.2)	4 (20.0)	0.030
Difference in acromiohumeral distance (mm)	4.3 (2.6–6.2)	4 (2.1–4.8)	0.563

Values are presented as median (interquartile range) or number (%). Continuous variables were analyzed using the Mann-Whitney U test, and Categorical variables were compared using Fisher exact test.

https://doi.org/10.12671/jmt.2025.00325

graphic outcomes of shoulder HA for complex proximal humeral fractures with a minimum follow-up of 3 years. Overall, the patients demonstrated moderate Constant scores and satisfactory pain control at the 3-year follow-up, with approximately 64% reporting satisfaction with the procedure. Radiographically, 39% of patients exhibited tuberosity absorption at 3 years postoperatively, which was associated with inferior clinical outcomes. These findings emphasize the importance of anatomical restoration for optimal functional recovery. Additionally, radiolucent lines were identified in 23% of the cases and glenoid arthrosis developed in 41% of the cases, suggesting that mid- to long-term monitoring is essential for these patients.

Interpretation/comparison with previous studies

As a standard treatment for proximal humeral fractures, shoulder HA is generally performed for complex comminuted fractures, dislocations, or head-split fractures. Mighell et al. [13] reported that 93% of patients who underwent HA for proximal humeral fractures were pain-free and satisfied with their clinical outcomes at follow-up, including American Shoulder and Elbow Surgeons (ASES) score and Simple Shoulder Test (SST) scores. Several reports have suggested HA for proximal humeral fractures because many patients have good functional results [14-16]. Implants have recently been developed for RSA. Therefore, RSA is becoming more common than HA for the treatment of proximal humeral fractures [17]. However, most studies have compared elderly patients, and RSA in young patients remains controversial. If plate fixation is difficult for proximal humeral fractures in relatively young patients, HA is still used as a primary treatment.

Gronhagen et al. [18] asserted that the classification of fractures was not correlated with the Constant score in the midterm follow-up and noted that the status of soft tissue, not just the fracture classification, was important as a postoperative result. We also found no correlation between the fracture type and postoperative results and could not objectively determine the preoperative state of the soft tissues. Gronhagen et al. [18] concluded that early postoperative surgery affects the outcome, which is an important factor already mentioned by several authors, and we could not analyze the correlation statistically because of the delayed operation in this study [13,19].

Many factors affect the functional outcomes of HA. The age of the patients, time to surgery after injury, the position of humeral stem and rotator cuff integrity were reported as important factors [20,21], and it is known that the anatomical reduction and union of greater tuberosity after surgery is the most important factor on postoperative function [5,19,22]. Boileau et al. [5] reported that the outcomes of 66 patients who underwent HA were related to displacement and malposition of the tuberosity. Initial malposition was observed in 27% of patients. Finally, it was reported that 50% of the cases showed an abnormal position of the tuberosity. In this case, the superior displacement of the implant, shoulder stiffness or weakness, and continuous pain were unsatisfactory. In our cases, nonunion or absorption of the tuberosity affected the postoperative prognosis. In addition, Boileau et al. [5] described factors related to malunion of the tuberosity, such as initial replacement of the implant, malposition of the tuberosity, and age >75 years. Anatomical union of the tuberosity is the most important factor in the HA. Moreover, rehabilitation should be delayed in such patients.

Antuna et al. [23] also described age as an important factor. Elderly individuals have relatively poor bone quality, which affects the healing of the tuberosity, and rehabilitation also shows poor functional outcomes. We also found that preservation of tuberosity healing was a key determinant of postoperative function.

The reported incidence of glenoid arthrosis varies depending on the radiographic definition and follow-up duration. However, there are few cases in which reoperation is required, even in cases of glenoid arthrosis [19,24]. Gronhagen et al. [18] found 35% of these cases and no such correlation, but interpreted it as having poor results in postoperative Constant scores. Mighell et al. [13] observed radiologic changes in degenerative joints in six of eight patients (72%). Two of them involved dissociation of the implant, and one case involved nonunion of the tuberosity. To solve this problem, reoperation was performed. At the time of reoperation, the patient had severe arthritis of the glenoid, concomitant glenoid replacement was performed at the time of reoperation. In our study, glenoid arthrosis was observed in 41% of patients, but the effect on postoperative results was not statistically significant. However, in our cases, it is thought that midterm follow-up was not sufficient to determine the progression of the degenerative lesion to the joint, and long-term follow-up is needed to

determine the effect of the degenerative change in the joint on the prognosis.

Limitations

First, it had a retrospective design with a moderate sample size, which may limit the strength of the statistical inferences. Second, although all patients were followed up for at least 3 years, long-term outcomes beyond this period (e.g., at 5 or 10 years) were not assessed. Third, our radiographic assessments (tuberosity healing, glenoid changes, and AHD) were based on plain radiographs, which may not fully capture the three-dimensional anatomic details. Despite these limitations, our study offers valuable insights into the midterm behavior of HA in proximal humeral fractures, highlighting the importance of tuberosity healing and early detection of glenoid changes. Future prospective multicenter studies with long-term follow-up and advanced imaging modalities (e.g., CT and 3D reconstruction) are needed to better delineate the factors that influence sustained outcomes after HA.

Generalizability

These findings are most generalizable to patients in Korea with proximal humeral fractures treated with HA because internal fixation is not feasible due to severe comminution or poor bone quality, using similar surgical technique and rehabilitation. Generalizability to other populations, surgeons, implant systems, and healthcare settings may be limited. In addition, because this was a single-cohort study without a non-HA comparison group, the results should not be interpreted as comparative effectiveness versus reverse shoulder arthroplasty or fixation strategies.

Conclusions

Shoulder HA for complex proximal humeral fractures provided satisfactory pain relief and functional recovery at the 3-year follow-up, when adequate tuberosity healing was achieved. However, tuberosity absorption was associated with poorer long-term outcomes. Continuous radiographic monitoring and precise surgical reconstruction of the tuberosities are essential to obtain optimal results.

Article Information

Author contributions

Conceptualization: SJC, SWK. Data curation: KHJ. Formal analysis: KHJ, MHC, SWK. Investigation: KHJ, SWK. Methodology: KHJ, SWK. Writing-original draft: SJC, MHC, SWK. Writing-review & editing: SJC, SWK. All authors read and approved the final manuscript.

Conflicts of interest

No potential conflict of interest relevant to this article was reported.

Funding

This work was supported by a 2-Year Research Grant of Pusan National University.

Data availability

Contact the corresponding author for data availability.

Acknowledgments

We respectfully dedicate this manuscript to the memory of Young-Kyu Kim, MD, PhD (1959-2025; former professor, Department of Orthopedic Surgery, Gil Medical Center, Gachon University College of Medicine, Incheon, Korea), whose passing in August 2025 preceded the submission of this work. Dr. Kim's pioneering contributions to the conception, design, and execution of this study reflect his lifelong dedication to advancing the field of shoulder arthroplasty. His scientific rigor and clinical expertise continue to guide our research endeavors.

Supplementary materials

None.

References

1. Hasler A, Ker A, Grubhofer F, et al. Clinical and radiographic long-term outcomes of hemiarthroplasty for complex proximal humeral fractures. J Shoulder Elbow Surg 2024;33:698-706.
2. Ferrel JR, Trinh TQ, Fischer RA. Reverse total shoulder arthroplasty versus hemiarthroplasty for proximal humeral fractures: a systematic review. J Orthop Trauma 2015;29:60-8.

https://doi.org/10.12671/jmt.2025.00325

3. Boyle MJ, Youn SM, Frampton CM, Ball CM. Functional outcomes of reverse shoulder arthroplasty compared with hemiarthroplasty for acute proximal humeral fractures. J Shoulder Elbow Surg 2013;22:32-7.
4. Essilfie AA, Gamradt SC. The role for shoulder hemiarthroplasty in the young, active patient. Clin Sports Med 2018;37:527-35.
5. Boileau P, Krishnan SG, Tinsi L, Walch G, Coste JS, Molé D. Tuberosity malposition and migration: reasons for poor outcomes after hemiarthroplasty for displaced fractures of the proximal humerus. J Shoulder Elbow Surg 2002;11:401-12.
6. Kralinger F, Schwaiger R, Wambacher M, et al. Outcome after primary hemiarthroplasty for fracture of the head of the humerus. A retrospective multicentre study of 167 patients. J Bone Joint Surg Br 2004;86:217-9.
7. Gadea F, Alami G, Pape G, Boileau P, Favard L. Shoulder hemiarthroplasty: outcomes and long-term survival analysis according to etiology. Orthop Traumatol Surg Res 2012;98:659-65.
8. Zhao Y, Zhu Y, Lu Y, Li F, Jiang C. Long-term outcomes of shoulder hemiarthroplasty for acute proximal humeral fractures. Int Orthop 2023;47:1517-26.
9. Parsons IM 4th, Millett PJ, Warner JJ. Glenoid wear after shoulder hemiarthroplasty: quantitative radiographic analysis. Clin Orthop Relat Res 2004;(421):120-5.
10. Bijur PE, Silver W, Gallagher EJ. Reliability of the visual analog scale for measurement of acute pain. Acad Emerg Med 2001;8(12):1153-7.
11. Torrens C, Martínez-Díaz S, Ruiz A, Gines A, Cáceres E. Assessment of radiolucent lines in cemented shoulder hemi-arthroplasties: study of concordance and reproducibility. Int Orthop 2009;33:165-9.
12. Reuther F, Muller S, Wahl D. Management of humeral head fractures with a trauma shoulder prosthesis: correlation between joint function and healing of the tuberosities. Acta Orthop Belg 2007;73:179-87.
13. Mighell MA, Kolm GP, Collinge CA, Frankle MA. Outcomes of hemiarthroplasty for fractures of the proximal humerus. J Shoulder Elbow Surg 2003;12:569-77.
14. Agarwal S, Rana A, Sharma RK. Functional outcome after primary hemiarthroplasty in three or four part proximal humerus fracture: a short term followup. Indian J Orthop 2016;50:590-4.
15. Bosch U, Skutek M, Fremerey RW, Tscherne H. Outcome after primary and secondary hemiarthroplasty in elderly patients with fractures of the proximal humerus. J Shoulder Elbow Surg 1998;7:479-84.
16. Dimakopoulos P, Potamitis N, Lambiris E. Hemiarthroplasty in the treatment of comminuted intraarticular fractures of the proximal humerus. Clin Orthop Relat Res 1997;(341):7-11.
17. LaMartina J 2nd, Christmas KN, Simon P, et al. Difficulty in decision making in the treatment of displaced proximal humerus fractures: the effect of uncertainty on surgical outcomes. J Shoulder Elbow Surg 2018;27:470-7.
18. Gronhagen CM, Abbaszadegan H, Revay SA, Adolphson PY. Medium-term results after primary hemiarthroplasty for comminute proximal humerus fractures: a study of 46 patients followed up for an average of 4.4 years. J Shoulder Elbow Surg 2007;16:766-73.
19. Kwon YW, Zuckerman JD. Outcome after treatment of proximal humeral fractures with humeral head replacement. Instr Course Lect 2005;54:363-9.
20. Demirhan M, Kilicoglu O, Altinel L, Eralp L, Akalin Y. Prognostic factors in prosthetic replacement for acute proximal humerus fractures. J Orthop Trauma 2003;17:181-8.
21. Robinson CM, Page RS, Hill RM, Sanders DL, Court-Brown CM, Wakefield AE. Primary hemiarthroplasty for treatment of proximal humeral fractures. J Bone Joint Surg Am 2003;85:1215-23.
22. Frankle MA, Mighell MA. Techniques and principles of tuberosity fixation for proximal humeral fractures treated with hemiarthroplasty. J Shoulder Elbow Surg 2004;13:239-47.
23. Antuna SA, Sperling JW, Cofield RH. Shoulder hemiarthroplasty for acute fractures of the proximal humerus: a minimum five-year follow-up. J Shoulder Elbow Surg 2008;17:202-9.
24. Plausinis D, Kwon YW, Zuckerman JD. Complications of humeral head replacement for proximal humeral fractures. Instr Course Lect 2005;54:371-80.

JMT Journal of Musculoskeletal Trauma

pISSN 3058-6267 · eISSN 3058-6275
J Musculoskelet Trauma 2026;39(2):156-161
https://doi.org/10.12671/jmt.2025.00381

Clinical and radiographic outcomes of elastic stable intramedullary nailing for pediatric humeral shaft fractures: a retrospective case series

Kang-San Lee[1,2], Dongju Shin[1], Sang Hee Kim[1], Il Seo[1], Tae-Hoon Kim[1], Sung Jung Kim[1]

[1]W Institute for Orthopedic Trauma and Joint Surgery, W General Hospital, Daegu, Korea
[2]Daegu Top Union Orthopedic Surgery Clinic, Daegu, Korea

Background: Pediatric humeral shaft fractures are uncommon and are generally treated conservatively, with satisfactory clinical outcomes reported in most cases. However, conservative management often necessitates prolonged immobilization and frequent outpatient follow-up visits, and it carries an inherent risk of residual angular or translational deformity. Elastic stable intramedullary nailing (ESIN) provides a simple and minimally invasive method of fracture fixation that offers adequate stability without disrupting the periosteal blood supply, thereby permitting early mobilization and promoting rapid bone union. The purpose of this study was to evaluate the clinical and radiological outcomes of ESIN fixation in pediatric patients with humeral shaft fractures.

Methods: The medical records of pediatric patients with humeral shaft fractures who underwent ESIN fixation between January 2015 and November 2025 were retrospectively reviewed. Data collected included patient demographics, mechanism of injury, fracture location, number of elastic nails used, time to union, degree of residual angulation, range of motion (ROM), and postoperative complications.

Results: The mean age of the patients was 10.0 years (range, 7 to 15 years). The mean time to radiographic union was 5.4 weeks (range, 2.4 to 10.4 weeks). The mean coronal angulation was 0.2° (range, –9.1° to 5.8°), while the mean sagittal angulation was –1.3° (range, –6.9° to 5.3°). No cases of infection, nerve injury, or nail migration were observed during the follow-up period. At the final follow-up assessment, all patients demonstrated full shoulder and elbow ROM, with no residual deformity or pain reported.

Conclusions: In this small retrospective case series, ESIN fixation resulted in favorable union rates and excellent functional outcomes in pediatric humeral shaft fractures.

Level of evidence: IV.

Keywords: Child; Humeral fractures; Intramedullary fracture fixation; Bone nails; Treatment outcome

Original Article

Received: December 4, 2025
Revised: January 20, 2026
Accepted: January 23, 2026

Correspondence to:
Sung Jung Kim
W Institute for Orthopedic Trauma and Joint Surgery, W General Hospital, 1632, Dalgubeol-daero, Dalse-gu, Daegu 42642, Korea
Tel: +82-53-522-5561
Email: os1947@msn.com

Introduction

Background

Pediatric humeral shaft fractures are relatively uncommon injuries, accounting for approximately 2%–5% of all long-bone fractures in children [1,2]. Most cases can be successfully managed with conservative treatment such as functional bracing or cast immobilization, given the strong remodeling potential of the growing bone [3]. How-

ever, prolonged immobilization often causes discomfort, requires frequent outpatient follow-ups, and carries a risk of angular or translational deformity, particularly in older children and adolescents [4].

Elastic stable intramedullary nailing (ESIN) has become an established minimally invasive fixation technique for pediatric long-bone fractures [5,6]. This method provides stable fixation without disrupting the periosteal blood supply, allowing early joint motion and reliable bone union [7]. While ESIN has been successfully reported in several Asian studies, clinical series focusing on its role in achieving early mobilization and minimizing the burden of prolonged immobilization in this population remain limited [5].

Purpose

The purpose of this study was to evaluate the clinical and radiologic outcomes of ESIN for pediatric humeral shaft fractures, with particular focus on its potential for rapid functional recovery, based on our institutional experience.

Methods

Ethics statement

We conducted this study in compliance with the principles of the Declaration of Helsinki. Ethical approval for this study was obtained from the Public Institutional Review Board (PIRB) via the e-IRB system of the Ministry of Health and Welfare, Republic of Korea. The requirement for informed consent was waived due to the retrospective nature of the study (IRB No. P01-202512-01-001).

Study design

This study is a retrospective, single-center case series.

Setting

This study was conducted at W Institute for Orthopedic Trauma and Joint Surgery, W General Hospital (Daegu, Korea). The medical records of patients aged under 18 years who underwent surgical treatment for humeral shaft fractures at our institution between January 2015 and November 2025 were retrospectively reviewed.

Patients were followed postoperatively through scheduled outpatient visits, with radiographic and clinical assessment of union typically performed at weekly intervals until healing criteria were met. Final outcomes were assessed at the last follow-up visit.

Surgical intervention

The surgical indications at this institution included displaced humeral shaft fractures with angulation exceeding age-dependent limits (≥30° in children <10 years, ≥20° in older children), or unstable alignment after closed reduction. Other indications included open fractures, polytrauma, and associated nerve injury.

All surgeries were performed by orthopedic surgeons specializing in pediatric or upper extremity trauma. Anesthesia was administered as either brachial plexus block or general anesthesia, depending on the patient's age and level of cooperation. The patient was placed in a supine position on a radiolucent table with the injured arm draped free, and fluoroscopy was used throughout the procedure.

A posterior entry technique through the distal humeral cortex was used in all cases. A small longitudinal incision was made over the posterior aspect of the distal humerus just proximal to the olecranon fossa. The triceps muscle was bluntly split to expose the posterior cortex, and an awl was used under fluoroscopic guidance to create the entry portal into the medullary canal (Fig. 1).

A single or double prebent titanium elastic nail (diameter, 2.0–3.0 mm) was chosen, with a diameter approximately one-third of the narrowest portion of the medullary canal [8]. In smaller humeri, the available canal diameter and posterior entry approach sometimes limited the maximal

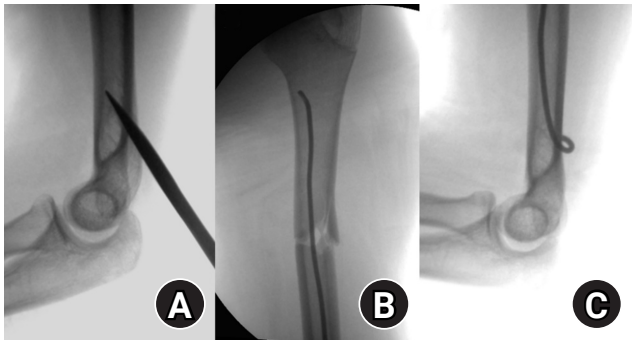

Fig. 1. Intraoperative fluoroscopic images demonstrating the surgical technique of elastic stable intramedullary nailing for a pediatric humeral shaft fracture. (A) The entry point was created at the posterior cortex of the distal humerus using an awl under fluoroscopic guidance. (B) The prebent elastic nail was advanced across the fracture site under continuous fluoroscopic visualization. (C) The distal ends of the nails were contoured and buried subcutaneously to minimize soft-tissue irritation.

nail size, so a single nail was used to avoid excessive force during insertion. When the canal width allowed, two nails were inserted to achieve optimal end-point divergence and three-point elastic fixation. Proper alignment and rotational stability were confirmed under fluoroscopic control. After satisfactory reduction and fixation were achieved, the nail was cut and impacted beneath the posterior cortex to prevent soft-tissue irritation. Postoperatively, the arm was supported in a simple sling for comfort. Early gentle shoulder and elbow motion was initiated within the first postoperative week, and full range of motion (ROM) was allowed once radiographic callus formation was evident. All implants were removed after radiologic union was achieved (Fig. 2).

Participants

During the study period, a total of seven patients aged under 18 years underwent surgical treatment for humeral shaft fractures at our institution. Among them, two patients were treated with plate fixation due to distal shaft fracture location, which limited the feasibility of achieving stable fixation with ESIN, and were therefore excluded from the analysis. The remaining five patients who underwent ESIN were included in this study.

Variables

Medical records and radiographs provided patient age/sex, injury mechanism, and fracture site. Surgical variables included details like elastic nail count. Primary radiologic outcome variables were bone union time, removal time, follow-up time, and final follow-up angulation (coronal/sagittal planes). Clinical outcome variables were shoulder/elbow range of motion or ROM, residual pain, and complications.

Data sources/measurement

Data were from the electronic medical records of this hospital. Radiologic assessments included bone union and postoperative angulation in both the coronal (varus/valgus) and sagittal (anterior/posterior) planes on anteroposterior and lateral radiographs, measured at the final follow-up. Positive values were defined as valgus or anterior angulation, whereas negative values indicated varus or posterior angulation. Bone union was defined as the earliest appearance of bridging callus formation on at least three cortices on radiographs, accompanied by the absence of tenderness at the fracture site. Union time was recorded at the postoperative visit (typically at weekly intervals) when these radiographic and clinical criteria were

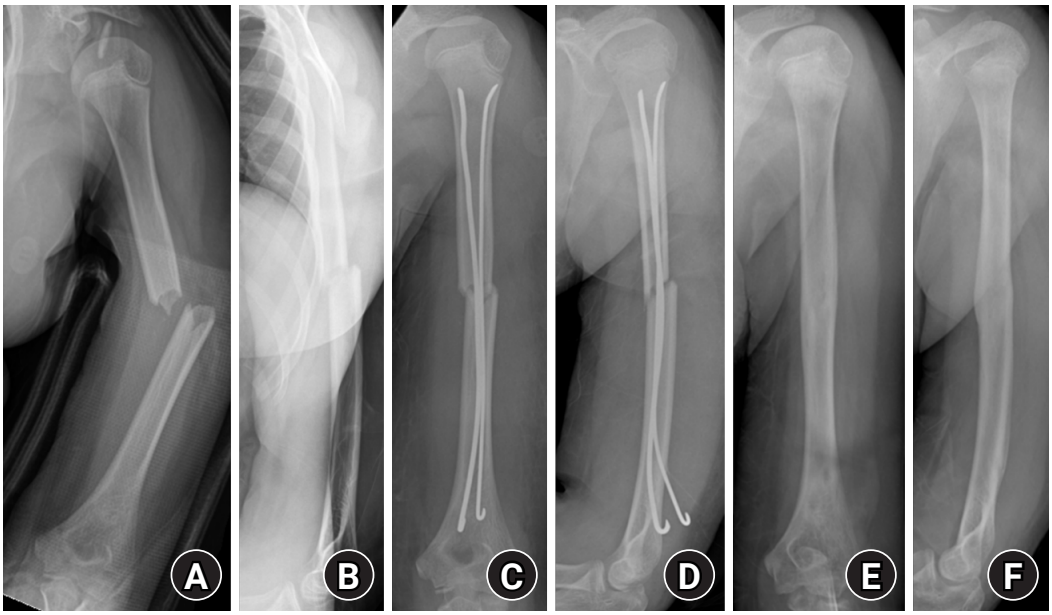

Fig. 2. Radiographs of a representative case demonstrating successful bone healing following elastic stable intramedullary nailing fixation. (A, B) Preoperative anteroposterior and lateral radiographs showing a midshaft humeral fracture. (C, D) Immediate postoperative radiographs demonstrating satisfactory fracture alignment and stable fixation with elastic nails. (E, F) Follow-up radiographs obtained after implant removal showing complete bone union and restoration of normal humeral alignment.

https://doi.org/10.12671/jmt.2025.00381

first met. Implant removal was scheduled once union was achieved; however, the exact timing varied depending on each patient's circumstances, such as school schedule and outpatient availability. Clinical results were evaluated based on shoulder and elbow ROM, residual pain, and complications such as nonunion, infection, nail migration, or reoperation.

Bias

Because this was a retrospective case series of surgically treated patients, selection bias and confounding by indication are possible; operative treatment was chosen based on fracture characteristics and clinical considerations at the institution. To reduce selection bias within the ESIN cohort, we included consecutive pediatric humeral shaft fracture cases treated with ESIN during the study period and extracted variables using predefined radiographic and clinical criteria.

Study size

There was no sample size estimation.

Statistical methods

Continuous variables were summarized using means and ranges. Given the small sample size, descriptive statistics were primarily used, and no inferential statistical analyses were performed. All statistical calculations were performed using IBM SPSS ver. 26.0 (IBM Corp.). There were no missing data in this study.

Results

A total of five patients (four males and one female; mean age, 10 years; range, 7–15 years) were included in the study (Table 1). The mechanisms of injury consisted of falls from height in one patient, a traffic accident in two, and a slip down in two. The mean follow-up period was 18.7 weeks (range, 11.1–25.9 weeks). The mean bone union time was 5.4 weeks (range, 2.4–10.4 weeks). At the final follow-up, the mean coronal (varus/valgus) angulation was 0.2° (range, –9.1° to 5.8°), and the mean sagittal (anterior/posterior) angulation was –1.3° (range, –6.9° to 5.3°) (Table 2).

No cases of infection, nerve injury, or nail migration were observed. At the final follow-up, all patients achieved full shoulder and elbow ROM without residual pain or deformity, and no patient required early implant removal due to irritation or discomfort.

Discussion

Key results

This study demonstrated that ESIN provided consistent bone union and favorable functional outcomes in most pediatric humeral shaft fractures. The technique offers several advantages, including minimal soft-tissue disruption, preservation of the periosteal blood supply, and the potential for early joint mobilization. All patients achieved solid bone union within an average of 5.4 weeks and regained full shoulder and elbow motion without pain or deformity. Notably, bridging callus formation was observed as early as

Table 2. Radiologic outcomes

Variable	Mean (range)
Union time (wk, n=5)	5.4 (2.4 to 10.4)
Coronal angulation (°)	0.2 (–9.1 to 5.8)
Sagittal angulation (°)	–1.3 (–6.9 to 5.3)

Table 1. Demographic, clinical, and radiologic characteristics of patients

Case	Age (yr)/ sex	Side	Mechanism of injury	Fracture site	No. of nails	Union time (wk)	Removal time (wk)	Follow-up time (wk)	Coronal angulation (°)	Sagittal angulation (°)	Final range of motion	Complication
1	8/Male	Right	Slip down	Mid	1	2.4	3.4	11.1	3.1	5.3	Full	None
2	15/Male	Left	Traffic accident	Mid	1	3.2	6.4	20.6	5.8	–2.5	Full	None
3	10/Male	Right	Traffic accident	Mid	1	10.4	18.9	20.4	–9.1	–1.0	Full	None
4	7/Female	Right	Fall from height	Proximal	1	3.4	3.6	15.7	0.8	–1.2	Full	None
5	10/Male	Left	Slip down	Mid	2	7.4	25.9	25.9	0.5	–6.9	Full	None

Positive values indicate valgus or anterior angulation; negative values indicate varus or posterior angulation.

2.4 weeks in some cases, which may reflect the preserved periosteal blood supply.

Interpretation/comparison with previous studies

Several studies have discussed the mechanical stability of flexible intramedullary nailing in long-bone fractures. Lascombes et al. [8] emphasized that the stability of elastic nailing depends on the ratio between nail diameter and the medullary canal width, suggesting that insufficient nail occupancy may reduce construct rigidity and lead to delayed union or loss of alignment. In addition, Johnson et al. [9] conducted a biomechanical study evaluating the influence of the nail's length beyond the fracture site on overall construct stability. They reported that fixations extending less than two bone diameters beyond the fracture were grossly unstable, showing significantly reduced bending resistance and higher displacement under load. In contrast, fixations extending at least three diameters maintained sufficient stiffness and load-bearing capacity, highlighting the importance of adequate working length for stable fixation. Integrating these findings with the present study, adequate nail diameter and sufficient working length are essential to achieve stable fixation and prevent loss of alignment in pediatric humeral shaft fractures. However, it should be noted that these biomechanical principles are largely derived from studies on lower-extremity long bones, where greater nail occupancy is generally feasible.

In the pediatric humerus, the medullary canal is often substantially narrower, which may limit the ability to achieve the "adequate" nail diameter suggested by biomechanical studies. Despite this limitation, the present series demonstrated favorable alignment maintenance and union, which may be partly attributable to the lower mechanical loading demands of the upper extremity.

Although the present study did not directly compare ESIN with conservative treatment, previous literature has discussed differences in angular correction between the two approaches. In a comparative study between conservative and surgical treatment for pediatric humeral shaft fractures, Canavese et al. [3] reported better correction of angular deformity in the surgically treated group compared with the nonoperative group. In contrast, Hannonen et al. [10] demonstrated that even though surgical fixation for pediatric humeral shaft fractures has become more common in recent years, most cases still achieve satisfactory union and function with conservative management. Considering the generally accepted limits of angular deformity in nonoperative management (approximately 20°–30° in younger children and 15°–20° in older children), the present study demonstrated superior alignment correction, suggesting that ESIN can provide more reliable angular control while allowing early rehabilitation in carefully selected cases [10].

Limitations

The retrospective design and small number of cases limit the generalizability of the findings, and statistical interpretation should be approached with caution. The follow-up duration was relatively short, precluding the evaluation of long-term functional or radiographic outcomes such as remodeling or residual deformity. Because no control group was available, direct comparison with conservative treatment or other fixation methods could not be made. Nevertheless, this study provides valuable insight into the practical indications and limitations of ESIN for pediatric humeral shaft fractures.

Clinical implication

These findings support previous reports that ESIN provides stable fixation and predictable healing for humeral shaft fractures in skeletally immature patients.

Conclusions

In this small retrospective series, ESIN provided reliable alignment maintenance and favorable functional recovery, allowing early mobilization in appropriately selected pediatric humeral shaft fractures. While most fractures can be successfully managed nonoperatively, ESIN may serve as a useful surgical option when unacceptable angulation or instability persists after closed reduction. Larger comparative studies are warranted to further clarify its indications.

Article Information

Author contributions

Conceptualization: DS, SJK. Data curation: KSL, SHK, IS. Formal analysis: THK. Investigation: KSL, IS. Methodology: KSL, SJK. Project administration: SJK. Visualization: KSL, SHK. Writing-original draft: KSL. Writing-review & editing: all authors. All authors read and approved the final manuscript.

https://doi.org/10.12671/jmt.2025.00381

Conflicts of interest
No potential conflict of interest relevant to this article was reported.

Funding
None.

Data availability
Contact the corresponding author for data availability.

Acknowledgments
None.

Supplementary materials
None.

References

1. Caviglia H, Garrido CP, Palazzi FF, Meana NV. Pediatric fractures of the humerus. Clin Orthop Relat Res 2005;432:49-56.
2. O'Shaughnessy MA, Parry JA, Liu H, Stans AA, Larson AN, Milbrandt TA. Management of paediatric humeral shaft fractures and associated nerve palsy. J Child Orthop 2019;13:508-15.
3. Canavese F, Marengo L, Cravino M, et al. Outcome of conservative versus surgical treatment of humeral shaft fracture in children and adolescents: comparison between non-operative treatment (Desault's bandage), external fixation and elastic stable intramedullary nailing. J Pediatr Orthop 2017;37:e156-63.
4. van de Wall BJ, Ochen Y, Beeres FJ, et al. Conservative vs. operative treatment for humeral shaft fractures: a meta-analysis and systematic review of randomized clinical trials and observational studies. J Shoulder Elbow Surg 2020;29:1493-504.
5. Li J, Wu J, Zhang Y, et al. Elastic stable intramedullary nailing for pediatric humeral shaft fractures under ultrasonographic guidance: a retrospective study. Front Pediatr 2021;9:806100.
6. Marengo L, Nasto LA, Michelis MB, Boero S. Elastic stable intramedullary nailing (ESIN) in paediatric femur and tibia shaft fractures: comparison between titanium and stainless steel nails. Injury 2018;49 Suppl 3:S8-11.
7. Annabell L, Shore BJ, Hedequist DJ, Hogue GD. Evaluation and management of pediatric humeral shaft fractures. J Am Acad Orthop Surg 2023;31:265-73.
8. Lascombes P, Haumont T, Journeau P. Use and abuse of flexible intramedullary nailing in children and adolescents. J Pediatr Orthop 2006;26:827-34.
9. Johnson CW, Carmichael KD, Morris RP, Gilmer B. Biomechanical study of flexible intramedullary nails. J Pediatr Orthop 2009;29:44-8.
10. Hannonen J, Sassi E, Hyvönen H, Sinikumpu JJ. A shift from non-operative care to surgical fixation of pediatric humeral shaft fractures even though their severity has not changed. Front Pediatr 2020;8:580272.

JMT Journal of Musculoskeletal Trauma

pISSN 3058-6267 · eISSN 3058-6275
J Musculoskelet Trauma 2026;39(2):162-173
https://doi.org/10.12671/jmt.2025.00367

NSAID-induced suppression of type X collagen and VEGF expression in the early phase of rat femoral fracture healing

Maria Zafar[1], Rana Mohammad Zeeshan[1], Safia Tasawar[1], Muhammad Saad Ilyas[2], Amer Aziz[2], Uruj Zehra[1]

[1]Department of Anatomy, University of Health Sciences, Lahore, Pakistan
[2]Department of Orthopedic & Spine Surgery, Ghurki Trust Teaching Hospital, Lahore, Pakistan

Background: The current literature presents conflicting evidence regarding the effects of nonsteroidal anti-inflammatory drugs (NSAIDs) on fracture healing. This experimental study aimed to evaluate and compare the histological and immunohistochemical changes during femoral fracture healing in rats treated with a nonselective cyclooxygenase (COX) inhibitor (diclofenac sodium) and a selective COX-2 inhibitor (celecoxib).

Methods: Thirty-six male Wistar (standard outbred) albino rats weighing 200–400 g underwent standardized mid-diaphyseal femoral fracture surgery. The animals were randomized into three groups (n=12 per group): group 1 received diclofenac sodium, group 2 received celecoxib, and group 3 served as the control group and received 1 mL of distilled water orally once daily. Six rats from each group were euthanized at the end of the 2nd and 7th weeks after fracture for sample collection. Histological examination was complemented by immunohistochemical analysis, and the expression of type X collagen and vascular endothelial growth factor (VEGF) was assessed using the immunoreactive score (IRS) method.

Results: Healing scores were significantly higher in the control group at both time points (2nd week, P=0.01; 7th week, P=0.03). At the 2nd week, rats treated with diclofenac sodium demonstrated significantly greater fibrosis (P=0.01), and by the 7th week, they exhibited impaired bone formation (P=0.003) along with increased bone defects (P=0.01). IRS values for type X collagen and VEGF were significantly higher in the control group than in both treatment groups during the 2nd week (P=0.01 and P=0.005, respectively).

Conclusions: These findings suggest that, in this rat model, NSAIDs, particularly nonselective COX inhibitors, may disrupt the early phases of bone repair by affecting hypertrophic chondrocyte differentiation and reducing angiogenic activity. Although these results indicate a potential risk to optimal healing, they are preclinical observations, and their relevance to clinical fracture management should be interpreted with caution.

Level of evidence: V.

Keywords: Bone fractures; Non-steroidal anti-inflammatory drugs; Fracture healing; Cyclooxygenase inhibitors

Original Article

Received: November 18, 2025
Revised: February 17, 2026
Accepted: March 4, 2026

Correspondence to:
Uruj Zehra
Department of Anatomy, University of Health Sciences, Lahore, Pakistan
Tel: +92-336-478-5095
Email: uruj.zehra@gmail.com

Introduction

Background

Bone fractures represent one of the most prevalent public health challenges worldwide. In 2019 alone, approximately 178 million new fracture cases were reported

globally, reflecting a 33.4% increase compared to previous years. Additionally, the total number of individuals living with fractures reached 455 million, marking a staggering 70.1% increase since 1990 [1]. The region of Asia has a higher prevalence of individuals at high fracture risk with most cases being osteoporotic fractures in women [2].

Fracture healing is a complex process that starts with the activation of immune and inflammatory responses. Macrophages, neutrophils, and platelets play a pivotal role in the initial phase of bone healing by releasing a wide array of pro-inflammatory cytokines and growth factors [3]. These include tumor necrosis factor-alpha, platelet-derived growth factor (PDGF), bone morphogenetic proteins (BMPs), vascular endothelial growth factor (VEGF), transforming growth factor-beta, and various interleukins (IL-1, IL-6, IL-10, IL-11, IL-12, and IL-23), all of which are essential for initiating and regulating the healing cascade. These signaling molecules organize a cascade of cellular events that are essential for initiating and sustaining the healing process at the fracture site [3-5]. The two key factors on which successful fracture healing primarily depends are a favorable biological environment with sufficient vascularization and a mechanically stable environment [6]. Previous studies have highlighted the central role of VEGF in fracture healing. VEGF promotes the development of a supportive vascular network that synergizes osteogenic factors such as BMP-2, and it drives the angiogenic responses necessary for cartilage resorption and subsequent bone formation. Enhanced vasculogenesis and angiogenesis increase the delivery of progenitor cells, nutrients, oxygen, and minerals essential for matrix deposition and mineralization. As repair progresses into later stages, chondrocytes within the cartilaginous callus cease proliferation, undergo hypertrophy, and begin producing type X collagen. These hypertrophic chondrocytes also express Osterix, a potent inducer of VEGF, which facilitates vascular invasion and the recruitment of chondroclasts into the hypertrophic cartilage [7,8]. However, several intrinsic and extrinsic factors can potentially disrupt or impair this healing process [6]. One such factor influencing fracture healing is the use of nonsteroidal anti-inflammatory drugs (NSAIDs), which are frequently prescribed for their analgesic and anti-inflammatory properties [9]. Despite their widespread use in clinical practice, the impact of NSAIDs on bone healing remains controversial. Numerous studies have investigated their effects, with findings ranging from delayed or impaired healing to no significant impact. The variability in results is often attributed to differences in the type of NSAID used, dosage, duration of administration, and the specific stage of healing during which the drug is administered. This ongoing debate underscores the need for cautious consideration when prescribing NSAIDs in the context of bone fractures [10].

NSAIDs are often preferred over other analgesics in the management of fractures due to their dual action providing both effective pain relief and anti-inflammatory benefits [11]. However, prolonged administration of NSAIDs has been associated with an increased risk of delayed union, malunion, and nonunion of fractures. In contrast, some studies have reported no significant impact on bone healing, leaving the role of NSAIDs in fracture repair a subject of ongoing debate [9].

It is believed that due to the inhibition of cyclooxygenase (COX) enzymes by NSAIDs, the synthesis of prostaglandins is reduced which participate in different processes of healing and repair leading to repressive effect on fracture healing. Prostaglandins promote the process of angiogenesis and collagen synthesis thus enhancing the healing process [10]. Based on the current literature regarding NSAID exposure and bone healing, there is a clear need for further research to better elucidate the mechanisms of action of different classes of NSAIDs and their specific effects on the various phases of fracture repair [9].

Objectives

In the current study we hypothesized that NSAID administration reduces collagen type X (COLX) and VEGF expression during fracture healing. This was investigated through detailed histological analysis and by determining the proportion and localization of COLX and VEGF in healing fractures.

Methods

Ethics statement

This study was conducted following approval from the Ethical Review Committee of the institute (approval No. UHS/Reg-21/ERC/510) and in accordance with institutional guidelines for medical and biomedical animal research.

Study design

Standard outbred Wistar albino rats were used as a fracture model in the current study as a sequence of biological events during fracture healing in these rats such as inflammation, callus formation, endochondral ossification, and remodeling closely parallel human fracture healing [12].

Sample size was determined using the resource equation approach, which is appropriate for experimental animal studies where prior effect size estimates are limited. Based on this method, the minimum required sample size was calculated to be eight animals per group to achieve an adequate degree of freedom for error. To further increase statistical power and improve the detection of biologically meaningful differences, the sample size was increased to twelve animals per group. This calculation was based on the total number of animals per group and was not dependent on subdivision by time points; despite postoperative losses, the overall sample size per group remained above the calculated minimum requirement. Accordingly, a total of thirty-six healthy adult male Wistar albino rats (200–400 g) were randomly allocated to three groups using a lottery method.

To minimize potential confounders, the animals were kept separately in the institutional animal facility in small groups of 2–3 adult rats per cage under standardized conditions, including a well-ventilated environment maintained at a temperature of 23±2 °C, relative humidity of 55%±5%, and a 12-hour light/dark cycle. Cage location was not systematically varied; all animals were provided with a standard laboratory rodent diet and had free access to water. Surgical procedures, drug administration, and outcome assessments were conducted according to a standardized protocol and in the same order across groups where feasible. Any sick rats found during the research procedure were excluded from the study, in addition, animals who underwent any surgical complications or died both during and after surgery were also excluded from the study.

Surgical procedure and induction of fracture

Rats were given antibiotic enrofloxacin (5–10 mg/kg) prophylactically just before the surgery and anesthetized with mixture of Ketamine 80–100 mg/kg and Xylazine 5–10 mg/kg given intramuscularly [13]. A vertical midline incision was made under aseptic and sterile conditions, beginning from the mid-thigh and extending over the knee joint, positioned medial to the patella and the extensor mechanism, on either the right or left limb as required. The quadriceps and extensor mechanism were displaced laterally. The distal end of the femur and the proximal end of the tibia were exposed after subluxation of the patella and extensor mechanism laterally. An entry hole in the medullary canal was created in the middle of the groove between the condyles of the femur [13]. Intramedullary reaming was done with the passage of a guidewire. The mid-diaphyseal fracture of femur was induced by a surgical hammer and retrograde intramedullary nailing was done (Supplementary material). The skin was closed in layers with the help of a Vicryl suture, postoperatively, the animals were monitored constantly until full recovery from anesthesia, followed by hourly observations for the first 8 hours postoperatively. Therapeutic dose of tramadol (10 mg/kg body weight) was administered intramuscularly once after surgery to all animals to keep them pain free [14].

Grouping and administration of NSAIDs

The animals were randomly divided into three groups using a lottery method, each comprising 12 rats. Group 1 received a nonselective NSAID (diclofenac sodium) administered once daily at a dosage of 5 mg/kg body weight/day [15], while group 2 was treated with a selective COX-2 inhibitor (celecoxib) at a dosage of 4 mg/kg body weight/day [16]. Both drugs were given orally and started from the first postoperative day. Group 3 served as the control group and was administered 1 mL of distilled water orally once daily (Table 1).

Animals were monitored daily by trained personnel for behavioral signs of pain or distress, including reduced mobility, guarding behavior, altered grooming, and changes in food or water intake. A predefined rescue analgesia protocol and humane endpoints were established; however, no animal required additional analgesic intervention or early euthanasia during the study period.

Additional postoperative analgesics were not administered to the control group, as two of the experimental groups were already receiving NSAIDs. This approach was adopted to avoid potential confounding effects of additional pharmacological agents on bone healing outcomes and to minimize bias related to drug interactions.

https://doi.org/10.12671/jmt.2025.00367

Table 1. Grouping of experimental animals, method of treatment, and drug dosage

Group	Intervention	Frequency and route of administration	Duration (wk)	No. of animals and day of sacrifice
A (n=11)	Diclofenac sodium 5 mg/kg in 1 mL of distilled water	Once daily orally from postoperative day 1 until the day before euthanasia	2	5 on PD 15
			7	6 on PD 49
B (n=12)	Celecoxib 4 mg/kg in 1 mL of distilled water	Once daily orally from postoperative day 1 until the day before euthanasia	2	6 on PD 15
			7	6 on PD 49
C (n=11)	1 mL of distilled water	Once daily orally from postoperative day 1 until the day before euthanasia	2	5 on PD 15
			7	6 on PD 49

PD, postoperative day.

Dissection and radiograph

Half of the animals from each group were euthanized and dissected at the end of the 2nd week (15th postoperative day). The other half of the animals were sacrificed at the end of 7th week (49th postoperative day). The dissected limbs of animals sacrificed at 7th week were radiographed laterally to evaluate the healing of bone.

Histological and immunohistochemical evaluation

The fractured femur was fixed in 10% formalin for 72 hours and then decalcified in 20% ethylenediaminetetraacetic acid solution (pH 8) for 4–5 days in a vacuum oven and paraffin blocks were made after tissue processing. Alcian blue hematoxylin/orange G (ABH/OG) staining was done on 5 μm thick sections to assess the healing bone based on modified Lane and Sandhu method [17]. This method scores from 0–10 each for newly formed bone, newly formed cartilage, evidence of hypertrophic cartilage, newly formed fibrous tissue, and remnant defect size. Scoring increased with increased newly formed bone, cartilage and hypertrophied cartilage, while it decreased with an increase of fibrous tissue and bone defect between fractured ends.

ABH/OG-stained sections are used to appreciate architecture of the callus, as cartilage stains blue, immature bone gray, mature bone orange, erythrocytes and soft tissue appear pink to red and fibrous connective tissue violet.

Immunohistochemical analyses of COLX and VEGF were also done on 3 μm sections using polyclonal primary antibody (PA5-115039 and ABCLONAL A12303 respectively). The intensity and percentage expression were analyzed based on immunoreactive scoring system [18]. In brief, immunoreactivity was evaluated using the immunoreactive score (IRS), calculated by multiplying the percentage of positive cells (0–4) by staining intensity (0–3). The resulting IRS values were categorized as: 0–1, negative; 2–3, mild; 4–8, moderate; and 9–12, strongly positive.

Reliability analysis

For histological and IRS scoring reliability analysis, the first two authors performed independent evaluations of radiographs and slides (for histology and immunohistochemistry). They also performed the same analysis twice on radiographs and slides by blinding the group allocation with one-month interval to assess intraobserver variation. Both inter and intraobserver agreement of each radiographic finding, histological manifestation and the total score were statistically analyzed using intraclass correlation coefficients (ICC), which demonstrated good to excellent agreement (ICC, 0.7–0.9).

Statistical analysis

Data were analyzed using IBM SPSS ver. 26.0 (IBM Corp.). Quantitative variables were summarized as median with interquartile range due to nonnormal data distribution. Normality was assessed using the Shapiro–Wilk test. Comparisons among the three groups for histological and immunohistochemical parameters were performed using the Kruskal-Wallis test, followed by Dunn's post hoc test for pairwise comparisons where appropriate. Correlations between numerical variables were evaluated using Spearman's rank correlation coefficient. Inter- and intraobserver reliability were assessed using intraclass correlation coefficients. A P-value ≤0.05 was considered statistically significant.

Results

General health of the animal during experimental period

Two animals (one from each diclofenac and control

groups) died on the first postoperative day without any obvious reason from the sample cohort of 36 animals leaving a total of 11 animals in diclofenac and control group while 12 in celecoxib. During daily morning and afternoon inspection of animals to monitor health, movement, and food intake behavior, two animals of the same cage were found to have minor wounds at 14th day on their nonoperative leg, due to fighting and injuring each other, which was taken care of by antiseptic dressing. Throughout the remaining experimental period, these animals stayed healthy, no further sickness, disease, or change in behavior was noticed.

Radiographic findings

The radiographs of nearly 90% of the animals treated with diclofenac and 65% of those treated with celecoxib by the end of 7th week postoperative still showed the gap between the two edges of the healing bones and were marked as persistent radiolucent fracture lines by two observers. In contrast, all animals in the control group exhibited well-formed bony callus (Fig. 1).

General histological architecture

In ABH/OG-stained sections the cartilage, immature and mature bone and fibrous connective tissue were appreciated quite well (Fig. 2). Lightly stained newly formed bone was seen surrounding the fractured ends. Bone defects appeared as tissue gap with cluster of newly formed chondrocytes present between and around fracture ends forming soft callus. Fibrosis was identified as groups of small fibroblasts present at the periphery of fractured ends and soft callus. Mature hypertrophied chondrocytes were observed as giant cells with large nucleus present on the junction of cartilage and newly formed bone tissue. The inter and intra observer ICC for all the histological parameters was excellent to fair.

Histological scoring at 2nd week

Among individual parameters, fibrosis scores were signifi-

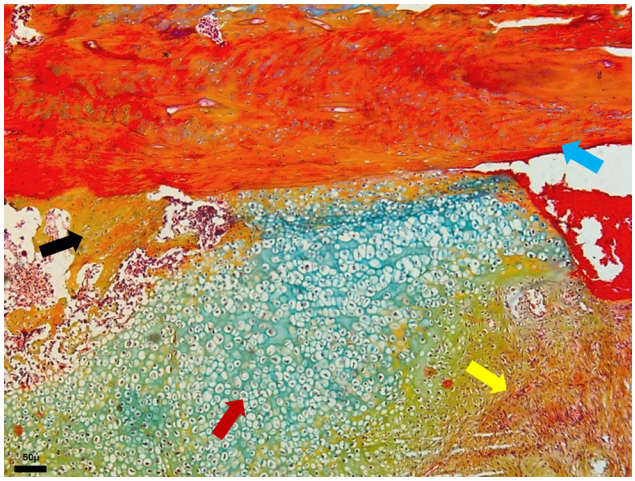

Fig. 2. Photomicrograph of an Alcian blue hematoxylin orange G (ABH/OG)-stained section from the celecoxib group at 2 weeks after fracture, demonstrating cartilage (red arrow), immature woven bone (black arrow), mature lamellar bone (blue arrow), and fibrous connective tissue (yellow arrow) (magnification, ×50).

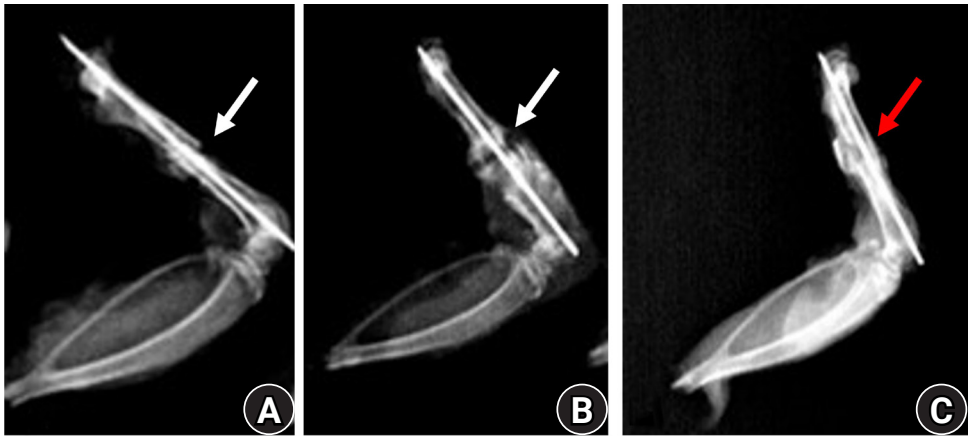

Fig. 1. Lateral radiographs of rat femora at 7 weeks after fracture. (A) The diclofenac group and (B) the celecoxib group show persistent radiolucent fracture lines (white arrows), defined as linear lucencies at the original fracture site indicating incomplete cortical bridging. (C) The control group demonstrates a consolidated bridging callus (red arrow) without residual fracture lucency.

https://doi.org/10.12671/jmt.2025.00367

cantly lower in the NSAID-treated groups (P=0.03) indicating greater fibrous tissue at the fracture site. Pairwise comparison using Dunn's post hoc test showed significant difference only between diclofenac group and controls (P=0.01). The overall healing scores were also found significantly lower in experimental animals (P=0.01) while pairwise comparison using Dunn's post hoc test showed significant difference only between diclofenac group and controls (P=0.004) (Table 2, Fig. 3).

Histological scoring at 7th week

At the 7th week, newly formed bone was significantly greater in the control group compared with the experimental groups (P=0.01). Pairwise comparisons using Dunn's post hoc test demonstrated a significant difference between the diclofenac and control groups (P=0.003). Bone defect scores were significantly lower in the diclofenac group (P=0.03) reflecting larger residual bone defects). Dunn's post hoc analysis revealed a highly significant difference between the diclofenac group and controls (P=0.01), as well as borderline significance between diclofenac and celecoxib groups (P=0.05) (Fig. 4). Total healing scores were significantly lower in experimental animals (P=0.03), with pairwise comparisons showing significant differences between the diclofenac group and controls (P<0.001) and between diclofenac and celecoxib groups (P=0.03) (Table 2).

Immunohistochemical expression of collagen X and VEGF

The immunohistochemical stained slides gave the variable expression of collagen X (COLX) and VEGF. The COLX staining was seen around the mature hypertrophied chondrocytes and near the newly formed bone, while VEGF expression was mostly near the newly formed bone, in extracellular matrix and around blood vessels.

The expression of COLX was less in percentage (P=0.01) and intensity (P=0.02) in experimental animals as compared to controls making IRS significantly lower in these

Table 2. Median and IQR of histological scores according to the modified Lane and Sandhu scoring method at weeks 2 and 7 in all three groups

Variable	Group	Cartilage	Bone formed	MHC	Fibrosis	Bone defect	Total
Second week	Diclofenac	3 (2–4.5)	1.5 (1–2)	5 (4.5–5.5)	5 (4.5–5.5)*	8 (3.5–9)	22 (17–25)*
	Celecoxib	3 (2.5–3)	2 (1–2.5)	5 (5–6)	7 (4.5–7)*	10 (9–10)	25 (24.5–27)*
	Control	3.5 (3–5)	2.5 (1.5–3)	6 (5.5–6)	8 (7–8)*	10 (10–10)	28.5 (28–30)*
Seventh week	Diclofenac	1.5 (1–2.5)	2 (1.5–2.5)*	2 (1–5)	3.5 (1.5–6.5)	1.5 (0.5–6)*	13.5 (9–19)*
	Celecoxib	4 (2–5)	4 (3–6)*	6 (5–7)	7 (3–7)	10 (6–10)*	31 (21.5–33)*
	Control	1 (1–5)	6 (5–8.5)*	6 (1–7.5)	7 (6–9)	10 (10–10)*	31 (29–34)*

Values are presented as median (IQR).
IQR, interquartile range; MHC, mature hypertrophic chondrocytes.
*P<0.05.

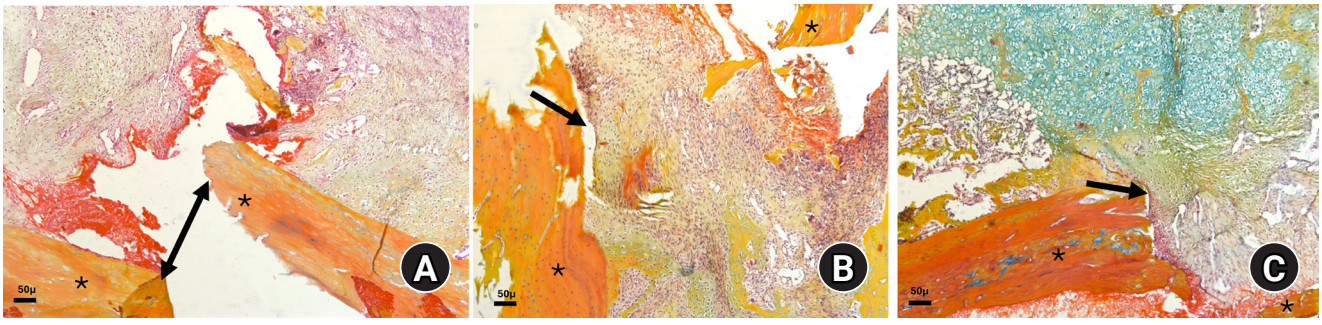

Fig. 3. Photomicrographs of Alcian blue hematoxylin orange G (ABH/OG)-stained slides illustrating fractured bone edges (*) with callus formation at 2 weeks after fracture in the three animal groups: (A) diclofenac group, (B) celecoxib group, and (C) control group (magnification, ×50). Notably, in the control group, the fracture gap is filled with soft callus tissue (black arrow), unlike in the two experimental groups, where the gap is partially filled with granulation tissue (double-sided and black arrows in A and B, respectively). The bluish staining in C indicates the presence of more cartilaginous tissue.

Fig. 4. Photomicrographs of Alcian blue hematoxylin orange G (ABH/OG)-stained slides illustrating fractured bone at 7 weeks after fracture in the three animal groups: (A) diclofenac group, (B) celecoxib group, and (C) control group (magnification, ×50). Notably, in the control group, the bone is almost completely healed (black arrow), whereas granulation tissue is still present in both the diclofenac and celecoxib groups (black arrows). The edges of the healing bone are also visible (*).

Table 3. Comparison of the median and IQR values for the immunohistochemical expression of VEGF and type X collagen in terms of percentage, intensity, and IRS

Variable	Groups	Immunomarker expression	Percentage scores	Intensity scores	Total scores
Week 2	Diclofenac	VEGF	1 (0.5–1.5)**	1 (0.5–1) **	1 (0.5–1.5) **
		Collagen X	2 (1.5–2)*	1 (1–1.5)*	2 (1.5–3)*
	Celecoxib	VEGF	2 (2–2)**	2 (1–2)**	4 (2–4)**
		Collagen X	3 (2.5–3)*	2 (2–3)*	6 (5–7.5)*
	Controls	VEGF	3 (3–3.5)**	3 (3–3)**	9 (9–10.5)**
		Collagen X	3.5 (3–4)*	3 (2.5–3)*	9 (8.5–10.5)*
Week 7	Diclofenac	VEGF	2 (1.5–2)	2 (1.5–2)*	3 (2–4)*
		Collagen X	1 (1–1.5)	1 (1–1.5)	1.5 (1–2)
	Celecoxib	VEGF	3 (1.5–3)	2 (1.5–2.5)*	6 (2.5–7.5)*
		Collagen X	2 (1.5–2.5)	2 (1.5–2.5)	4 (2.5–6)
	Controls	VEGF	1 (1–1.5)	1 (1–1)*	1 (1–1.5)*
		Collagen X	2 (1–2)	1.5 (1–2)	3 (1–4)

Values are presented as median (IQR).
IQR, interquartile range; VEGF, vascular endothelial growth factor; IRS, immunoreactive scoring.
*P<0.05, **P<0.01.

animals (P=0.01) in 2nd week (Table 3, Fig. 5). Pairwise comparisons using Dunn's post hoc test showed significantly lower percentage, intensity, and IRSs in the diclofenac group compared with the celecoxib group (P=0.05, P=0.04, and P=0.04, respectively) and the control group (P=0.003, P=0.009, and P=0.004, respectively). On the 7th week no significant difference was seen in the expression of COLX among animals.

VEGF expression was significantly reduced in experimental animals compared with controls, both in terms of percentage (P=0.005) and intensity (P=0.006), resulting in a significantly lower IRS (P=0.005) at the 2nd week (Table 3, Fig. 5). Pairwise comparisons using Dunn's post hoc test demonstrated significant differences in percentage, intensity, and IRSs between the diclofenac group and controls (P=0.001, P=0.002, and P=0.001, respectively), as well as between the celecoxib group and controls (P=0.04, P=0.04, and P=0.05, respectively).

At the 7th week, VEGF expression showed lower intensity in controls compared with experimental animals (P=0.03), resulting in a significantly higher total IRS in the experimental groups (P=0.03). Pairwise analysis using Dunn's post hoc test revealed a significant difference only between the celecoxib group and controls for intensity (P=0.03) and IRS (P=0.01).

https://doi.org/10.12671/jmt.2025.00367

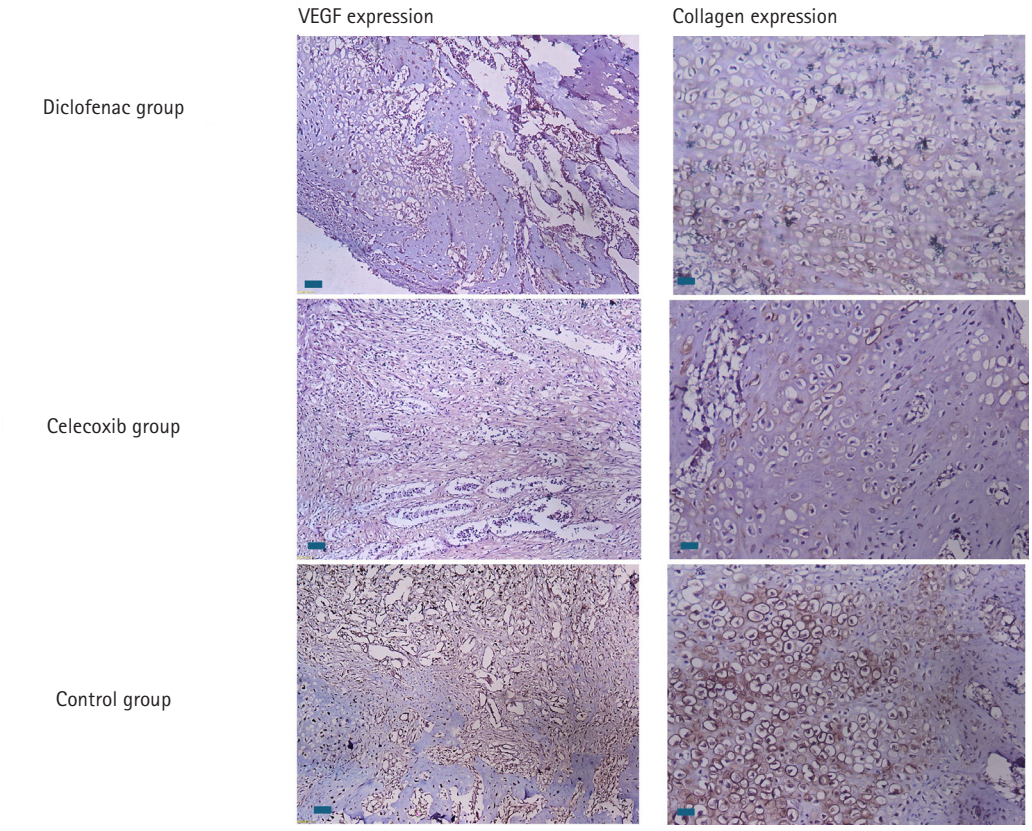

Fig. 5. Immunohistochemically stained sections showing the expression and intensity of vascular endothelial growth factor (VEGF) and type X collagen in all three groups at 2 weeks after fracture. Notably, expression is higher in the control group, as shown by the brown staining (scale bars, 50 μm; magnification, ×100).

Correlation between immunohistochemical expression and healing scores

The COLX and VEGF expression was seen to be in significant positive correlation with total healing score (r=0.76, P=0.002; r=0.66, P=0.01 respectively). While in the 7th week they did not show any significant correlation.

Correlation among immunohistochemical expression

Both VEGF and COLX were in significant positive correlation with each other in the 2nd week (r=0.7, P=0.006) while in the 7th week no correlation was seen.

Discussion

Key results

The current study revealed that by the second week, the experimental group receiving diclofenac sodium exhibited a significantly higher fibrosis at the fracture site and delayed bone healing. Furthermore, the expression of COLX and VEGF was notably lower in both experimental groups compared to the control group. By the seventh week, new bone formation was significantly reduced, with a large remaining bone defect between the fractured ends and a significant delay in bone healing in both experimental groups, particularly in the diclofenac sodium-treated animals. Additionally, VEGF expression was decreased in the control group at 7th week likely reflecting advanced healing with reduced angiogenic demand (Fig. 6). Pairwise comparisons indicate that the most consistent and significant differences are observed between the diclofenac and control groups, whereas celecoxib does not demonstrate uniformly significant differences compared to control across all histological endpoints.

Interpretation/comparison with previous studies

Radiographic examination of the fractured bones at the 7th

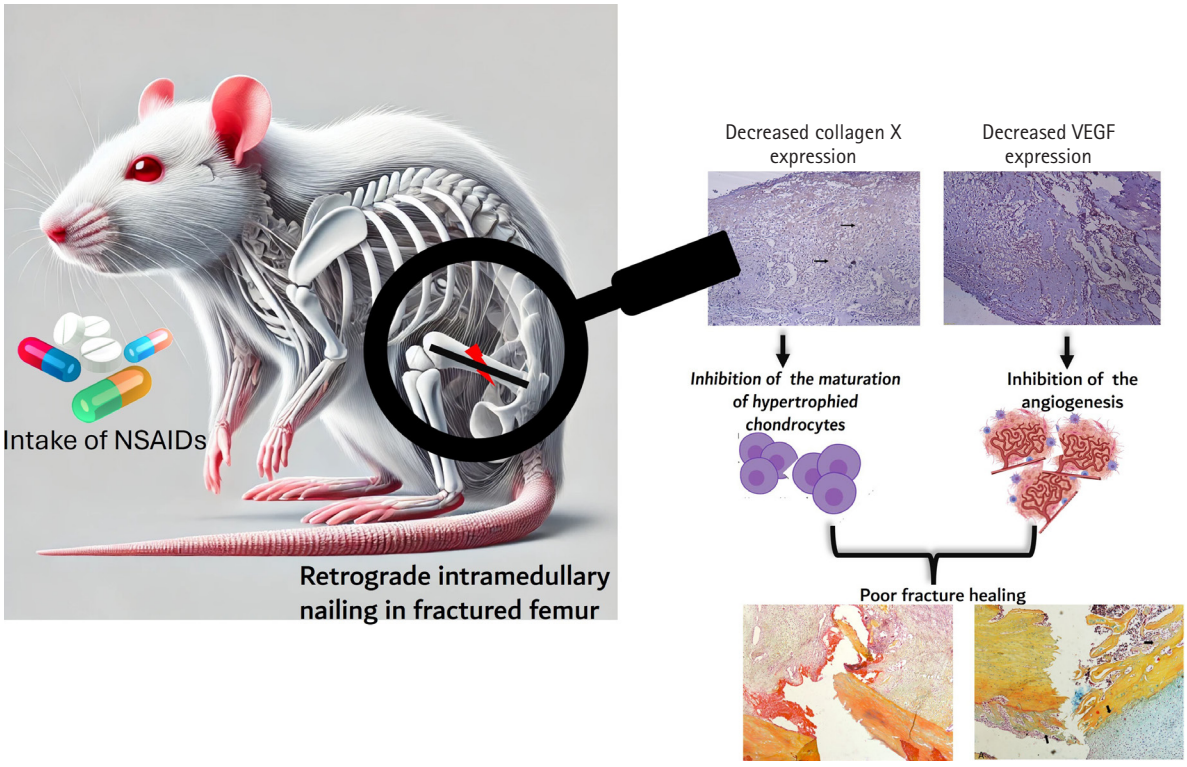

Fig. 6. Intake of NSAIDs reduce the expression of collagen X and vascular endothelial factors (VEGF) in early phase of rat femoral fracture healing. NSAIDs, anti-inflammatory drugs; VEGF, vascular endothelial growth factor.

week showed fracture lines specifically in the experimental animals treated with NSAIDs, which aligns with previous studies [19,20]. These findings were further supported by our histological analysis, which revealed larger bone defects and reduced new bone formation at both the 2nd and 7th weeks postoperation, particularly in animals treated with diclofenac sodium. Similar results have been observed in other animal studies, where NSAIDs, especially diclofenac, were found to delay healing by affecting callus remodeling, reducing bone production, and decreasing lamellar bone content in the callus tissue. This occurs due to the inhibition of prostaglandins during the early stages of healing. Prostaglandins, along with various other inflammatory mediators, are known to play a crucial role in osteoblast differentiation [21-23].

Despite strong evidence indicating that NSAIDs impair bone healing, a few studies suggest that NSAIDs have little or no effect on fracture healing outcomes [24,25]. However, the role of NSAIDs in reducing prostaglandin production, which is essential for regulating bone repair, particularly during the inflammatory phase [26], may provide the most plausible explanation for the findings in the current study. The inhibition of prostaglandins affects multiple signaling pathways and can delay bone healing by reducing osteoblast activity, increasing osteoclast activity, and impairing angiogenesis.

This explanation accounts for the decreased expression and intensity of COLX and VEGF staining in NSAID-treated animals compared to the control group, particularly at the 2nd week. Several previous studies have reported on VEGF expression in relation to NSAID treatment. For instance, Rofecoxib, a COX-2 inhibitor, has been shown to reduce blood flow and VEGF expression across the fracture gap at 4, 16, and 24 days postinjury in a mouse model [20]. Additionally, VEGF immunostaining within granulation tissues significantly decreased in animals treated with ketoprofen, a nonselective COX inhibitor, during a four-week study [27]. NSAIDs are known to impair cell proliferation by inhibiting angiogenesis, as observed in cancer studies, and it is likely that NSAID-induced nonunions occur through a similar mechanism [20]. However, a study on tibial fractures in mice found that NSAIDs had positive effects on vascular

https://doi.org/10.12671/jmt.2025.00367

density in the fracture gap during early healing, as compared to the control group [28]. Nevertheless, this study was unable to clarify the interaction between inflammation and angiogenesis.

Regarding COLX expression, there is a significant lack of data, as no study to date has specifically investigated its expression in relation to NSAIDs. However, it is well established that COLX plays a crucial role in endochondral ossification during fracture healing [29], as most fractures heal through this process, often involving some degree of cartilage formation. The relationship between COX inhibition and decreased COLX expression has been identified in a few in vitro studies, which suggest that COX inhibition may have negative effects on this process [30,31]. COLX is thought to facilitate bone formation during fracture healing by promoting matrix mineralization and angiogenesis. This also explains the linear correlation between the expressions of COLX and VEGF in the current study. Hypertrophic chondrocytes also express VEGF, which promotes vascularization. This process, in turn, accelerates cartilage matrix degradation through the invasion of vessels [32].

In the current study, at the 7th week, all three groups exhibited similar levels of COLX expression. This aligns with reports indicating that COLX expression peaks around the 14th day, coinciding with chondrocyte hypertrophy. A sharp decline in COLX levels is observed between days 14 and 42, as hypertrophic chondrocytes transition into osteoblasts, and the provisional COLX matrix is replaced by bone [8]. A similar process likely occurred in this study, which explains the lack of observable differences.

In the 7th week, VEGF expression remained consistent in experimental animals, whereas it decreased in controls. This suggests that bone healing in the fractured femur was not yet complete by the 7th week in experimental animals reflecting the later stages of remodeling, where neovascular support is still required as radiographic and histologic evidence showed the progressive union. As fracture healing transitions from the reparative to the remodeling phase, angiogenic activity does not cease abruptly; instead, it tapers gradually as woven bone is reorganized into lamellar bone. Various processes may influence the interplay between inflammation and angiogenesis. Macrophages, neutrophils, and key bone remodeling cells osteoclasts, osteoblasts, and osteocytes are known to produce angiogenic factors such as VEGF, FGF2, and PDGF, which can regulate directional angiogenesis and maintain the blood supply [33].

The strong correlation between COLX and VEGF expression and total healing scores in the 2nd week underscores the critical role of both factors in the formation and maintenance of bone tissue during fracture healing. As NSAIDs are known to inhibit the maturation of hypertrophied chondrocytes by blocking COX enzymes, leading to reduced COLX expression and delayed fracture healing [34], it is evident that COLX expression is essential for enhanced bone formation and improved fracture healing during the early stages. Moreover, reduced VEGF expression can hinder the development of vasculature across the fracture gap, delaying union. Limited VEGF expression disrupts communication between osteoblasts and the vasculature [35], which likely contributes to delays in the fracture healing process.

Limitations

This study has certain limitations, the most significant being its nature as an animal-based experimental model; therefore, the findings may not be directly translatable to fracture healing in humans due to interspecies differences in bone biology and healing dynamics. However, it is widely acknowledged that investigating the effects of NSAID administration on bone healing in clinical settings presents substantial methodological challenges, including difficulty in controlling confounding variables and accurately assessing healing outcomes. Therefore, *in vivo* experimental studies like this one remain a valuable and necessary source of evidence. The prolonged NSAID administration used in this study was intended to assess cumulative effects on fracture healing rather than to replicate routine short-term postoperative analgesic use. Although such exposure may exceed typical perioperative NSAID prescribing, prolonged NSAID use is common in patients with chronic musculoskeletal pain or inflammatory conditions. Nevertheless, extrapolation of dose and duration from animal models to clinical practice should be made with caution.

Implications

In addition, the study focused on histological and molecular endpoints at predefined time points and did not include long-term functional or biomechanical assessments of bone strength. Despite these limitations, the present study enhances our understanding of the biological mechanisms involved in bone repair and offers important insights into

the potential influence of NSAID use on the fracture healing process.

Conclusions

Use of nonselective and selective COX-2 NSAIDs delays fracture healing by reducing COLX and VEGF expression in the early stages of fracture healing, which correlates with reduced new bone formation, increased bone defect, and fibrous tissue at the fracture healing site. While our results suggest a potential risk for impaired bone repair, definitive clinical implications cannot be drawn from preclinical data alone. Further studies in humans are needed before firm recommendations can be made.

Article Information

Author contributions

Conceptualization: MSI, UZ. Data curation: MZ, RMZ, Formal analysis: UZ. Methodology: MSI, MZ, RMZ. Investigation: MZ, RMZ, ST, MSI. Resources: MZ, RMZ, MSI, AA, UZ. Supervision: UZ. Validation: ST, UZ. Project administration: MSI, AA, UZ. Visualization: MZ, RMZ, ST. Writing-original draft: UZ. Writing-review & editing: MZ, RMZ, ST, MSI, AA, UZ. All authors read and approved the final manuscript.

Conflicts of interest

No potential conflict of interest relevant to this article was reported.

Funding

None.

Data availability

Contact the corresponding author for data availability.

Acknowledgments

None.

Supplementary materials

Supplementary materials related to this article can be found online at https://doi.org/10.12671/jmt.2025.00367.

References

1. GBD 2019 Fracture Collaborators. Global, regional, and national burden of bone fractures in 204 countries and territories, 1990-2019: a systematic analysis from the Global Burden of Disease Study 2019. Lancet Healthy Longev 2021;2:e580-92.
2. Salari N, Ghasemi H, Mohammadi L, et al. The global prevalence of osteoporosis in the world: a comprehensive systematic review and meta-analysis. J Orthop Surg Res 2021;16:609.
3. Marsell R, Einhorn TA. The biology of fracture healing. Injury 2011;42:551-5.
4. Bahney CS, Zondervan RL, Allison P, et al. Cellular biology of fracture healing. J Orthop Res 2019;37:35-50.
5. Papachristou DJ, Georgopoulos S, Giannoudis PV, Panagiotopoulos E. Insights into the cellular and molecular mechanisms that govern the fracture-healing process: a narrative review. J Clin Med 2021;10:3554.
6. Sheen JR, Mabrouk A, Garla VV. Fracture healing overview. In: StatPearls. Treasure Island (FL): StatPearls Publishing; 2023.
7. Hu K, Olsen BR. The roles of vascular endothelial growth factor in bone repair and regeneration. Bone 2016;91:30-8.
8. Working ZM, Morris ER, Chang JC, et al. A quantitative serum biomarker of circulating collagen X effectively correlates with endochondral fracture healing. J Orthop Res 2021;39:53-62.
9. Al Farii H, Farahdel L, Frazer A, Salimi A, Bernstein M. The effect of NSAIDs on postfracture bone healing: a meta-analysis of randomized controlled trials. OTA Int 2021;4:e092.
10. Ozturan YA, Akin I. Comprehensive review of the impact of NSAIDs on bone healing outcomes in animal models: conflicting evidence and methodological considerations. Discov Med 2024;1:20.
11. Murphy PB, Kasotakis G, Haut ER, et al. Efficacy and safety of non-steroidal anti-inflammatory drugs (NSAIDs) for the treatment of acute pain after orthopedic trauma: a practice management guideline from the Eastern Association for the Surgery of Trauma and the Orthopedic Trauma Association. Trauma Surg Acute Care Open 2023;8:e001056.
12. Chakkalakal DA, Strates BS, Mashoof AA, et al. Repair of segmental bone defects in the rat: an experimental model of human fracture healing. Bone 1999;25:321-32.
13. De Giacomo A, Morgan EF, Gerstenfeld LC. Generation of closed transverse fractures in small animals. Methods Mol Biol 2014;1130:35-44.
14. Udegbunam R, Okereke H, Udegbunam S. Single versus repeated tramadol injection in laparotomized albino rats:

comparison of effects on hematology, serum biochemical parameters, and body weight gain. J Adv Vet Anim Res 2015;2:316.
15. Abbas SS, Schaalan MF, Bahgat AK, El-Denshary ES. Possible potentiation by certain antioxidants of the anti-inflammatory effects of diclofenac in rats. ScientificWorldJournal 2014;2014:731462.
16. Simon AM, O'Connor JP. Dose and time-dependent effects of cyclooxygenase-2 inhibition on fracture-healing. J Bone Joint Surg Am 2007;89:500-11.
17. Gultekin A, Unal M, Unlu M, Satoglu S. Effect of human amniotic fluid and membrane on fracture healing on rat fracture model. Med J Suleyman Demirel Univ 2020;27:105-12.
18. Fedchenko N, Reifenrath J. Different approaches for interpretation and reporting of immunohistochemistry analysis results in the bone tissue: a review. Diagn Pathol 2014;9:221.
19. Li KH, Cheng L, Zhu Y, Deng GB, Long HT. Effects of a selective cyclooxygenase-2 inhibitor (celecoxib) on fracture healing in rats. Indian J Orthop 2013;47:395-401.
20. Murnaghan M, Li G, Marsh DR. Nonsteroidal anti-inflammatory drug-induced fracture nonunion: an inhibition of angiogenesis? J Bone Joint Surg Am 2006;88 Suppl 3:140-7.
21. Beck A, Krischak G, Sorg T, et al. Influence of diclofenac (group of nonsteroidal anti-inflammatory drugs) on fracture healing. Arch Orthop Trauma Surg 2003;123:327-32.
22. Sandberg O, Aspenberg P. Different effects of indomethacin on healing of shaft and metaphyseal fractures. Acta Orthop 2015;86:243-7.
23. Menger MM, Stief M, Scheuer C, et al. Diclofenac, a NSAID, delays fracture healing in aged mice. Exp Gerontol 2023;178:112201.
24. Matsumoto MA, De Oliveira A, Ribeiro Junior PD, Nary Filho H, Ribeiro DA. Short-term administration of non-selective and selective COX-2 NSAIDs do not interfere with bone repair in rats. J Mol Histol 2008;39:381-7.
25. Inal S, Kabay S, Cayci MK, et al. Comparison of the effects of dexketoprofen trometamol, meloxicam and diclofenac sodium on fibular fracture healing, kidney and liver: an experimental rat model. Injury 2014;45:494-500.
26. Al-Waeli H, Reboucas AP, Mansour A, Morris M, Tamimi F, Nicolau B. Non-steroidal anti-inflammatory drugs and bone healing in animal models-a systematic review and meta-analysis. Syst Rev 2021;10:201.
27. Elgendy M, Elsayad G, Seleim M, et al. Flunixin meglumine enhanced bone fracture healing in rabbits associated with activation of early collagen deposition and enhancement of vascular endothelial growth factor expression. Animals (Basel) 2021;11:2834.
28. Lu C, Xing Z, Wang X, Mao J, Marcucio RS, Miclau T. Anti-inflammatory treatment increases angiogenesis during early fracture healing. Arch Orthop Trauma Surg 2012;132:1205-13.
29. Grant WT, Wang GJ, Balian G. Type X collagen synthesis during endochondral ossification in fracture repair. J Biol Chem 1987;262:9844-9.
30. Welting TJ, Caron MM, Emans PJ, et al. Inhibition of cyclooxygenase-2 impacts chondrocyte hypertrophic differentiation during endochondral ossification. Eur Cell Mater 2011;22:420-36.
31. Janssen MP, Caron MM, van Rietbergen B, et al. Impairment of the chondrogenic phase of endochondral ossification in vivo by inhibition of cyclooxygenase-2. Eur Cell Mater 2017;34:202-16.
32. Kodama J, Wilkinson KJ, Iwamoto M, Otsuru S, Enomoto-Iwamoto M. The role of hypertrophic chondrocytes in regulation of the cartilage-to-bone transition in fracture healing. Bone Rep 2022;17:101616.
33. Chim SM, Tickner J, Chow ST, et al. Angiogenic factors in bone local environment. Cytokine Growth Factor Rev 2013;24:297-310.
34. Cottrell JA, O'Connor JP. Pharmacological inhibition of 5-lipoxygenase accelerates and enhances fracture-healing. J Bone Joint Surg Am 2009;91:2653-65.
35. Hu K, Olsen BR. Osteoblast-derived VEGF regulates osteoblast differentiation and bone formation during bone repair. J Clin Invest 2016;126:509-26.

JMT Journal of Musculoskeletal Trauma

pISSN 3058-6267 · eISSN 3058-6275
J Musculoskelet Trauma 2026;39(2):174-180
https://doi.org/10.12671/jmt.2025.00388

Paradoxical hypertrophy as a cause of femoral insufficiency fractures analyzed through differences in force application in Korea: three case reports

Yong-Uk Kwon, Dae-Hyun Park, Hyoung-Gu Kang

Department of Orthopedic Surgery, Inje University Busan Paik Hospital, Inje University College of Medicine, Busan, Korea

Previous studies have extensively examined the association between femoral insufficiency fractures and prolonged bisphosphonate therapy. However, alternative etiologies remain insufficiently characterized. This study aimed to analyze nonpharmacologic factors associated with femoral insufficiency fractures, with particular emphasis on paradoxical cortical hypertrophy and altered biomechanical load distribution. We reviewed three cases of femoral insufficiency fracture that were surgically treated at our institution between January 2018 and January 2022. None of the patients had a history of bisphosphonate use. Clinical histories—including underlying comorbidities, prior surgical procedures, and radiographic findings—were evaluated. Serial radiographs obtained before and after fracture occurrence were analyzed to characterize fracture morphology and associated cortical changes. Case 1 involved a patient with posttraumatic hip synostosis; case 2 involved a patient with osteogenesis imperfecta; and case 3 involved a patient who had previously undergone intramedullary nailing for an intertrochanteric fracture. Lateral femoral bowing and cortical hypertrophy preceded fracture development in two cases, whereas focal cortical hypertrophy at the distal locking screw site was observed in the third case. No history of bisphosphonate therapy was identified in any patient. Fractures developed at sites characterized by increased cortical remodeling and abnormal load concentration. Femoral insufficiency fractures can occur in the absence of bisphosphonate therapy. Paradoxical cortical hypertrophy and altered biomechanical force distribution appear to be important contributing factors.
Level of evidence: IV.

Keywords: Stress fracture; Osteoporosis; Diphosphonates; Bone remodeling

Case Report

Received: December 13, 2025
Revised: January 29, 2026
Accepted: February 9, 2026

Correspondence to:
Dae-Hyun Park
Department of Orthopedic Surgery, Inje University Busan Paik Hospital, Inje University College of Medicine, 75 Bokji-ro, Busanjin-gu, Busan 47392, Korea
Tel: +82-51-890-6129
Email: spineparkdaehyun@gmail.com

Introduction

Insufficiency fractures are a subtype of stress fractures that occur when repeated and subthreshold stress is applied to normal or abnormal bones [1]. Stress fractures include both fatigue and insufficiency fractures, which are best understood as two contrasting processes with a similar end result. Fatigue fractures are caused by repeated and subthreshold loads upon normal bone, whereas insufficiency fractures are the result of repeated and subthreshold stress upon abnormal bone with deficient elastic resistance [2]. Although the term fatigue fracture may be occasionally used interchangeably with stress fracture, these fractures should be viewed as a subtype of

stress fracture. Meanwhile, a pathologic fracture is a break in a weakened bone that is caused by an underlying disease (Benign or malignant neoplasm, infection, metabolic bone disease etc.) [3]. Therefore, insufficiency fractures that occur in abnormal bones are stress fractures and belong to pathologic fractures, and fatigue fractures that occur in normal bones are stress fractures and belong to physiologic fractures (Fig. 1).

Insufficiency fractures most commonly involve the weight-bearing bones, particularly the pelvis, spine, femur and other axial skeleton sites [4,5]. In this study, we present cases of femoral insufficiency fractures occurring in the proximal femur, with a focus on analyzing the specific causative factors and clinical features observed in our patient cases.

The incidence of femoral insufficiency fractures increases with age, and their incidence is especially high in the elderly [4]. Many efforts have been made to identify the causes of femoral insufficiency fractures, and the most widely acknowledged risk factor at present is the long-term use of bisphosphonates to prevent osteoporosis [5]. Many studies have been conducted on this topic, and various case reports have been published to date. But, the published literature suggests that femoral insufficiency fractures have a different pathology than the standard osteoporotic fractures, and the atypical features of these fractures are rarely seen without long-term bisphosphonate therapy [5]. Rogers et al. [6] reported that the potential absolute risk associated with bisphosphonate use seems to be relatively small. In some studies, evidence from clinical and regulatory sources points out that insufficiency fractures can occur independently of bisphosphonate therapy, highlighting the need to consider alternative mechanisms such as biomechanical factors and comorbidities [6-8].

While bisphosphonate use remains a significant contributing factor, this study introduces several cases of femoral insufficiency fractures occurring without bisphosphonate exposure, aiming to discuss other possible nonpharmacologic etiologies and mechanisms involved.

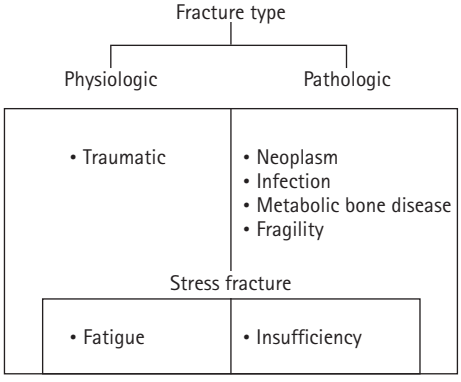

Fig. 1. Schematic diagram illustrating the classification of fractures.

Case reports

Ethics statement

This study was approved by Institutional Review Board (IRB) of Inje University Busan Paik Hospital (IRB No. 2023-05-044). The authors attest that informed consent was obtained from all individual patients or their legal guardians.

Case 1: synostosis of hip joint

A 58-year-old female patient visited our emergency room, complaining of pain in the right hip that occurred the day before her hospital visit. She had a history of restricted right hip range of movement following a dislocation of the right hip in her youth, and she typically walked with a cane. The day prior to her visit, while lying on her right side and sleeping, she developed pain in the right hip area without any history of trauma. Upon examination, the patient had a background of hypertension and exhibited a bone mineral density (BMD) of -0.1 in the femoral neck. Notably, she had no history of malignancy. Initial physical examination and computed tomography scans conducted upon her arrival did not reveal any signs of malignancy or infection at the fracture site, indicating a low likelihood of these conditions as contributing factors. Radiographic evaluations, including both hip anteroposterior and right axial views, demonstrated signs of synostosis involving the right femoral head and acetabulum. A fracture was observed in the subtrochanteric area of the right femur, characterized by a beak-shaped thickened cortex on the lateral side of the fracture site. Importantly, the radiographs obtained 3 years prior showed no abnormalities at the fracture site (Figs. 2, 3). Following the diagnosis, the patient underwent open reduction and internal fixation using a plate. Subsequent follow-up indicated successful bone union at the fracture site.

Case 2: osteogenesis imperfecta

An 8-year-old female patient visited our emergency room complaining of pain in the left thigh that began on the day of her visit. She slipped and directly injured her thigh upon falling to the left. Initial examination revealed normal laboratory findings, including serum calcium levels of 9.0 mg/dL and inorganic phosphorus levels of 4.7 mg/dL. Radiographic evaluations, including anteroposterior and lateral views of the left femur, demonstrated a transverse irregular fracture line in the proximal one-third area of the left femur, accompanied by lateral cortex hypertrophy. Importantly, the possibility of malignancy or infection as contributing factors to the fracture was considered low. Two years prior, the patient had visited the pediatric department of our hospital due to concerns about her height, which was below that of her peers. Following genetic testing, she was diagnosed with osteogenesis imperfecta and has since been monitored by both the pediatrics and orthopedics departments. At that time, lateral bowing of both femurs was observed in both lower extremities during standing anteroposterior evaluations (Figs. 4, 5). She had previously undergone epiphysiodesis on both femurs due to genu valgum. After diagnosis, the patient underwent open reduction and internal fixation using an ender nail. Follow-up evaluations indicated successful bone union at the fracture site.

Fig. 2. Radiograph obtained 3 years earlier of a 58-year-old female patient presenting with a right subtrochanteric femoral fracture (anteroposterior view).

Case 3: distal locking screw of intramedullary nail

A 73-year-old female patient visited our emergency room complaining of pain in the left thigh that had begun approximately a month ago. She had undergone intramedullary nail fixation for a left femoral intertrochanteric fracture 9 years prior and reported no history of recent trauma. The patient had initially sought treatment at another hospital for her left thigh pain and was discharged after conservative management. However, she experienced sudden se-

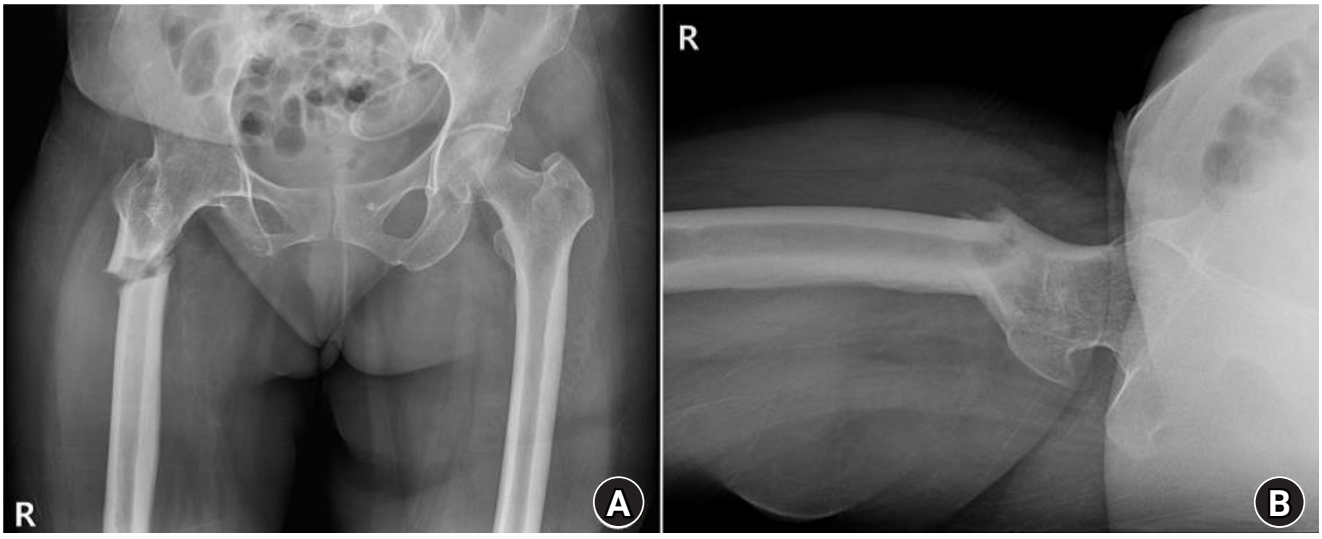

Fig. 3. Radiographs of the same patient presenting with a right subtrochanteric femoral fracture (Russell-Taylor classification type 1). (A) Anteroposterior view. (B) Axial view.

https://doi.org/10.12671/jmt.2025.00388

Fig. 4. Prefracture radiograph of an 8-year-old female patient who presented with a proximal one-third fracture of the left femur (bilateral lower-extremity standing anteroposterior view).

vere pain accompanied by a breaking sound while walking. Upon examination, her BMD at the L3-4 levels was noted to be -3.1. The patient also had a history of rheumatoid arthritis and hypertension, with no history of cancer. Radiographic evaluations, including anteroposterior and lateral views of the left femur, revealed a left femoral shaft fracture and metal breakage at the distal locking screw fixation site of the previously inserted intramedullary nail. Notably, when the patient first visited the other hospital, a hypertrophy and microfracture were observed at the lateral site of the distal locking screw insertion (Figs. 6, 7). Following the diagnosis, the patient underwent intramedullary fixation using a long nail. Subsequent follow-up evaluations indicated successful bone union at the fracture site.

Discussion

All three patients had no history of taking bisphosphonates. Hypertrophy of the femur lateral cortex was observed at the fracture site in all three patients. The first patient with synostosis of the hip joint had no range of motion of the right hip joint. As the weight-bearing force was not properly distributed during walking, femur lateral bowing was induced, and tensile force was continuously applied to the lateral cortex of the proximal femur. The second patient

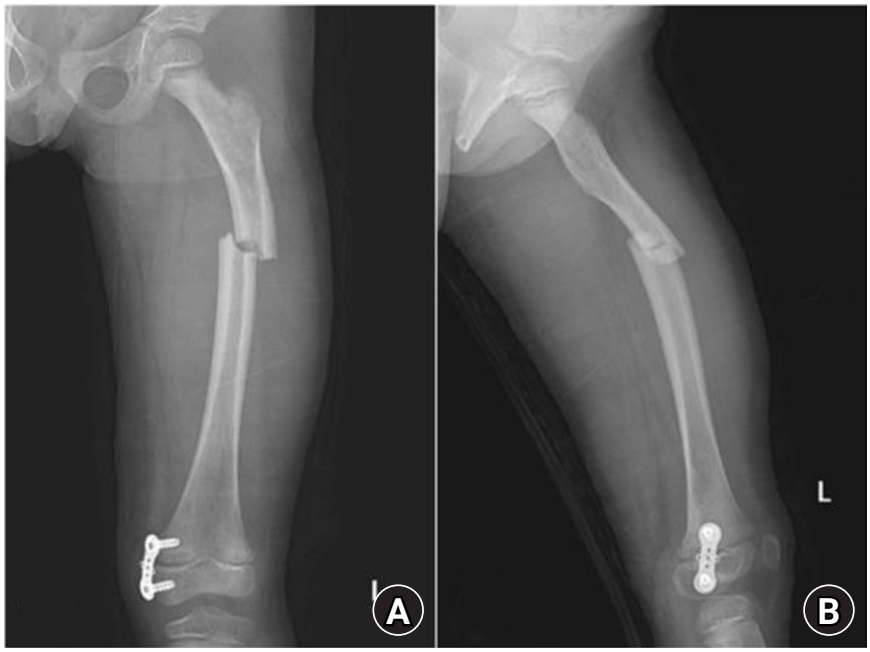

Fig. 5. Radiographs of the same patient with a proximal one-third fracture of the left femur. (A) Anteroposterior view. (B) Lateral view.

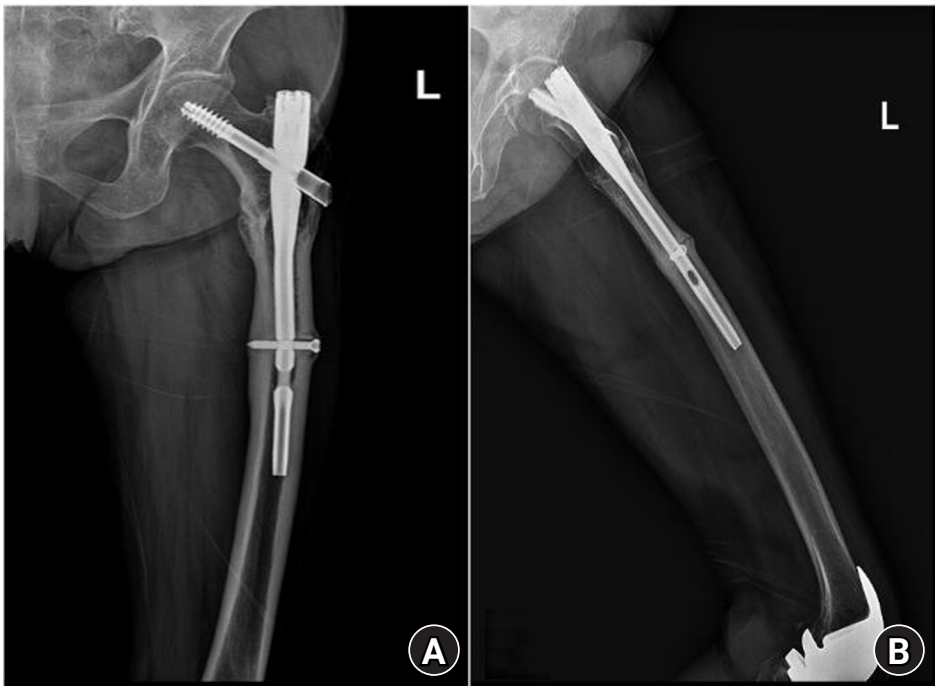

Fig. 6. Prefracture radiographs of a 73-year-old female patient who subsequently presented with a femoral shaft fracture demonstrating cortical hypertrophy and microfracture. (A) Anteroposterior view. (B) Lateral view.

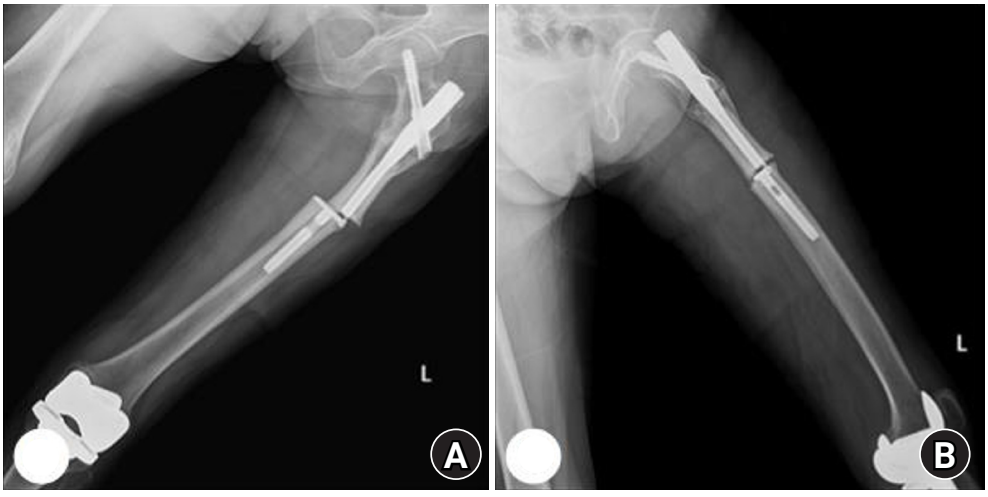

Fig. 7. Radiographs of the same patient with a femoral shaft fracture and implant failure. (A) Anteroposterior view. (B) Lateral view.

had an underlying disease of osteogenesis imperfecta. As a result, the weakened femur showed lateral bowing, and similarly, tensile force acted upon weight-bearing. The other patient underwent intramedullary nail fixation due to a previous femoral intertrochanteric fracture. As the distal locking screw of the intramedullary nail exerted a sustained tensile force on the femur lateral cortex, hypertrophy also occurred around the distal locking screw head.

Since their initial approval, bisphosphonates have been widely used for the prevention of low-energy fractures. This drug is widely considered first-line therapy and the mainstay of primary and secondary insufficiency fracture prevention. However, despite short- and mid-term success, concerns regarding long-term bisphosphonate use and the

https://doi.org/10.12671/jmt.2025.00388

associated increased risk of insufficiency fractures of the femur have grown over the past 5 years. Several studies have been conducted to determine the association between long-term use of bisphosphonates and femoral insufficiency fractures. While caution is required for long-term use of bisphosphonates, a clear relationship with femoral insufficiency fractures has not yet been established. Accordingly, other causes that can lead to insufficiency fractures have been raised. Long-term glucocorticoid use is known to be associated with the development of insufficiency fractures, with estimates suggesting that over half of chronic glucocorticoid users will develop reduced BMD and fractures. Additionally, prolonged bed rest can lead to disuse osteoporosis due to increased bone resorption and decreased bone formation along with the effect of nutritional factors. Nevertheless, in our study, we aim to report the occurrence of insufficiency fractures related to the patient's bone deformity and force application rather than other environmental or external factors.

In patients with abnormal bones, whether osteoporotic, bowing, or those who have undergone previous surgery, the opposite of Wolff's law may occur. An adequate understanding of Wolff's law is essential for contextualizing our hypothesis. Proposed by the German anatomist and surgeon Julius Wolff in the 19th century, Wolff's law states that the bone of a healthy animal will adapt to the loads under which it is placed. When a load is applied, bony growth occurs on the side that receives compression force, while bony resorption occurs on the side that experiences tensile force (Fig. 8). Although Wolff's law is primarily applicable to healthy bones, patients with femoral insufficiency fractures do not possess normal healthy bones; instead, they have bones that are osteoporotic, exhibit bowing for various reasons, or have undergone previous surgeries. Therefore, we have termed this phenomenon "paradoxical hypertrophy."

The phenomenon of paradoxical hypertrophy, which we have named, is thought to arise from several factors. First, tensile force is applied to the lateral cortex due to femoral lateral bowing, and as microfractures and bone healing are repeated in this area, hypertrophy occurs. This hypertrophy of the lateral cortex becomes vulnerable to impact, leading to fractures even with minimal force. Femoral lateral bowing not only progresses with age but can also be exacerbated by the patient's underlying disease or anatomical deformity. The second reason is that hypertrophy occurs at the distal locking screw insertion site in patients who have previously had femoral intramedullary nailing. Similarly, as force is applied to the femur lateral cortex by the head of the distal locking screw, hypertrophy occurs in that area due to repeated microfracture and bone healing. In patients using bisphosphonates, the process of bone resorption is inhibited, leading to an impaired bone remodeling cycle and altering bone mineral and matrix properties, which increases susceptibility to fractures. However, in these three cases, the mechanism is not due to reduced bone turnover from medication, but rather to situations where microdamage accumulates. Initial microfractures fail to heal adequately and are re-injured by new stress, leading to excessive osteoclast-mediated resorption that inhibits normal remodeling and results in the formation of incomplete callus. This mechanism, while opposite to that of bisphosphonate action, ultimately leads to similar outcomes.

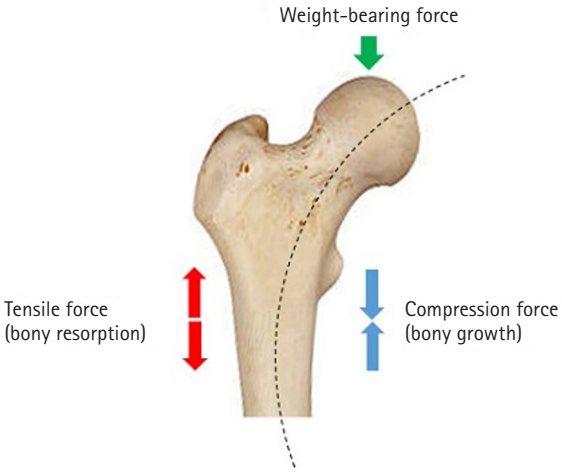

Fig. 8. Schematic illustration of Wolff's law.

In accordance with the American Society for Bone and Mineral Research (ASBMR) [9,10] diagnostic criteria, each case can be evaluated for insufficiency fractures based on clinical history, imaging findings, and the absence of significant trauma. All three patients demonstrated characteristic features of insufficiency fractures, including specific deformities and forces acting on the femur. In doing so, it is essential to consider the unique circumstances surrounding each case, which collectively suggest that the mechanism of insufficiency fractures may differ from that traditionally associated with long-term bisphosphonate use.

Until now, long-term use of bisphosphonates was thought to be the main cause of femoral insufficiency fractures. However, as demonstrated in our study, repetitive force applied to the femur lateral cortex leads to hypertrophy as a result of microfracture repetition and inadequate healing, culminating in insufficiency fractures in that area.

Article Information

Author contributions

Conceptualization: YUK. Methodology: YUK. Supervision: DHP. Visualization: HGK. Writing–original draft: YUK, HGK. Writing–review & editing: YUK, DHP, HGK. All authors read and approved the final manuscript.

Conflicts of interest

No potential conflict of interest relevant to this article was reported.

Funding

None.

Data availability

Not applicable.

Acknowledgments

None.

Supplementary material

None.

References

1. Pentecost RL, Murray RA, Brindley HH. Fatigue, insufficiency, and pathologic fractures. JAMA 1964;187:1001-4.
2. Fayad LM, Kawamoto S, Kamel IR, et al. Distinction of long bone stress fractures from pathologic fractures on cross-sectional imaging: how successful are we? AJR Am J Roentgenol 2005;185:915-24.
3. Matcuk GR Jr, Mahanty SR, Skalski MR, Patel DB, White EA, Gottsegen CJ. Stress fractures: pathophysiology, clinical presentation, imaging features, and treatment options. Emerg Radiol 2016;23:365-75.
4. Court-Brown CM, McQueen MM. Global forum: fractures in the elderly. J Bone Joint Surg Am 2016;98:e36.
5. Isaacs JD, Shidiak L, Harris IA, Szomor ZL. Femoral insufficiency fractures associated with prolonged bisphosphonate therapy. Clin Orthop Relat Res 2010;468:3384-92.
6. Rogers LF, Taljanovic M. FDA statement on relationship between bisphosphonate use and atypical subtrochanteric and femoral shaft fractures: a considered opinion. AJR Am J Roentgenol 2010;195:563-6.
7. Ha YC, Cho MR, Park KH, Kim SY, Koo KH. Is surgery necessary for femoral insufficiency fractures after long-term bisphosphonate therapy? Clin Orthop Relat Res 2010;468:3393-8.
8. Rudran B, Super J, Jandoo R, et al. Current concepts in the management of bisphosphonate associated atypical femoral fractures. World J Orthop 2021;12:660-71.
9. Shane E, Burr D, Ebeling PR, et al. Atypical subtrochanteric and diaphyseal femoral fractures: report of a task force of the American Society for Bone and Mineral Research. J Bone Miner Res 2010;25:2267-94.
10. Shane E, Burr D, Abrahamsen B, et al. Atypical subtrochanteric and diaphyseal femoral fractures: second report of a task force of the American Society for Bone and Mineral Research. J Bone Miner Res 2014;29:1-23.

https://doi.org/10.12671/jmt.2025.00388

JMT Journal of Musculoskeletal Trauma

pISSN 3058-6267 · eISSN 3058-6275
J Musculoskelet Trauma 2026;39(2):181-183
https://doi.org/10.12671/jmt.2026.00038

Sacral stress fracture mimicking sacroiliac pathology in two young adults: a reminder to systematically review the sacrum on hip/sacroiliac magnetic resonance imaging

Nihal Karayer Özgül[1], Sami Özgül[2]

[1]Department of Physical Medicine and Rehabilitation, Mugla Sitki Kocman University, Mugla, Turkey
[2]Department of Radiology, Mugla Sitki Kocman University, Mugla, Turkey

To the Editor,

Sacral stress fracture is an important yet frequently underrecognized cause of buttock and low-back pain. It may be overlooked on magnetic resonance imaging (MRI) studies obtained primarily for hip or sacroiliac (SI) indications, particularly when image review is focused on intraarticular hip pathology or suspected inflammatory sacroiliitis. Because bone marrow edema in the sacral ala lies adjacent to the SI joint, it may be mistaken for SI pathology when joint margins are not deliberately assessed; preservation of the SI joint space and articular surfaces, with edema centered in the sacral wing rather than within the joint, favors a sacral stress fracture pattern. Diagnostic delay is clinically meaningful, as symptoms may persist, additional investigations may be pursued, and effective conservative management may be postponed [1-3]. Here, we describe two young adults without typical predisposing factors in whom the diagnosis was not identified on the initial MRI report, underscoring the value of systematic sacral review even in younger patients. In this letter, we use "stress fracture" as an umbrella term encompassing fatigue fractures (abnormal or repetitive load on otherwise normal bone) and insufficiency fractures (physiologic load on weakened bone). Given the patients' age, the absence of fragility risk factors, and age-appropriate dual-energy X-ray absorptiometry (DXA) Z-scores, the imaging patterns are most consistent with fatigue-type sacral stress fractures, while acknowledging that borderline or low-normal 25-hydroxyvitamin D levels may represent a modifiable contributing factor rather than clear metabolic bone disease.

A 30-year-old female healthcare worker presented with localized deep gluteal pain. A hip MRI was performed; however, the initial report did not address the sacrum. Following clinical–radiologic correlation and targeted re-evaluation, the MRI demonstrated findings consistent with a unilateral sacral stress fracture pattern involving the sacral ala. MRI assessment included fluid-sensitive sequences covering the sacral alae, specifically coronal short tau ınversion recovery (STIR) and fat-suppressed T2-weighted images with a field of view encompassing the sacrum (Fig. 1). This appearance may be misinterpreted as nonspecific periarticular marrow edema if the sacrum is not deliberately incorporated into the imaging search pattern [1,3]. Laboratory testing did not suggest overt metabolic bone disease, with calcium and parathy-

Letter to the Editor

Received: January 12, 2026
Revised: January 14, 2026
Accepted: January 14, 2026

Correspondence to:
Sami Özgül
Department of Radiology, Mugla Sitki Kocman University, Kotekli, Mentese, Mugla, Turkey
Tel: +90-507-306-82-12
Email: supersamo48@gmail.com

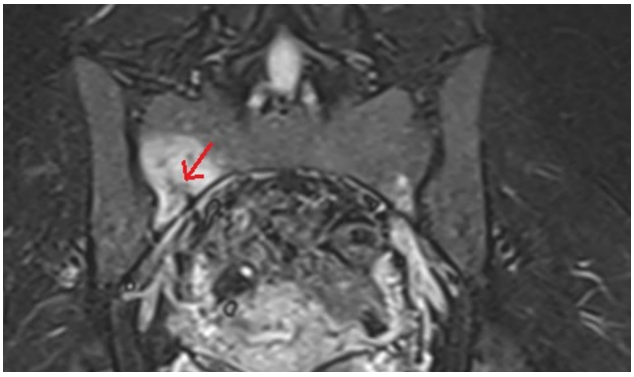

Fig. 1. Hip magnetic resonance imaging (patient A). Imaging demonstrates a unilateral sacral ala stress fracture pattern with surrounding marrow edema, best appreciated on fluid-sensitive sequences. The arrow indicates bone marrow edema in the sacral ala with a visible fracture line.

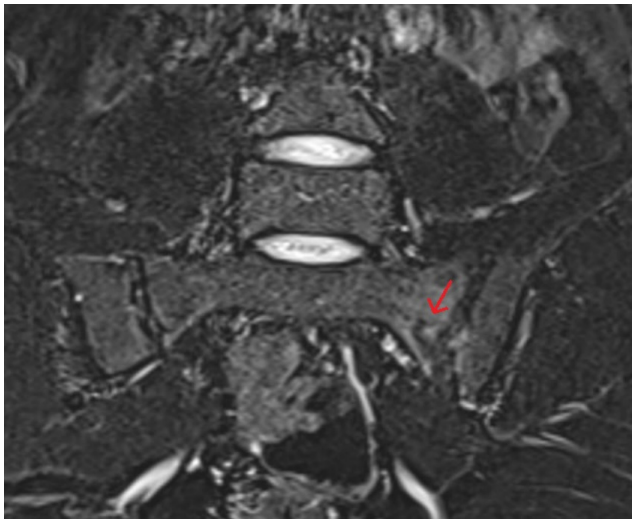

Fig. 2. Sacroiliac magnetic resonance imaging (patient B). Retrospective review of the sacrum reveals a sacral ala stress fracture pattern with marrow edema, despite an initially unremarkable report. The arrow indicates bone marrow edema in the sacral ala with a visible fracture line.

roid hormone levels within reference ranges, borderline or low-normal 25-hydroxyvitamin D levels, and age-appropriate DXA Z-scores. The patient was treated conservatively with activity modification and use of a sitting cushion, with substantial symptomatic improvement. Symptoms improved within approximately six weeks, and she returned to baseline activity by 2 months.

A 23-year-old male student presented with low-back pain. He denied trauma and did not report a clear recent change in training or impact activity, which contributed to an initial diagnostic focus on SI pathology. Pelvic radiography raised concern for a possible SI joint abnormality, and SI MRI was subsequently obtained. The MRI was initially interpreted as unremarkable. On careful retrospective review of the sacrum, a sacral stress fracture pattern involving the sacral ala was identified and subsequently confirmed in consultation with radiology. The MRI protocol included coronal STIR and fat-suppressed T2-weighted sequences with coverage of the sacral wings, enabling detection of characteristic bone marrow edema patterns (Fig. 2). Laboratory testing did not suggest overt metabolic bone disease, with calcium and parathyroid hormone levels within reference ranges, borderline or low-normal 25-hydroxyvitamin D levels, and age-appropriate DXA Z-scores. At an 8-week follow-up, pain had resolved, and the patient had returned to daily activities.

These two presentations emphasize two practical considerations. First, although sacral fractures are often associated with advanced age and bone fragility, sacral stress fractures should remain in the differential diagnosis of buttock or low-back pain in young adults, even in the absence of commonly cited predisposing factors such as osteoporosis, pelvic irradiation, prolonged corticosteroid exposure, metabolic bone disease, or marked repetitive overuse [4]. Second, an initial MRI report that is described as normal or noncontributory does not fully exclude sacral stress fracture when the protocol is tailored to the hip or SI joints and the sacrum is not explicitly scrutinized [2,3]. A simple and readily implementable safeguard is to incorporate a brief "sacrum check" into routine review of hip and SI MRI examinations, particularly when symptoms localize to the posterior pelvis [1,2]. This recommendation is especially pertinent because SI MRI interpretation is subject to recognized pitfalls, and focal sacral abnormalities may be either overcalled or undercalled when the primary diagnostic focus is inflammatory SI disease [5].

Early recognition supports timely conservative management and may reduce diagnostic drift toward inflammatory SI disease, particularly when imaging findings are subtle or unilateral [2,3,5].

Ethics statement

Written informed consent for publication of deidentified

https://doi.org/10.12671/jmt.2026.00038

clinical and imaging information was obtained from both individuals.

Article Information

Author contributions

Conceptualization: NKO, SO. Data curation: NKO, SO. Resources: NKO, SO. Visualization: NKO. Writing-original draft: NKO, SO. Writing-review & editing: NKO, SO. All authors read and approved the final manuscript.

Conflicts of interest

No potential conflict of interest relevant to this article was reported.

Funding

None.

Data availability

Not applicable.

Acknowledgments

None.

Supplementary materials

None.

References

1. Lyders EM, Whitlow CT, Baker MD, Morris PP. Imaging and treatment of sacral insufficiency fractures. AJNR Am J Neuroradiol 2010;31:201-10.
2. Kim YY, Chung BM, Kim WT. Lumbar spine MRI versus non-lumbar imaging modalities in the diagnosis of sacral insufficiency fracture: a retrospective observational study. BMC Musculoskelet Disord 2018;19:257.
3. Sudhir G, Kalra KL, Acharya S, Chahal R. Sacral insufficiency fractures mimicking lumbar spine pathology. Asian Spine J 2016;10:558-64.
4. Yoder K, Bartsokas J, Averell K, McBride E, Long C, Cook C. Risk factors associated with sacral stress fractures: a systematic review. J Man Manip Ther 2015;23:84-92.
5. Badr S, Jacques T, Lefebvre G, Boulil Y, Abou Diwan R, Cotten A. Main diagnostic pitfalls in reading the sacroiliac joints on MRI. Diagnostics (Basel) 2021;11:2001.

JMT Journal of Musculoskeletal Trauma

Instructions for authors

Enacted from January 1, 1988
Last revision: December 1, 2025

1. GENERAL INFORMATION

The *Journal of Musculoskeletal Trauma* is the official publication of the Korean Orthopaedic Trauma Association (KOTA), and is published in academic collaboration with the Thai Orthopaedic Trauma Society (TOTS) and the Taiwan Orthopaedic Trauma Association (TOTA) as Affiliated Societies. It is an international, peer-reviewed, open-access journal dedicated to advancing the science, education, and clinical care of musculoskeletal trauma. The journal was first launched in 1988 and is published quarterly on the 25th of January, April, July, and October. As of October 2024, the official language of the journal has been changed to English.

The journal covers a wide range of topics related to musculoskeletal injuries, including but not limited to: prevention, diagnosis, treatment, and rehabilitation of fractures, dislocations, and soft tissue injuries of both the extremities and the axial skeleton; advances in surgical techniques, implants, and prosthetic devices; biomechanical and biological research related to trauma and tissue healing; rehabilitation strategies for functional recovery; and clinical and translational research bridging basic science and clinical practice.

We invite submissions of original articles, reviews, case reports, technical notes, letters to the editor, and editorials that contribute to the advancement of musculoskeletal trauma care. Manuscripts submitted to JMT should be prepared according to the following instructions. The journal adheres to the Recommendations for the Conduct, Reporting, Editing, and Publication of Scholarly Work in Medical Journals (http://www.icmje.org/icmje-recommendations.pdf) from the International Committee of Medical Journal Editors (ICMJE).

2. ARTICLE PROCESSING CHARGE

There are no author fees for manuscript processing or publication in the journal, as all costs are covered by the publisher, the Korean Orthopaedic Trauma Association, unless the policy changes. Therefore, it is a platinum open-access journal.

3. RESEARCH AND PUBLICATION ETHICS

The journal adheres to the guidelines for research and publication described in the Committee on Publication Ethics (COPE) Guidances (https://publicationethics.org/resources/guidelines) the ICMJE Recommendations (https://www.icmje.org), and the Good Publication Practice Guideline for Medical Journals (https://www.kamje.or.kr/board/view?b_name=bo_publication&bo_id=14). Furthermore, all processes addressing research and publication misconduct shall follow the flowcharts of COPE (https://publicationethics.org/resources/flowcharts). Any attempts to duplicate publications or engage in plagiarism will lead to automatic rejection and may prejudice the acceptance of future submissions.

Statement of Human and Animal Rights

Clinical research should be conducted in accordance with the World Medical Association's Declaration of Helsinki (https://www.wma.net/what-we-do/medical-ethics/declaration-of-helsinki/). Any investigations involving humans and animals should be approved by the Research Ethics Committee (REC) or the Institutional Review Board (IRB) and Animal Care Committee, respectively, of the institution where the experiment was performed. JMT will not consider any studies involving humans or animals without appropriate approval. Such approval, along with the approval number and the name of the IRB or REC institution, should be stated in the Methods section of the manuscript. Informed consent must be obtained from patients participating in clinical investigations, unless waived by the IRB. In the case of an animal study, a statement should be provided indicating that the experimental procedures, such

as the breeding and the use of laboratory animals, was approved by the REC of the institution where the experiment was performed or that it does not violate the rules of the REC of the institution or the National Institutes of Health (NIH) Guide for the Care and Use of Laboratory Animals (Institute of Laboratory Animal Resources, Commission on Life Sciences, National Research Council). The authors should preserve raw experimental study data for at least 1 year after the publication of the paper and should present this data if required by the Editorial Board.

Protection of Privacy, Confidentiality, and Written Informed Consent

The ICMJE has recommended the following statement for the protection of privacy, confidentiality, and written informed consent: The rights of patients should not be infringed without written informed consent. Identifying details (patients' names, initials, hospital numbers, dates of birth, or other personal or identifying information, protected healthcare information) should not be published in written descriptions. Images of human subjects should not be used unless the information is essential for scientific purposes and explicit permission has been given as part of the consent. For individuals who cannot provide consent independently, including those from vulnerable populations—such as minors, the elderly, racial or ethnic minorities, individuals with certain health conditions, or those who are socioeconomically disadvantaged—consent should be obtained from a legally authorized representative or parent/guardian. Even where consent has been given, identifying details should be removed if they are not essential. If identifying characteristics are altered to protect anonymity, authors should provide assurances that such alterations do not distort scientific meaning. If consent has not been obtained, it is generally not sufficient to anonymize a photograph simply by using eye bars or blurring the face of the individual concerned.

Conflict of Interest

Authors are responsible for disclosing any financial support or benefit that might affect the content of the manuscript or might cause a conflict of interest. When submitting the manuscript, the author must attach a conflict of interest statement (https://e-jmt.org/authors/copyright_transfer_agreement.php). All authors should disclose their conflicts of interest, i.e., (1) financial relationships (such as employment, consultancies, stock ownership, honoraria, or paid expert testimony), (2) personal relationship, (3) academic competition, and (4) intellectual passion. These conflicts of interest must be included as a footnote on the title page. Each author should certify the disclosure of any conflict of interest with their signature.

Originality, Plagiarism, and Duplicate Publication

Redundant or duplicate publication refers to the publication of a paper that overlaps substantially with one already published. Upon receipt, submitted manuscripts are screened for possible plagiarism or duplicate publication using Crossref Similarity Check. If a paper that might be regarded as duplicate or redundant had already been published in another journal or submitted for publication, the author should notify the fact in advance at the time of submission. Under these conditions, any such work should be referred to and referenced in the new paper. The new manuscript should be submitted together with copies of the duplicate or redundant material to the editorial committee. If redundant or duplicate publication is attempted or occurs without such notification, the submitted manuscript will be rejected immediately. If the editor was not aware of the violations and of the fact that the article had already been published, the editor will announce in the journal that the submitted manuscript had already been published in a duplicate or redundant manner, without seeking the author's explanation or approval.

Secondary Publication

It is possible to republish manuscripts if the manuscripts satisfy the conditions for secondary publication of the ICMJE Recommendations, available from: https://www.icmje.org/ as follows:

(1) Certain types of articles, such as guidelines produced by governmental agencies and professional organizations, may need to reach the widest possible audience. In such instances, editors sometimes deliberately publish material that is also published in other journals with the agreement of the authors and the editors of those journals.

(2) Secondary publication for various other reasons, in the same or another language, especially in other countries, is justifiable and can be beneficial provid-

ed that the following conditions are met. The authors have received approval from the editors of both journals (the editor concerned with secondary publication must have a photocopy, reprint, or manuscript of the primary version). The priority of the primary publication is respected by a publication interval of at least one week (unless specifically negotiated otherwise by both editors).

(3) The paper for secondary publication is intended for a different group of readers; therefore, an abbreviated version could be sufficient. The secondary version faithfully reflects the data and interpretations of the primary version. The footnote on the title page of the secondary version informs readers, peers, and documenting agencies that the paper has been published in whole or in part and states the primary reference. A suitable footnote might read: "This article is based on a study first reported in the [title of a journal, with full reference]."

Authorship

Authorship credit should be based on substantial contributions to all four categories established by the ICMJE: (1) substantial contributions to conception or design of the work, acquisition of data, and analysis and interpretation of data; (2) drafting the work or revising it critically for important intellectual content; (3) final approval of the version to be published; and (4) agreement to be accountable for all aspects of the work in ensuring that questions related to the accuracy or integrity of any part of the work are appropriately investigated and resolved.

- The contributions of all authors must be described. JMT has adopted the CRediT Taxonomy (https://credit.niso.org/) to describe each author's individual contributions to the work. The role of each author should be addressed on the title page.
- Correction of authorship: Requests for corrections in authorship (such as adding or removing authors, or rearranging the order of authors) after the initial manuscript submission and before publication should be explained in writing to the editor, in a letter or email signed by all authors. A completed copyright assignment form must be submitted by every author.
- Role of corresponding author: The corresponding author takes primary responsibility for communication with the journal during the manuscript submission, peer review, and publication process. The corresponding author typically ensures that all of the journal's administrative requirements, such as providing the details of authorship, ethics committee approval, clinical trial registration documentation, and conflict of interest forms and statements, are properly completed, although these duties may be delegated to one or more co-authors. The corresponding author should be available throughout the submission and peer-review process to respond to editorial queries in a timely manner, and after publication, should be available to respond to critiques of the work and cooperate with any requests from the journal for data, additional information, or questions about the article.
- Contributors: Any researcher who does not meet all four ICMJE criteria for authorship discussed above but contributes substantively to the study in terms of idea development, manuscript writing, conducting research, data analysis, and financial support should have their contributions listed in the Acknowledgments section of the article.

Process for Managing Research and Publication Misconduct

When the journal faces suspected cases of research and publication misconduct, such as redundant (duplicate) publication, plagiarism, fraudulent or fabricated data, changes in authorship, undisclosed conflict of interest, ethical problems with a submitted manuscript, appropriation by a reviewer of an author's idea or data, and complaints against editors, the resolution process will follow the flowcharts provided by COPE (http://publicationethics.org/resources/flowcharts). The discussion and decision on the suspected cases are carried out by the Editorial Board.

Editorial Responsibilities

The Editorial Board will continuously work to monitor and safeguard publication ethics: guidelines for retracting articles; maintenance of the integrity of academic records; preclusion of business needs from compromising intellectual and ethical standards; publishing corrections, clarifications, retractions, and apologies when needed; and excluding plagiarized and fraudulent data. The editors maintain the following responsibilities: responsibility and

authority to reject and accept articles; avoid any conflict of interest with respect to articles they reject or accept; promote the publication of corrections or retractions when errors are found; and preserve the anonymity of reviewers.

Artificial Intelligence (AI) Guideline

JMT adheres to the following guidelines specified by the ICMJE regarding the use of AI tools. These measures are essential to ensuring academic integrity and ethical standards.

- AI cannot be listed as an author: AI tools cannot be listed or cited as authors due to their inability to take responsibility for errors.
- Reliability, responsibility, and permissible use of AI: Authors are fully responsible for the reliability, accuracy, originality, and integrity of their manuscripts when using AI tools. They must take complete responsibility for any plagiarism or false information generated by AI. AI-generated content cannot be cited as a primary source. The use of AI tools is permissible only for language editing or formatting assistance, and such use must be transparently disclosed.
- Data privacy and confidentiality: Authors must ensure that no confidential, sensitive, or personally identifiable data are entered into AI tools.
- Disclosure of AI use: Authors must disclose the use of AI tools at the time of manuscript submission. This disclosure should include the specific tools used, their model names, versions, manufacturers, and the role of the AI in the process. This information should be included in the Methods or Acknowledgments section, with detailed prompts included where relevant.
- Prohibition on AI-generated images and videos: AI-generated images or videos, which lack societal consensus on copyright, cannot be included in submitted manuscripts. However, exceptions may be made if AI is essential to the research design or methodology, in which case it must be explained in the Methods section.
- Restrictions for peer reviewers: Peer reviewers are prohibited from uploading manuscripts to external AI tools during the review process. If AI tools are used to support any part of the review, reviewers must transparently disclose this in their peer review reports.
- Editor's authority: the editor may refuse to proceed with the review of a paper if inappropriate use of AI is detected. Additionally, this policy may evolve in response to advancements in technology and societal agreements.

4. EDITORIAL POLICY

Copyright

Copyright in all published material is owned by the Korean Orthopaedic Trauma Association. Authors must agree to transfer copyright (https://e-jmt.org/authors/copyright_transfer_agreement.php) during the submission process. The corresponding author is responsible for submitting the copyright transfer agreement to the publisher. In addition, if excerpts from other copyrighted works are included, the authors must obtain written permission from the copyright owners and credit the sources in the article.

Open-Access License

JMT is an open-access journal. Articles are distributed under the terms of the Creative Commons Attribution License (https://creativecommons.org/licenses/by-nc/4.0/), which permits unrestricted non-commercial use, distribution, and reproduction in any medium, provided the original work is properly cited. Authors do not need permission to use tables or figures published in JMT in other journals, books, or media for scholarly and non-commercial purposes. For any commercial use of material from this open-access journal, permission must be obtained from Korean Orthopaedic Trauma Association (email: office@e-jmt.org).

Article Sharing (Author Self-Archiving) Policy

JMT is an open-access journal, and authors who submit manuscripts to JMT may share their research in several ways, including on preprint servers, social media platforms, at conferences, and in educational materials, in accordance with our open-access policy. Authors may deposit the accepted manuscript or published version in institutional repositories, provided that the original source (JMT, DOI, and publisher information) is clearly cited. All shared versions must include a link to the official publication on the JMT website. Commercial use of the published content is not permitted unless explicitly authorized by the publisher. Submitting the same manuscript to multiple

journals is strictly prohibited. This policy may be updated in response to changes in copyright law, licensing agreements, or publisher requirements.

Registration of Clinical Trial Research

It is recommended that any research that deals with a clinical trial be registered with a clinical trial registration site, such as http://cris.nih.go.kr, or other primary national registry sites accredited by the World Health Organization (https://www.who.int/clinical-trials-registry-platform/network/primary-registries) or clinicaltrial.gov (http://clinicaltrials.gov/), a service of the United States National Institutes of Health.

Data Sharing Policy

JMT encourages data sharing wherever possible unless this is prevented by ethical, privacy, or confidentiality matters. Authors wishing to do so may deposit their data in a publicly accessible repository and include a link to the DOI within the text of the manuscript.

- Clinical Trials: JMT accepts the ICMJE Recommendations for data sharing statement policy. Authors may refer to the editorial, "Data Sharing Statements for Clinical Trials: A Requirement of the International Committee of Medical Journal Editors," in the Journal of Korean Medical Science (https://dx.doi.org/10.3346/jkms.2017.32.7.1051).

Archiving Policy

In accordance with the Korean Library Act, the full text of the JMT can be archived in the National Library of Korea. JMT provides electronic archiving and preservation of access to the journal content in the event the journal is no longer published, by archiving in the National Library of Korea (https://www.nl.go.kr/archive/search.do) and the National Library of Korea can permanently preserve submitted JMT papers.

Preprint Policy

A preprint can be defined as a version of a scholarly paper that precedes formal peer review and publication in a peer-reviewed scholarly journal. JMT allows authors to submit preprints to the journal. It is not treated as duplicate submission or duplicate publication. JMT recommends that authors disclose the existence of a preprint with its DOI in the letter to the editor during the submission process. Otherwise, a plagiarism check program—Similarity Check (Crossref) or Copy Killer—may flag the results as containing excessive duplication. A preprint submission will be processed through the same peer-review process as a usual submission. If a preprint is accepted for publication, the authors are recommended to update the information on the preprint site with a link to the published article in JMT, including the DOI at JMT. It is strongly recommended that authors cite the article in JMT instead of the preprint in their next submission to journals.

5. MANUSCRIPT SUBMISSION AND PEER-REVIEW PROCESS

Online Submission

All manuscripts should be submitted online via the journal's website (https://submit.e-jmt.org/) by the corresponding author. Once you have logged into your account, the online system will lead you through the submission process in a step-by-step manner. In case of any trouble, please contact the editorial office (Email: office@e-jmt.org).

Screening after Submission

The screening process will be conducted after submission. If the manuscript does not fit the aims and scope of the Journal or does not adhere to the Instructions to authors, it may be returned to the author immediately after receipt and without a review. Before review, all submitted manuscripts are inspected using "Similarity Check powered by iThenticate (https://www.crossref.org/services/similarity-check/), a plagiarism-screening tool. If an excessively high similarity score is found, the Editorial Board will do a more profound content screening. The criterion for similarity rate for further screening is usually 25%; however, the excess amount of similarity in specific sentences may be also checked in every manuscript. The settings for Similarity Check screening are as follows: It excludes quotes, a bibliography, small matches of 6 words, small sources of 1%, and the Methods section.

Peer-Review Process

All papers, including those invited by the Editor, are subject to peer review. Manuscripts will be peer-reviewed by two

accredited experts in the musculoskeletal trauma care with one additional review by a prominent member of our Editorial Board. The editor is responsible for the final decision whether the manuscript is accepted or rejected.

- The journal uses a single-blind peer-review process: the reviewers are aware of the identity of the authors, but the authors do not know the identity of the reviewer. During the peer-review process, reviewers may interact directly or exchange information (e.g., via submission systems or email) only with the editor, which is known as "independent review."
- JMT's average turnaround time from submission to decision is 6 weeks.
- Decision letter will be sent to corresponding author via registered email. Reviewers can request authors to revise the content. The corresponding author must indicate the modifications made in their item-by-item response to the reviewers' comments. Failure to resubmit the revised manuscript within 4 weeks of the editorial decision is regarded as a withdrawal.
- The editorial committee has the right to revise the manuscript without the authors' consent unless the revision substantially affects the original content.
- After review, the Editorial Board determines whether the manuscript will be accepted for publication. Once rejected, the manuscript does not undergo another round of review.
- All articles in JMT include the dates of submission, revision, acceptance, and publication on their article page. No information about the review process or editorial decision process is published on the article page.

Submission by Editors

All manuscripts from editors, employees, or members of the Editorial Board are processed in the same way as other unsolicited manuscripts. During the review process, submitters will not engage in the selection of reviewers or the decision process. Editors will not handle their manuscripts even if the manuscripts are commissioned.

The conflict of interest declaration should be added as follows.

Conflicts of Interest: OOO has been an Editorial Board member of Journal of Musculoskeletal Trauma since OOO but has no role in the decision to publish this article. No other potential conflicts of interest relevant to this article were reported.

Feedback after Publication

If the authors or readers find any errors or contents that should be revised, it can be requested from the Editorial Board. The Editorial Board may consider erratum, corrigendum, or a retraction. If there are any revisions to the article, there will be a CrossMark description to announce the final draft. If there is a reader's opinion on the published article with the form of Letter to the editor, it will be forwarded to the authors. The authors can reply to the reader's letter. Letter to the editor and the author's reply may be also published.

Appeals of Decisions

Any appeal against an editorial decision must be made within 2 weeks of the date of the decision letter. Authors who wish to appeal a decision should contact the Editor-in-Chief, explaining in detail the reasons for the appeal. All appeals will be discussed with at least one other associate editor. If consensus cannot be reached thereby, an appeal will be discussed at a full editorial meeting. The process of handling complaints and appeals follows the guidelines of COPE. JMT does not consider second appeals.

6. MANUSCRIPT PREPARATION

Authors are required to submit their manuscripts after reading the following instructions. Any manuscript that does not conform to the following requirements will be deemed inappropriate and may be returned.

General Requirements

- All manuscripts should be written in English.
- The manuscript must be written using Microsoft Word and saved as ".doc" or ".docx" format. The font size should be 11 points. The body text must be left-aligned, double-spaced, and presented in a single column. The left, right, and bottom margins must be 3 cm, but the top margin must be 3.5 cm.
- The page numbers should be placed in Arabic numerals at the center of the bottom margin, starting from the abstract page.
- Only standard abbreviations should be used. Abbrevi-

ations should be avoided in the title of the manuscript. Abbreviations should be spelled out when first used in the text and the use of abbreviations should be kept to a minimum.
- The names of manufacturers of equipment and non-generic drugs should be given.
- Authors should express all measurements in conventional units, using International System (SI) units.
- P-value from statistical testing should be expressed as capital P.

Reporting Guidelines for Specific Study Designs

For the specific study design, it is recommended that authors follow the reporting guidelines, such as CONSORT (http://www.consort-statement.org) for randomized controlled trials, STROBE (http://www.strobe-statement.org) for observational studies, and PRISMA (http://www.prisma-statement.org) for systematic reviews and meta-analyses. A good source of reporting guidelines is the EQUATOR Network (https://www.equator-network.org/) and NLM (https://www.nlm.nih.gov/services/research_report_guide.html).

Types of Manuscripts

- The manuscript types are divided into original articles, review articles, case reports, technical notes, letters to the editor, editorial, and other types.
- Original Articles: Original articles should be written in the following order: title page, abstract (within 300 words), keywords, main body (introduction, methods, results, discussion, and conclusions), acknowledgments (if applicable), references (up to 30), tables, figure legends, and figures.
- Review Articles: Review articles should focus on a specific topic. The format of a review article is flexible. Publication of these articles will be decided upon by the Editorial Board.
- Case Reports: Case reports should be a report on a single case or an analysis of a few cases to add to the clinical spectrum. Case reports should be written in the following order: title page, abstract (within 200 words), keywords, main body (introduction, case report, and discussion), acknowledgments (if applicable), references (up to 10), tables, figure legends, and figures.
- Technical Notes: Technical notes should be written in the following order: title page, abstract (within 200 words), keywords, main body (introduction, technique, and discussion), acknowledgments (if applicable), references (up to 20), tables (if applicable), figure legends, and figures. The total word count should not exceed 1,500 words.
- Letters to the Editor: The journal welcomes readers' comments on recently published articles or orthopedic topics of interest. Letters to the editor should not exceed 1,000 words, excluding references, tables, and figures. A maximum of 5 references and total 4 figures or tables are allowed.
- Editorials: Editorials are invited by the editors and should be commentaries on articles recently published in the journal. Editorial topics could include active areas of research, fresh insights, and debates in the field of orthopedic surgery. Editorials should not exceed 1,000 words, excluding references, tables, and figures. A maximum of 10 references and total 4 figures or tables are allowed.
- Systematic Reviews and Meta-Analyses: Systematic reviews and meta-analyses should provide a comprehensive and structured overview of published material on a clearly defined subject. Authors must describe in detail how the evidence was identified, including the sources searched and the inclusion and exclusion criteria applied. Meta-analyses should quantitatively synthesize the results of two or more studies to address a specific research question or association. All systematic reviews and meta-analyses submitted to JMT must adhere to the PRISMA guidelines (http://www.prisma-statement.org).

Table 1. Recommended maximums for articles submitted to JMT[a]

Type of article	Abstract (word)	Text (word)[b]	References	Tables & Figures
Original Article	Structured, 300	NL	30	NL
Review	Unstructured, 300	NL	NL	NL
Systematic Review	Structured, 300	NL	NL	NL
Case Report	Unstructured, 200	1,500	10	NL
Technical Note	Unstructured, 200	1,500	20	NL
Letter to the Editor	-	1,000	5	4
Editorial	-	1,000	10	4

[a]The requirements for the number of references, tables and figures and length of the main text can be consulted with the Editorial Office; [b]Excluding abstract, tables, figures, acknowledgments, and references.

Format of Manuscript Title page

- The title page must include the title, the authors' names,

affiliations, and the corresponding author's name and contact information. The corresponding author's contact information must include their name and email. In addition, a running title must be provided, with a maximum of 50 characters, including spaces.

Abstract and keywords

Each paper should begin with an abstract not exceeding 300 words (for original articles and reviews). The abstract for original articles should state the background, methods, results, and conclusions in each paragraph in a brief and coherent manner. Relevant numerical data should be included. Below the abstract, keywords should be provided (maximum of 5). Authors are encouraged to use the MeSH database to find Medical Subject Headings at http://www.nlm.nih.gov/mesh/meshhome.html. The structured abstract should be divided into the following sections.

- Background: The rationale, importance, or objectives of the study should be described briefly and concisely in one to two sentences. The objective should be consistent with that stated in the Introduction.
- Methods: The procedures conducted to achieve the study objective should be described in detail, together with relevant details concerning how data were obtained and analyzed and how research bias was adjusted.
- Results: The most important study results and analysis should be presented in a logical manner with specific experimental data.
- Conclusions: The conclusions drawn from the results should be described in one to two sentences and must align with the study objective.
- Level of evidence: Author should make the final determination of the study design and level of evidence based on the Centre for Evidence Based Medicine guidelines. Authors may refer to the definitions in the Level of Evidence table (https://www.cebm.ox.ac.uk/files/levels-of-evidence/cebm-levels-of-evidence-2-1.pdf).

Main Body

- All articles using clinical samples or data and those involving animals must include information on the IRB/IACUC approval or waiver and informed consent. An example is shown below. "We conducted this study in compliance with the principles of the Declaration of Helsinki. The study protocol was reviewed and approved by the Institutional Review Board of OO (No. OO). Written informed consent was obtained / Informed consent was waived."
- Description of participants: Ensure the correct use of the terms "sex" (when reporting biological factors) and "gender" (identity, psychosocial, or cultural factors), and, unless inappropriate, report the sex and/or gender of study participants, the sex of animals or cells, and describe the methods used to determine sex and gender. If the study was done involving an exclusive population, for example, in only one sex, authors should justify why, except in obvious cases (e.g., ovarian cancer). Authors should define how they determined race or ethnicity and justify their relevance.
- Introduction: State the background or problem that led to the initiation of the study. Introduction is not a book review, rather it is best when the authors bring out controversies which create interest. Lead systematically to the hypothesis of the study, and finally, to a restatement of the study objective, which should match that in the Abstract. Do not include conclusions in the Introduction.
- Methods: Describe the study design (prospective or retrospective, inclusion and exclusion criteria, duration of the study) and the study population (demographics, length of follow-up). Explanations of the experimental methods should be concise, yet enable replication by a qualified investigator.
- Results: This section should include detailed reports on the data obtained during the study. All data in the text must be presented in a consistent manner throughout the manuscript. All issues which the authors brought up in the method section need to be in result section. Also, it is preferred that data be in figures or tables rather than a long list of numbers. Instead, numbers should be in tables or figures with key comments on the findings.
- Discussion: The first paragraph of the discussion should deal with the key point in this study. Do not start with an article review or general comment on the study topic. In the Discussion, data should be interpreted to demonstrate whether they affirm or refute the original hypothesis. Discuss elements related to the purpose of the study and present the rationales that support the conclusion drawn by referring to relevant literature. Discussion needs

some comparison of similar papers published previously, and discuss why your study is different or similar from those papers. Care should be taken to avoid information obtained from books, historical facts, and irrelevant information. A discussion of study weaknesses and limitations should be included, followed by a brief conclusion that clearly states the answer to the research question or hypothesis. Conclusions must be drawn only from the study results, and authors should verify that their data firmly support these conclusions. The conclusions in the text and those in the abstract must be consistent.

- Article Information: This section should include details on Author Contributions, Conflicts of Interest, Funding, Data Availability, Acknowledgments, and Supplementary Materials. If any of these items are not applicable, authors must indicate "None."
- The contributions of all authors must be described using the CRediT (https://credit.niso.org/) taxonomy of author roles.
- References must be numbered with superscripts according to their quotation order. When more than two quotations of the same authors are indicated in the main body, a comma must be placed between a discontinuous set of numbers, whereas a dash must be placed between the first and last numerals of a continuous set of numbers: "Kim et al. [2,8,9] insisted…" and "However, Park et al. [11-14] showed opposing research results."
- Figures and tables used in the main body must be indicated as "Fig." and "Table." For example, "Magnetic resonance imaging of the brain revealed… (Figs. 1-3).
- ORCID: We recommend that the open researcher and contributor ID (ORCID) of all authors be provided. To have an ORCID, authors should register in the ORCID website (http://orcid.org/).

References

- References are recommended as 30 for original articles, 10 for case reports, and 20 for technical notes.
- All references must be cited in the text. The number assigned to the reference citation is according to the first appearance in the manuscript. References in tables or figures are also numbered according to the appearance order. Reference numbers in the text, tables, and figures should in a bracket ([ ]).
- List all authors when there are six or fewer. When there are seven or more authors, list only the first three authors followed by "et al."
- Authors should be listed by surname followed by initials.
- The journals should be abbreviated according to the style used in the list of journals indexed in the NLM Journal Catalog (http://www.ncbi.nlm.nih.gov/nlmcatalog/journals).
- Overlapping page numbers (e.g., 2025-2026) should omit the repeated numerals (e.g., 2025-2026 should be written as 2025-6).
- References to unpublished material, such as personal communications and unpublished data, should be noted within the text and not cited in the References. Personal communications and unpublished data must include the individual's name, location, and date of communication.
- Examples of references are as follows: Journal article

① Journal

1. Song HK, Cho WT, Choi WS, Sakong SY, Im S. Acute compartment syndrome of thigh: ten-year experiences from a level I trauma center. J Musculoskelet Trauma 2024;37:171-4.
2. MacKechnie MC, Shearer DW, Verhofstad MH, et al. Establishing consensus on essential resources for musculoskeletal trauma care worldwide: a modified Delphi study. J Bone Joint Surg Am 2024;106:47-55.
3. Raats JH, Ponds NH, Brameier DT, et al. Agreement between patient- and proxy-reported outcome measures in adult musculoskeletal trauma and injury: a scoping review. Qual Life Res 2024 Aug 23 [Epub]. https://10.1007/s11136-024-03766-1

② Book & Book chapter

4. Townsend CM, Beauchamp RD, Evers BM, Mattox K. Sabiston textbook of surgery. 21st ed. Elsevier; 2021.
5. Meltzer PS, Kallioniemi A, Trent JM. Chromosome alterations in human solid tumors. In: Vogelstein B, Kinzler KW, eds. The genetic basis of human cancer. McGraw-Hill; 2002. p. 93-113.

③ Homepage/Web site

6. World Health Organization (WHO). World health statistics 2021: a visual summary [Internet]. WHO; 2021 [cited 2023 Feb 1]. Available from: https://www.who.int/data/stories/world-health-statistics-2021-a-visual-summary

④ Preprint

7. Sharma N, Sharma P, Basu S, et al. The seroprevalence

and trends of SARS-CoV-2 in Delhi, India: a repeated population-based seroepidemiological study [Preprint]. Posted 2020 Dec 14. medRxiv 2020.12.13.20248123. https://doi.org/10.1101/2020.12.13.20248123

For more on references, refer to the NLM's "Samples of Formatted References for Authors of Journal Articles." https://www.nlm.nih.gov/bsd/uniform_requirements.html#journals

Figures and Figure Legends

Figures should be cited in the text and numbered using Arabic numerals in the order of their citation (e.g., Fig. 1). Figures are not embedded within the text. Each figure should be submitted as an individual file. The figure legends should begin on the next page after the last table. Every figure has its own legend. Abbreviations and additional information for any clarification should be described within each figure legend. Footnotes below the figure should follow the order of abbreviation first, followed by symbols. Symbols should be marked with small alphabet letters in the order of their usage, such as [a], [b], [c], or asterisks (*) for statistical significance. Figure files are submitted in EPS, TIFF, or PDF formats. The requirement for minimum resolutions is dependent on figure types. For line drawings, 1,200 dpi are required. For grey color works (i.e., pictures of gel or blots), 600 dpi is required. For color or half-tone artwork, 300 dpi is required. The files should be named according to the figure number.

- Staining techniques used should be described. Photomicrographs with no inset scale should have the magnification of the print in the legend.
- Papers containing unclear photographic prints may be rejected.
- Remove any writing that could identify a patient.
- If any tables or figures are taken or modified from other papers, authors should obtain permission through the Copyright Clearance Center (https://www.copyright.com/) or from the individual publisher, unless they are from open-access journals under the Creative Commons License. For tables or figures from an open-access journal, simply verify the source of the journal precisely in the accompanying footnote. Please note the distinction between a free access journal and an open-access journal: it is necessary to obtain permission from the publisher of a free-access journal for using tables or figures published therein. Examples are shown below:

  Reprinted (Modified) from Tanaka et al. [48], with permission of Elsevier.

  Reprinted (Modified) from Weiss et al. [2], according to the Creative Commons License.

Tables

- Tables should be numbered sequentially with Arabic numerals in the order in which they are mentioned in the text.
- If an abbreviation is used in a table, it should be defined in a footnote below the table.
- Additional information for any clarification should be designated for citation using alphabetical superscripts [a], [b], [c] or asterisks (*) for statistical significance. The explanation for superscript citation should follow these examples: [a]Not tested.

  *P< 0.05, **P< 0.01, ***P< 0.001.
- Tables should be understandable and self-explanatory, without references to the text.
- If a table has been previously published, it should be accompanied by the written consent of the copyright holder, and the footnote must acknowledge the original source.

7. MANUSCRIPT PROCESSING AFTER ACCEPTANCE

Final Version

After the paper has been accepted for publication, the authors should submit the final version of the manuscript. The names and affiliations of the authors should be double-checked, and if the originally submitted image files were of poor resolution, higher-resolution image files should be submitted at this time. Symbols (e.g., circles, triangles, squares), letters (e.g., words, abbreviations), and numbers should be large enough to be legible on reduction to the journal's column widths. All symbols must be defined in the figure caption. If references, tables, or figures are moved, added, or deleted during the revision process, renumber them to reflect such changes so that all tables, references, and figures are cited in numeric order.

Manuscript Corrections

Before publication, the manuscript editor will correct the manuscript such that it meets the standard publication format. The authors must respond within two days when the manuscript editor contacts the corresponding author for revisions. If the response is delayed, the manuscript's publication may be postponed to the next issue.

Proof

The authors will receive the final version of the manuscript as a PDF file. Upon receipt, the authors must notify the editorial office (or printing office) of any errors found in the file within two days. Any errors found after this time are the responsibility of the authors and will have to be corrected as an erratum.

Errata and Corrigenda

To correct errors in published articles, the corresponding author should contact the journal's Editorial Office with a detailed description of the proposed correction. Corrections that profoundly affect the interpretation or conclusions of the article will be reviewed by the editors. Corrections will be published as corrigenda (corrections of the author's errors) or errata (corrections of the publisher's errors) in a later issue of the journal.

NOTICE: These recently revised instructions for authors will be applied beginning with the January 2026 issue.

Checklist

☐ Manuscript in MS-WORD (DOC, DOCX) format.

☐ Double-spaced typing with 12-point font.

☐ Sequence of title page, abstract and keywords, introduction, methods, results, discussion, and conclusions, acknowledgments, references, tables, and figure legends. All pages and manuscript text with line should be numbered sequentially, starting from the abstract.

☐ Title page with article title, authors' full name(s) and affiliation(s), address for correspondence (including telephone number, and email address), running title (less than 50 characters), and acknowledgments, if any.

☐ Abstract in structured format up to 300 words for original articles. Keywords (up to 5) from the MeSH.

☐ All table and figure numbers are found in the text.

☐ Figures as separate files, in TIFF, JPG, GIF, or PPT format.

☐ References listed in proper format. All references listed in the reference section are cited in the text and vice versa.

JMT Journal of Musculoskeletal Trauma

Copyright transfer agreement and COI disclosure

Manuscript Title _____

I. Copyright Transfer Form

The authors hereby transfer all copyrights in and to the manuscript titled above, in all forms and media, whether now known or hereafter developed, to the Korean Orthopaedic Trauma Association effective upon the manuscript's acceptance for publication in the *Journal of Musculoskeletal Trauma*. The authors retain all proprietary rights other than copyright, such as patent rights.

Everyone listed as an author on this manuscript has made a substantial, direct, and intellectual contribution to the work and assumes public responsibility for its content. This manuscript represents original work that has not previously published and is not currently under consideration for publication in any other journal.

List the names of all authors in the correct order.

_____

_____

_____

The corresponding author signs this copyright agreement on behalf of all the co-authors.

Name(s) of the corresponding author(s): _____

Signature: _____ Date: _____

JMT Journal of Musculoskeletal Trauma

Conflict of interest form

Manuscript Title _____

_____

As an integral part of the online submission process, Journal of Musculoskeletal Trauma policy requires that each author confirms whether he or she has any conflicts of interest or financial support to declare and to provide any such details.

Signature
By signing this conflict of interest form, each and every undersigned author agrees to the following: To the best of my knowledge, I have no relevant financial relationships except as follows (please list any possible exceptions below the author name).

Author Name_____ Signed_____ Date_____(DD/ MM/ YY)

_____

Author Name_____ Signed_____ Date_____(DD/ MM/ YY)

_____

Author Name_____ Signed_____ Date_____(DD/ MM/ YY)

_____

Author Name_____ Signed_____ Date_____(DD/ MM/ YY)

_____

Author Name_____ Signed_____ Date_____(DD/ MM/ YY)

_____

Author Name_____ Signed_____ Date_____(DD/ MM/ YY)

_____